40097

National Library of Canada **Bibliothèque nationale du Canada**

CANADIAN THESES ON MICROFICHE

THÈSES CANADIENNES SUR MICROFICHE

NAME OF AUTHOR/*NOM DE L'AUTEUR* Iain Bruce

TITLE OF THESIS/*TITRE DE LA THÈSE* The Field Estimation of Shear Strength on Rock Discontinuities

UNIVERSITY/*UNIVERSITÉ* University of Alberta

DEGREE FOR WHICH THESIS WAS PRESENTED/ *GRADE POUR LEQUEL CETTE THÈSE FUT PRÉSENTÉE* Ph. D

YEAR THIS DEGREE CONFERRED/*ANNÉE D'OBTENTION DE CE GRADE* 1978

NAME OF SUPERVISOR/*NOM DU DIRECTEUR DE THÈSE* Dr. D. M. Cruden

Permission is hereby granted to the NATIONAL LIBRARY OF CANADA to microfilm this thesis and to lend or sell copies of the film.

The author reserves other publication rights, and neither the thesis nor extensive extracts from it may be printed or otherwise reproduced without the author's written permission.

L'autorisation est, par la présente, accordée à la BIBLIOTHÈQUE NATIONALE DU CANADA de microfilmer cette thèse et de prêter ou de vendre des exemplaires du film.

L'auteur se réserve les autres droits de publication; ni la thèse ni de longs extraits de celle-ci ne doivent être imprimés ou autrement reproduits sans l'autorisation écrite de l'auteur.

DATED/*DATÉ* Oct 10/1978 SIGNED/*SIGNÉ* Iain Bruce

PERMANENT ADDRESS/*RÉSIDENCE FIXE*
10840 - 33 Ave
Edmonton Alberta
T6J 3C1

NL-91 (3-74)

National Library of Canada

Cataloguing Branch
Canadian Theses Division

Ottawa, Canada
K1A 0N4

NOTICE

The quality of this microfiche is heavily dependent upon the quality of the original thesis submitted for microfilming. Every effort has been made to ensure the highest quality of reproduction possible.

If pages are missing, contact the university which granted the degree.

Some pages may have indistinct print especially if the original pages were typed with a poor typewriter ribbon or if the university sent us a poor photocopy.

Previously copyrighted materials (journal articles, published tests, etc.) are not filmed.

Reproduction in full or in part of this film is governed by the Canadian Copyright Act, R.S.C. 1970, c. C-30. Please read the authorization forms which accompany this thesis.

THIS DISSERTATION
HAS BEEN MICROFILMED
EXACTLY AS RECEIVED

Bibliothèque nationale du Canada

Direction du catalogage
Division des thèses canadiennes

AVIS

La qualité de cette microfiche dépend grandement de la qualité de la thèse soumise au microfilmage. Nous avons tout fait pour assurer une qualité supérieure de reproduction.

S'il manque des pages, veuillez communiquer avec l'université qui a conféré le grade.

La qualité d'impression de certaines pages peut laisser à désirer, surtout si les pages originales ont été dactylographiées à l'aide d'un ruban usé ou si l'université nous a fait parvenir une photocopie de mauvaise qualité.

Les documents qui font déjà l'objet d'un droit d'auteur (articles de revue, examens publiés, etc.) ne sont pas microfilmés.

La reproduction, même partielle, de ce microfilm est soumise à la Loi canadienne sur le droit d'auteur, SRC 1970, c. C-30. Veuillez prendre connaissance des formules d'autorisation qui accompagnent cette thèse.

LA THÈSE A ÉTÉ
MICROFILMÉE TELLE QUE
NOUS L'AVONS REÇUE

NL-339 (3/77)

THE UNIVERSITY OF ALBERTA

THE FIELD ESTIMATION OF SHEAR STRENGTH ON ROCK DISCONTINUITIES

by

© IAIN BRUCE

A THESIS
SUBMITTED TO THE FACULTY OF GRADUATE STUDIES AND RESEARCH
IN PARTIAL FULFILMENT OF THE REQUIREMENTS FOR THE DEGREE
OF DOCTOR OF PHILOSOPHY
IN
CIVIL ENGINEERING

DEPARTMENT OF CIVIL ENGINEERING

EDMONTON, ALBERTA
FALL, 1978

THE UNIVERSITY OF ALBERTA

FACULTY OF GRADUATE STUDIES AND RESEARCH

The undersigned certify that they have read, and recommend to the Faculty of Graduate Studies and Research, for acceptance, a thesis entitled " THE FIELD ESTIMATION OF SHEAR STRENGTH ON ROCK DISCONTINUITIES"

submitted by Iain Bruce

in partial fulfilment of the requirements for the degree of Doctor of Philosophy in Civil Engineering.

Supervisor

B. Stimpson

External Examiner

DATE 10 October 1978

TO BEARS EVERYWHERE

ABSTRACT

Two natural rock slides in the Canadian Rocky Mountains have been investigated following a model for rock slope investigations. The geology at each area was mapped in detail in the slide areas. The slides are simple and have occurred down the dip of bedding surface discontinuities. The scarps and lateral margins of the slides, where they existed, have been formed by near vertical joint sets striking approximately parallel and perpendiculr to the direction of sliding.

The rock masses underlying the slides were thrust into position along deep-seated faults. The failure surfaces at Jonas Creek have been gently folded. The assumed toes of the slides outcrop two thirds of the way up the valley wall. The slide at Jonas Creek has occurred within the Lower Cambrian Gog Group quartzites. The failure surfaces at Whitehorse Creek are planar and the toes of the slides are located near the bottom of a small valley. The slides occurred within the Mississippian Turner Valley Formation of limestones and dolomites.

A new method of measuring the roughness on the failure plane, utilizing only a CLAR compass and simple statistics, has been evaluated at both slide areas. The new method gives similar results to other methods of evaluating roughness over the small scales previously investigated. The new method , however, allows estimates of roughness on much larger scales which were previously unobtainable. The controlling scale of roughness appears to exist on the 0.30 m scale. The roughness varies substantially over short distances, however, and must be mapped in detail.

The frictional resistance of clean mating bedding surface discontinuities from both slide areas was evaluated in the laboratory using a direct shear apparatus and tilting table tests. Peak and ultimate shear strength values were evaluated for natural rough surfaces on 5cm x 5cm samples. The values of ϕ_b estimated using the direct shear test and the tilt table test were similar. The tilt table test results were easier to obtain , however, than the direct shear test results.

Results indicate that the commonly quoted 30 to 35° value for basic friction angles in rock may overestimate the basic friction angle acting in the field.

Back-analyses conducted on the slides indicated that the combinations of ϕ_b evaluated by tilt table and the field roughness on the 0.3 m scale yielded factors of safety varying from 1.07 to 1.34, a reasonable result.

Simple dynamic analyses conducted on the slides indicated that the movement of the slide debris was controlled by the laws of dry sliding friction.

ACKNOWLEDGEMENTS

The author of this thesis would like to thank his thesis supervisor Dr. Dave Cruden for the past four years of guidance, patience, and understanding. His topic suggestion, encouragement and field expertise have been greatly appreciated.

The author would especially like to thank his small bear Kathy, who helped gather the field data, who typed and edited this thesis, and who gave the author moral support for four long years.

The author would also like to thank professors Thomson, Morgenstern, Stimpson,and Eisenstein for their criticisms and suggestions.

The assistance and friendship of the staff at the University of Alberta, notably Mr.O. (Woody) Wood and Mr. Al. Muir , is immensely appreciated. I would also like to thank Scotty Rogers, Don Fushtey, Bob Billey and Ray Howells for their help. Special thanks also go to Hertha Yaroschuk and Eleanor Kangas for administrative assistance.

Special thanks go to Dan Mageau, Rex Tse and Marc Tremblay for their assistance in field mapping and testing.

The photographic assistance of Mr. W. Moranetz and Mr. H.Friedrich is appreciated.

I would also like to thank my fellow graduate students who helped with discussions about the thesis, notably Alan Gale, Bruce Kjartanson, Sergio daFontoura, Peter Kaiser, Jeff Weaver, Maurice Dusseault, John Simmons, Wayne Savigny and Davey Sego.

The financial assistance provided by Dr. Dave Cruden, The University Of Alberta Civil Department and provided by the National Research Council of Canada is gratefully acknowledged.

A special thanks is extended to Jasper Parks officials of Parks Canada who allowed sampling of the Jonas Creek Rock Slide and who cooperated by closing off the Banff-Jasper highway for an in-situ rock slide test.

TABLE OF CONTENTS

CHAPTER PAGE

I INTRODUCTION

1-1 General 1

1-2 Purpose And Scope 2

II THE GEOLOGY OF THE JONAS CREEK SLIDE AREA

2-1 Introduction 6

2-2 Location And Access 7

2-3 Previous Work 7

2-4 Surficial Geology 9

2-5 Stratigraphy 14

2-6 Structural Geology 16

2-7 Summary 23

III THE GEOLOGY OF THE WHITEHORSE CREEK SLIDE AREA

3-1 Introduction 41

3-2 Location And Access 42

3-3 Previous Work 43

3-4 Surficial Geology 44

3-5 Stratigraphy 47

3-6 Structural Geology 49

3-7 Summary 55

IV THE FIELD ESTIMATION OF THE TOPOGRAPHIC COMPONENT OF SHEAR STRENGTH

4-1 Introduction 72

4-2 Previous Techniques Used To Evaluate i 76

4-3 Previous Analysis Of Roughness Measurements 84

4-4 Theory Of Roughness Evaluation 88
4-5 Experimental Verification Of Roughness Evaluation .. 92
4-6 Correlation Of Variances With i 99
4-7 Discussion 105
4-8 Conclusions 106

V LABORATORY DETERMINATIONS OF SHEAR STRENGTH

5-1 Introduction 145
5-2 Previous Work In Shear Strength Evaluation 147
5-3 Sampling Locations 151
5-4 Sampling Procedure 153
5-5 Sample Preparation 154
5-6 Testing Apparatus And Procedure 158
5-7 Testing Program 162
5-8 Direct Shear Test Results 165
5-9 Roughness Evaluation Results 168
5-10 Results Of The Point Load Tests 171
5-11 Tilting Table Test Results 174
5-12 Tilting Table Test Results;Part 2 179
5-13 Summary Of Results 182
5-14 Recommendations 184

VI ROCK SLIDE BACK ANALYSES

6-1 Introduction 210
6-2 Slope Stability Methods 211
6-3 Geometry Of The Failure Mass 216
6-4 Pore Pressure Assumptions 217
6-5 Shear Strength Parameters 222
6-6 Discussion 223

6-7 Post Failure Behaviour 226

6-8 Conclusions 232

VII CONCLUSIONS

7-1 General 237

References Cited 245

Appendix A-1 261

Appendix A-2 263

Appendix A-3 271

Appendix A-4 274

LIST OF TABLES

Table	Description	Page
2-1	Physical Dimensions Of Jonas Creek Failure Surfaces.	25
3-1	Physical Dimensions Of Whitehorse Creek Failure Surfaces.	56
4-1	Range Of Dip And Dip Direction Values Found At Whitehorse Creek Using Fecker And Renger's Method.	109
4-2	The Operator Errors Established At Jonas Creek And Whitehorse Creek.	110
4-3	Summary Of The S(w) Values For The 0.3 m scale.	112
4-4	Summary Of Roughness On The 3.0 m Scale.	116
4-5	A Synthesis Of The Various i Angles Calculated Using Several Different Methods.	118
4-6	Summary Of The i Angles Found On Various Scales.	119
5-1	Summary Of Shear Test Results And Their Confidence Limits (Natural Surfaces).	186
5-2	Summary Of Direct Shear Test Results (Artificial Surfaces).	187
5-3	Summary Of i Angles Recorded Before And After Shear.	188
5-4	Comparison Of i Angles Measured On Profiles With Those Measured By LVDT During Shear.	189
5-5	Summary Of Uniaxial Compressive Strengths As Obtained By The Point Load Tester.	191
5-6	Summary Of CLA Values Encountered On The Artificial Surfaces.	192
5-7	A Summary Of Sliding Angles Øs, Measured By Tilting Table.	193
5-8	A comparison Between The Sliding Friction Angles From The Tilt Table.	194

LIST OF FIGURES

Figure		Page
1-1	Flow Chart Of A Slope Stability Analysis.	5
2-1	Location Map Of Jonas Creek .	26
2-2	Section Near Jonas Creek illustrating U Valley.	27
2-3	Simplified Surficial Geology Map Of Jonas Creek.	28
2-4	Structural Geology Map Of Part Of The Main Ranges.	29
2-5	Jonas Creek Stratigraphic Column.	30
2-6	Map Of The Jonas Creek Area Showing Data From Hughes.	31
2-7	Average Lineation On The Slickensided Surfaces Shown Relative To Average Joints And Bedding.	32
2-8	Structural Geology Map Of Jonas Creek.	33
2-9	Poles To The Joints Found At Jonas Creek.	34
2-10	Stereonet Analysis Illustrating How Endless Chain Ridge Is Stabilized.	35
3-1	Location Map Of Whitehorse Creek.	57
3-2	Valley Profile Adjacent To Whitehorse Creek Illustrating U Profile	58
3-3	A Surficial Geology Map Of The Area Surrounding The Whitehorse Creek Slide Area	59
3-4	Stratigraphic Column Of Whitehorse Creek Area.	60
3-5	Structural Geology Of Part Of The Rocky Mountain Foothills.	61
3-6	Structural Geology Map Of Whitehorse Creek.	62

3-7 Stereonet Of Poles To Bedding On The Failure Surface. 63

3-8 Stereonet Of Poles To Bedding Above The Slide Failure Surface. 64

3-9 Stereonet Used To Define The Fold Axis From Poles To Bedding. 65

3-10 Poles To Joints Measured At Whitehorse Creek. 66

4-1 Idealized Bilinear Failure Envelope. 120

4-2 Representation Of How ϕ, As, andV/Tan i, Varies With Normal Stress. 121

4-3 An Example Of A Natural Rock Profile. 122

4-4 A Representation Of How Fecker And Rengers Measured Surface Roughness. 123

4-5 Fecker And Rengers' Method Of Evaluating i On Different Scales. 124

4-6 Comparison Of Rengers' Profilograph Results With Fecker And Rengers' Compass Results. 125

4-7 Results From Fecker And Rengers' Data Illustrating Elliptical Outlines Of Compass Data. 126

4-8 Correlation Between Z2 And Friction Angle. 127

4-9 Barton's Experimental Results Relating Roughness Angle To Normal Stress. 128

4-10 Roughness Profiles Illustrating The Various JRC Values. 129

4-11 Comparison Of The Theoretical Line Of i=100/L And Fecker And Rengers' Data And Hoek And Bray's Interpretation. 130

4-12 Graph Illustrating Similarity In Trend Between Fecker And Rengers' Data And Maximum Range/2 And S(w) Values. 131

4-13 Results From Fecker And Renger's Approach at Stations 1 - 4 At Whitehorse Creek. 132

4-14 Schematic Diagram Of A Station With A Worked Example Showing How To Find The Operator Error. 133

4-15 Graph Illustrating The Similarity Between The Maximum S(w) Values And 47/ L. 134

4-16 Histogram Of i Angles Recorded From Profiles. 135

4-17 Topographic Profiles Measured Using A Theodolite To Determine i angles. 136

4-18 Experimentally Defined Relationship Linking S(w) With The Roughness Angle i. 137

4-19 Comparison Between Roughness Values Evaluated By Fecker And Rengers' Range/2 Versus S(w). 138

4-20 Relationship Between in Values And Z2 Values For Large Scale Profiles Measured At Jonas Creek And Whitehorse Creek. 139

4-21 Relationship Between Z2 Parameter And JRC Values. 140

4-22 Graph Illustrating The Relationship Between in Values And JRC Values. 141

5-1 Scale Effects Of Sample Size On Peak Friction Angles. 195

5-2 Schematic Diagram Of Sample Preparation. 196

5-3 Example Traces Recorded From Roughness Profiles Showing Some representative i Angles. 197

5-4 Schematic Drawing Of Sliding Test Statics. 198

5-5 An Example Of A Direct Shear Test Graph Result. 199

5-6 Mohr-Coulomb Envelope For The Results Of The 5 cm x 5 cm Direct Shear Tests At Jonas Creek . 200

5-7 Mohr-Coulomb Envelopes For The Results Of The 5 cm x 5 cm Direct Shear Tests At Whitehorse Creek. 201

5-8 Amplitude Distribution Of Asperities For A Test Surface. 202

5-9 Graphical Presentation Of The Relationships Between The i Angle Measured By LVDT During Shear Versus The Average Profile i Angle. 203

5-10 Graph Of Barton's Relationship Of Øp=Øb + 2i. 204

6-1 Failure Geometry Proposed By Barton. 229

6-2 Location Map Showing The Section Lines Illustrated In Figures 6-3 to 6-7. 230

6-3 Cross Section Of The North Slide At Jonas Creek. 231

6-4 Cross Section Of The Unfailed Slope At Jonas Creek. 232

6-5 Cross Section Of The South Slide At Jonas Creek. 233

6-6 Cross Section Through The Younger Slide At Whitehorse Creek. 234

6-7 Cross Section Through The Older Slide At Whitehorse Creek. 235

6-8 Figure Illustrating The Horizontal And Vertical Distances Travelled By The Centre Of Gravity Of The Failure Mass. 236

A-1-1 Sketch Map Illustrating Ramsden's Graphical Model 262

A-2-1 Results Of The In Situ Shear Test At Jonas Creek. 270

Results Of The Laboratory Shear Tests. 278

LIST OF PHOTOGRAPHIC PLATES

Plate	Description	Page
2-1	Air Photo Of The Jonas Creek Slide Area Showing Debris Outlines And Thicknesses.	36
2-2	Air Photo Pair Showing Jonas Creek Slide Debris Areas With Wavelike Surface Of The Debris.	37
2-3	Photograph Of The Failure Surface At Jonas Creek Showing Large Scale Cross Bedding.	38
2-4	Photograph Of The North Failure Plane Showing The Vertical Joints Which Occurred Between Beds.	39
2-5	Photograph Showing Variation In Joint Spacing On The North Slide.	40
3-1	Photograph Illustrating The Large Range In Debris Sizes at Whitehorse Creek.	67
3-2	Bedrock Geology Shown Overlain On An Air Photo Of The Slides At Whitehorse Creek.	68
3-3	Photograph Of Part Of The Failure Surface At Whitehorse Creek Showing Small Vertical Steps.	69
3-4	Photo Of The Scarp At Whitehorse Creek Showing The Vertical Joints Forming The Back And Side Scarps.	70
3-5	Air Photo Of The Entire Ridge At Whitehorse Creek.	71
4-1	A Profile Of A Bedding Plane At Jonas Creek Illustrating Various i Angles.	142
4-2	Air Photo Illustrating The Rough Bedding Plane Locations At Jonas Creek.	143
4-3	Air Photo Illustrating The Rough Bedding Plane Locations At Whitehorse Creek.	

TABLE OF ABBREVIATIONS

As = Shear Area Ratio.
c = Effective Cohesion Intercept.
C = Uniaxial Compressive Strength.
d = True Average Value Of The Dip Of A Discontinuity Set.
D = Core Diameter Of A Point Load Test Sample.
e = Operator Error
$E(\theta)$ = Expected Value Of Theta.
f = Average Coefficient Of Friction.
F = Force Recorded Across The Point Load Plattens.
i = Angle Of Inclination Of Asperities.
I = Value Used In The Point Load Tests.
J = Degree Of Interlock Along A Joint.
N =Normal Stress.
T = The Transition Stress At Which Shear Strength For A Joint Equals The Shear Strength Of The Intact Rock.
ϕp = Peak Friction Angle.
ϕb = Basic Friction Angle.
ϕm = Mineralogical Friction Angle Found On Smooth Rock Surfaces.
ϕs = Sliding Friction Angle Found On The Tilting Table.
S = Shear Stress.
S^2 = Variance.
S( ) = Standard Deviation.
θ = Measurement Of Dip.
V = Dilation Rate Due To Shear.
W = Roughness On A Single Discontinuity.
Z = Difference In Roughness Between Discontinuities.

Chapter I

Introduction

1-1 GENERAL

The necessity of finding new sources of raw materials has forced open pit mines to be excavated to depths in excess of 1000 m. Slopes of this height must be designed as steeply as possible, as excess excavation costs may be on the order of 5 to 15 million dollars per degree of slope angle (Brawner,1971). On the other hand oversteepening of a slope may lead to failures which could be dangerous to personnel and which could cost vast sums of money due to production delay and equipment loss. In order to design such deep steep slopes as safely and as economically as possible, the shear strength parameters acting along geologic discontinuities must be known.

The desire to create new structures and transportation corridors in mountainous terrain also necessitates the evaluation of rock slope stability. Under these circumstances, the evaluation of slope stability is critical, as very often slope failures may lead to loss of life; an unacceptable consequence of inadequate slope design.

In the latest state of the art paper on rock slope stability at the recent meeting of the International Society for Rock Mechanics, Hoek and Londe (1974) indicated that the results of tests on small samples of clean mating discontinuities, found in well indurated rock, often overestimate the shear strengths found to be acting in the field.

Krahn (1974) indicated that future research in rock mechanics should be concentrated along the lines of estimating and understanding the field shear strength behaviour of rock slopes. Krahn also indicated that there is still a great need for detailed case histories of slides to confirm or disprove the reliability of analyses based on direct shear tests performed in the lab, and to evaluate the topographic component of roughness acting along discontinuities in the field.

Brawner (1971) also indicated the necessity of case studies:

> "We are desperately in need of case studies and analysis of field failures to test theoretical concepts. Only then will real practical progress be made."

1-2 PURPOSE AND SCOPE

The purpose of this thesis was first and foremost to design and evaluate a simple method of predicting field scale values of roughness in order to predict field scale values of shear strength. The theoretical model for this approach was established by Patton (1966). The measurement of ϕb, the basic frictional component of shear strength, by a simple tilting apparatus was compared and evaluated with more conventional direct shear test methods. The tilt table tests were also compared with direct shear test results reported earlier by Coulson (1972), and other tilt test results by Cawsey and Farrar (1976), Hencher (1976) and Barton and Choubey (1977). It was hoped that the investigation of the slide areas studied would help to fill in the void in case histories pointed out by Brawner (1971).

The thesis investigation was carried out and reported upon in a fashion similar to that expected in a slope stability investigation. A suitable framework for this type of investigation was presented by Hoek and Bray (1974) in the form of a slope stability flow chart(Figure 1-1). The initial parts of this flow chart (steps 1 through 6), which were used in this investigation, were examined in detail and are reported in the thesis in the order presented by Hoek and Bray.

Chapters 2 and 3 summarize the geological conditions found at the sites of the slide areas being investigated. These lie in the Canadian Rocky Mountains at Jonas Creek and at Whitehorse Creek. Chapters 2 and 3 synthesize the geological data obtained from geologic reports, topographic maps, and field work carried out in the vicinity of each slide.

Chapter 4 presents the theoretical basis of the measurement of roughness. The results of the application of this theory to the slide areas studied are compared with previously proposed methods of roughness evaluation.

Chapter 5 summarizes the results of laboratory investigations of shear strength using a conventional direct shear apparatus. In addition a new method of evaluating Øb is presented and evaluated.

Chapter 6 presents the results of back-analyses performed for each slide area investigated. The results of these analyses are then compared with the field estimation of shear strength composed of Øb and the measured field roughness. The dynamics of the slides and a model for slide movement are discussed.

Chapter 7 summarizes the thesis results.

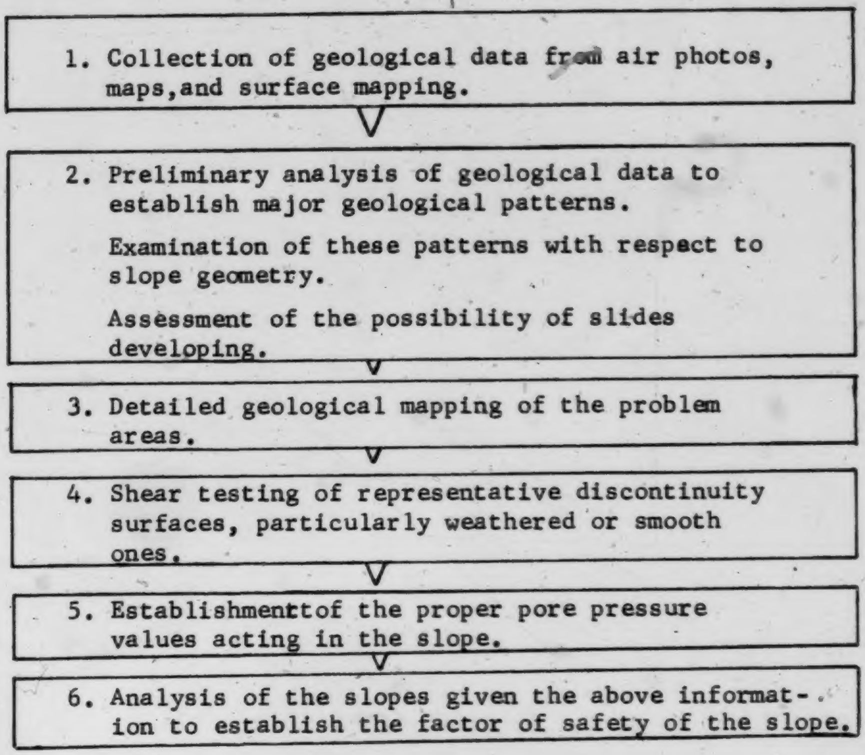

1. Collection of geological data from air photos, maps,and surface mapping.
2. Preliminary analysis of geological data to establish major geological patterns.

   Examination of these patterns with respect to slope geometry.

   Assessment of the possibility of slides developing.
3. Detailed geological mapping of the problem areas.
4. Shear testing of representative discontinuity surfaces, particularly weathered or smooth ones.
5. Establishmenttof the proper pore pressure values acting in the slope.
6. Analysis of the slopes given the above information to establish the factor of safety of the slope.

FIGURE 1-1 Flow Chart Of A Slope Stability Analysis. (Modified After Hoek And Bray,1974).

CHAPTER II

The Geology Of The Jonas Creek Slide Area

2-1 INTRODUCTION

This chapter summarizes the results of geological investigations carried out in and around the failure surfaces of two rock slides on Jonas Ridge in Jasper National Park. The slides are separated by a large mass of unfailed material still in situ on Jonas Ridge. Both slides have been recognized and discussed qualitatively by several authors including Coleman (1911), Hughes (1955), and Baird (1963). Both slides occurred between 1885 and 1893 (Flanagan, 1978 and Coleman, 1911).

Previous workers in areas surrounding the slide have established the regional relationships with respect to the stratigraphy and structural geology. These results were augmented with detailed mapping of the slide area, a prerequisite for this type of investigation. This field work was carried out during the summers of 1976 and 1977.

2-2 LOCATION AND ACCESS

The Jonas Creek study area lies within the Main Ranges of the Rocky Mountains (Price and Mountjoy , 1970). The mountain side underlying the slide area is referred to as Jonas Ridge by Hughes (1955), and is situated on a southern extension of Endless Chain Ridge, on the east side of the Sunwapta River Valley, about 93 km south of the town of Jasper. The coordinates of the slide are 117° 24' W longitude and 52° 26' N latitude. The Sunwapta River occupies the valley floor and also traverses part of the rock slide debris which forms small rapids in some areas. Elevations in the area range from about 1500 m above sea level (ASL) at the river to 3000 m ASL at the top of the ridge behind the slides. Figure 2-1 summarizes the location data and some pertinent geographic details.

Access to the slide area from either Jasper or Banff can be had via highway 93, a two lane hard covered road which traverses the slide debris 60 m above the valley bottom.

2-3 PREVIOUS WORK

Previous exploration in the area surrounding Jonas Creek has been meagre. Hughes (1955) mapped the structure and lithology of the bedrock formations of the Sunwapta and

Southesk map areas (NTS No's 83C/6, 83C/11). The Jonas Creek rock slides lie near the central portion of this region. Other work has been done in the areas adjacent to Jonas Creek. Pertinent areas are shown on Figure 2-1.

Mountjoy and Aitken (1963) investigated the early Cambrian and late Precambrian paleocurrents in Banff and Jasper Parks.

Charlesworth et.al. (1967) studied the structures and provenance of the Precambrian Formations of the region around Jasper townsite. Although both of these reports deal with areas somewhat removed from Jonas Creek, the dominant NW-SE linear trends found in the Rockies and the great lateral extent of the original depositional environment (North, 1966) make it possible to correlate similar lithologies over great distances. The rock types studied by Mountjoy and Aitken, or the sedimentary depositional environments investigated by Charlesworth et. al. in their respective areas, are similar to those found at Jonas Creek.

Price and Mountjoy (1970), as part of a Geological Survey of Canada project named Operation Bow-Athabasca, synthesized the gross geologic structures found in the eastern Rocky Mountains between the Bow and the Athabasca Rivers. This investigation was conducted as part of a reconnaissance survey on a scale of 1 cm = 8.4 km, but nevertheless contributes valuable information with respect to the structural geology near Jonas Creek.

Road logs are available for the Jasper to Banff highway from the 24th International Congress of Geology held in Montreal (1972) . None of the logs are very detailed however and can only be used as general guides. Guide books covering the area were presented by Stott and Taylor (1972) and Wheeler et. al. (1972).

Cook (1975) mapped an area of the Banff- Jasper highway south of the North Saskatchewan River crossing to Lake Louise. This area which exhibits stratigraphic and structural domains similar to those at Jonas Creek is also marked on Figure 2-1.

In 1975 , Bayrock and Reimchen mapped the surficial geology of Banff and Jasper Parks. Reconnaisance maps on a scale of 1:50,000 were produced which fitted as overlays onto standard NTS topographic maps.

2-4 SURFICIAL GEOLOGY

The surficial geology in the Jonas Creek area was first mapped by Hughes (1955). Details are vague, however, and no surficial maps were presented. Hughes reported (page 108) that there was little evidence in the form of striations, glacial grooving or moraines to support the fact that the Sunwapta Valley had been glaciated even though the valley does have a broad U shape (Figure 2-2). Hughes did note (page 113) that colluvium covered a large portion of the study area mostly in the form of talus cones and rock slide debris.

Hughes (page 113) was one of the first to document the rockslides being studied here. Hughes (1955) states,

> "A rockslide crosses the Banff-Jasper highway at mile 47.5. At this locality quartzite beds of the Jonas Creek Formation broke away from Jonas Ridge and slid westward with enough momentum to carry them across Sunwapta River."

Baird (1963) also recognized the presence of the Jonas Creek slides and hypothesized on the basis of the age of the trees present, that it took place at least 70 to 80 years ago.

More recent surficial reconnaissance mapping of Jasper Park was performed by Bayrock and Reimchen (1976) from air photos. A small part of their final map series surrounding the Jonas Creek slide is shown in Figure 2-3. An outline of the rock slide scarps and the slide debris has been added to the map however, as the rock slides were not shown on the original map. The two steep, near vertical back scarps exposed on the ridge above the highway, the nearly planar well exposed failure surface on one slide, the irregular but steep side scarps or flanks, and the accumulation of highly disorganized broken rock fragments in the valley bottom, fit into the general description of a rock slide outlined by Ritchie (1958, p.56-57) and leave little doubt that the study area does indeed encompass two rock slides.

Bayrock and Reimchen's map illustrates that the floor of the Sunwapta Valley, other than the alluvial deposits found within the river banks, consists of bouldery rolling moraine from 2 m to 12 m deep. This fact in conjunction with the U shaped valley and the proximity to present day glaciers establishes beyond reasonable doubt that the valley was glaciated.

Rubbly colluvial aprons, varying in thickness from 0.0 m to 2.0 m deep blanket the bedrock on the lower half of the valley walls. Bare rock makes up the upper portions of the exposed ridges.

The surficial geology of the slide debris was mapped in detail. The debris on the lower part of the slope consisted of all sizes of particles, from sand grains up to large flat blocks 3 m square and up to 1 m thick. One very large block of debris, 20 m wide and 30 m long was found on the upper slope very close to the exposed failure surfaces. This block was still relatively intact and so had probably not travelled very far with respect to the rest of the debris which had been broken up in transit. All of the debris blocks were identified as the Gog Group quartzites. There was no evidence of any other material type in the debris.

Debris from the north slide travelled over 1 km vertically and 4 km horizontally, measured from the top of the scarp to the toe of the debris. Debris from the north slide crossed the Sunwapta River to the opposite side of the valley. The debris from the south slide, which constitutes a larger mass, has also travelled 1 km vertically but only 3 km horizontally. The volumes of slid mass were 2.1×10^6 cubic meters for the north slide and 4.5x10^6 cubic meters for the south slide. The volume of the unfailed mass separating the two failures is approximately 2.1x10^6 cubic meters. Table 2-1 summarizes the physical dimensions of the slide debris.

Debris thickness from both slides was mapped by traversing the debris in a grid pattern and estimating the depth of rock at each point of the grid. The estimates of thickness in meters are shown on the air photo in Figure 2-4. The estimated thickness of debris varies from 1 m to 10 m and averages about 3 m thick. The debris outlines for both slides are shown in detail on Plate 2-1. The air photos shown are Government of Alberta photos numbers 2107-5210x No.s 132-133. They have a scale of 1:33,333.

Examination of an air photo stereo pair of the slides reveals a pattern of ridges and troughs in the debris (Plate 2-2). Cruden (1974) points out that these are normal occurrences in rock slides where debris flow has been impeded by pronounced topographic barriers. The crests of the ridges are shown on the air photos by a dashed line. The wavelike pattern which has an amplitude varying from 3 m to 6.5 m is superimposed on the much larger scale valley topography. The ridges in the debris may have been formed by several small slides occurring in sequence, with the leading edges of each slide running into the trailing edges of the older slide in front causing a bulge in the topography. However, they may also be due to one large slide exhibiting an internal wavy pattern. The largest bulge, denoted by number 1 on Plate 2-2, coincides with a major break in slope that occurs between the steep dip slope of the valley wall and the flatter valley floor and may result from the slowing down of the rock mass due to the slope change.

A pattern of ridges is also seen on the valley floor to the northwest and southeast of the slide debris. These ridges are caused by differential erosion along bedding planes. The bedrock ridges are much closer spaced and have much less topographic expression than the ridges in the debris, especially near the slide margins. In addition the curved debris ridges do not follow the trend of the relatively straight bedrock ridges, and so it would appear that the ridges found in the debris are not associated with the bedrock ridges found on the valley floor.

The outer margins of the debris are very sharp as there has been very little scatter of the individual blocks. A margin no wider than 1 m can be traced along both sides of the debris separating the failed debris blocks from the undisturbed moraine on the valley floor. In places near the north margin of the north slide, the debris is only one block thick. This contrasts greatly with the leading margin of the south slide which varies from 3 m to 10 m high, reclines at an angle close to 40°, and is slightly curved in plan (Plate 2-1). Both debris outlines are lobate and tongue shaped, a pattern often associated with rock slides (Cruden, 1974).

2-5 Stratigraphy

The rock found on the southern extension of Endless Chain Ridge in the vicinity of the slides, belongs to the Lower Cambrian Gog Group. This sequence of rock, deposited 550-570 million years before present (MYBP), consists of massive clean quartz sandstones and quartzites with thin shale lens interbeds (Cook, 1975).

Field mapping carried out during 1976 and 1977 indicated the quartzite beds at Jonas Creek vary in thickness from 0.10 m to at least 1.0 m. The quartzite is primarily honey coloured with minor inclusions of hematite or limonite which gives the rock a pink hue upon weathering. Hughes (1955) reported the presence of thin blue-green shale lenses in the vicinity of Jonas Creek. A small discontinuous lens of this shale was found during field exploration near the middle of the north slide failure plane at Jonas Creek. This lens, however, was less than 3 m long and varied from 0 to 6 cm in thickness. There was no other evidence of shale either on the slope surface or in the debris.

Cross-bedding structures have been reported in the Gog quartzites by Mountjoy and Aitken (1963) and Cook (1975). Cross-bedding at Jonas Creek, found during field work, existed on all scales.

Plate 2-3 is a photograph of large scale cross-bedding observed on the slope at Jonas Creek. The cross-bedding dip at Jonas Creek was parallel to the rock slide failure direction and thus may have contributed significantly to the down dip roughness angle acting on the failure surface. Further discussions with respect to the variations in roughness are detailed in Chapter 4.

The Gog Group as a whole, according to Stott and Taylor (1972) varies in thickness from 600-2200 m in the Southern Rocky Mountains. North (1966) suggested that the average thickness is close to 600 m. Hughes (1955) stated that the Gog Group was approximately 1500 m in the vicinity of Jonas Creek. This number agrees very closely with the thickness estimated from the structural geology map reproduced from Price and Mountjoy (1970) in Figure 2-4. The Gog Group exhibits great lateral persistence as well as depth and can be traced along strike for 130 km in the vicinity of Endless Chain Ridge (Figure 2-4).

The base of the Gog is defined by a disconformity separating the clean pinkish-white arenaceous Gog Group from the green argillaceous metasediments of the Precambrian Windermere Group (North, 1966). The top of the Gog Group is defined by a thin layer of limestone often referred to as the Peyto Member of the Mount Whyte Formation (Cook, 1975). Neither the Windermere nor the Mount Whyte Formations are included in the rock slides. Figure 2-5 is a stratigraphic summary of the formations in the vicinity of Jonas Creek. The slides occurred in the upper third of the Gog Group according to Hughes map (1955).

2-6 STRUCTURAL GEOLOGY

The structures of the East Main Ranges of the Rocky Mountains are dominated by thrust faults which dip to the southwest, curve gently concavely upward and flatten out with depth. Thrusts generally follow the sedimentary layering of the rock or cut up steeply through the more competent layers. The thrust plates are generally thick and flat but may in some areas be very gently folded (Price and Mountjoy, 1970). Figure 2-4 illustrates a section expanded from Price and Mountjoy showing this type of gross structure in the vicinity of Endless Chain Ridge and Jonas Ridge.

Previous work by Hughes (1955), indicated that the quartzite constituting Endless Chain Ridge and Jonas Ridge had been thrust into position as a single block which had not sustained any appreciable internal deformation. Figure 2-6 illustrates the results of detailed mapping in the area of Jonas Creek.

In order to supplement the information derived from Hughes and others, detailed mapping was undertaken over the slide areas on Jonas Ridge. The failure planes of the two well defined slides were separated by a large mass of rock which has remained stable. The unfailed mass outlined on Plate 2-1 is of the same order of magnitude in volume as the masses involved in the two neighbouring slides(Table 2-1). The presence of this mass between the two slides appears anomalous as there are no apparent changes of lithology or structure which would have caused a change in slope stability.

The failure surface of the north slide consists of a series of parallel bedding surfaces which stepped up through the stratigraphic section as the failure surface increases in elevation. Figure 2-7 is a stereonet illustrating the average bedding orientations. Near vertical joints striking parallel to the bedding strike, but not perpendicular to the bedding dip, constitutes the front face of each step. Plate 2-3 illustrates one of these steps. A structural geology map of the failure surfaces showing station locations and bedding and joint orientations is shown in Figure 2-8.

The scarp of the South Slide and the lateral margins of both slides are well defined by steep joints continuous over several meters. Approximately 100 joint orientations were measured over the mapped area. The results of this mapping, illustrated on structural diagrams in Figure 2-9 indicates that the joints belong to two orthogonal joint sets with strikes close to 40° and 135° . The dips range from 60° to the northeast to 70° to the southwest for the northwest-southeast striking joints. The joint set striking northeast-southwest had dips varying from 85° northwest through 90° to 85° southeast. The strikes of these joint sets coincide very closely with the strikes of System 1 joint sets defined by Babcock (1974) in Central Alberta.

Babcock hypothesized that these joints were formed by horizontal stresses imposed by the Laramide Orogeny. However the joints defined by Babcock were perpendicular to the flat lying bedding of the prairies. The joints found at Jonas Creek were not perpendicular to bedding. As a result,although superposition of the System 1 joint set strike implies that the Jonas Creek joints are similar in tectonic origin to the System 1 sets, the fact that the beds are not perpendicular to bedding implies that the joints at Jonas Creek due to the influence of a local stress regime, may not completely reflect the same regional stresses found by Babcock.

Currie and Reik (1977) while studying the joint pattern around a fold in the Rocky Mountain Foothills found that one steeply dipping fold limb had joint sets which departed from being normal to bedding by 20° to 50°. They concluded from their studies that the existence of this joint set orientation is a normal accompaniment to the advanced stages of deformation in fold limbs. They also reported that this phenomenon has been recorded by Stearns (1967) and Friedman and Stearns (1971) in less deformed bedding with dips of less than 30°. It would appear then that one possible cause of the joint sets at Jonas Creek are the result of the combination of stresses imposed by the Laramide Orogeny with variations in dip orientations imposed by the formation of local folds. Joints may also arise from the effects of glacial action, erosion and seismicity.

The joint spacing at Jonas Creek varied from several centimeters to several meters and was responsible for controlling the dimensions of the debris blocks. The mean joint spacing recorded was 0.65 m. Plate 2-4 illustrates the variations in joint spacing which are found over very short distances.

Contrary to Hughes findings (1955) the block of quartzite which constitutes Jonas Ridge has been folded. A fold with a radius of curvature of 2.4 km is present near the upper half of the ridge. The presence of the fold was discovered by the use of a dip isogon map. The average dips of all the bedding surfaces recorded were plotted on a map of the slide area and three distinct 5° bands were defined. The map in figure 2-8 ilustrates how the bedding dip increases from a minimum dip of 28° near the bottom of the exposed failure surface to a maximum recorded dip of 39° near the scarp. The location of this gentle fold explained why the failure surface has daylighted so high up the dip slope of the valley wall.

Reconnaissance mapping of Jonas Ridge south of the rock slide revealed a similar trend in bedding orientations near the top of the slope. This trend was not reported by Hughes (1955).

The fold was apparently formed by the buckling of individual layers which slipped past each other. This often leads to the formation of slickenslides and lineations. However, only one small polished and slickensided area, about 10 m square, was present on one part of a bedding plane on the north failure surface (Figure 2-8) The striae on the polished block had an average trend of 224° and plunge of 28° (Figure 2-7) .The lineation trends were parallel to the bedding dip direction and were both parallel and perpendicular to the strikes of the previously defined joint sets. One other larger area of slickensides (20 m x 30 m) was found in the debris below the failure plane. This block however was not in situ and so orientations were of little use.

A stereonet illustrating the interrelationships of the structural elements is shown in Figure 2-7. The combination of the fold striae parallel to dip, the orthogonal joint sets striking parallel and perpendicular to the dip direction and the approximate fold axis perpendicular to dip direction, indicates that this surface underwent deformation due to flexural slip folding (Ramsay, 1967) .

The influence of the flexural slip surface is probably not large as only small areas of slickensides were found. The weathering resistance of quartzite coupled with the fact that the slide is 89 ± 4 years old (Section 2-1), implies that weathering would not have removed exposed areas of slickensides. It would appear that little deformation occurred between layers and so the flexural slip surface influence on slope stability is minimal. The amount of flexural slip is a function of the curvature of the folds which in this case was very small. This again implies that the area of the failure surface which underwent flexural slip was probably small.

If slickensides had been present prior to failure, but had been removed by crushing during failure, then the presence of slickensides is irrelevant. However, the compressive strength of this rock, coupled with the known normal loads applied along this failure surface, make this possibility unlikely. Only if sliding occurred along the smooth slickensided surface without causing surface damage would the presence of slickensides influence slope stability. This possibility is further discussed in Chapter 7 when dealing with the back analysis.

In addition to the large scale fold found by dip isogon mapping, a series of small amplitude folds with axes at right angles to the large fold axis were found on the north slide failure surface. These symmetrical folds have wavelengths of approximately 200 feet, interlimb angles of 176° to 178° and amplitudes ranging from 0.5 m to 1.0 m. The folds were discovered using a new technique evaluated by Ramsden (1977) . This technique is outlined in Appendix A-1. The folds are perpendicular to the overall bedding strike and hence did not alter the down dip roughnesses on the failure surface. As a result these folds played no part in the overall slope stability. Their presence implies that the regional stress distribution, inferred from the joint orientation and the orientation of the folded failure surface, was more complicated than originally surmised.

The flexural slip fold has occurred within a fault block that has been bodily tilted to an average inclination of 30-35°. Two major thrust faults mapped by Hughes (1955) and Price and Mountjoy (1970) running parallel to bedding on both sides of Endless Chain Ridge and Jonas Ridge, are primarily responsible for this configuration. The faults are outlined on Figure 2-4. The courses of the Sunwapta River and Poboktan Creek appear to be structurally controlled by these faults. The gap between Endless Chain Ridge and the southern extension upon which the slides are located, may be the reflection of a tear fault associated with these two major thrusts. This gap forms the north margin of the north rock slide. No other structural control of the rock slide by large scale faulting was observed. It would therefore appear that no slippage took place within the fault block other than that associated with the flexural slip deformation. It is quite possible therefore to have bedding surfaces, along which there has been no significant previous movement, tilted into position along deep thrust faults. The representative friction values within these beds should be equivalent to peak friction angles.

The site of the two major rock slides being studied is the only area along the Endless Chain Ridge or its' continuation, where a major rock slide has taken place. Coincidentally, this area is the only area along the ridge where the bedding dips directly into the valley and bedding strike is parallel to the valley wall. In all other locations the strike of the valley wall, taken from NTS map 83C/6, is rotated 20° away from the bedding strike (Figure

2-6). The strike of the ridge in the vicinity of the slide is 135°. The strike of the ridge to the northwest and southeast of the slide area is 115°. The average bedding strike at Jonas Creek is 135°. The bedding strikes recorded by Hughes (1955) along Endless Chain Ridge to the north and Jonas Ridge to the south also have an average strike of approximately 135°. This has two effects. The difference of 20° between the bedding and the trend of the valley wall is enough to lower the apparent dip of the bedding into the valley by about 2-3° (Figure 2-10). On a marginally stable slope this decrease in the dip of the potential failure surface can be important. More significantly however,, due to the non-parallelism of the valley with the bedding directions, no single bedding surface daylights near the bottom of the valley. As a result any blocks which do become mobile and try to move down dip run into other bedding planes which are not daylighted and which therefore cannot fail. As a result only minor failures of single loose blocks can occur. This allows talus cones to build up at the base of the slopes but does not allow major failures to occur.

2-7 SUMMARY

The two rock slides at Jonas Creek occurred within 0.18 km of each other between 85 and 93 years ago. The slides are separated by an unfailed part of Jonas Ridge approximately equal in volume to each of the failed masses.

Failure has occurred along several gently curved bedding surfaces discontinuities all of which are contained within the Lower Cambrian Gog Group Quartzites. The bedding discontinuities have dips which vary from 28° to 39° and which have an average strike of 135°. The failure did not occur along tectonically produced structures such as flexural slip surfaces or faults. The failure surface of the north slide stepped up through the bedding as elevation increased. The south slide failure surface was obscured by debris. Near vertical joints, which are parallel and perpendicular to strike form the lateral scarps of both slides and the back scarp of the south slide.

Failure has apparently occurred at this location due to the spatial coincidence of the bedding surfaces and the trend of the valley wall. Elsewhere along the ridge, the valley wall deviates from the bedding strike by approximately 20° and has thus decreased the potential for a large slide.

TABLE 2-1

Physical dimensions of the Jonas Creek Slides And Failure Surfaces.

slide	width	length	vertical travel	horizontal travel	volume
north	0.37km	0.37km	0.88km	3.25km	2.1 x 10^6m^3
south	0.37km	0.61km	0.92km	2.50km	4.5 x 10^6m^3
unfailed mass	0.18km	0.61km	-------	-----	2.1 x 10^6m^3

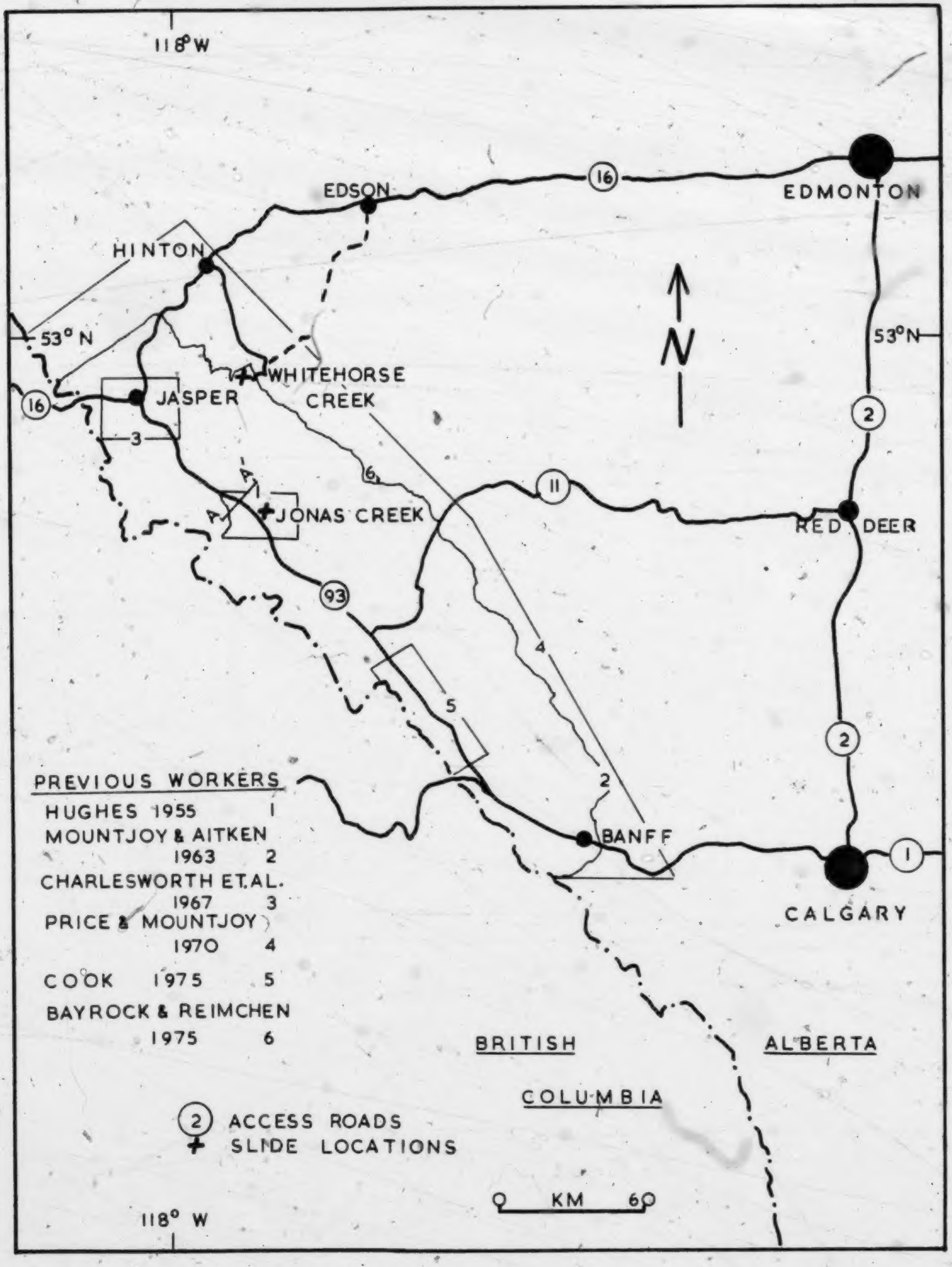
118°W
EDMONTON
EDSON
HINTON
16
53° N
53°N
WHITEHORSE CREEK
JASPER
3
2
6
11
JONAS CREEK
RED DEER
93
4
5
2
BANFF
1
CALGARY
N
PREVIOUS WORKERS
HUGHES 1955 1
MOUNTJOY & AITKEN 1963 2
CHARLESWORTH ET.AL. 1967 3
PRICE & MOUNTJOY 1970 4
COOK 1975 5
BAYROCK & REIMCHEN 1975 6
BRITISH COLUMBIA
ALBERTA
② ACCESS ROADS
+ SLIDE LOCATIONS
0 KM 60
118° W

FIGURE 2-1 Location Map Of Jonas Creek.

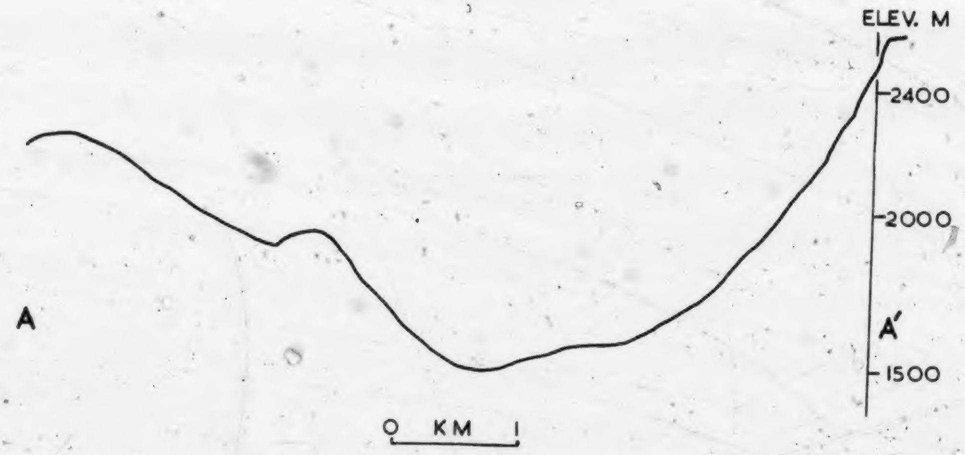
ELEV. M
2400
2000
1500
A
A'
0 KM 1

FIGURE 2-2 Section Near Jonas Creek Illustrating U Valley (Section Line On Figure 2-1).

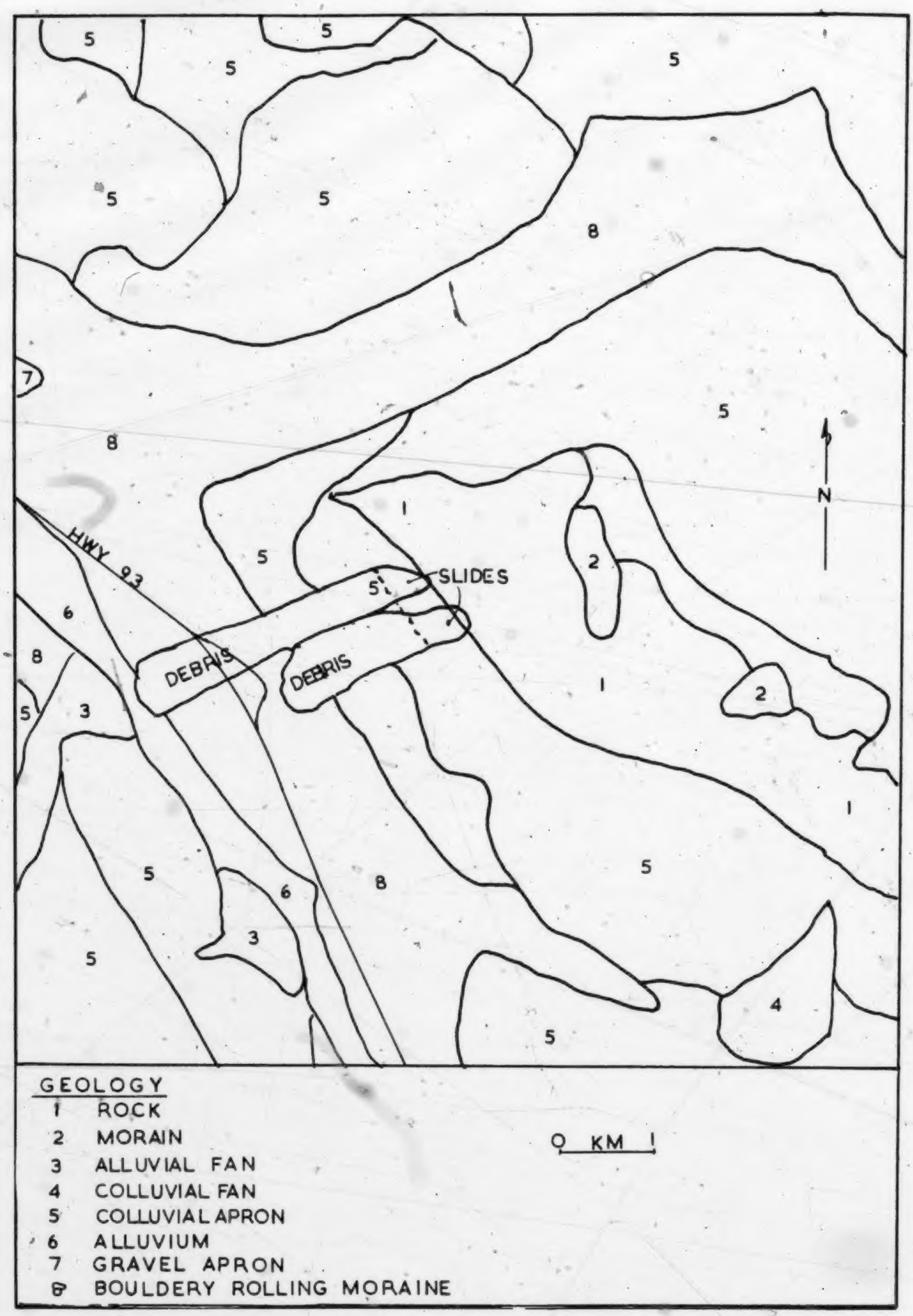
5
5
5
5
5
5
8
7
8
5
N
1
5
HWY 93
SLIDES
5
2
6
8
DEBRIS
DEBRIS
1
2
5
3
1
5
6
8
3
5
5
4
5
GEOLOGY
1 ROCK
2 MORAIN
3 ALLUVIAL FAN
4 COLLUVIAL FAN
5 COLLUVIAL APRON
6 ALLUVIUM
7 GRAVEL APRON
8 BOULDERY ROLLING MORAINE
0 KM 1

FIGURE 2-3 Simplified Surficial Geology Map Of Jonas Creek (Modified After Bayrock and Reimchen, 1975).

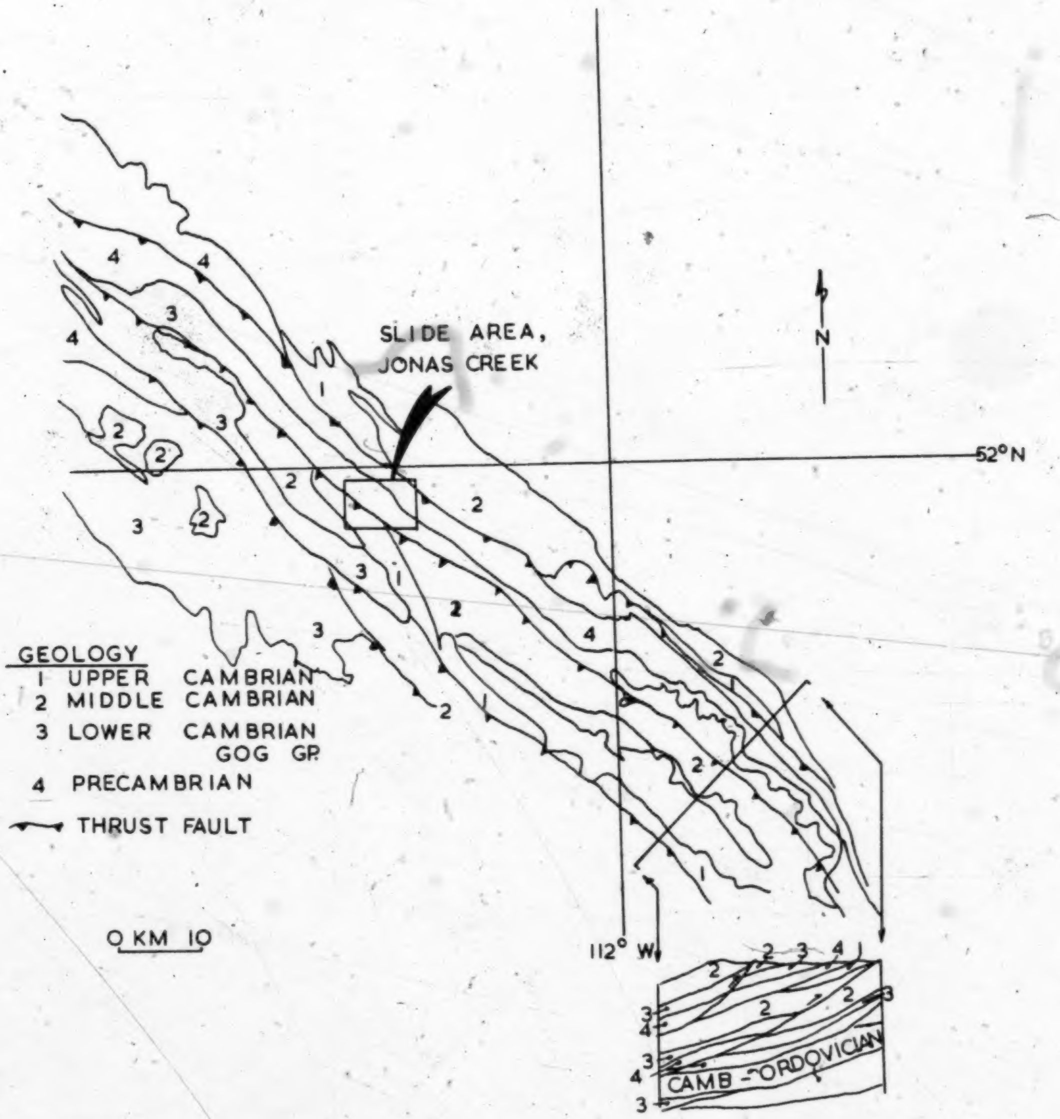
SLIDE AREA, JONAS CREEK
N
52°N
112° W
GEOLOGY
1 UPPER CAMBRIAN
2 MIDDLE CAMBRIAN
3 LOWER CAMBRIAN GOG GP.
4 PRECAMBRIAN
THRUST FAULT
0 KM 10
CAMB - ORDOVICIAN
1
2
3
4

FIGURE 2-4 Structural Geology Map Of Part Of The Main Ranges.
(Modified After Price And Mountjoy, 1970).

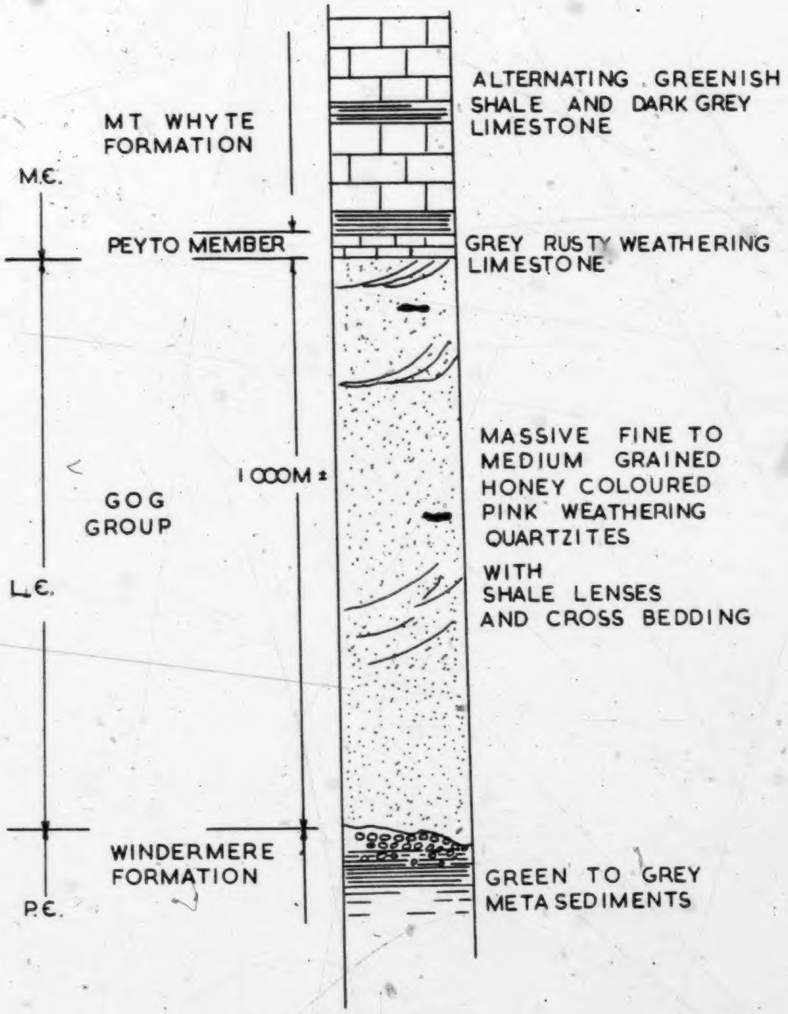
MT WHYTE
FORMATION
ALTERNATING GREENISH
SHALE AND DARK GREY
LIMESTONE
M.Є.
PEYTO MEMBER
GREY RUSTY WEATHERING
LIMESTONE
1000M±
GOG
GROUP
MASSIVE FINE TO
MEDIUM GRAINED
HONEY COLOURED
PINK WEATHERING
QUARTZITES
WITH
SHALE LENSES
AND CROSS BEDDING
L.Є.
WINDERMERE
FORMATION
GREEN TO GREY
METASEDIMENTS
P.Є.

FIGURE 2-5 Jonas Creek Stratigraphic Column(Modified After Cook,1975 And Hughes,1955).

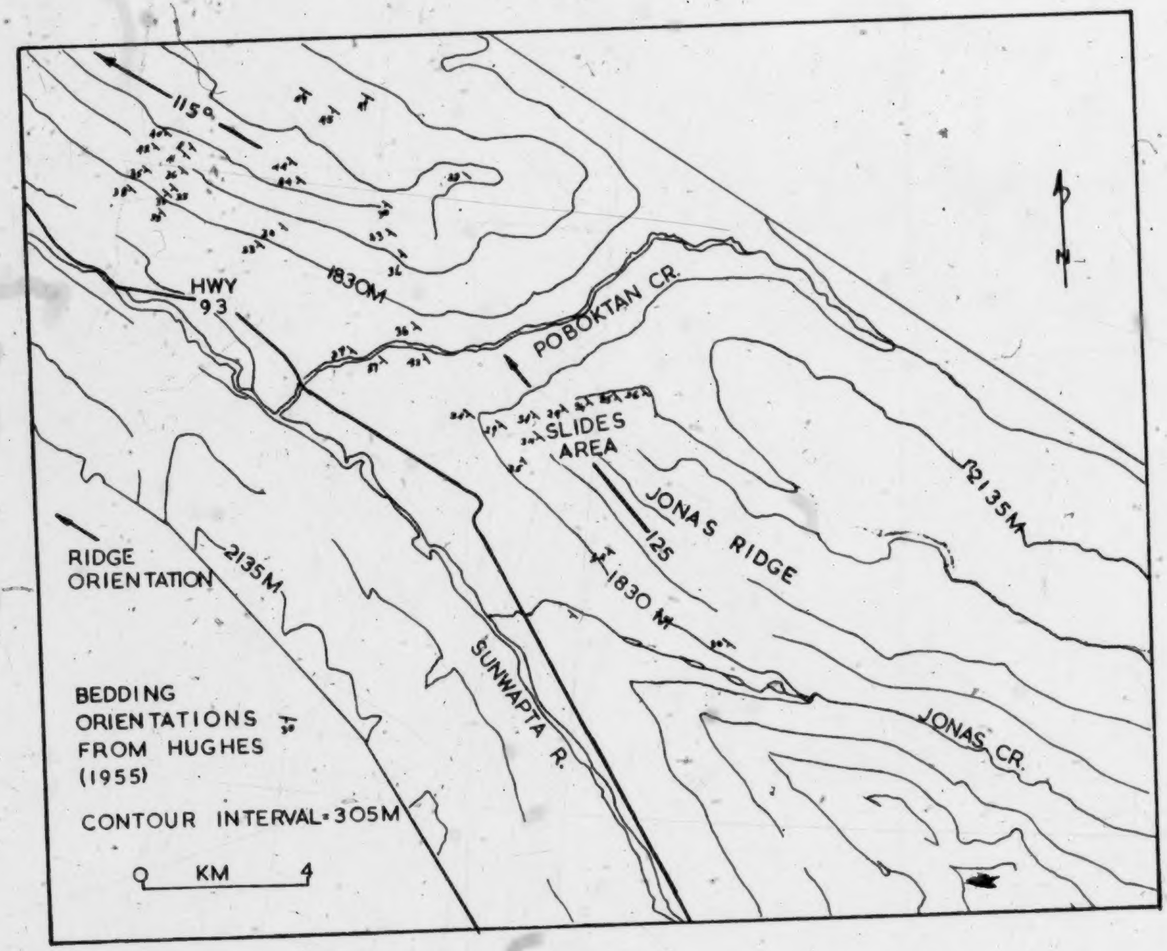
115°
HWY 93
1830M
POBOKTAN CR.
SLIDES AREA
JONAS RIDGE
125
1830 M
2135M
JONAS CR.
SUNWAPTA R.
2135M
N
RIDGE ORIENTATION
BEDDING ORIENTATIONS FROM HUGHES (1955)
CONTOUR INTERVAL=305M
0 KM 4

FIGURE 2-6 Map Of Jonas Creek Area Showing Data From Hughes (Modified After Hughes, 1955).

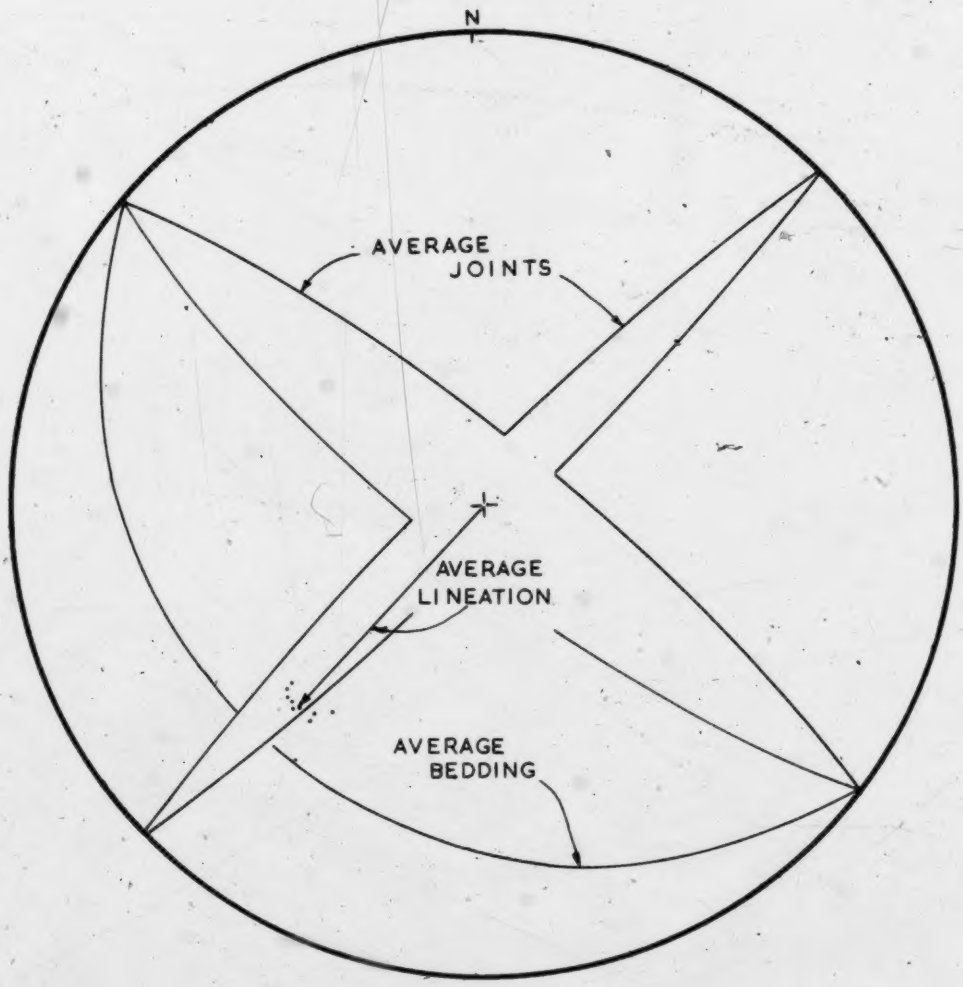
N
AVERAGE JOINTS
AVERAGE LINEATION
AVERAGE BEDDING

FIGURE 2-7 Average Lineation Found On The Slickensided Surfaces Shown Relative To Average Joints And Bedding.

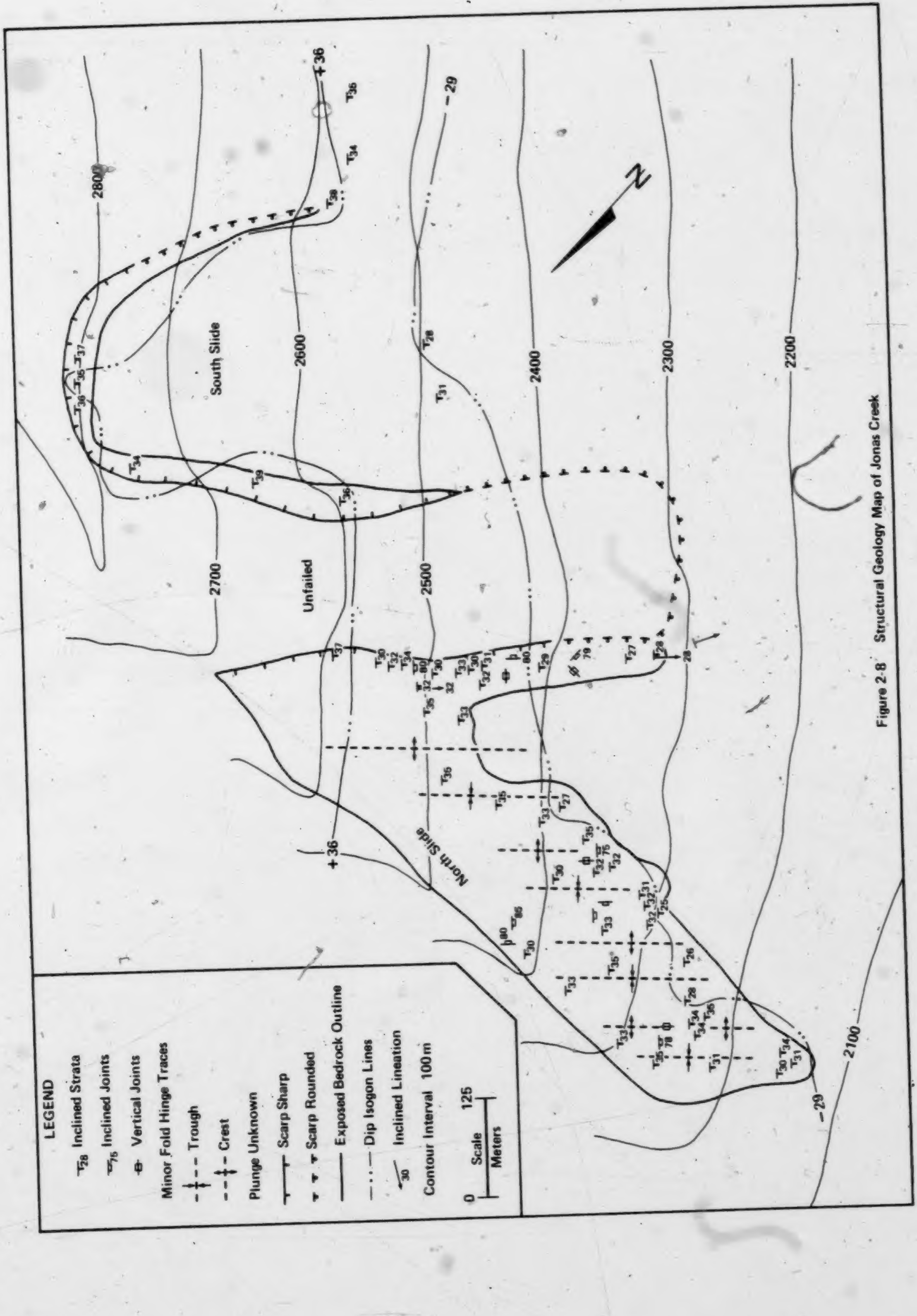
LEGEND
Inclined Strata
Inclined Joints
Vertical Joints
Minor Fold Hinge Traces
Trough
Crest
Plunge Unknown
Scarp Sharp
Scarp Rounded
Exposed Bedrock Outline
Dip Isogon Lines
Inclined Lineation
Contour Interval 100 m
Scale
Meters
0
125
N
South Slide
Unfailed
North Slide
2800
2700
2600
2500
2400
2300
2200
2100
+36
-29

Figure 2-8 Structural Geology Map of Jonas Creek

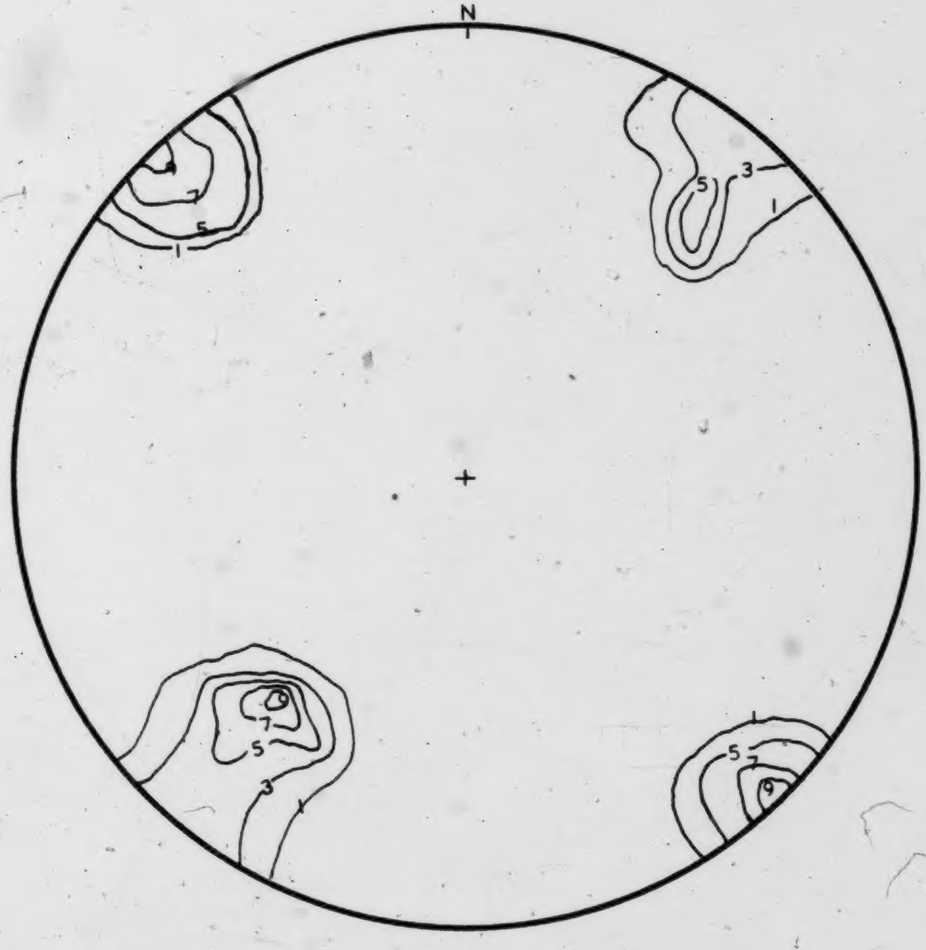
N
9
7
5
1
5
3
1
9
7
5
3
1
1
5
7
9

FIGURE 2-9 Poles To The Joints Found At Jonas Creek.

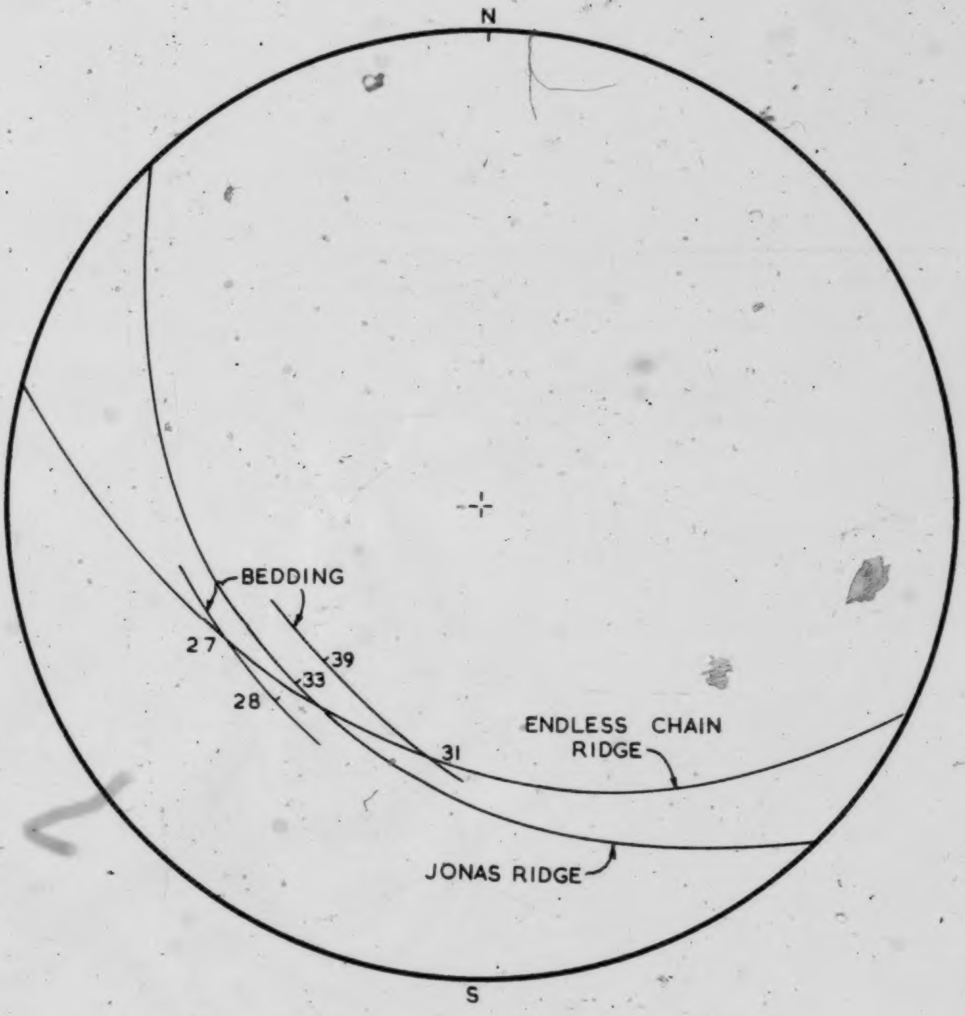
N
BEDDING
27
39
33
28
31
ENDLESS CHAIN RIDGE
JONAS RIDGE
S

FIGURE 2-10 Stereonet Analysis Illustrating How Endless Chain Ridge Is Stabilized .

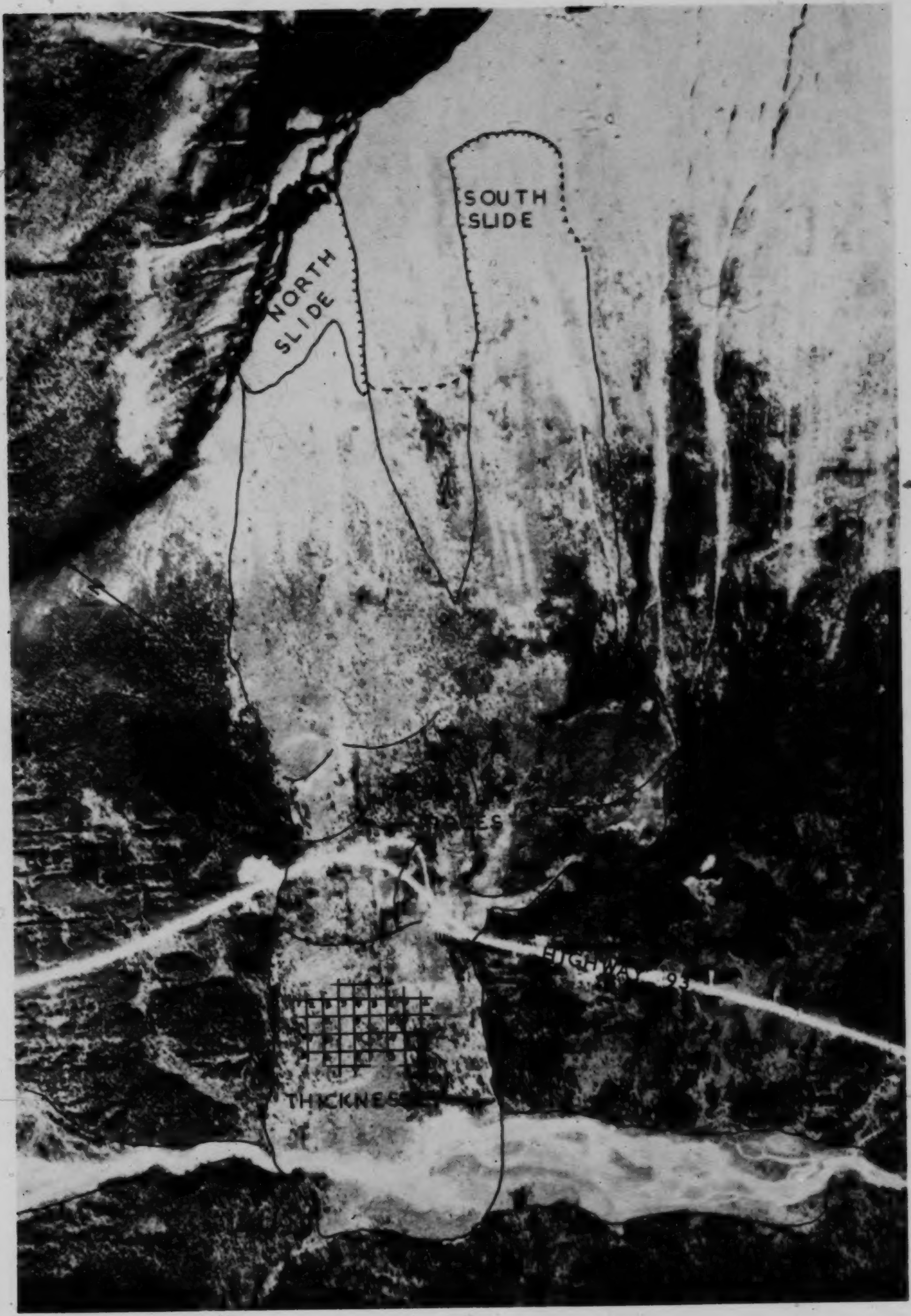
SOUTH SLIDE
NORTH SLIDE
HIGHWAY 93
THICKNESS

PLATE 2-1 Air Photo Of The Jonas Creek Slide Area Showing Debris Outlines And Thicknesses.

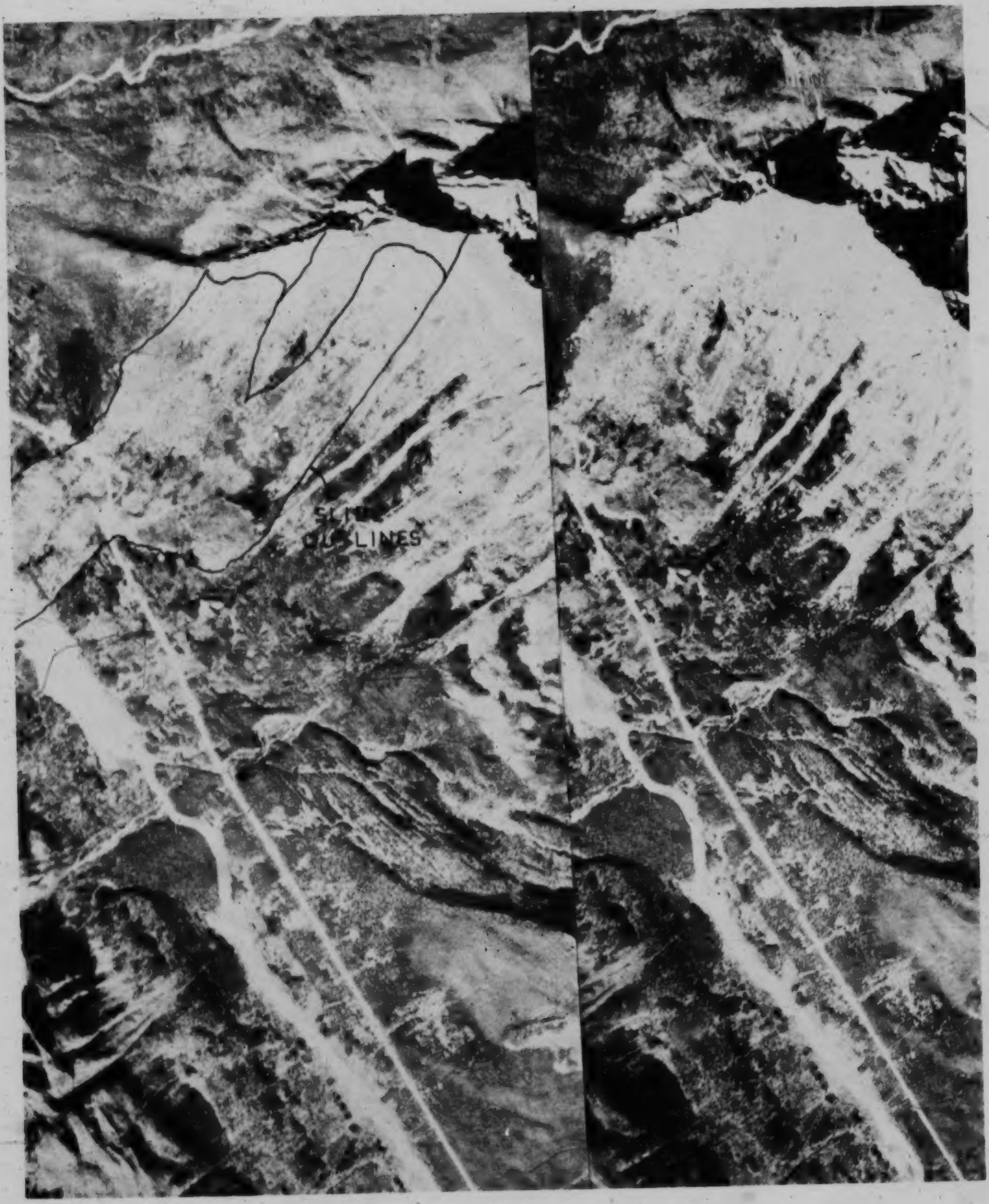
SLIDE
OUTLINES

PLATE 2-2 Air Photo Pair Showing Jonas Creek Slide Areas With Wavelike Surface Of The Debris.

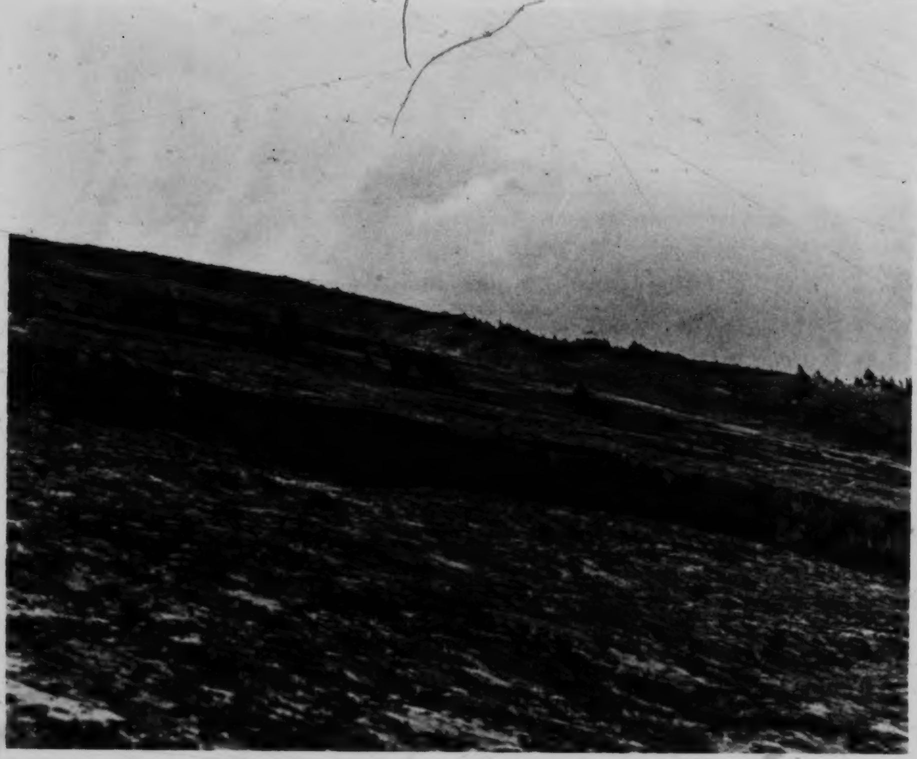

PLATE 2-3 Photograph Of The Failure Surface At Jonas Creek Showing Large Scale Cross Bedding.

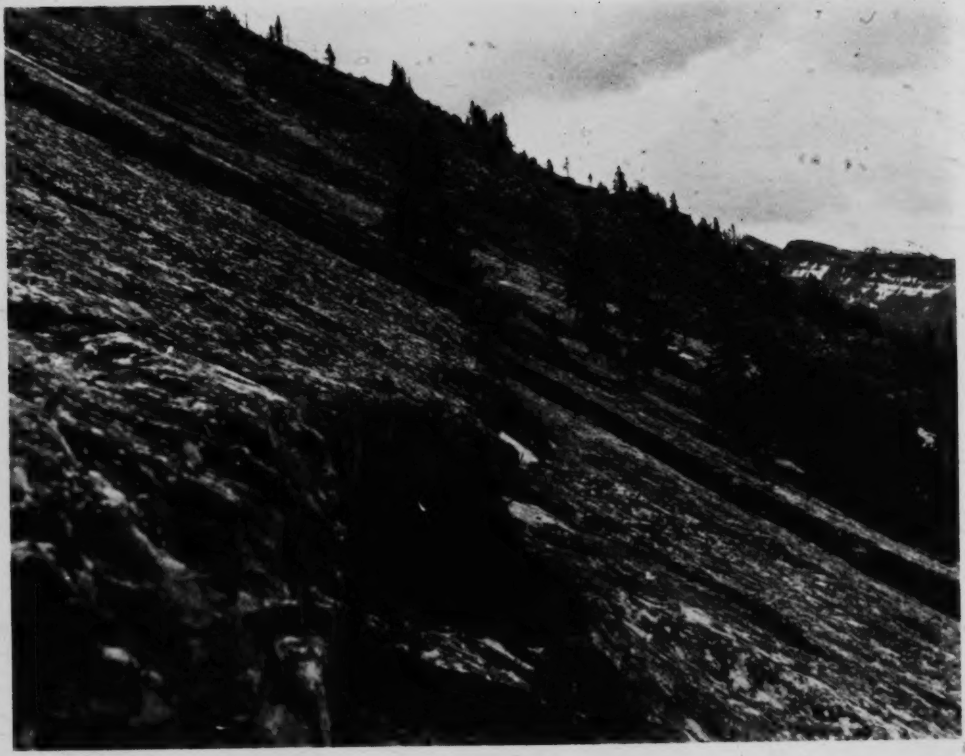

PLATE 2-4 Photograph Of The North Failure Plane Showing The Vertical Joints Which Occurred Between Beds.

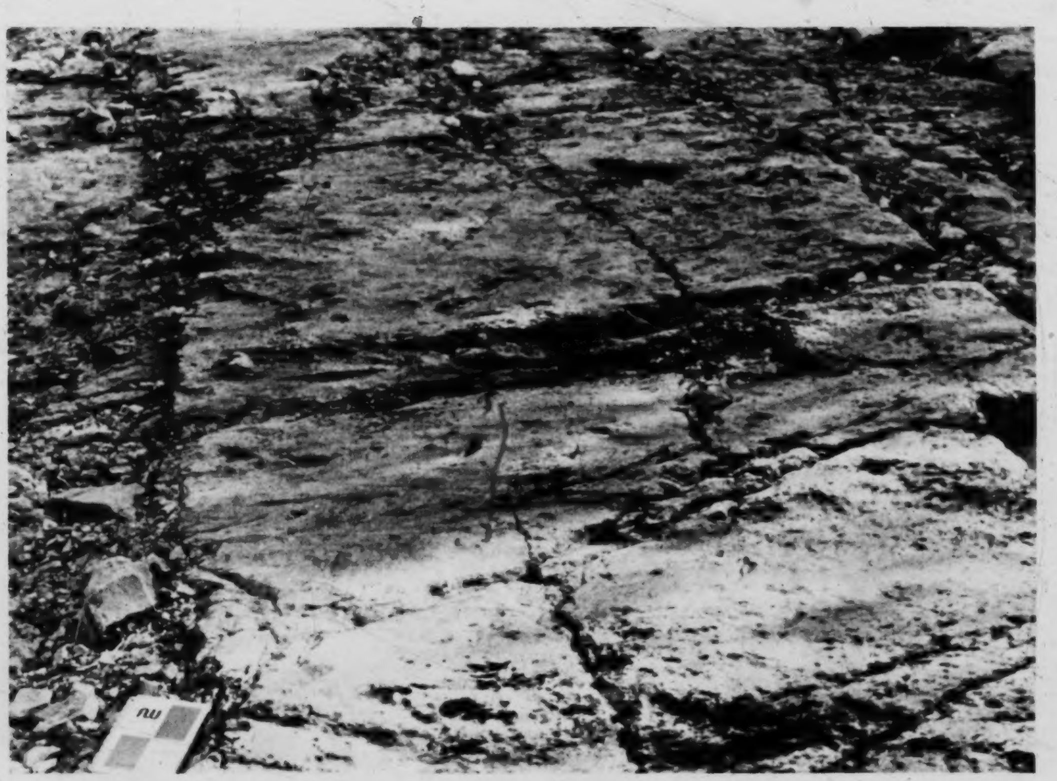

PLATE 2-5 Photograph Showing Variation In Joint Spacing On The North Slide.

CHAPTER III

The Geology Of The
Whitehorse Creek Slide Area

3-1 INTRODUCTION

Chapter 3 summarizes the geologic investigations carried out on a rock slide and a rock slide scar at Whitehorse Creek. These two rock slides have occurred beside each other in the Rocky Mountain Foothills near the town of Cadomin. Both slides are prehistoric in age.

The older of the two slides no longer has any debris left on the valley bottom. However, the presence of a steep back scarp and south lateral scarp along with a well exposed failure surface leave little doubt that a slide had occurred here. The absence of debris, possibly removed by glaciers or flowing water, indicates the great age of the slide. Long periods of weathering may have altered the surface roughness along the failure plane and hence the roughness originally acting at the time of failure. For these reasons the failure surface was not examined in detail.

The younger slide surface seemed relatively fresh. The debris overlies the till which indicates that the slide is post glacial in age. As a result, most of the mapping was concentrated on and around the younger slide exposure.

The stratigraphy at Whitehorse Creek has been well defined by previous authors but very little work has been done with respect to the structural and surficial geology of the area. As a result, detailed mapping of the younger of the two slides was conducted during the summers of 1976 and 1977 to supplement the available published information of the area and to allow evaluations of slope stability.

3-2 LOCATION AND ACCESS

The Whitehorse Creek rock slides are situated on the eastern flanks of the Rocky Mountain Foothills about 5 km south of the town of Cadomin. The coordinates of the rock slide are 117° 23' W longitude and 53° 00' N latitude (Figure 3-1). The slides have occurred on a southwest facing valley wall above an unnamed creek which enters Whitehorse Creek, a tributary of the McLeod River. Elevations in the vicinity of the slides vary from approximately 1800 m ASL near the toe of the existing slide debris to 2300 m ASL near the west of the ridge behind the younger slide.

The slide area can be reached by car from the town of Edson, Alberta via Highway 47, a secondary gravel road which leads to Cadomin. Access can also be gained by Highway 40, a partially paved two lane access road which goes from the town of Hinton, straight south to Cadomin. A forestry road continues south of Cadomin over the bridge at Whitehorse Creek. From this point an abandoned gravel quarry road gives final access to the rock slide area.

3-3 PREVIOUS WORK

The bedrock geology of the Whitehorse Creek area was originally mapped by B.R. MacKay in 1929. MacKay mapped the structural features and stratigraphic relationships of the Cadomin and Mountain Park map sheets (NTS No. 83C/14 and 83F/3). The Whitehorse Creek slide lies in the middle of this area. No report was published to accompany this map. Further studies of the Mississippian stratigraphy in similar structural environments in the foothills south and west of Cadomin have been conducted by several authors and summarized by Moore (1958) and Macauley et. al. (1966).

MacQueen (1966) studied the Mississippian stratigraphy of the Cadomin area in detail and correlated this cyclic stratigraphy with changing depositional environments. Macqueen's report describes in detail the rock formations outcropping in the MacLeod River Valley 2.6 km south east of the rock slides (Figure 3-1).

The structural geology of the area has not previously been mapped in detail but a reconnaissance map of the general stratigraphy and structure of the Rocky Mountains prepared by Price and Mountjoy (1970) as part of the GSC Operation Bow-Athabasca, encompasses the Whitehorse Creek slide area.

Reconnaissance maps of the surficial geology of the foothills area north of 52° latitude were prepared on a 1:50,000 scale by Bayrock and Reimchen (1975). No previous surficial maps had been made of the area. The study areas investigated by the respective authors are outlined in Figure 3-1.

3-4 SURFICIAL GEOLOGY

The surficial geology of the Whitehorse Creek slide area was first mapped by Bayrock and Reimchen (1975) as part of a reconnaissance programme to evaluate the erosion potential of surficial materials in the Rocky Mountain Foothills north of 52° latitude. The rock slide area under investigation was recognized as such by Bayrock and Reimchen and is located in the top centre of the map.

Bayrock and Reimchen indicate that the Whitehorse Creek Valley walls, adjacent to the valley in which the slides occurred, are covered with classical Wisconsin age tills. A poorly defined U shaped valley profile (Figure 3-2) suggests this interpretation. The bottom of the valley , within the banks of the creek, is covered with alluvium. The area surrounding the rock slides has been mapped as colluvium with no mention of till.

Field mapping around the periphery of the slides has revealed the presence of sandy till on the sides of the unnamed creek valley beside the debris. The areal limits of this till sheet were not mapped but it would seem reasonable to suggest that this till was equivalent to one of those mapped by Bayrock and Reimchen less than 500 m away. The till found in this valley consists of large boulders, sand and silt and ranges in thickness from 2-12 m. The surficial geology of the area surrounding the slide is summarized in Figure 3-3. The locations of the till outcrops mapped are also shown in Figure 3-3.

Alluvial deposits have formed in the water course of the unnamed creek which flows below the debris of the younger slide. Downstream of the debris the creek course is very narrow and steep. Lenses of gravelly alluvium varying from 0-0.1 m thick and covering areas up to 0.3 m^2, can be found in this valley covering the bedrock. Upstream of the debris a large flat area of alluvium covering the width of the valley floor, which appears to be recently formed fine grained sedimentary deposits, conceals the creek. This deposit probably formed when the debris from the younger slide filled the valley. The creek now flows underground and exits in the form of a spring southeast of the debris.

The debris from the younger slide varies from blocks 10 m^2 by 8 m thick to sand size particles (Plate 3-1). All of the debris visible was identified as dolomite of the

Turner Valley Formation. The debris moved approximately 0.8 km horizontally and about 0.33 km vertically measured from the top of the scarp to the toe of the debris. The total volume of the slide mass was approximately 2.3 x 10^6 m^3. Table 3-1 summarizes the physical dimensions of the slide.

The centre of the debris is approximately 35.0 m thick and thins gradually on all edges. Thicknesses were estimated from a topographic map of the slide area constructed on a 1:4,800 scale. The outline of the debris is tear drop shaped. The leading edge of the debris has crossed the path of the unnamed creek and pushed against the valley wall opposite the rock slide causing the debris to pile up. The margins of the debris are not well defined. The blocks are scattered over a distance of 10-15 m in all directions and vary in places from small piles of debris which have gathered on the outside debris margin to large blocks isolated from the main body of the slid mass. No debris from the older slide remains in the area.

The outcrops of bedrock in the area adjacent to the slide have been mapped in detail and are discussed in Section 3-6. The remaining areas have been mapped as colluvium following the example of Bayrock and Reimchen (1975).

3-5 STRATIGRAPHY

The bedrock stratigraphy around the Whitehorse Creek area was first defined on a large scale by MacKay (1929). He identified the bedrock underlying the ridge from which the slide occurred as Mississippian Rundle Group limestones. The Rundle Group has since been subdivided into several Formations.

In Southern Alberta the Livingstone and Mount Head Formations make up the Rundle Group while in the foothills of Central Alberta the equivalent sequence is divided into the Pekisko, Shunda, Turner Valley and Mount Head Formations (Moore,1958 and Macauley et.al., 1966). The detailed stratigraphy of the Cadomin area was mapped by MacQueen (1966) and a type section along a railway cut in the MacLeod River Valley was defined. The location of this section is shown on Figure 3-1. The rock formations were visually extrapolated from the type section across the MacLeod River to the end of the unnamed ridge which extends southwest from the rock slides. From here the formation contacts were worked out on the ground along the ridge and used to define the stratigraphy of the slides.

The following lithologic descriptions of the various formations are modified after MacQueen (1966).

Three formations outcrop on the ridge in the vicinity of the rock slide study area. The stratigraphic column pertaining to these is shown in Figure 3-4. The oldest formation recognized in the area, the Shunda Formation, has been informally divided into 4 units in the Cadomin area by MacQueen. The Shunda Formation outcrops on the steep slope northwest of the younger slide. The upper unit of this formation is the only one of any consequence, however, as it lies directly below the failure surface of the younger slide. The Upper Shunda unit consists of about 3 m to 5 m of easily recognizable fine grained to very fine grained brown weathering dolomite. The top of this unit is defined by the first appearance of massively bedded (greater than 10 cm thick) brown weathering crystalline dolomites of the Turner Valley Formation.

The 34 m thick Turner Valley Formation has been subdivided by MacQueen into two units separated by a 6 m thick bed of fine grained crystalline dolomite which contains up to 20% chert bands, chert nodules and silicified brachiopods. The Lower Turner Valley (16 m thick) and the Upper Turner Valley (12 m thick) are very similar in nature and can not be distinguished on the basis of lithology. MacQueen describes the whole formation as a fine to medium crystalline, brown weathering dolomite. The unit is porous and resistant. Syringopora tabulate corals may be found in the lower part of the formation and were found at many of the stations on the younger slide surface. The upper part of the formation is less porous than the lower part and shows traces of cross bedding. The top of the Turner Valley Formation, as defined by MacQueen, is placed at the base of a weathered zone of brecciated microcrystalline dolomite.

According to MacQueen, the Mount Head Formation in the Cadomin area consists of 60 m of unfossiliferous predominantly microcrystalline to fine crystalline dolomites with local interbeds of green dolomitic mudstones. Some of the beds exhibit irregular hummocky surfaces with well developed mud cracks. The Mount Head Formation outcrops above the slide area on a flatter part of the slope and was not involved in the slope failure.

Field mapping in the vicinity of the failure planes established that the older slide slid along the 6 m thick marker bed dividing the Turner Valley Formation into two units. The failure plane of this slide is well exposed in most places. The back scarp and the eastern lateral margin of the older slide consist of the upper half of the Turner Valley Formation. The failure plane of the younger slide was located within the lower part of the Turner Valley Formation just above the Shunda Formation contact. The back scarp was approximately 30 m to 35 m high and consists of the remaining thickness of Turner Valley Formation.

The bedrock geology of the slide area is shown overlain on an air photograph in Plate 3-2. This photo is a Government of Alberta photo # AS1266-34-244 with a scale of 1:21,000.

3-6 STRUCTURAL GEOLOGY

The study area at Whitehorse Creek lies within the eastern half of the structural subprovince of the Rocky Mountains known as the Front Ranges. Structure in this province is dominated by thick relatively flat thrust plates that have been gently deformed into broad open folds. The rocks consist of a thick sequence of competent carbonates Upper Paleozoic in age (Price and Mountjoy, 1970). Figure 3-7 is a reproduction of the part of the structural geology map compiled by Price and Mountjoy for Operation Bow-Athabasca. This map illustrates how the Mississippian rocks at Cadomin have been thrust up into position along the Bighorn Thrust Fault. No other reports dealing with the structural geology of this area were available.

In order to supplement this information on a scale small enough to be of use in a rock slope back analysis, detailed structural mapping of the bedrock around the failure surface was carried out. The results are summarized in Figure 3-6. Both slide surfaces and scarps were mapped but the majority of the stations were located on and around the younger failure surface.

The failure surfaces of both slides consisted of a series of parallel bedding planes which step up through the lithologic section as the failure surface increases in elevation. The steps varied from 12 cm to 30 cm high and in most cases are formed by joints which run obliquely down the bedding surface. Plate 3-3 is an example of one such bedding surface found near the southeast margin of the younger rock slide.

The average orientations of the bedding surfaces at each of 48 stations, based on 15 individual readings per station, were plotted on a stereonet and the average bedding plane was established with a dip direction and dip of 206° and 30° (Figure 3-7) . There were no large scale variations in orientation on the failure surface. Bedding planes near the failure surface varied in thickness from 0.2 m to 0.6 m and averaged 0.3 m. MacQueen noted the presence of large scale cross bedding within the upper part of the Turner Valley Formation. Cross bedding with an amplitude of about 0.30 m and dips varying from 38° to 20° were found in one location on the eastern margin of the ancient slide. This location was on the south west margin of the older slide near the top of the Turner Valley Formation (Figure 3-6). No cross bedding was readily visible near the failure surfaces of either slide.

Bedding orientations were also taken at 7 stations on bedrock outcrops on the unfailed portion of the ridge above the back scarps of both slides. The average bedding dip in this location decreased to approximately 20° although the dip directions are almost the same, 202° as opposed to 206°, (Figure 3-8). There was no surface expression of a fault or a tight fold in the vicinity of the rock slide scarps which would explain the variation in attitudes. However on the basis of bedding orientations a hypothetical fold axis with a trend of 112° to 116° and a plunge of 0° was defined and marked on Figure 3-6. This fold, which has an axis parallel to bedding may be the result of thrust faulting which moved the bedding to its present location.

A small tight fold was observed on the surface of the younger slide near the northwest corner of the failure surface 120 m below the back scarp(Figure 3-6). The fold could be traced 150 m along strike before it died out. The beds involved in the fold were only 2 m thick as measured in the steeply dipping limb. The centre of the fold was hollow and the fold actually consisted of a series of flat bedding surfaces which had buckled at several discrete points. The thin skin nature of the fold implied that it was a superficial gravity structure probably related to interbed slip which occurred during or following the slope failure. The fold axis defined from the bedding had a trend of 120° and a plunge of 0° (Figure 3-9). This axis was parallel to the bedding strike as would be expected in a fold controlled by interbed slip.

Near vertical orthogonal joint sets form the vertical elements of both back and side scarps (Plate 3-4). The poles to 75 joints were plotted on a stereonet and the average joint strikes of 46° and 148° were defined (Figure 3-10). These joints form a crossing pattern on the slope surface which has controlled the orientation of the back scarps of both slides. The relationship between the scarps and the joint orientation is shown in Figure 3-6.

The strikes of the joint sets are very similar to those defined at Jonas Creek (40° and 135° , Section 2-6) and to those defined as System 1 joints (55°, 140°) which Babcock (1974) hypothesized as being the result of the Laramide Orogeny. Similar to Jonas Creek, the dips of both joint sets vary from 5° to 10° on either side of vertical and as such neither set is perpendicular to bedding. Again following the argument of Friedman and Stearns (1971), outlined in section 2-6, it would appear that the joint orientations at Whitehorse Creek are the result of the interrelationship between regional and local stresses imposed during deformation. Joint spacing varied from 0.2 m to 3.0 m with an average spacing close to 0.6 m.

There was no evidence of faulting or flexural slip folding having taken place along the failure surfaces of either slide although other evidence of thrust faulting and folding could be observed in the mountains around the slide area. However, the northwest corner of the younger slide, which apparently was daylighted prior to failure and which is now marked by a steep scarp, may reflect the presence of a transverse structural element such as a tear fault or a normal fault.

The block of Mississippian rocks forming the unnamed ridge which failed is overlain by Triassic sandstones and shales which are exposed in the bottom of the unnamed creek valley southwest of the slides. These beds range in thickness from 0.1 m to 0.3 m thick and are heavily jointed with joint spacing which generally equals the bed

7

thicknesses.

The unnamed ridge which trends NW-SE is covered by loose colluvium, with large unstable blocks and tension cracks present. (Plate 3-5). There are no major slides however along the ridge southeast of the study area. The reason for this is probably twofold:

1) During the early stages of the investigation, when the stratigraphy was being traced from the type section to the rock slide area, a series of bedding orientations were recorded close to the southwest end of the unnamed ridge (Point D, Plate 3-5). The bedding at this location had an average dip direction of 182° and a dip of 15° and as a result the slope was much more stable at this location. The loose blocks and tension cracks which appear to be quite old, could be linked with postglacial periglacial environments causing downslope creep or heaving of joint blocks (Washburn, 1973). The photograph used by Washburn to illustrate these processes strongly resembles the surface topography found near locations B and C on Plate 3-5.

2) The part of the ridge southeast of the slides which has not failed, does not have the Turner Valley Formation daylighted at the valley wall bottom. Below the area which did fail a small creek probably removed the toe support of the end of the ridge daylighting the middle zone of the Turner Valley Formation initiating the older slide. However at point A on Plate 3-5, the unnamed creek which was trending parallel to the bedding on the ridge cuts to the

south into the Triassic sandstones. So underneath the older slide, the Lower Turner Valley is probably not daylighted and hence failure within this unit has not occurred. The toe support along the rest of the ridge has not been removed either by the unnamed creek or Whitehorse Creek and so failure has not occurred. At the southeast end of the ridge where Whitehorse Creek has exposed the Turner Valley Formation the bedding dip is much lower and hence failure has again been avoided.

3-7 SUMMARY

The two rock slides at Whitehorse Creek have occurred on two separate failure planes within the Mississippian Turner Valley Formation. The failure surfaces are both planar and both step up through bedding as elevations increase. There is no visible evidence that faulting or folding led to slickensided failure surfaces. The back and lateral scarps are formed by near vertical joints with strikes of 46° and 148° . An open fold has been hypothetically mapped behind the failure scarp. North of this fold hinge the bedding dips 7° less than the bedding involved in the failure. This decrease of 10° accounts for the stability of the rock slope above and to the north of the failure planes.

TABLE 4-1

Physical Dimensions of the Whitehorse Creek Slides And failure surfaces.

Slide	width	length	vertical travel	horizontal travel	volume
older	0.28km	0.38km	-----	------	-----
younger	0.40km	0.38km	0.31km	0.79km	$2.3 \times 10^6\ m^3$

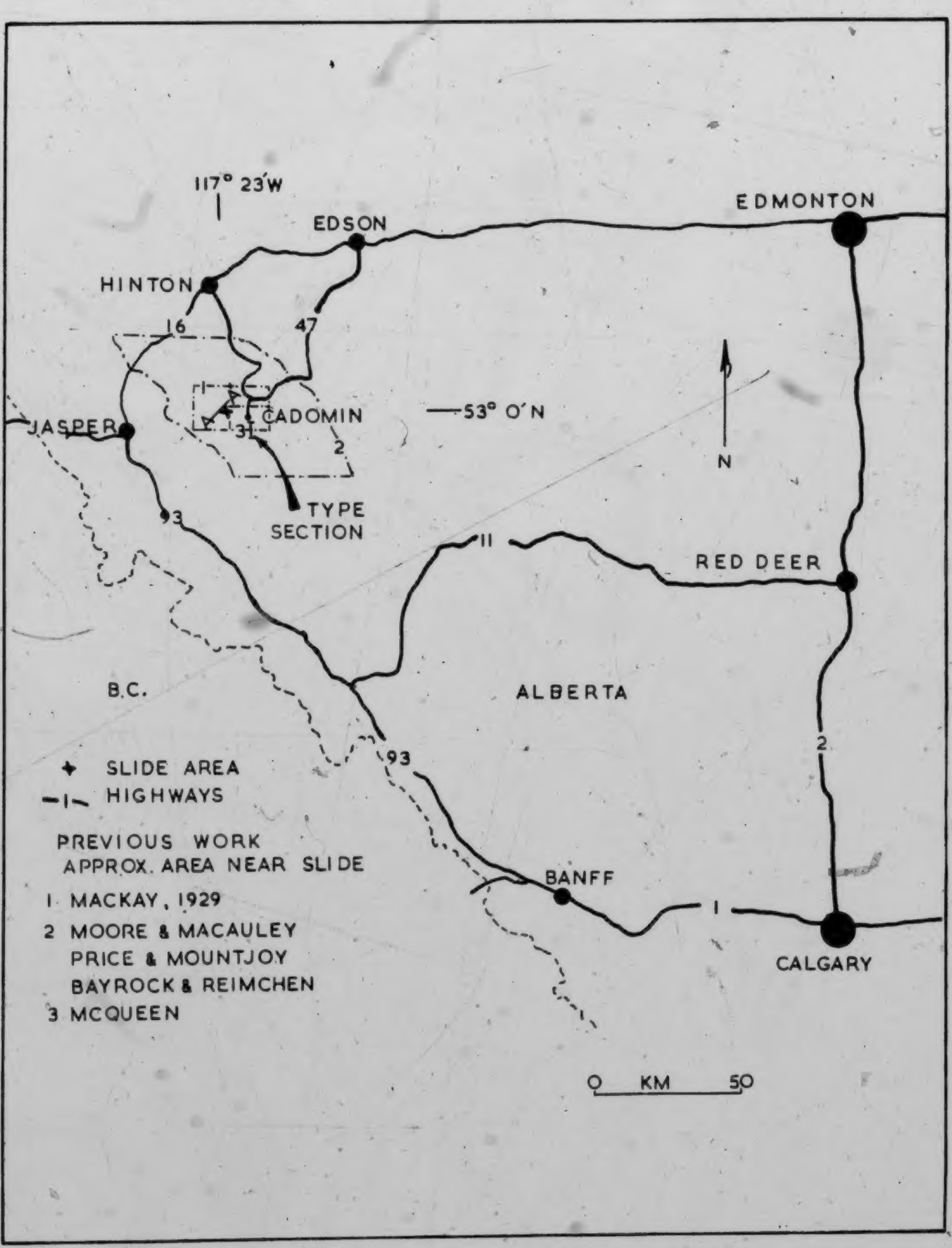
117° 23'W
EDSON
EDMONTON
HINTON
16
47
1
2
3
CADOMIN
53° 0'N
JASPER
2
N
TYPE SECTION
93
11
RED DEER
B.C.
ALBERTA
93
2
✦ SLIDE AREA
-1- HIGHWAYS
PREVIOUS WORK
APPROX. AREA NEAR SLIDE
1 MACKAY, 1929
2 MOORE & MACAULEY
PRICE & MOUNTJOY
BAYROCK & REIMCHEN
3 MCQUEEN
BANFF
1
CALGARY
0 KM 50

FIGURE 3-1 Location Map For Whitehorse Creek.

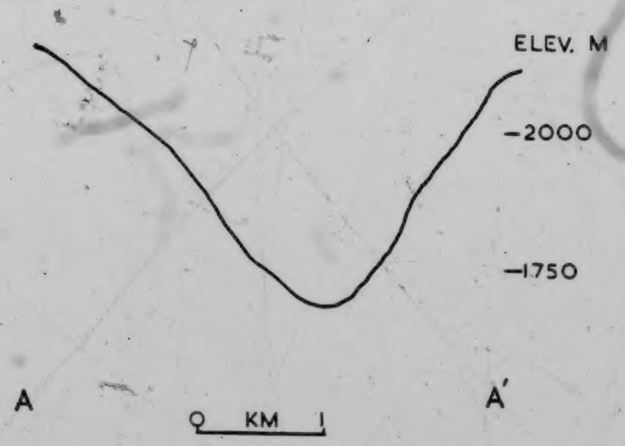
ELEV. M
-2000
-1750
A
A'
0 KM 1

FIGURE 3-2 Valley Profile Adjacent To Whitehorse Creek Illustrating U Profile. (Section Line On Figure 3-1)

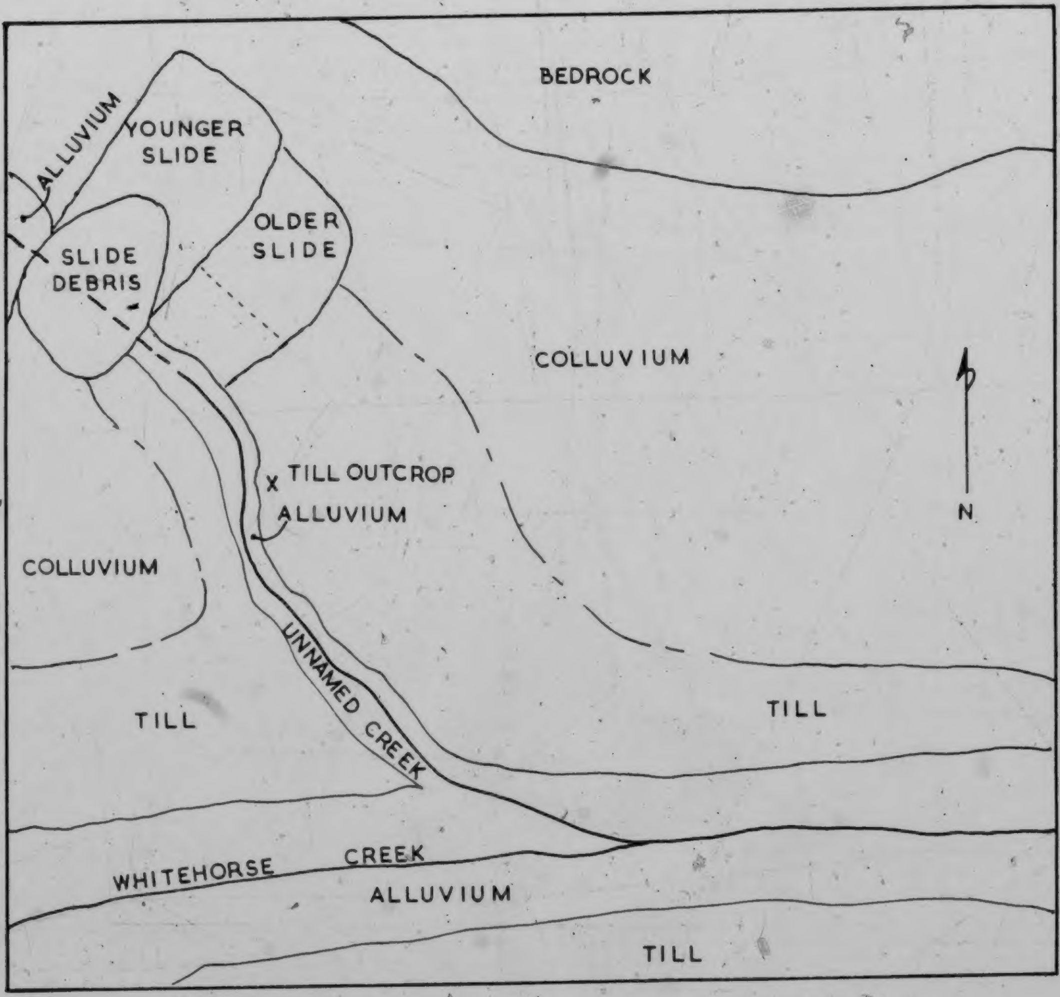
BEDROCK
ALLUVIUM
YOUNGER SLIDE
OLDER SLIDE
SLIDE DEBRIS
COLLUVIUM
X TILL OUTCROP
ALLUVIUM
N
COLLUVIUM
UNNAMED CREEK
TILL
TILL
WHITEHORSE CREEK
ALLUVIUM
TILL

FIGURE 3-3 A Surficial Geology Map Of The Area Surrounding The Whitehorse Creek Slide Are (Modified After Bayrock And Reimchen, 1975).

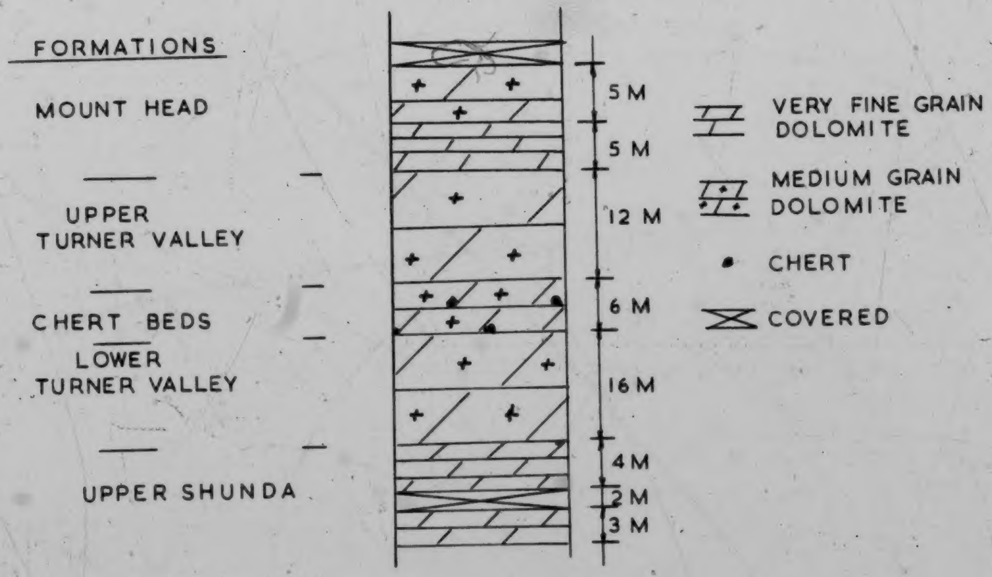
FORMATIONS
MOUNT HEAD
UPPER TURNER VALLEY
CHERT BEDS
LOWER TURNER VALLEY
UPPER SHUNDA
5 M
5 M
12 M
6 M
16 M
4 M
2 M
3 M
VERY FINE GRAIN DOLOMITE
MEDIUM GRAIN DOLOMITE
CHERT
COVERED

FIGURE 3-4 Stratigraphic Column Of Whitehorse Creek Area (Modified After MacQueen, 1975).

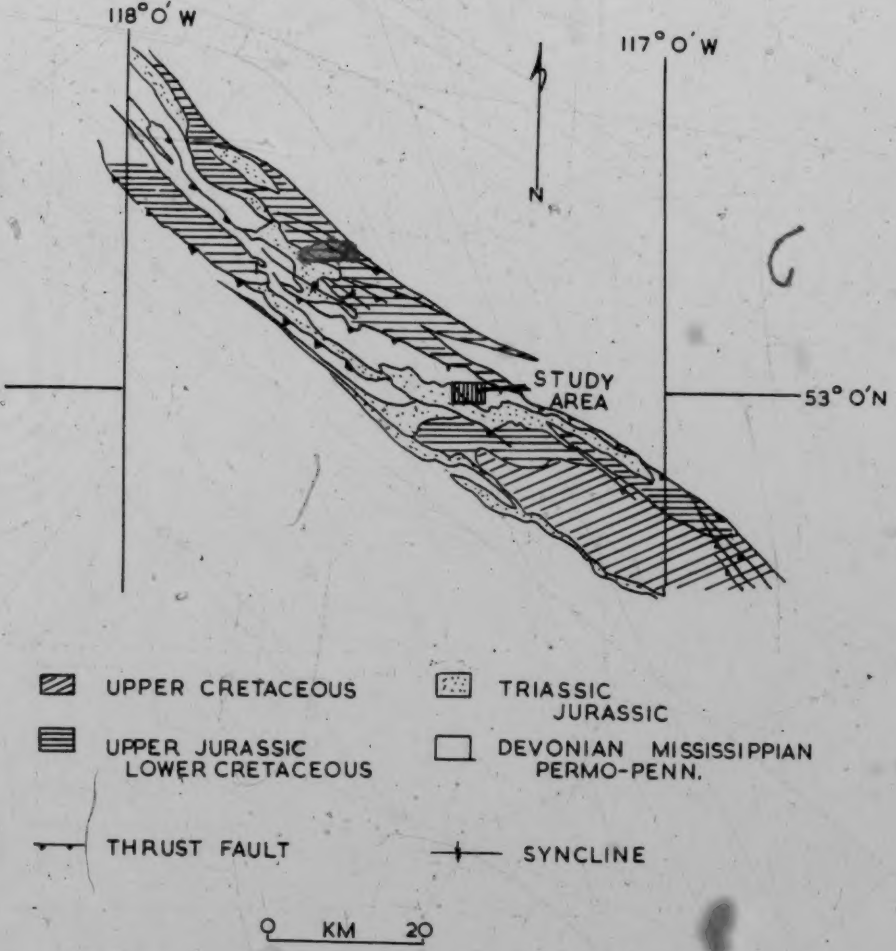
118° 0' W
117° 0' W
N
STUDY AREA
53° 0' N
UPPER CRETACEOUS
TRIASSIC JURASSIC
UPPER JURASSIC LOWER CRETACEOUS
DEVONIAN MISSISSIPPIAN PERMO-PENN.
THRUST FAULT
SYNCLINE
0 KM 20

FIGURE 3-5 Structural Geology Of Part Of The Rocky Mountain Foothills (After Price And Mountjoy , 1970).

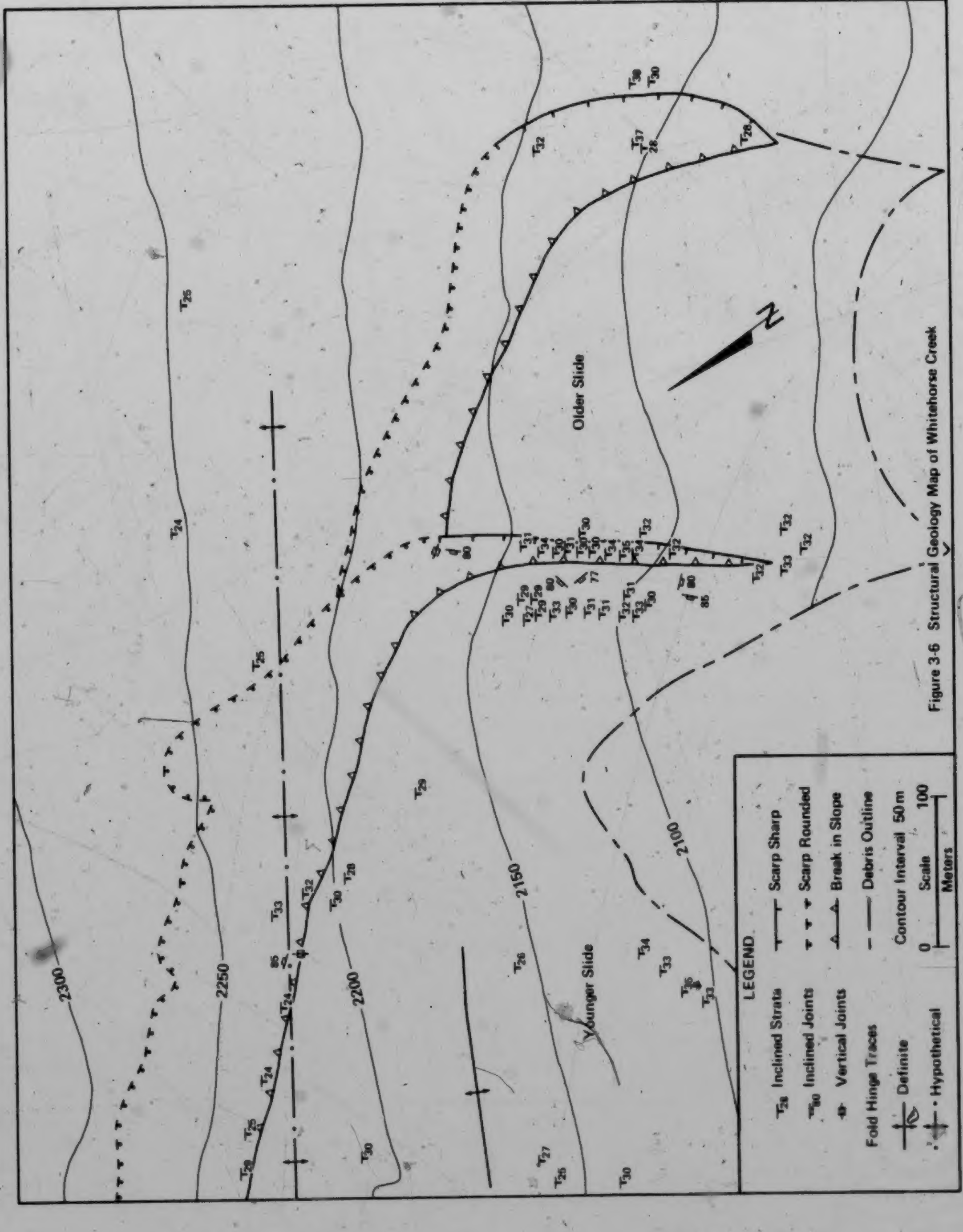
2300
2250
2200
2150
2100
Older Slide
Younger Slide
N
LEGEND
Inclined Strata
Inclined Joints
Vertical Joints
Fold Hinge Traces
Definite
Hypothetical
Scarp Sharp
Scarp Rounded
Break in Slope
Debris Outline
Contour Interval 50 m
Scale
0
100
Meters

Figure 3-6 Structural Geology Map of Whitehorse Creek

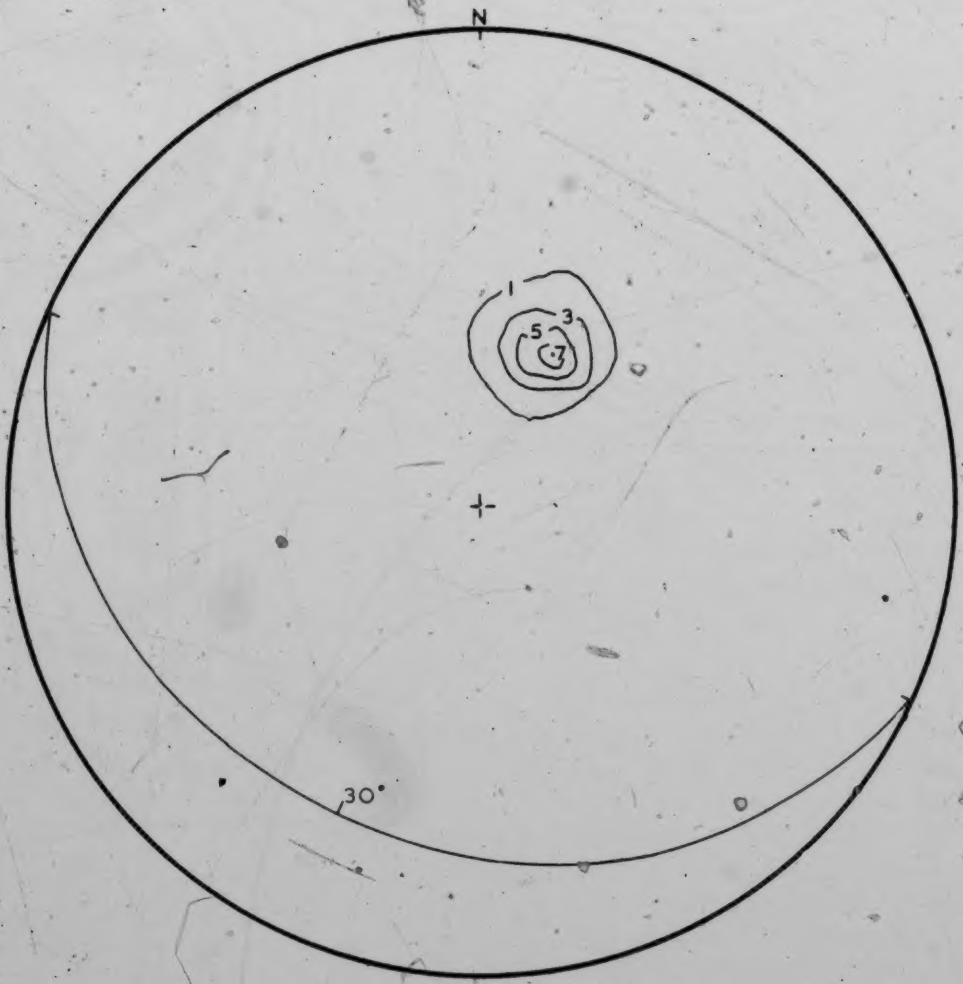

FIGURE 5-7 Stereonet Of Poles To Bedding On The Failure Surface.

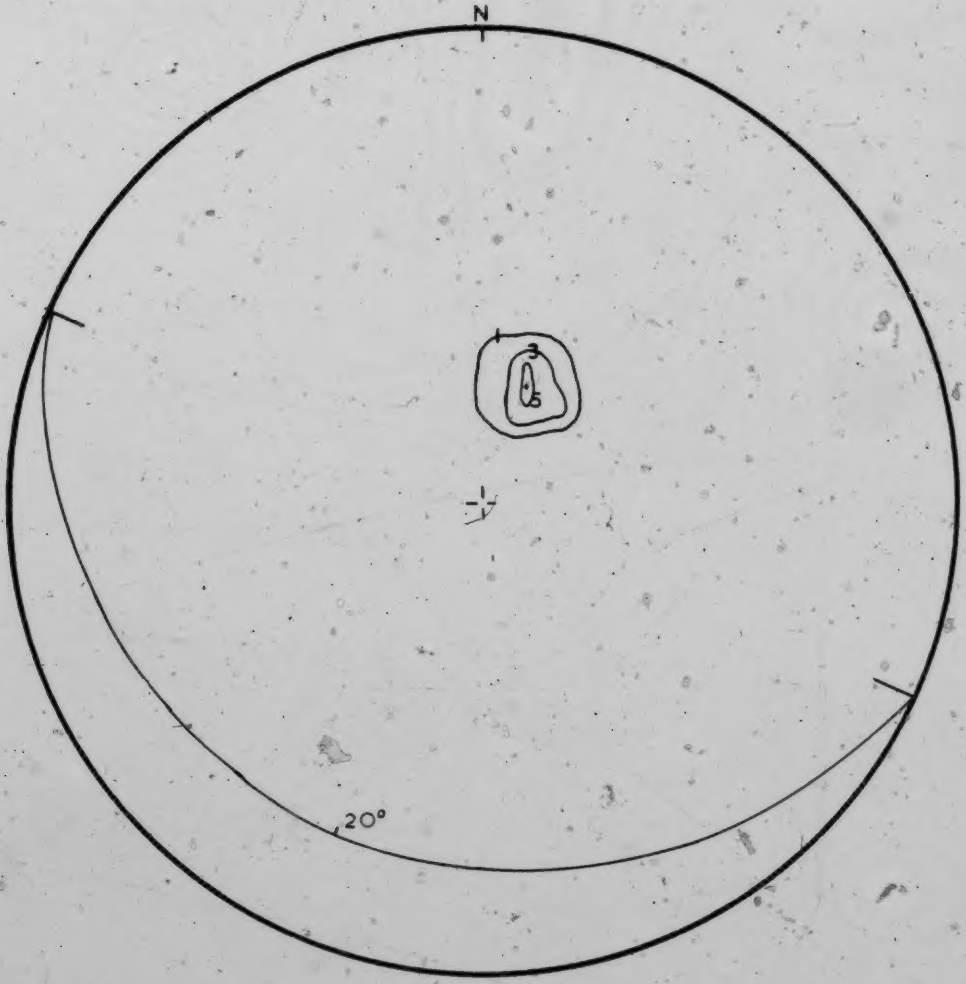

FIGURE 3-8 Stereonet Of Poles To Bedding Above The Slide Failure Surface.

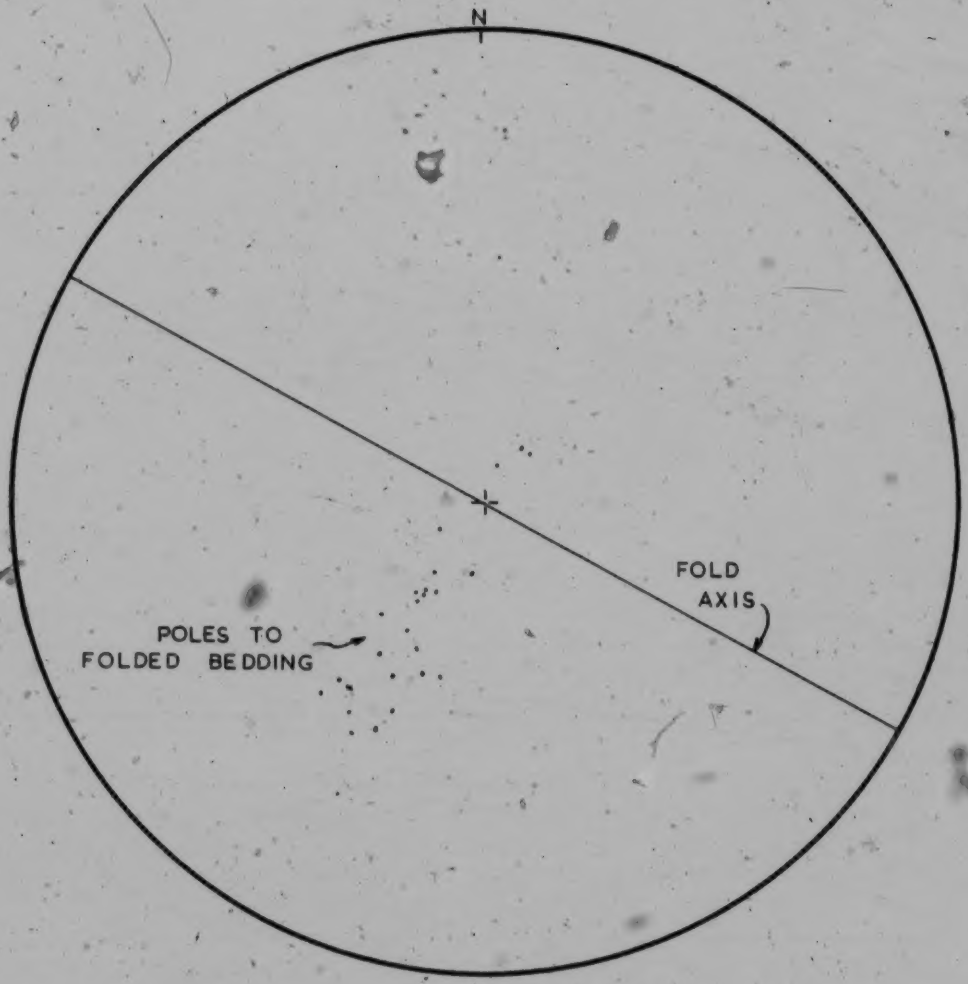
N
FOLD
AXIS
POLES TO
FOLDED BEDDING

GIGURE 5-9 Stereonet Used To Define The Fold Axis From Poles To Bedding.

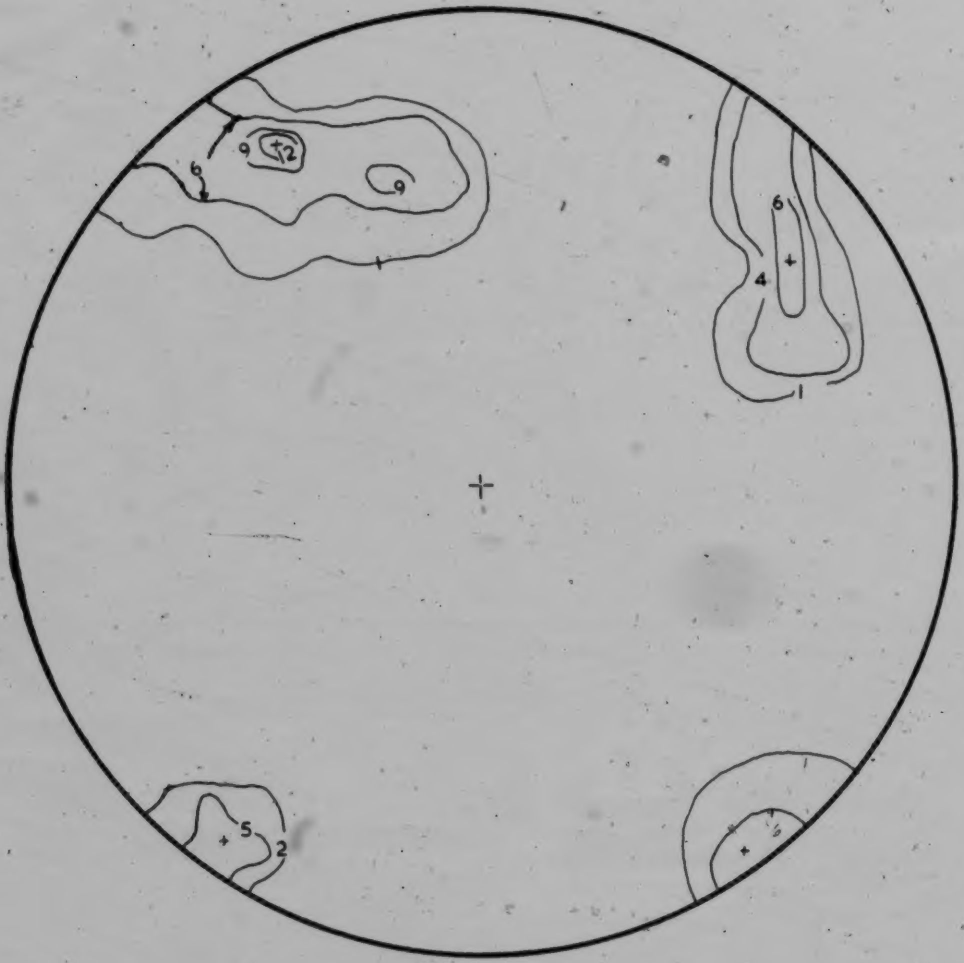
6
9
12
9
1
6
4
1
5
2
1

Figure 5-10 Poles To Joints Measured At whitehorse Creek.

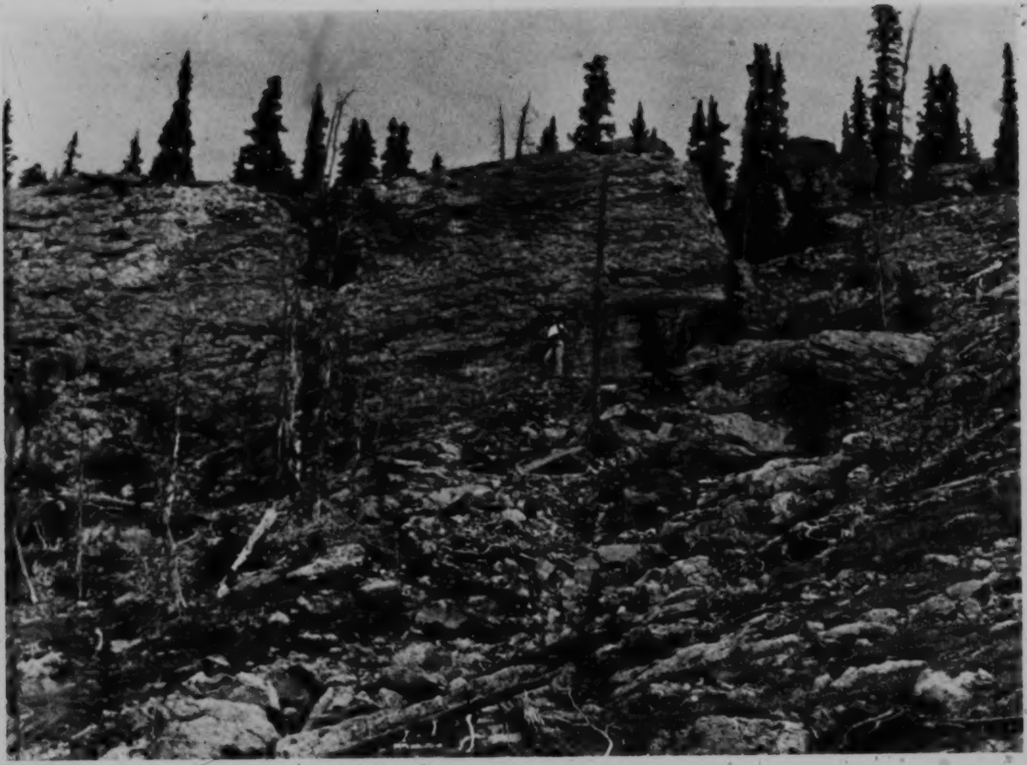

PLATE 3-1 Photograph Illustrating Large Range Of Debris Sizes At Whitehorse Creek.

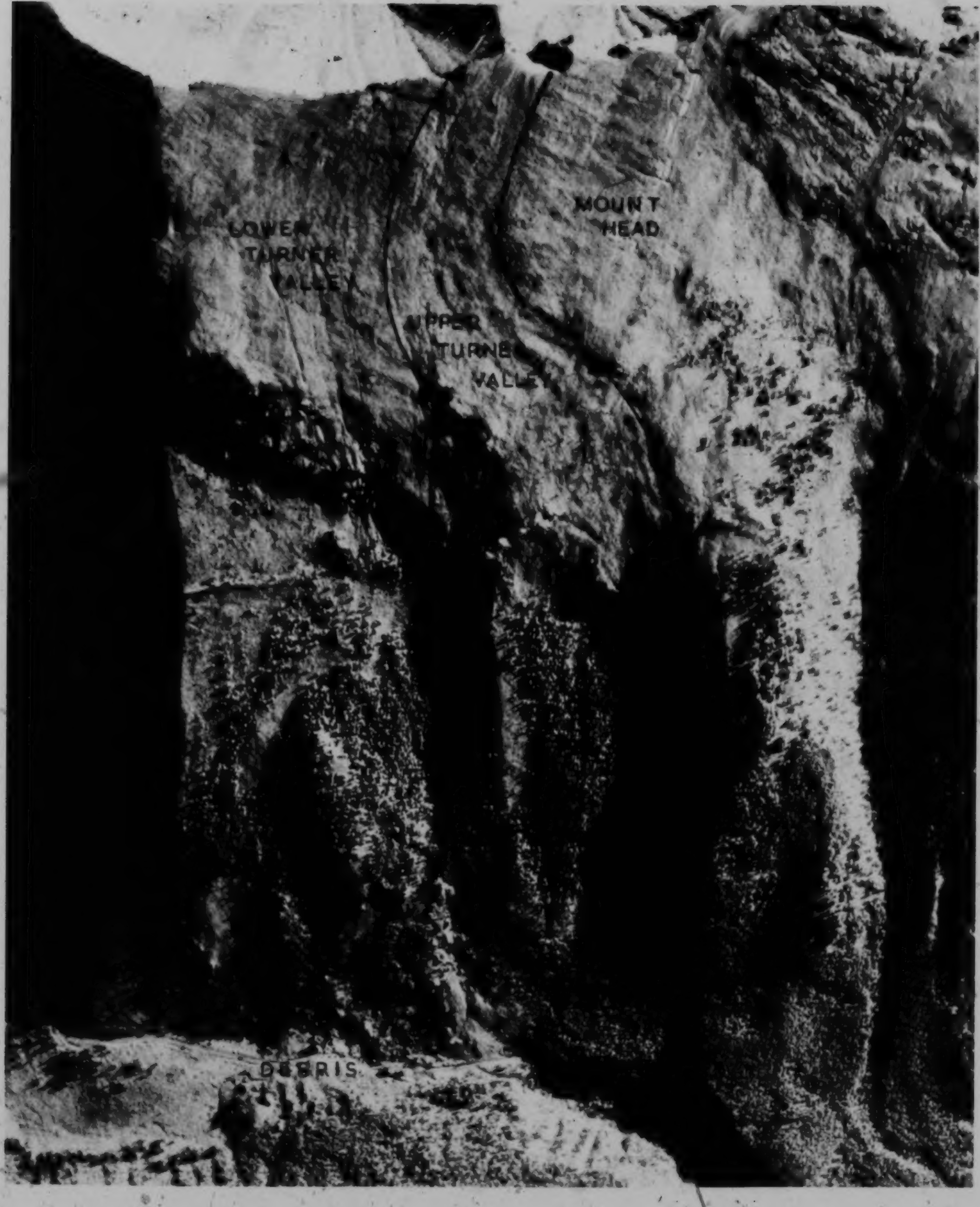
LOWER
TURNER
VALLEY
UPPER
TURNER
VALLEY
MOUNT
HEAD
DEBRIS

Plate 3-2 Bedrock Geology Shown Overlain On An AirPhoto Of The Slides At Whitehorse Creek.

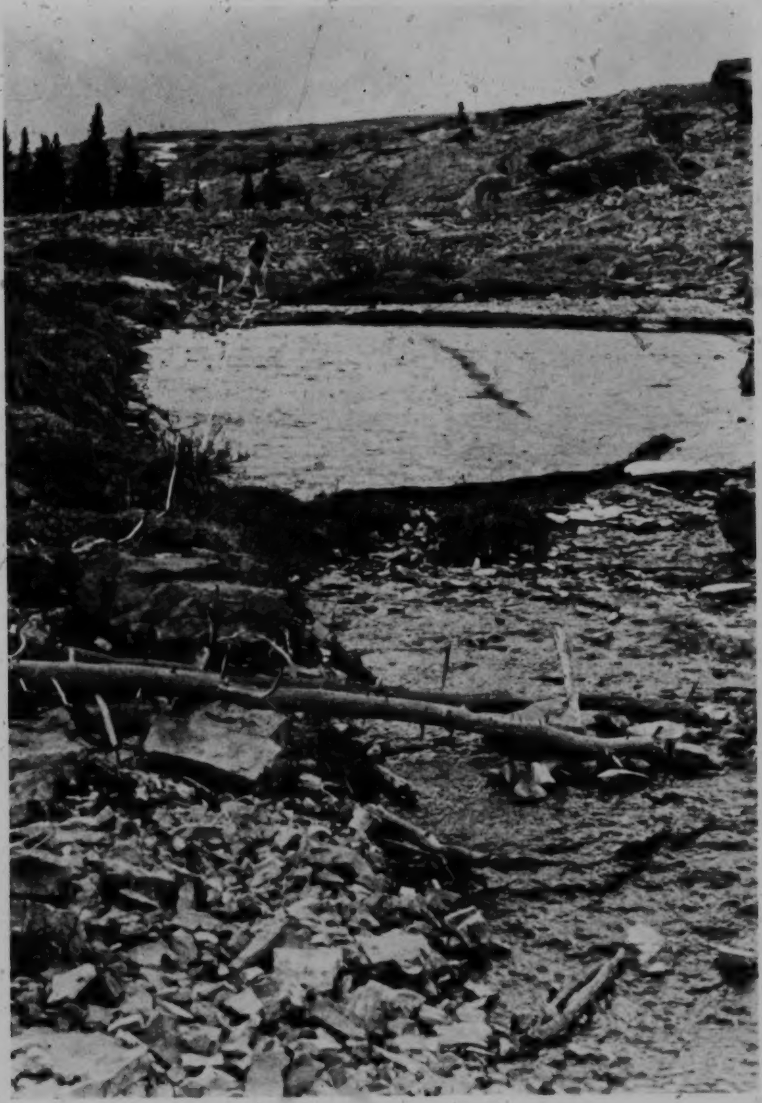

PLATE 3-3 Photograph Of Part Of The Failure Surface At Whitehorse Creek Showing Small Vertical Steps.

PLATE 3-4 Photo Of The Scarp At Whitehorse Creek Showing Vertical Joints Forming Back And Side Scarps.

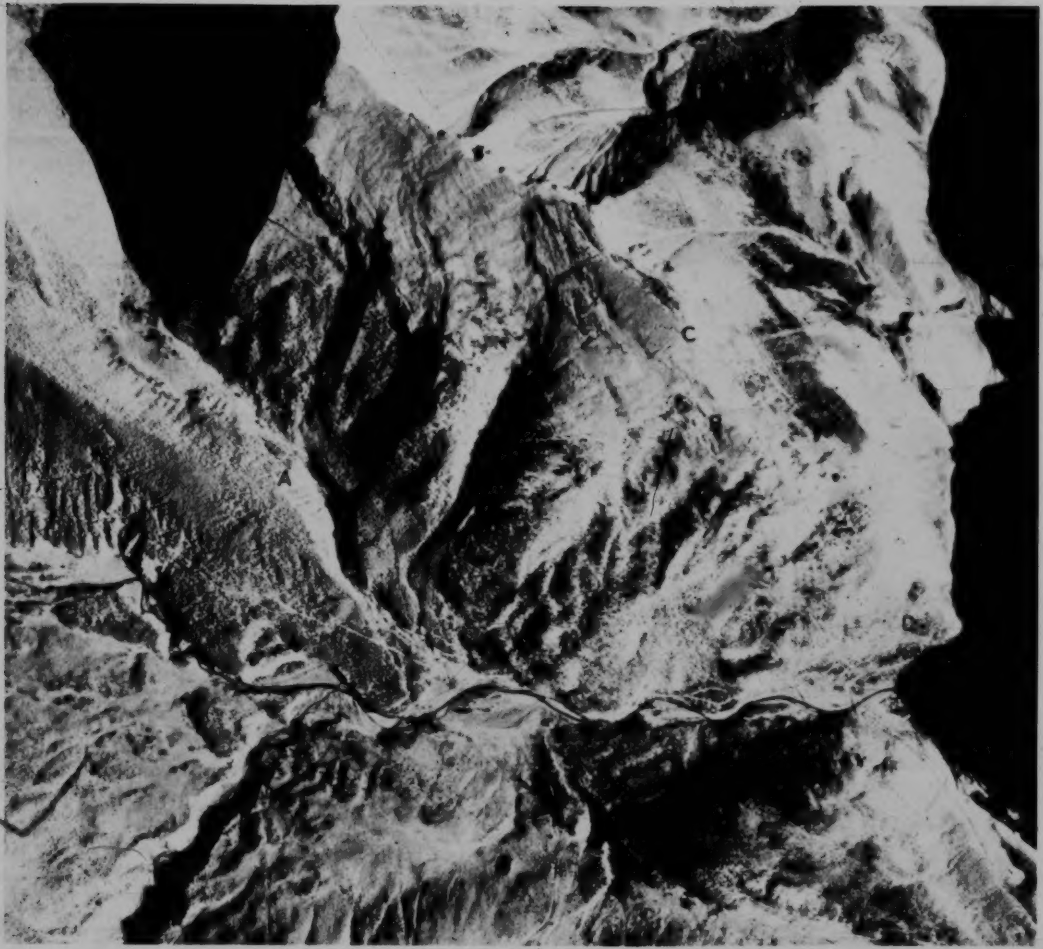

PLATE 3-5 Air Photo of The The Entire Ridge At Whitehorse Creek. Note The Point A Where The Small Creek Changes Direction, Boulders At B, And Cracks At C.

CHAPTER IV

The Field Estimation Of The Topographic Component Of Shear Strength

4.1 INTRODUCTION

Terzaghi (1962) noted that the stability of rock slopes depends upon the shear strengths mobilized along structural discontinuities in a rock mass as opposed to the shear strength of intact rock materials. Ripley and Lee (1961), after conducting a series of shear tests on some representative natural discontinuities, concluded that the peak shear strengths developed along these discontinuities were highly dependent upon the geometry of the natural surfaces.

Over the past decade this approach has been analyzed and refined and it is now generally accepted that the shearing resistance along rock discontinuities arises from two separate components; ϕb, the frictional resistance generated between two flat surfaces sheared past each other and the angle i, an indicator of the topographic component of shear resistance.

In an attempt to separate and quantify the two components of shear resistance, Patton (1966) performed a series of shear tests on plaster specimens with various known topographies. By using flat surfaces with no visible topographic component Patton defined ϕb by the expression

$$T = N \tan \phi b \qquad 4.1$$

where T = shear stress

N = normal stress

and ϕb= the basic friction angle of the material.

The peak friction angle developed on a surface with a topography of regularly inclined teeth (Figure 4.1) yielded the equation

$$S = c + N \tan (\phi b + i) \qquad 4.2$$

where c = an effective cohesion intercept

and i = the angle of inclination of the teeth or asperities forming the geometric component.

At low normal loads, the inclined teeth forced the upper half of the sample to dilate at an angle i from the direction of shear. The resulting straight line Mohr envelope had a slope of (ϕb+i) which passed through the origin. At high normal loads where dilation did not occur the asperities were sheared through giving rise to an effective cohesion intercept and a much lower angle of friction similar in magnitude to ϕb (Figure 4-1). The resulting bi-linear law of shear strength although somewhat over simplified was beneficial in explaining the observed behaviour in rock shear tests.

Ladanyi and Archambeault (1970) realized that the shearing through of asperities occurred over a range of normal loads and that i values on a natural rock surface varied with position and scale. They concluded that the combination of these variables led to a curved Mohr envelope for real rock materials and proposed the following equation to represent this;

$$T = \frac{N(1-As)(V+f) + As\ j\ C(m-1)/n(1+n)(N/j\ C)}{1-(1-As)\ V\ f} \qquad 4.3$$

where N = normal stress, T= shear stress

n = the ratio between cohesion and tensile strength

V = the dilation rate due to shear

As = shear area ratio, f = average coefficient of friction

j= degree of joint interlock, m = $(n+1)^{1/2}$

and C = uniaxial compressive strength.

Although this equation may be conceptually correct it is very difficult to evaluate some of the parameters such as As,V and j. It is interesting to point out however that in the case of low normal loads where no shearing through occurs, that is As=0, equation 4.3 reduces to equation 4.2.

Ladanyi and Archambeault (1970), on the basis of laboratory experiments on plaster models, defined the variation in As and V empirically as

$$As = 1-(1-N/Nt)\ \exp.k \qquad 4.4$$

$$\text{and } V = \{(1-N/Nt)\ \exp.L\}\ \tan i \qquad 4.5$$

where K = 4.0 and L = 1.5, both empirically defined values,

and Nt =the transition stress defined as the point where the shear strength envelope for a discontinuity intersects the envelope defined for intact rock.

The graphical relationships linking V, As and N are shown in Figure 4-2.

Hoek and Bray (1977) combined the above equations 4.3, 4.4 and 4.5, to form the equation;

$$T/N=\frac{N/C(1-N/C)^{1.5}\{(1-N/C)^{4}\tan i+\tan \phi\} + 0.232\{1-(1-N/C)^{1.5}\}\{1+10N/C\}^{.5}}{1-\{(1-N/C)^{5.5}\tan i \text{ x } \tan \phi\}} \tag{4.6}$$

Using the empirical values of K and L the ratio of T/N can now be evaluated knowing tan i and tan ϕ.

In the examples shown in Figure 4-2, the normal stress varies from 0 to Nt, which is approximately 100, mPa, and variations in the values of ϕ and i over this range are noticeable. However for many slope stability problems N is limited, often to less than 1500 KPa, and within this range the Mohr envelope can be represented by a straight line and hence one value of i. The value of 1500 KPa is greater than twice the value of the maximum normal stress acting at either the Jonas Creek or Whitehorse Creek rock slides. Using the empirical equation (equation 4.5), and assuming values of Nt, and i, of 100 mPa and 10° respectively, the value of i varies less than 1° over the range of normal stresses which may be expected in near surface workings.

The practical application of the simple $\phi b+i$ concept with respect to slope stability has been limited to date by our inability to evaluate the large scale i values found in the field. This thesis is an attempt to remedy this situation.

4.2 Previous Techniques Used to Evaluate i

Patton (1966) applied his bi-modal failure theory (5.2) to a series of natural rock slopes located in the Rocky Mountains of Canada and the United States. By photographing profiles of natural slopes, then projecting the profile photos onto a screen, Patton was able to reproduce the bedding surface profiles in the laboratory. He obtained a measure of the roughness by averaging the angles of deviation of small straight line segments from the mean orientation of the surface profile. Reproduction of small scale (3m long) profiles by this process is very simple. However, in places where profiles cannot be obtained, or in areas too large to be photographed, this technique is not applicable.

On the basis of the recorded roughness profiles and a qualitative evaluation of slope stability, Patton (1966) concluded that there were three scales of roughness present on the failure surfaces; first order irregularities with wavelengths of 60 cm and second order irregularities with wavelengths of approximately 6 to 10 cm and third order irregularities with scales less than 1 cm. Figure 4-3 is a sample profile recorded by Patton showing the various scales recorded along with some of the representatives i angles. The average i angles measured on the slope profile for first order irregularities appeared to be a good estimate of i for the natural rock slopes investigated. The second order irregularities lost their effectiveness when they were sheared through or otherwise overridden by natural processes (Deere, Patton et. al. 1967). Patton (1966) did not report on scales of roughness greater than first order.

Patton (1966) suggested that to estimate i where the failure plane is not exposed, a representative profile could be measured on a similar neighbouring discontinuity. This hypothesis has yet to be tested.

In an effort to evalute i on several different scales Rengers (1970) developed a stereo microscope and a mechanical roughness tracer to record discontinuity surface profiles varying in length from 0.1 to 100 cm.

Rengers (1970) stated,

> "On the obtained profiles (of different scales due to different recording methods) measuring points are laid with a mutual distance of L, measured parallel to ref which is usually taken as 1mm. From each point on the profile, correction lines are drawn to other points at various distances (step sizes) n x L. The step

> sizes are chosen so that n x L x 1/Profile Scale (=n.L') equalizes one of the 36 real step sizes used in this method... The correction lines make positive and negative angles of i with the reference line."

"Ref" refers to the reference plane lying parallel to the approximate orientation of the whole rock surface. Figure 4-4 illustrates this procedure.

Rengers plotted the tangent of the maximum i angles found against the scale of the step sizes and noted that the effective i angle between asperities decreased as the measuring base length (n.L) between asperities increased (Figure 4-4). However, no attempt was made to correlate any of these measurements or trends with an evaluation of discontinuity shear strength (Øb+i). Due to equipment limitations only the roughness on discontinuities less than 2 m long was evaluated. This method of evaluating variations in i is both time consuming and laborious and in addition requires expensive special equipment (Fecker and Rengers, 1971).

Fecker and Rengers (1971) described a somewhat simpler technique of evaluating field roughness on approximately the same 2 m scale. A CLAR compass with interchangeable base plates of 5.5, 11.0, 21.0, and 42.0 cm in diameter was used to record the measurements of discontinuity orientations (Figure 4-5). The scatter in the readings taken randomly over the discontinuity reflected the roughness of the rock surface. The change in scatter brought about by changing the size of the base plates reflected the changes of i with scale.

The poles of the resulting measurements were plotted on a polar equal area net and all the data rotated such that the mean orientation of the outcrop face fell at the stereonet centre. A line was then drawn enclosing all the poles for any given size of base plate. A qualitative comparison revealed that rougher discontinuities had a much greater scatter of poles than smoother discontinuities and on any given surface the amount of scatter decreased as the size of the base plate increased (Figure 4-6). The maximum scatter angles recorded using this three dimensional technique in a direction parallel to those evaluated using Rengers' profilograph on the same discontinuity at the same scales gave very similar results (Figure 4-6).

The primary advantages of the technique developed by Fecker and Rengers are the speed and simplicity with which a measure of i can be evaluated. However, when scales larger than 2m have to be evaluated this advantage is lost. Extrapolation of this technique implies either the use of compass base plates of unmanageable size in the field or extrapolation of the data over very large ranges; a practice which would almost certainly lead to gross inaccuracies.

Fecker and Rengers (1971) note that i angles can be evaluated in any direction from the final stereonet plots. However closer scrutiny shows that the plots are not symmetrical and often appear at the center of the stereonet as an elliptical group of points. At stations investigated using this technique the range in dip direction was approximately 2 to 3 times greater than the range in dip (Table 4-1). Cruden and Charlesworth (1976) have shown that the ratio of the dip error to the strike error is equal to the sine of the true dip of the discontinuity being measured. As a result, for a discontinuity dipping at approximately 30°, the error in the dip should be approximately 1/2 of the error associated with the strike. This result is partially a function of the instrument error, the range in values found by duplicating a single measurement at precisely the same point in space (Section 4-8).

Woodcock (1976) stated that for planes exhibiting low to medium dip the error in recording the dip is less than 2° whereas the error in recording the strike may vary up to 15°. Fecker and Rengers' recording technique has no means of assessing this variable instrument error and as a result it is impossible to distinguish the stereonet scatter caused by instrument error from the scatter caused by surface roughness. Instrument errors in some instances could be considerably larger than the variations caused by surface roughness. It is therefore not correct to evaluate the surface roughness from a stereonet without correction for instrument errors. No case histories were cited by Fecker and Rengers to correlate various values of roughness with i angles existing in the field.

Krahn (1974) used a small scale mechanical roughness tracer to record the profiles of natural discontinuities on 5cm and 15cm long samples. The traces were then digitized to form a series of discrete x-y points which were stored on a computer magnetic tape. From this digital data, several numeric characterizations of surface roughness often used by mechanical engineers were calculated. These were the CLA, the centre line average, RMS, the root mean square value and the Z2 and Z3 parameters. The RMS is defined numerically as

$$x=n$$

$$\mathrm{RMS} = 1/n \qquad Y^2\,dx \qquad\qquad 4.7$$

$$x=0$$

where n = number of amplitude measurements

Y = the amplitude of roughness about a mean of zero

and dx = a constant distance between amplitude readings.

The CLA is represented by

$$x=L$$

$$\mathrm{CLA} = 1/L \qquad Y\,\,dx \qquad\qquad 4.8$$

$$x=0$$

where L = distance over which the readings are taken.

The RMS differs from the CLA in magnitude only and is

11% larger.

The Z2 parameter is basically the RMS of the first derivative of the surface profile and is defined as;

$$Z2 = 1/L \int_{x=0}^{x=L} (dy/dx)^2 \, dx \qquad 4.9$$

The Z3 parameter is the RMS of the second derivative of the profile and reveals the roundness of the profile peaks

$$Z3 = 1/L \int_{x=0}^{x=L} (d^2x/dx^2)^2 \, dx \qquad 4.10$$

Krahn (1974) recorded the profiles of limestone samples extracted from the debris of the Frank Slide prior to performing a series of direct shear tests. The roughness characterizations found from these profiles were plotted against the peak friction angles found for the samples and a linear correlation between $\emptyset p$ and the Z2 parameter was defined (Figure 4-8). This result theoretically makes it possible to define the peak friction angle of a sample by recording the sample profile and calculating Z2. Krahn concluded however that this approach was not practical as the time and effort involved in calculating Z2 is much greater than performing a 5cm x 5cm direct shear test.

The obvious extension to this work required the characterization of the Z2 parameter on a larger field scale but extrapolation of this technique was not successful. Krahn (1974) measured three profiles with a maximum length of 1.5 m in the field but concluded that these were not representative of the large scale roughnesses found on natural slopes. Equipment limitations and small exposures of failure surfaces prohibited the use of this technique over a larger area. In addition no large scale shear tests could be run to define a correlation between the large scale i and the in situ angle of friction. Krahn did conclude on the basis of a back analysis that the i angle acting on very large surfaces was extremely small. This conclusion, however, is highly dependent upon the choice of ϕb, which as will be demonstrated in Chapter 5 is a variable parameter and is highly dependent on geological interpretation.

Barton (1971) tried to avoid the problem of measuring i angles on several scales by correlating the effective asperity inclination to the uniaxial compressive strength of the unweathered rock material. After conducting a series of shear tests on plaster specimens and plotting the results on a graph of log (C/N) versus i (Figure 4-9), Barton obtained the relationship

$$i = 10 \log (C/N) \qquad 4.11$$

where C = uniaxial compressive strength of the intact rock and

N = normal stress acting during shear.

The shear strength along a discontinuity was then given by

$$T = N \tan(JRC \log (C/N) + \phi b) \qquad 4.12$$

where JRC = the joint roughness coefficient, a modifier dependent on the roughness profile of the sample

and ∅b = the basic friction angle assumed by Barton to be 30 degrees.

Unfortunately the problem of estimating i has not been totally avoided as it is still necessary to evaluate the JRC. Barton's technique was to trace the profile of a rock surface then compare the trace with a set of standard profiles which had known JRC values (Figure 4-10). Recent work by Tse (1978) has shown that a straight line correlation exists between the JRC values defined by Barton and the Z2 parameters of Barton's standard profiles. This eliminates the qualitative comparisons previously used and thus numerically evaluates JRC for any sample. The problem of obtaining large scale profiles has not been eliminated however, and so for field use the JRC still has to be assessed qualitatively.

4-3 Previous Analyses of Roughness Measurements

Hoek and Bray (1974) in summarizing the previous work of Patton (1966) and Barton (1971) suggest that variations in shear strength due to scale effect were not properly taken into account. In an attempt to overcome this discrepancy Hoek and Bray graphically linked the work of Barton (Figure 4-9) with the results of Fecker and Rengers (Figure 4-6) to obtain a graph of the effective i angle versus the scale of measurements (s) over which the i angle was evaluated (Inset Figure 4-11). The original points defined by Fecker and Rengers (1972) shown in Figure 4-11 were enclosed by two straight lines drawn by Hoek and Bray (1974). These lines however, are poor fits to the data points shown. Further, they imply that for scales greater than 10m, i is equal to zero. However, large scale folds with wavelengths of 10 m and larger are found in the Rocky Mountains and the variations in dip created by these folds are considerably greater than zero degrees. It is interesting to note that this technique has since been abandoned by Hoek and Bray (1977).

Cruden (personal communication, 1974) has investigated the theoretical behaviour of variations in i with scale. Cruden assumed that a true profile of a natural surface could be approximated by a large number (n) of straight line elements (dL). This implies that as n approaches infinity, the profile y=f(x) is everywhere continuous and differentiable. These small lines, treated as unit vectors make angles θ with the mean orientation of the surface.

Cruden assumed that the Von Mises circular normal distribution accurately reflected the distribution of the orientations of the vectors data so that the length R, the resultant of the n unit vectors is given by

$$R = n(1 - 1/2\ k') \qquad 4.13$$

where k' is the best estimate of k

and k is the standard deviation of a Von Mises distribution given by $M(0,k)$.

For large values of R the Von Mises distribution can be approximated by the Normal Distribution represented by

$$N(0,k^{-1/2}) \tag{4.14}$$

The mean of n observations from a normal distribution is normally distributed with parameters

$$(0,kn^{-1/2}) \tag{4.15}$$

where 0 = mean and

$kn^{-1/2}$ is the standard deviation.

Therefore, the lines of length dL from a profile, have a distribution about the true orientation of a plane given by

$$N\ (0,(kn)^{-1/2}) \tag{4.16}$$

However $n=L/dL$ and therefore the distribution of lines of length L becomes

$$N\ (0,(kL/dL)^{-1/2}) \tag{4.17}$$

which implies that

$$i = x\,L^{-1/2} \qquad 4.18$$

where x is a constant.

Figure 4-11 illustrates the similarity in results between the experimental data of Fecker and Rengers and the theoretical distribution defined by Cruden. Equation 4.18 may be a basis for extrapolating i to large scales but it has yet to be verified experimentally. In summary then, the concept of measuring Øb in the laboratory and evaluating an i angle at the appropriate field scale appears to follow accepted guidelines published by Patton (1966), and more recently by Hoek and Bray (1974) and Goodman (1976). No method has yet been reported which can be used as a satisfactory design tool for evaluating i at large field scales.

A new technique for evaluating large scale roughness in the field has been derived which uses only a geological compass to record data. The simple two dimensional method works in areas of poor bedrock exposure and requires no special equipment. Only a pocket calculator is required to evaluate the results. This new technique is a modification of a method presented by Kerrich (1974) and is outlined in section 4-5.

4-4 Theory Of Roughness Evaluation

The two dimensional model was contrived by Kerrich (1974) to evaluate the mean orientation of a family of discontinuities for design purposes. Kerrich evaluated the scatter in joint dips by computing a mean dip and a variance for each joint set. The variances of the readings were treated as errors which had to be removed in order to delineate the true orientation of a discontinuity set for rock slope design purposes. Using a similar technique but considering the variances as roughness indicators instead of errors, it is possible to evaluate the variances or standard deviations in joint orientations and to correlate these statistics with i angles evaluated independently by other methods. The following is a summary of the theory as developed by Kerrich (1974).

θ is a measurement of the dip of a discontinuity on any fabric element. Assume the fabric element is planar within the scale of the outcrop being examined.

Assume that

$$\theta = d + z + w + e \qquad 4.19$$

where e is partially the observational error due to the instrument and the operator, and partially a measure of the very small scale roughness at any location. The error e is introduced by replicating a measurement at any given spot on the surface.

w is the error associated with trying to define the true orientation of a single joint surface. w represents the roughness of a single discontinuity.

z is the differences in roughness found on different discontinuities in the same set on the same outcrop.

and d is the true average value of dip of a discontinuity set.

For every set of discontinuities an indefinitely large number or population of possible dip measurements exists. This population possesses position and scatter, respectively represented by $E(\theta)$ and $\text{sigma}^2(\theta)$. Similarly the remaining variables z, w, and e also possess expected values and variances.

Assuming that z, w and e are all random and independent variables with zero expected values

then

$$E(\theta) = d + 0 + 0 + 0 \qquad 4.20$$

and

$$\text{sigma}^2(\theta) = \text{sigma}^2(z) + \text{sigma}^2(w) + \text{sigma}^2(e) \qquad 4.21$$

(after Kerrich 1974)

Let θj, $j=1,n$, be a random sample of dip measurements. The sample has a mean given by

$$E(\theta) = \sum_{j=1}^{n} \theta j/n \qquad 4.22$$

and a variance estimated by

$$S^2(\theta) = \sum_{j=1}^{n} (\theta j - \theta')^2 / n-1 \qquad 4.23$$

The expected value of θ, θ', the mean of the recorded dip values, is an estimate of d. The expected value of the variance, $S^2(\theta)$, is an estimate of the variance sigma $^2(\theta)$. Therefore $S^2(\theta)$ is also an estimate of sigma^2(z)+sigma^2(w)+sigma^2(e). However, what we need is an estimate of sigma^2(w) or sigma^2(w)+sigma^2(z). A distinction between sigma^2(w) and sigma^2(z) only becomes necessary when the roughnesses measured differ significantly between discontinuities.

Evaluation of sigma^2(e) is necessary in order to remove the influence of operator error from the above data.

The method of analysis suggested by Fecker and Rengers does not distinguish between the various types of roughness outlined above and indeed the roughnesses measured by Fecker and Rengers are estimates of z+w+e grouped together.

In order to evaluate $S^2(e)$, repeated samples of the discontinuity orientation are taken at the same point. Variations in placement of the compass and reading of the compass lead to small variations in the recorded dips. The rougher the surface the harder it is to replace the compass in the exact same position which increases the operator error $S^2(e)$.

By repeating this procedure at several locations on a single discontinuity $S^2(w)$ can be evaluated. By varying the distances between measuring locations it is possible to evaluate $S^2(z)$ and $S^2(w)$ on several different scales. As long as the mean values (i.e. the $E(\theta)$ from which the variances are being calculated), do not change significantly, the distances between stations, and hence the scale of $S^2(w)$ can be extended over very large areas.

The mathematical reduction of the data is simple. A mean and a variance were calculated for each scale investigated. Analysis of variance tests were performed on all the calculated means to test whether all were samples from one population (Walpole, 1968).

The variances calculated for any given scale were also tested for homogeneity using Bartlett's test (Walpole,1968,p.299) Upon completion of the statistical tests, all of which are based upon variances, the variances were reduced to standard deviation values. The standard deviations were more practical as these quantities were similar in magnitude to both Patton's and Fecker and Rengers results.

In addition, the standard deviation is a more efficient estimation of dispersion than the half range. An estimate of roughness using standard deviations requires fewer observations than an estimate using the range for a given level of confidence. For large samples the difference in efficiency is very large (Cruden and Charlesworth, 1976). In addition the standard deviation in a normally distributed set of data is proportional to the data range. The range values, however, are dependent on the sample size while the standard deviation is independent of sample size. Furthermore, as the distribution of estimates of the standard deviations for normal populations is well known, estimates of precision for various confidence limits can easily be made.

The use of the standard deviation as a roughness indicator improves the technique forwarded by Fecker and Rengers. The parallelism of the lines in Figure 4-12 indicates how the simple two dimensional technique gives similar results to the already accepted method developed by Fecker and Rengers.

4.5 Experimental Verification of Roughness Evaluation

Roughness was estimated on the basis of over 1800 bedding surface measurements taken at both Jonas Creek and Whitehorse Creek rock slides. Preliminary work consisted of taking measurements with a CLAR geological compass to establish the structural domains found on the rock surface. These mapping results were discussed earlier in Chapters 2 and 3 and will not be dealt with further.

Measurements were recorded from the first four stations occupied at Whitehorse Creek using a CLAR compass placed on 1.9 cm thick plywood discs 10 cm, 20 cm and 50 cm in diameter to verify the universality of Fecker and Rengers results (1971). A set of readings was also taken using only the square aluminum back of the compass which measured 4 cm by 4 cm. The poles to the compass base plate at each station for each size of base plate were plotted on a polar equal area net and a line enclosing all the points was drawn to represent the range in orientation data. The results from station 1 are illustrated in Figure 4-13.

The method simulated as closely as possible that of Fecker and Rengers (1971). Fecker and Rengers maintained that the use of a stereonet allowed the calculation of the roughness in any direction. The previous arguments with respect to operator error would indicate this to be incorrect. In all the cases reported by Fecker and Rengers (Figure 4-7) and for those stations recorded at Whitehorse Creek the range of the dip of the poles to the bedding surfaces was approximately 1/2 the range of the dip directions as predicted by Cruden and Charlesworth (1976). Table 4-1 is a summary of the ranges in dip and dip direction established at Whitehorse Creek.

The maximum dip deviation, estimated to be one half the range of dips measured in the dip direction, was recorded for each disc size and a graph of maximum dip deviation versus base plate diameter was constructed (Figure 4-12).

The trend of decreasing maximum range in i associated with increasing disc diameter closely mirrors the trend of the data gathered using Fecker and Rengers' method which combines dip and dip direction. The trend of Fecker and Rengers' data is also shown in Figure 4-12 for comparison. The dip data recorded using the CLAR compass on the wooden disc was analyzed in order to compare the new roughnesses established with those established by Fecker and Rengers method. The maximum value of S(w), the standard deviation for each disc size, was plotted versus s, the disc diameter and is also shown on Figure 4-12.

The similarity in the results is illustrated by the near parallelism of the lines depicting surface roughness variations.

The new method of analysis is preferred, however, due to

1) The use of a standard deviation value as opposed to range values.
2) The influence of operator error can be evaluated and removed.
3) The data can be reduced very easily.

The data from Whitehorse Creek, recorded at an early stage in the field exploration programme, appeared to verify the new method of evaluating roughness. As a result a standardized system for measuring and recording the data was established.

A cross with 0.3 m long arms parallel and perpendicular to the estimated dip direction of the discontinuity surface, was marked with water soluble paint on the exposed rupture surface at the desired station location. Figure 4-14 is a schematic drawing accompanied by field data recorded for one such station at Whitehorse Creek. Three observations of dip and dip direction were recorded at the centre of the cross and at the end of each arm to evaluate S(e) the standard deviation of operator error and the 0.03 m scale of roughness combined. The five resulting dip values of S(e) were then averaged to produce 1 value of S(e) per station. A sample calculation is shown in Figure 4-14. Table 4-2 summarizes the S(e) values of dip measurements found at the rock slides investigated. It is apparent from this table that the S(e) values of dip were reasonably constant at each area studied. Comparison of the variances at each area revealed that all individual S(e) values belonged to one population.

The quartzite bedding surfaces at Jonas Creek on this 0.03 m scale were relatively smooth. The corresponding average S(e) value was 1.2°. The dolomite surface at Whitehorse Creek was slightly rougher in places due to differential weathering around chert nodules and the formation of micro-karst features such as karren. The average S(e) value at Whitehorse Creek reflected this change in roughness. The average value of S(e) at Whitehorse Creek was 1.6°. It was reassuring to note also that the higher values of S(e), measured at Whitehorse Creek, corresponded well with qualitative evaluations of roughness made during the field mapping.

The next scale of roughness evaluated consisted of the 0.30 m scale. This size lay midway between Patton's first and second order irregularity scale. In order to evaluate this scale the 3 measurements of dip recorded at each point of the station crosses were averaged to produce one value. The five resulting dips were then used to produce a mean and a standard deviation S(w) for each station.

The variances, $S^2(w)$, were tested for homogeneity using Bartlett's test (Walpole, 1968) and it was found that values of S(w) could be separated into two separate populations with standard deviations above and below 4.50°. The majority of the standard deviations at Jonas Creek were less than 4.50° and averaged 2.90°. The higher values of S(w) ranged from 4.50° to 7.35° and averaged 5.45°.

These groups were referred to as normal and rough standard deviations for further analysis. These results are summarized in Table 4-3. Inspection of these results indicates that roughness on this scale can vary radically over small distances (see bedding surface #10 at Jonas Creek, Table 4-3).

At Whitehorse Creek the majority of the normal surfaces had standard deviations averaging 2.79° while the rough surfaces averaged 6.85° and ranged as high as 9.10°. Again, a high degree of variability could be seen in the roughnesses within short distances. Qualitative evaluations of roughness made in the field are shown in Table 4-3 and it is reassuring to note that the areas exhibiting high standard deviations had been previously evaluated as rough. Field evaluation of roughness in a qualitative fashion between stations on any given bedding surface seemed to reflect the roughnesses evaluated using standard deviations. Evaluations of roughness between bedding surfaces were more difficult as the stations were not within sight of each other.

Evaluation of S(w) on the 3.0 m scale of roughness was accomplished by grouping together all the stations on one bedding plane. The stations were all 3.0 m apart and each had a mean dip value derived from the five averages on the 0.30 m scale. Analysis of variance tests were conducted on all the bedding planes to test whether the dip means on the 0.30 m scale belonged to one population. In addition the new set of variances was tested for homogeneity using Bartlett's test. No significant differences existed in either case.

The standard deviations on the 0.3m scale were used to divide bedding surfaces into rough or smooth categories. (Table 4-3). This distinction was noted in Table 4-4, a summary of the 3.0 m scale of roughness. The qualitative field evaluations of roughnesses were also noted.

At Jonas Creek, the average standard deviation on the 3.0 m scale of roughness, for the beds defined as smooth on the 0.30 m scale of roughness, was slightly greater than the average standard deviation of the rough beds. This implied that extrapolation of roughnesses from small scales to large scales would lead to incorrect results. At Whitehorse Creek however, the rough bedding planes defined by the smaller 0.3m scale S(w) agreed well with the 3.0 m scale S(w) values. As a result, even though there was no statistical difference between families the beds were kept separated into rough and smooth groups at this stage. They were grouped together at a later stage, however, to evaluate the next larger scale of roughness.

On the basis of the above finding it would appear that roughnesses on the various scales must be evaluated independently as small scale roughness may not always reflect the roughness at larger scales.

Results for Jonas Creek on the 3.0 m scale indicate that the average standard deviation for all the bedding surfaces measured was 3.16° but varied from 2.17° to 4.35° . Comparison of these variances failed to find any significant differences between bedding surfaces at the 95% confidence level. This would tend to support Patton's hypothesis that roughness may be evaluated on similar discontinuities when the original or incipient failure surfaces are concealed.

At Whitehorse Creek, 5 of the 7 bedding surfaces analyzed at the 3.0 m scale had standard deviations which averaged 3.09° and ranged from 2.65° to 3.81°. These results were similar in nature to Jonas Creek results. The remaining two bedding planes, however, which prior to any calculations had qualitatively been evaluated as very rough had an average variance of 5.46° and ranged from 4.60° to 6.32°.

The next larger scale, the 30.0 m scale, was evaluated using all the data collected over each failure surface. In the first instance, because there was no significant difference between bedding surfaces on the 3.0 m scale, it was possible to group the average dips from each individual bedding surface together to evaluate the roughness. Because the failure surface at Jonas Creek steepened perceptibly with elevation (Chapter 2) only those bedding surfaces which exhibited similar dips were compared. The surface was divided into 3 zones of dip: those dips less than 30°, dips ranging from 30° to 35° and those dips greater than 35°. There were insufficient stations to compute the large scale roughnesses on the sections with dips greater than 35° and less than 30°. Only the large scale roughness for the intermediate dips was found. The bedding surface measurements grouped in this manner were used to calculate a mean and hence a standard deviation for this scale at each slide. The large scale standard deviation was 1.45° and 2.65° at Jonas Creek and Whitehorse Creek respectively.

4-6 Correlation of Variances with i

In order to illustrate the compatibility of the new method of analysis with other techniques the maximum values of standard deviation S(w) for each scale size were plotted on a graph. The average values or the minimum values could also have been used. A line connecting the points defined by $i = x\ (L^{-1/2})$, previously established as a good theoretical model for roughness variation, was also plotted on the graph. The near parallelism of the lines shown in Figure 4-15 illustrates that the new two dimensional technique gives a true representation of the surface roughness. In addition, as has been previously noted, the indicator S(w) can be correlated with the qualitative evaluations of roughness made in the field.

Compilation and removal of S(e), the operator error, and the 0.03 m scale of roughness combined isolated the values of S(z) and S(w) on the larger scales of roughness. The 0.03m scale of roughness can easily be evaluated during shear testing of small scale (5 cm x 5 cm) laboratory samples. In addition the i angles established at this scale are at least as small as Patton's second -order irregulanities and hence are of little significance. (Deere et. al. 1967). The remaining values of standard deviations represent values of i existing on the rock surface at different scales. These standard deviations, in order to be useful, must be correlated with actual i angles by independent techniques.

The first method emulated Patton's technique of photographing bedding surface profiles. Plate 4-1 is a sample photograph taken in the vicinity of areas previously mapped by compass. The average i angles, found by Patton (1966) to be the controlling i values, were then recorded for scales varying from 10 cm to 10 m.

The i angles reported by Patton for first-order irregularities varied from 10° to 20°. The first order irregularities measured in Figure 4-16 ranged from 2°-25° thereby supporting the use of this procedure. Figure 4-16 shows a set of histograms illustrating how the i values varied from each scale of roughness. All the i values measured on the photos were absolute values, therefore only one half of the histogram has been drawn. The means and standard deviations of the i values measured from the photos at various scales are shown on Figure 4-16.

In addition, slope profiles approximately 30 m and 60 m long were recorded on exposed bedding surfaces at both Jonas Creek and Whitehorse Creek rock slides using conventional surveying techniques. Figure 4-17 illustrates these profiles. The 0.30 m scale i angles measured from these profiles ranged from 1° to 22° and agreed well with the values for this scale reported by Patton (1966). An example of the various i angle means and standard deviations for the 60 m long Jonas Creek profile can be seen in the histograms in Figure 4-16.

Compass readings were systematically taken along the profiles established by photos or transit and the average i angles measured from the profiles were compared with the values of standard deviations calculated for various scales. A graph linking the S(w) values on all scales with the respective average i values was constructed and is shown in

Figure 4-18. The means and standard deviations of the S(w) and i values give rise to the points and error bars in Figure 4-18. The points without error bars indicate the measuring scales which had only one S(w) value. A straight line correlation was established which made it possible to evaluate the i angles acting on all the scales previously examined.

The half ranges of the data scatter, suggested by Fecker and Rengers (1971) to be an accurate reflection of the i angles existing on a slope, were compared with the standard deviations measured for the four original stations at Whitehorse Creek. The correlation between the two, illustrated in Figure 4-19 is a straight line relationship defined by

$$R/2 = 1.1 + 1.08\ i_n \qquad 4.26$$

where R/2 refers to the i value defined by Fecker and Rengers' technique

and in is the i angle established using the new S(w) method.

A similar comparison was made between the i angles predicted using the new technique with those predicted using Krahn's Z2 method. The profiles from Jonas Creek and Whitehorse Creek were digitized using points 0.3 m apart and the Z2 values were calculated. The Z2 values were then converted to Øb+i values using figure 4-8. The Øb value of 7°, shown on the graph in figure 4-8 as the ordinate intercept, was then subtracted from the Øp values in order to define the topographic component, i.

Manipulation of the Z2 parameters defined for the profiles yielded i angles of 13° and 11° for Jonas Creek and 9° for Whitehorse Creek. These i values, designated as iz, were compared with i values evaluated using the new method on the 0.3m scale.

The new values were 6.2°, 6.2° and 4.0° for Jonas Creek and Whitehorse Creek respectively. The Z2 values were also calculated for the 3.0m scale. The i values for this scale corresponded to 5° and 4° for Jonas Creek but unfortunately there were not enough points on the Whitehorse Creek exposure to compute a reliable estimate of a large scale Z2. The average i angles for the 3.0m scale at Jonas Creek corresponded to 1.4° and 1.3°. An attempt was made on the basis of only these 5 points to define a straight line relationship linking the i values defined by the Z2 parameter with the new method (Figure 4-20). The relationship was found to be;

$$iz = 2.5° + 1.5\ in \qquad 4.27$$

where iz is the i angle defined by Krahn

and in is the i value estimated from S(w) values using Figure 4-18.

This relationship is of little consequence however as it is often impossible to evaluate Z2 on large scales due to the lack of surface exposure. Neverthless it is reassuring to note that a straight line relationship exists between the two techniques.

Finally the technique proposed by Barton (1971) was used in conjunction with the relationship defined by Tse (1978) to define JRC values from the Z2 profile parameters. The relationship defined by Tse is given by

$$JRC = -7.5 + 86.8\ Z2 \qquad 4.28$$

This is illustrated in Figure 4-21.

The JRC values defined by this expression,corresponding to the previously calculated Z2 values of the large profiles, were 5.52, 2.31 and 0.75 for the 0.3m scale. The values of the JRC estimated for the 3.0m scale gave negative numbers which were of no physical significance. These were therefore equated to zero.

The correlation between i values and JRC values is defined by Barton as

$$ib = JRC \log(C/N) \qquad 4.29$$

where ib refers to Barton's i values.

For the normal loads found at both Jonas Creek and Whitehorse Creek the ratio of C/N has a maximum value of 100 (Barton, 1974b), which reduces the above equation to

$$ib = (JRC) \times 2 \qquad 4.30$$

The resulting i values calculated from the JRC values noted previously correspond to 1.0°, 4.6°, 1.5°, 0° and 0°. The resulting low i angles may indicate a sensitivity of the JRC to measure i at low roughness values. A straight line relationship linking the new i values with the JRC values was defined from the above 5 points. This relationship is given by

$$JRC = -1.32 + 0.79 \text{ in} \qquad 4.31$$

and is shown in Figure 4-22.

The application of this relationship based on so little data would be irresponsible at this time. However this preliminary finding does imply that large-scale now roughnesses can be evaluated quantitatively and used in Barton's relationship. Table 4-5 is a summary of all the equations and i angles discussed above.

4-7 Discussion

A review of the results from the previous section illustrates several important observations.

On the 0.30 m scale of roughness, a large range of variances was observed which could be split roughly into 2 populations. The full significance of these roughnesses only becomes obvious when the stations and their respective standard deviations or i values were plotted on an air photo. Plate 4-2 is a map of Jonas Creek showing the failure surfaces and the station locations. All the stations found on the exposed failure surface had a standard deviation cut off established by statistical tests which separated the results into normal or rough surfaces. No standard deviations greater than 4.5° were found anywhere other than around the edge of the unfailed mass sitting between the two failure surfaces.

At Whitehorse Creek 7 of the 8 anomalously high standard deviations are located near the slide margins

(Plate 4-3). The remaining high standard deviation is on the failure plane. The implications of this result are noteworthy. The first order irregularities, thought by Patton to be the controlling factor in slope stability appear to play a large role in the stability at Jonas and Whitehorse Creek rock slides. Failures only occurred where the 0.30m scale of i angles were less than 7° (s(w)=4.5°) and did not occur in areas with i angles greater than 7°.

On the 3.0m and 30.0 m scales of roughness no significant patterns could be established which could be used to distinguish stable from unstable slopes. The standard deviations on the 3.0 and 30.0m scales as a whole were lower than those found on the 0.3m scale. This implied that if and when the first order irregularity strength was overcome by natural processes only a lower or equivalent value of i was available on the slopes studied and hence failure could not be avoided. A summary of the i angles found at the various scales is given in Table 4-6.

4-8 Conclusions

The problem of evaluating various topographic components of roughness on a large field scale has not been satisfactorily dealt with in the past. However a new method has been designed and tested which appears to fit all the necessary requirements. The new method can evaluate roughness angles on scales from 0 to 30.0m, maximizes the use of small areas of exposed failure surface, and does not need special equipment to record data. A simple analysis which can be carried out on a pocket calculator is used to estimate i values.

Results indicate that, at Jonas Creek and Whitehorse Creek, failure is controlled by first order, 0.30m scale irregularities. The tremendous variation which can occur in roughness over small scales should be noted. The i angles vary from 0.5° to about 14° within a distance of less than 15m along the south margin of the north slide at Jonas Creek. It is therefore imperative that the 0.3m scale of roughness be well documented over the face of a site map regardless of the bedding surface exposed. The lowest value of i at this scale will doubtless control the topographic component of shear strength along a given bedding plane.

Observations of these failed slopes show that the i angles have decreased or remained approximately equal as the measuring scale has increased. As a result, if the small scale i angle is overcome, only smaller i angles remain and failure cannot be averted. The decline of the i angles with an increase in scale is what might be expected at random.

The i values for all scales are statistically equivalent from bedding plane to bedding plane. This result was implied by Patton (1966) when he suggested estimating the i angles on various surfaces.

The low i angles recorded for large scales of roughness agree with Krahn's conclusion that i is close to zero on failed slopes. This conclusion may not apply to all slopes.

It is based on a biased sample as failure has already occurred in the slopes measured. Further studies of stable slopes may be necessary prior to the acceptance of this tool as a design method.

The application of this new method of evaluating roughness will ensure that large scale roughnesses can be measured. In addition, many of the measurements will have to be taken in order to define the orientation of the rupture surface.

The analyses carried out at Jonas Creek and Whitehorse Creek are 2-dimensional in nature and have only been carried out with respect to dip values due to the planar nature of the slides. Deviations in strike can also be evaluated and hence roughness in the strike direction can be evaluated.

In cases where failure does not occur directly down dip, such as in a wedge failure, calculations of roughness may have to be carried out on values of apparent dips, calculated by a stereonet analysis prior to treatment using the new method of evaluating roughness.

TABLE 4-1

Range of dip and dip direction values found at Whitehorse Creek using Fecker and Renger's method

STATION #	RANGE IN	PLATE DIAMETERS (cm)		
		50	20	10
1	dip	5	6	6
	dip direction	13	17	10
2	dip	3	6	8
	dip direction	11	18	19
3	dip	5	6	8
	dip direction	5	18	13
4	dip	2	6	6
	dip direction	6	9	8

TABLE 4-2

S(e), The operator error values established at Jonas Creek and Whitehorse Creek.

JONAS CREEK		WHITEHORSE CREEK	
STATION #	S(e)	STATION #	S(e)
200	1.03	100	1.03
201	1.22	101	0.85
202	1.15	103	1.32
203	1.21	104	0.57
204	1.16	105	0.89
205	1.26	106	1.00
207	1.18	107	2.28
208	1.79	108	1.07
209	1.73	109	0.84
215	0.69	110	1.55
216	1.53	111	2.06
217	0.63	112	1.10
219	0.93	114	1.12
220	1.46	115	2.72
222	1.53	123	0.55
224	1.00	124	2.80
226	1.82	131	1.36

TABLE 4-2 CONTINUED

300	1.16	132	1.34
301	0.63	133	1.57
302	1.57	134	3.52
303	1.00	135	3.33
304	0.81	136	0.76
305	0.58	137	0.81
306	0.89	138	2.76
307	1.10	139	1.95
308	3.12	146a	1.48
309	0.45	146b	1.91
310	0.81	147a	2.15
311	0.68	147b	1.44
312	1.29	147c	1.79
AVG.	1.18	AVG.	1.60

TABLE 4-3

Summary of the S(w) values for the 0.3 m scale.

JONAS CREEK

BED Pl.#	STAT.#	S(w)	Field Evaluation
1	200	3.08	smooth
1	201	2.47	smooth
1	202	3.01	smooth
2	203	4.37	rougher
2	204	3.03	than
2	205	3.49	B.P.1
3	207	3.19	rougher
3	208	3.48	than
3	209	1.95	B.P.1
10	215	5.22	
10	216	6.12	
10	217	3.08	
11	219	2.33	
12	220	2.56	
13	222	4.50	
14	224	4.78	
15	226	2.52	

TABLE 4-3 CONTINUED

16	300	1.60	
16	301	2.20	
17	302	3.31	
17	303	3.61	
17	304	4.52	moderately
17	305	4.28	rough
17	306	1.81	
17	307	3.72	
18	308	6.96	
18	309	1.85	
18	310	5.04	
19	311	7.35	
	1 19		
	312	4.55	
Rough Avg.		5.45	
Smooth Average.		2.90	

TABLE 4-3 CONTINUED

Summary of S(w) values for the 0.3 m scale

WHITEHORSE CREEK

BED PL.#	STA.#	S(w)	field roughness
1	1	2.10	smooth
1	1	2.10	
1	1	4.43	
1	35	2.74	
3	4	1.90	
3	5	1.00	
3	6	2.61	
3	37	3.59	
4	7	9.10	very
4	38	3.85	rough
4	39	5.16	
5	8	3.54	
5	9	1.76	rough
6	10	6.86	
7	11	3.16	
8	12	3.19	
9	14	1.34	
9	15	5.76	
10	16	3.42	

TABLE 4-3 CONTINUED

11	22	6.15
12	31	2.43
12	32	2.24
12	33	3.87
12	34	3.24
13	24	3.11
15	46a	2.41
15	46b	6.16
16	47a	3.97
16	47b	1.70
16	47c	3.36
Rough Average.		6.85
Smooth Average.		2.79

TABLE 4-4

Summary of roughness on the 3.0 m scale

JONAS CREEK

BED. PL.#	ROUGHNESS	S(w)	Roughnesses from Table 4-3
1	smooth	2.53	smooth
2	rougher	3.78	smooth
3	rougher still	4.36	smooth
10	rough	3.26	rough
17	med. rough	3.22	rough
18	med. rough	2.83	rough
19	rough	2.17	rough
Average S(w)		3.16	

TABLE 4-4 CONTINUED

WHITEHORSE CREEK

BED.PL.#	ROUGHNESS	S(w)	from Table 4-3
1	smooth	2.98	smooth
3	smoother	2.65	smooth
4	rough	6.32	rough
5	med.rough	2.81	smooth
12	very rough	3.81	smooth
T1 15	med.rough	4.60	rough
16	no estimate	3.22	smooth

Average S(w) for smooth beds	3.09
Average S(w) for rough beds	5.46

TABLE 4-5

A Synthesis Of The Various i Angles Calculated Using Several Methods

SCALE	S²(w)	ip	if	ib	iz		
0.30 m	18.0	6.2	7.8	11.0	13.0		
	13.6	6.2	7.8	4.6	11.0		
	16.7	4.0	5.4	1.5	9.0		
3.0 m	7.1	1.4		0.0	5.0		
	2.4	1.3		0.0	4.0		
	1.4	1.8				5.7	0.7
	6.2	3.5		16.8		6.0	
30.0 m	5.4	1.3					
	3.4	0.7					
	1.3	1.9					

The values of iz,ib,if can only be evaluated on the 0.3 m scale. S(w) are values found using the new method of evaluating roughness.

ip are i values found using Patton's profiling technique.

if values found to be given by if=1.1 + 1.08 in.

iz values found using the calculated Z2 parameters from Figure 4-17.

ib values calculated from JRC values estimated using Z2 in conjunction with Tse's formula and i=2JRC after Barton.

TABLE 4-6

Summary of i angles found on the various scales.

JONAS CREEK

SCALE	AVERAGE i	RANGE IN i
0.3 m	3.8° (normal)	1° to 7.0°
0.3 m	8.9° (rough)	7.0° to 12.9°
3.0 m	3.2°	2.2° to 4.4°
30.0 m	0.3°	single value only

WHITEHORSE CREEK

SCALE	AVERAGE i	RANGE IN i
0.3 m	3.5° (normal)	0.0° to 7.0°
0.3 m	11.8° (rough)	7.0° to 16.3°
3.0 m	4.1° (normal)	3.2° to 5.6°
3.0 m	8.9° (rough)	7.2° to 10.7°
30.0 m	2.8°	single value only

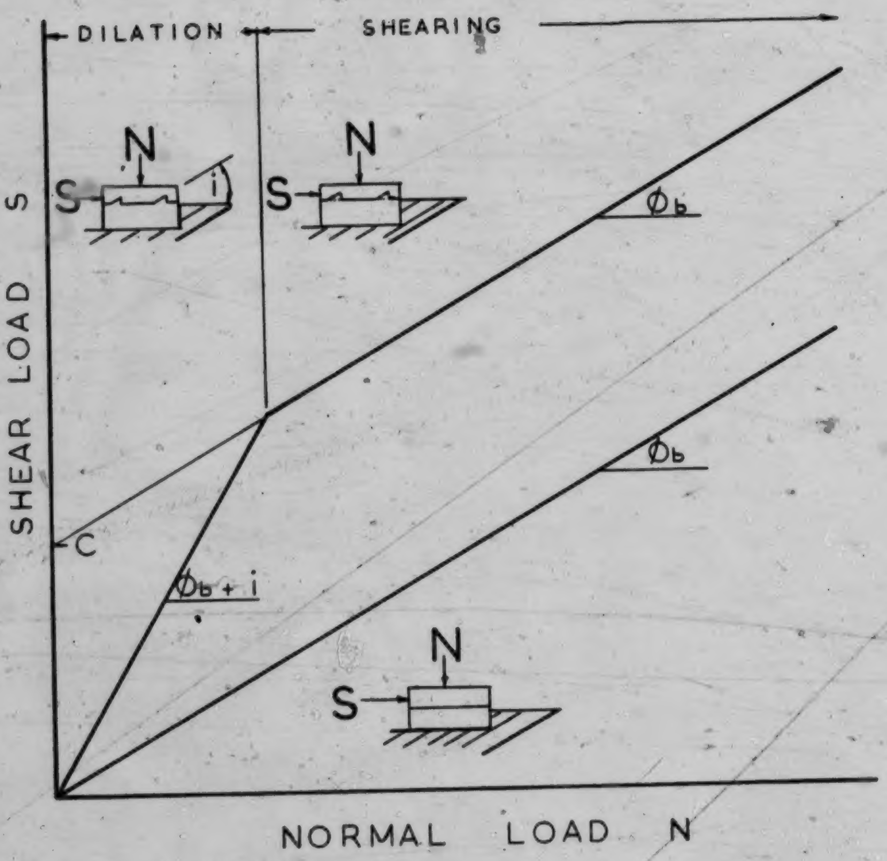
DILATION
SHEARING
SHEAR LOAD S
NORMAL LOAD N
N
S
i
N
S
ϕ_b
ϕ_b
C
$\phi_b + i$
N
S

FIGURE 4-1 Idealized Bilinear Failure Envelope (After Patton ,1966).

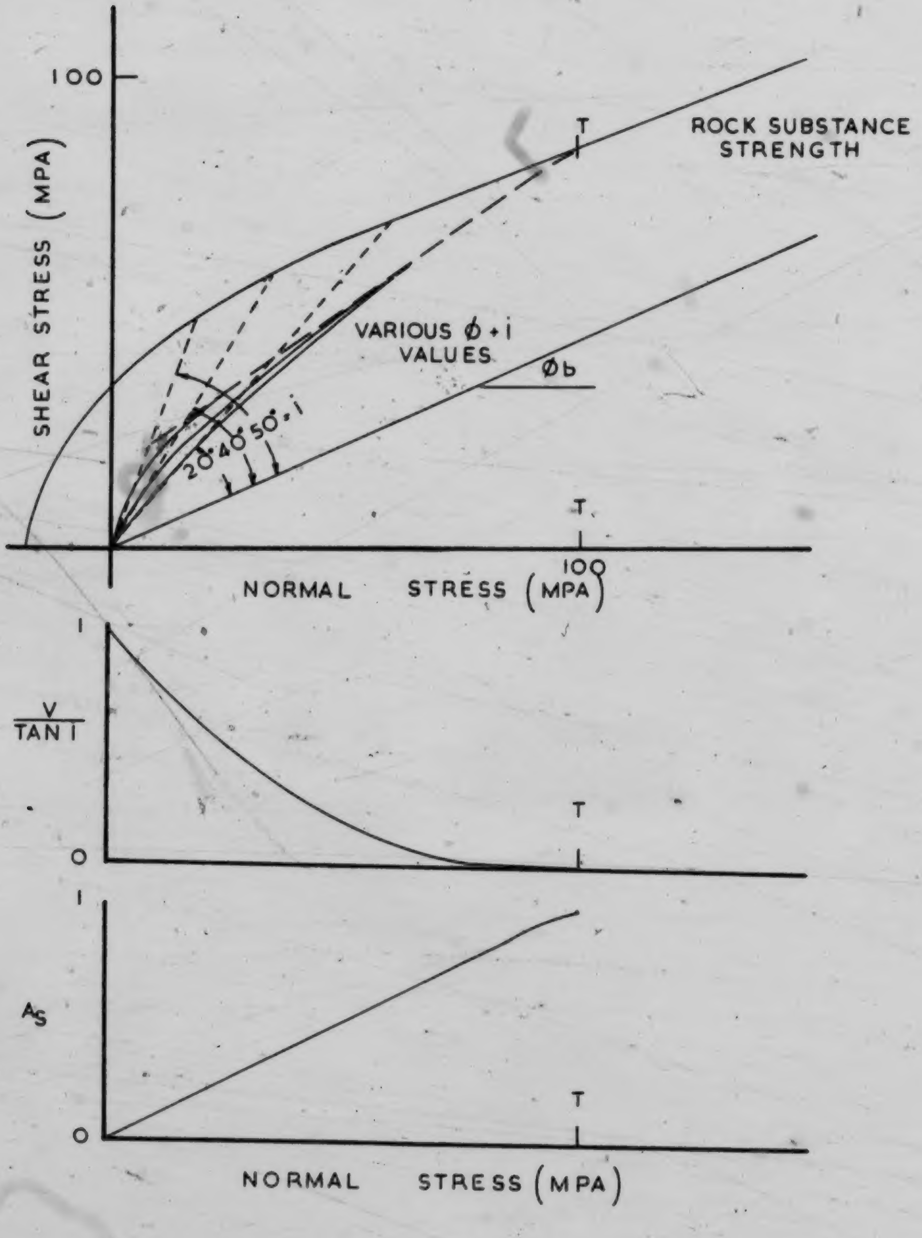

FIGURE 4-2 Representation Of How ϕ, As, and V/Tan i Varies With Normal Stress (After Ladanyi and Archambeault, 1970).

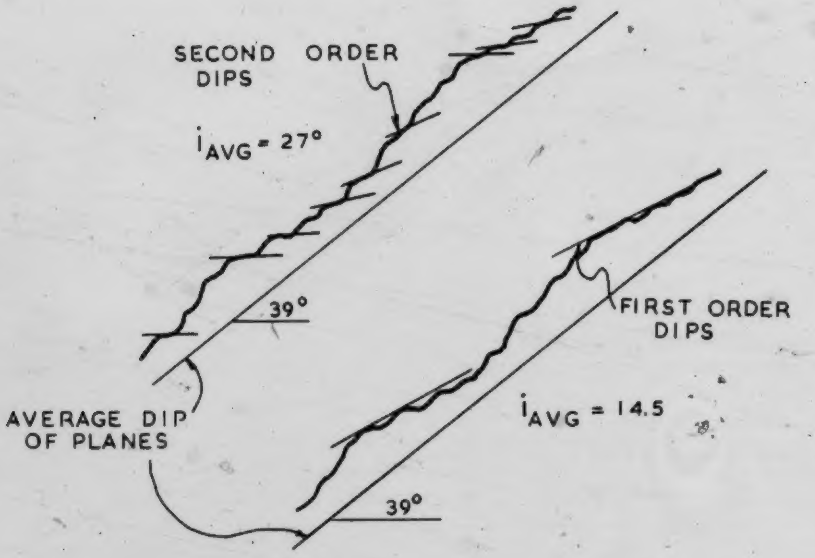
SECOND ORDER DIPS
$i_{AVG} = 27°$
39°
FIRST ORDER DIPS
$i_{AVG} = 14.5$
AVERAGE DIP OF PLANES
39°

FIGURE 4-5 An Example Of A Natural Rock Profile (After Patton, 1966)

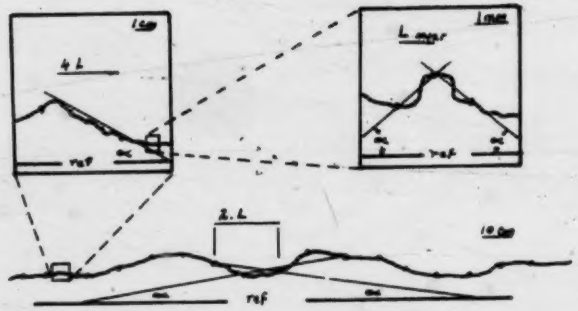
1cm
4 L
ref
α
1mm
L micr
α
ref
α
2.L
10cm
α
ref
α

MEASURING SURFACE ROUGHNESS FOR DIFFERENT SCALES.

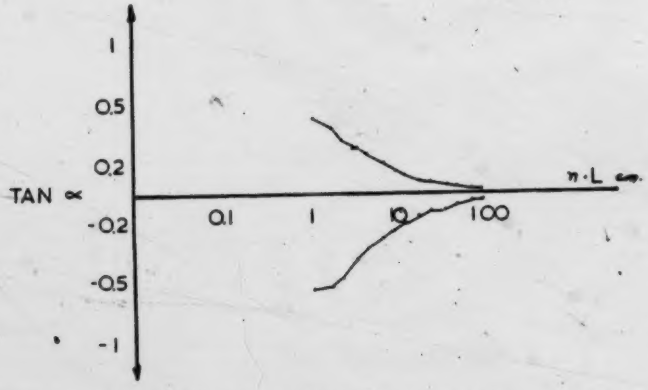

MAXIMUM VALUES OF TAN ∝ FOR DIFFERENT SCALES.

FIGURE 4.4 A Representation Of How Fecker And Rengers' Measured Surface Roughness Showing How Measurements Vary With Scale.

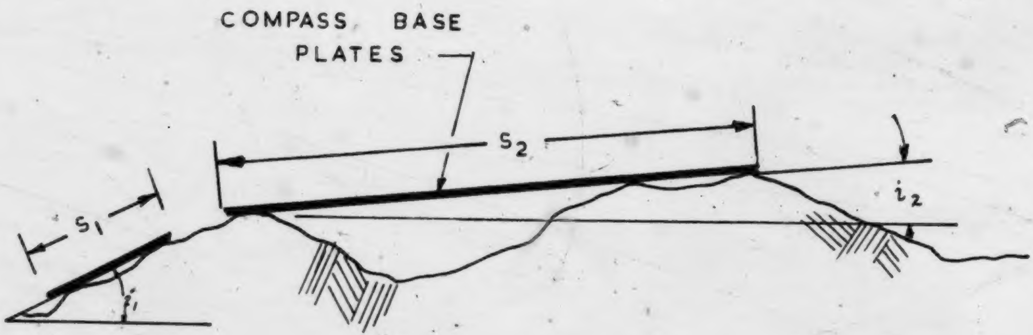
COMPASS BASE
PLATES
S_2
S_1
i_1
i_2

FIGURE 4-5 Fecker and Rengers' Method Of Evaluating i on Different Scales.

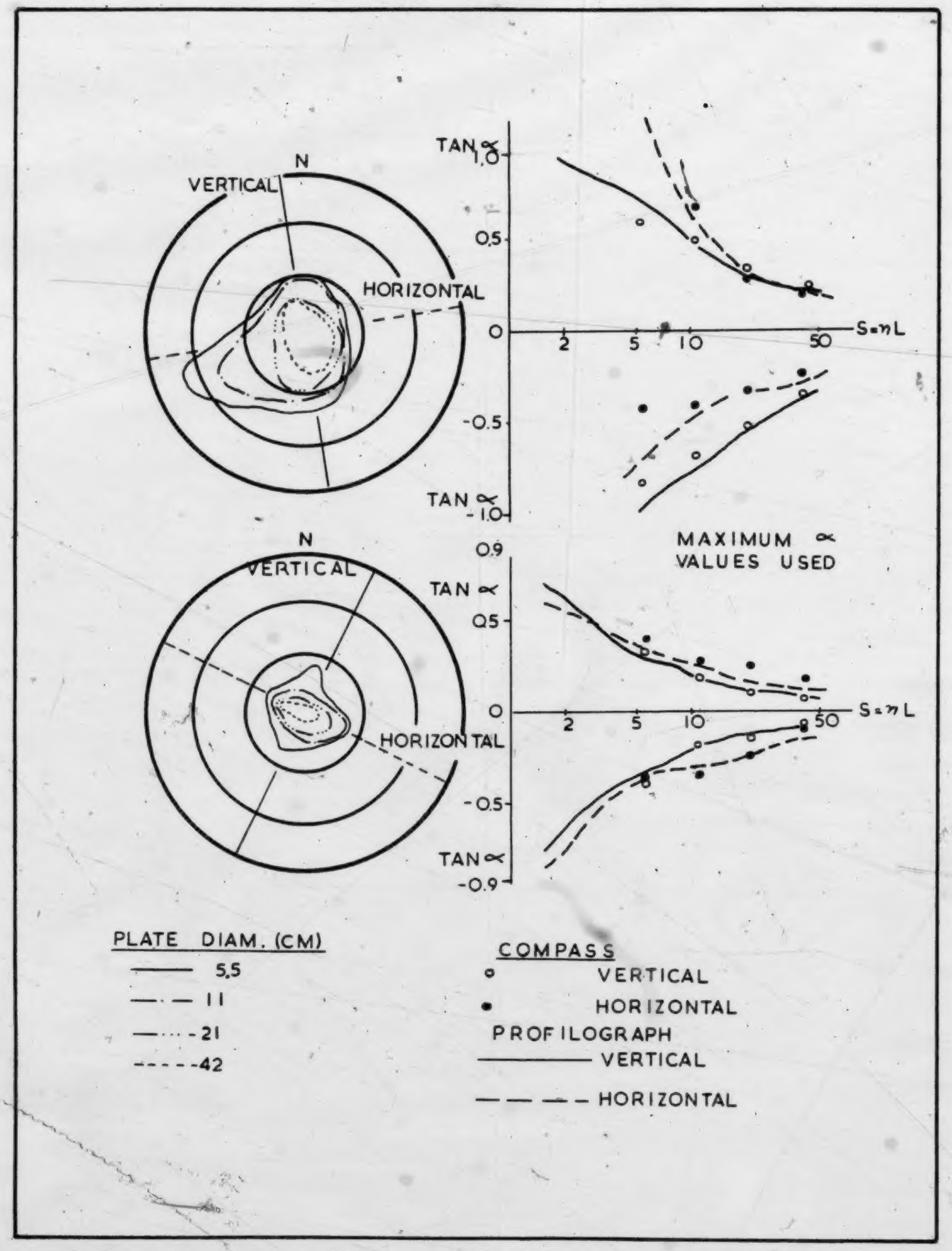

FIGURE 4-6 Comparison Of Rengers' Profilograph Results With Fecker And Rengers' Compass Results.

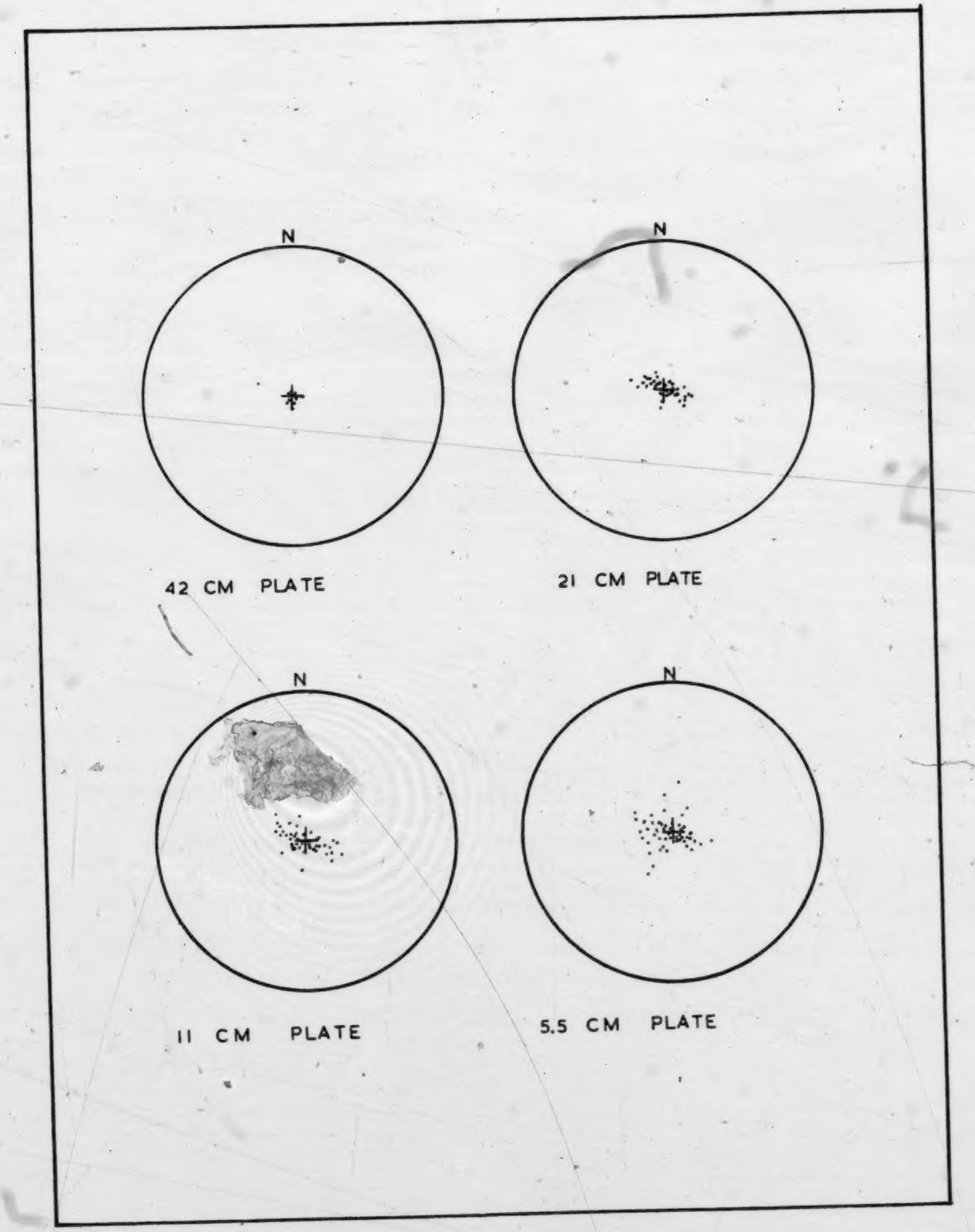

42 CM PLATE

21 CM PLATE

11 CM PLATE

5.5 CM PLATE

FIGURE 4-7 Results From Fecker And Rengers' Data Illustrating Elliptical Outlines Of Compass Data.

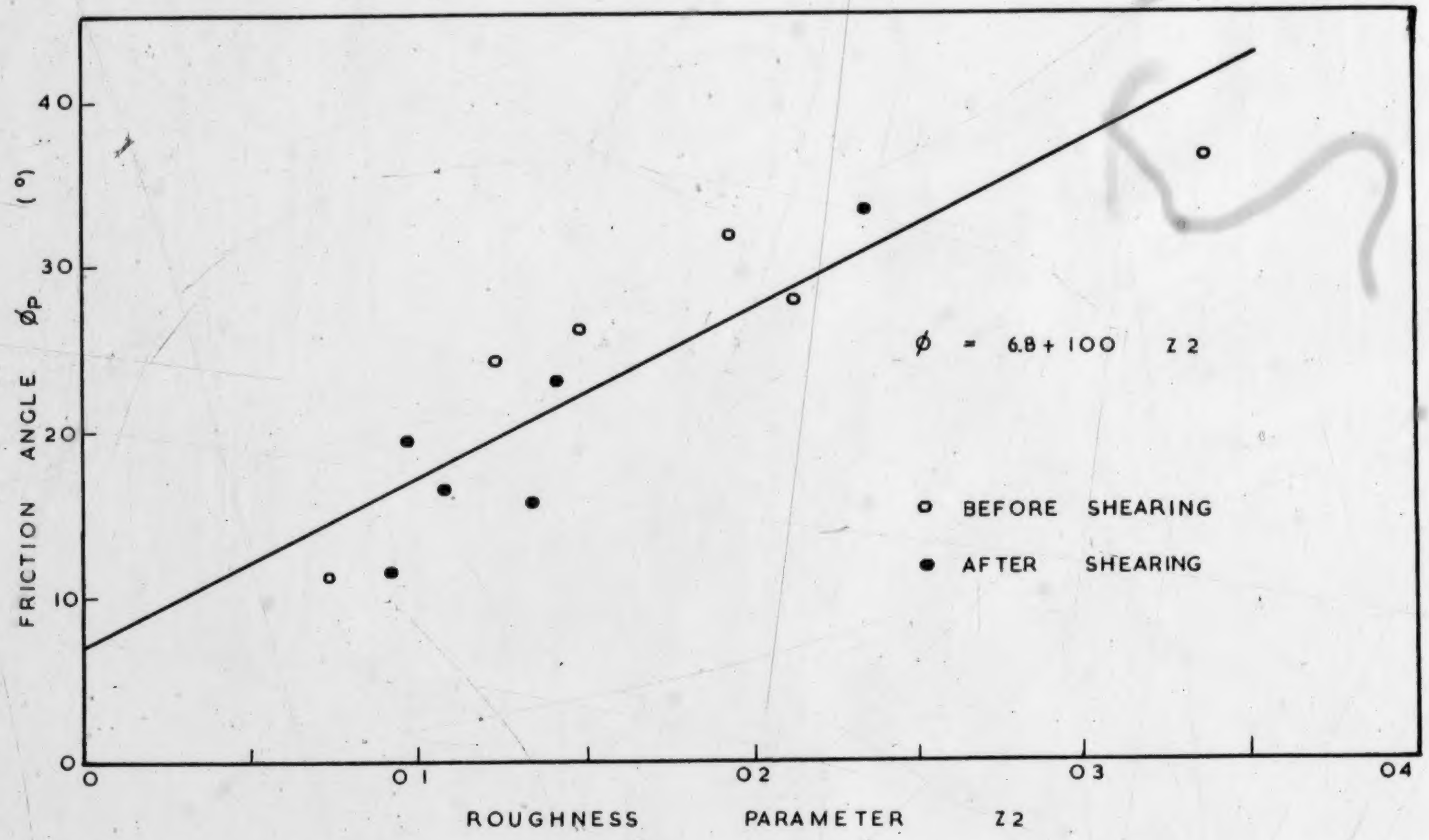

FIGURE 4-8 Correlation Between Z2 And Friction Angle (After Krahn, 1977)

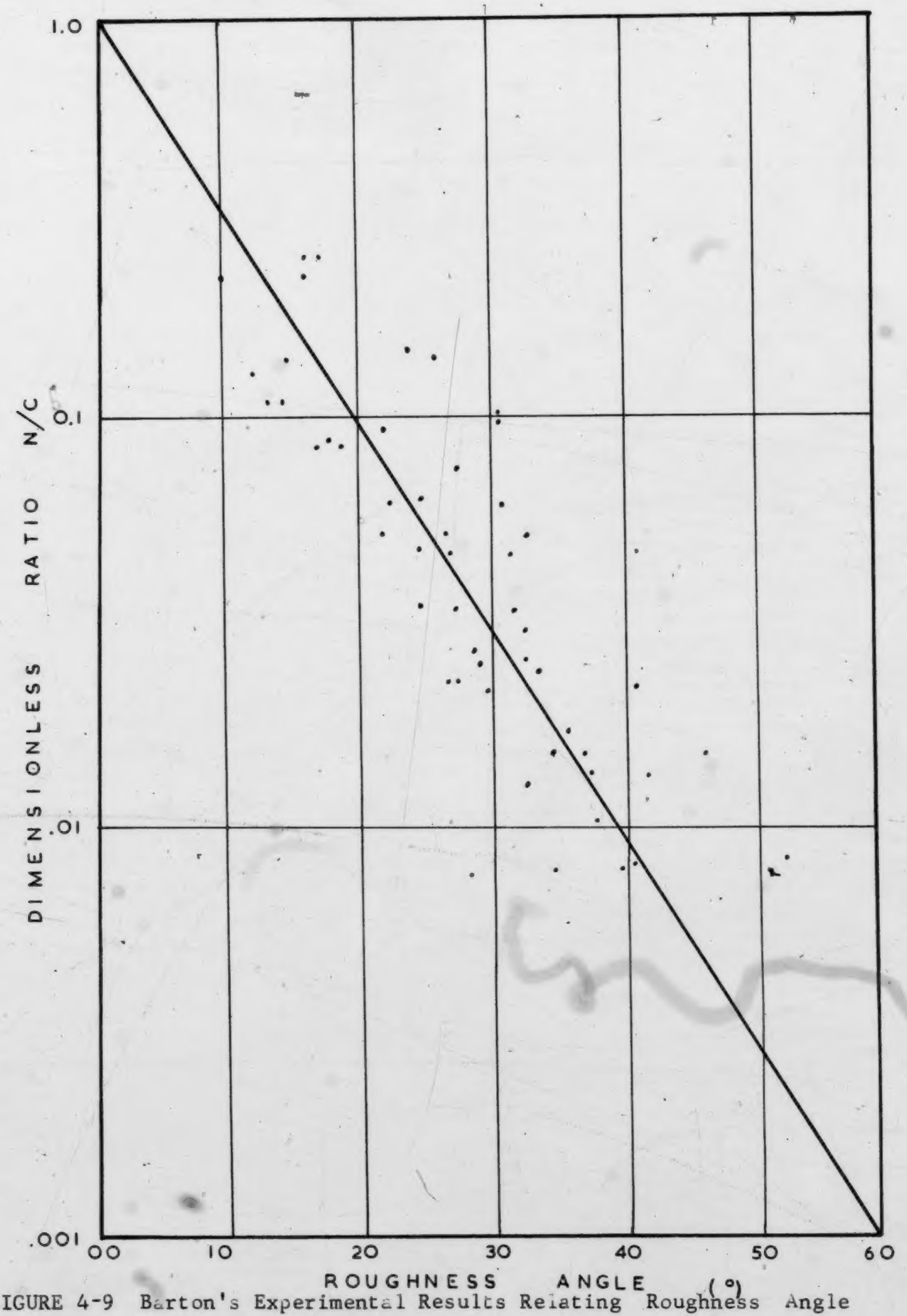

FIGURE 4-9 Barton's Experimental Results Relating Roughness Angle To Normal Stress.

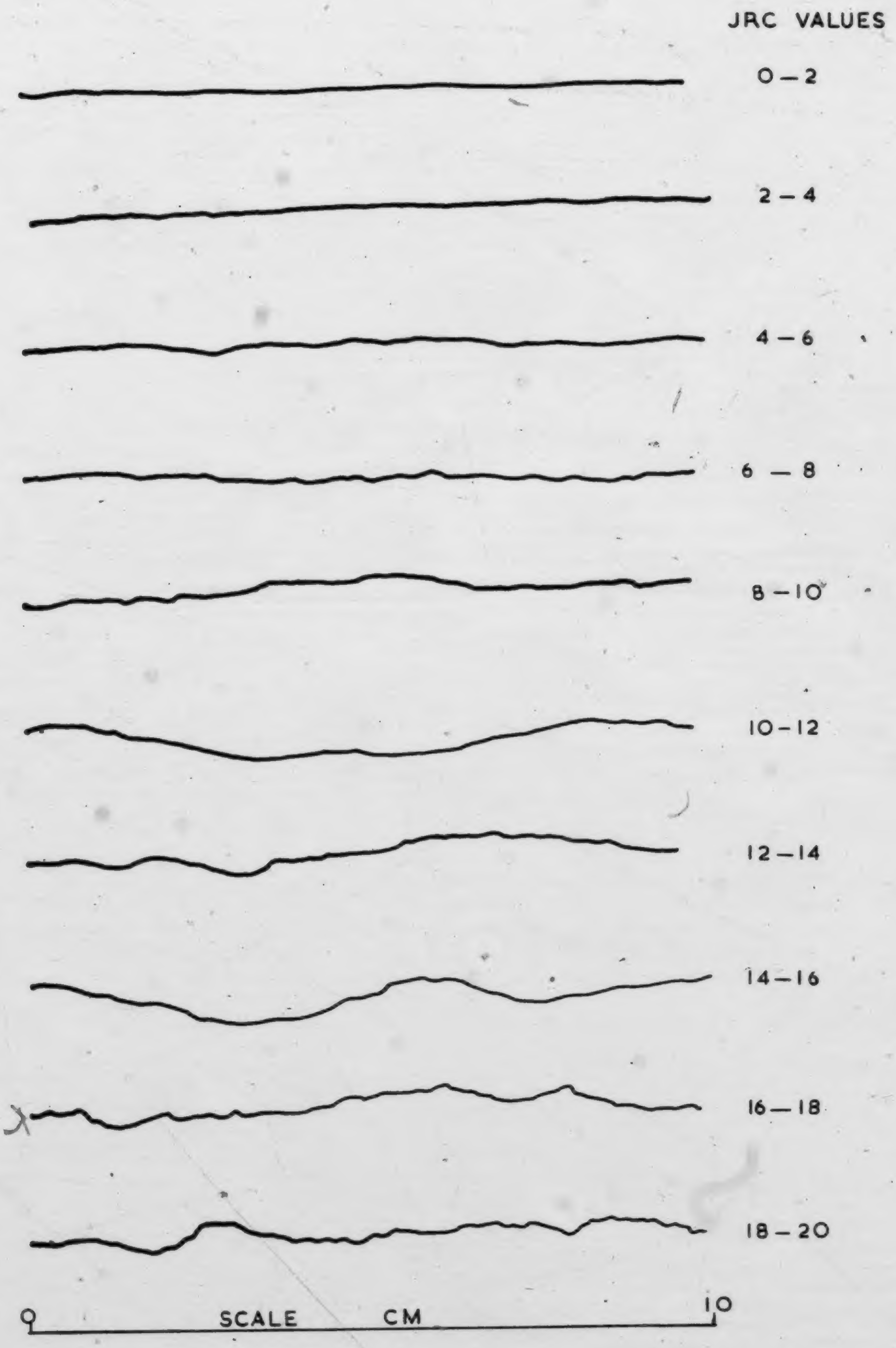
JRC VALUES
0 – 2
2 – 4
4 – 6
6 – 8
8 – 10
10 – 12
12 – 14
14 – 16
16 – 18
18 – 20
0
SCALE CM
10

FIGURE 4-10 Roughness Profiles Illustrating The Various JRC Values (After Barton, 1977)

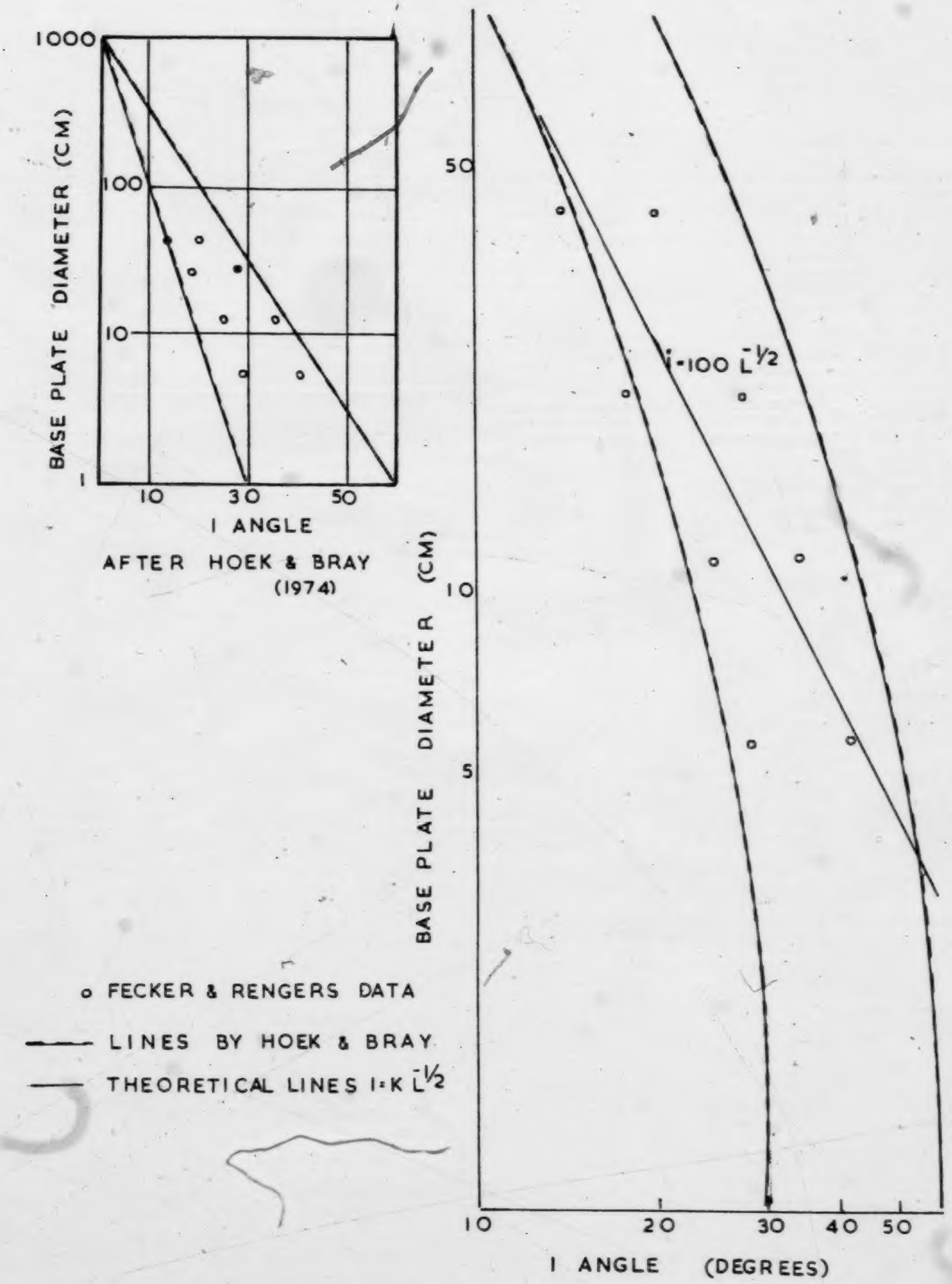

FIGURE 4-1^1 Comparison between The Theoretical line of $i= 100/L^{-1/2}$ And Fecker And Renger's Data as Interpreted By Hoek And Bray (1974).

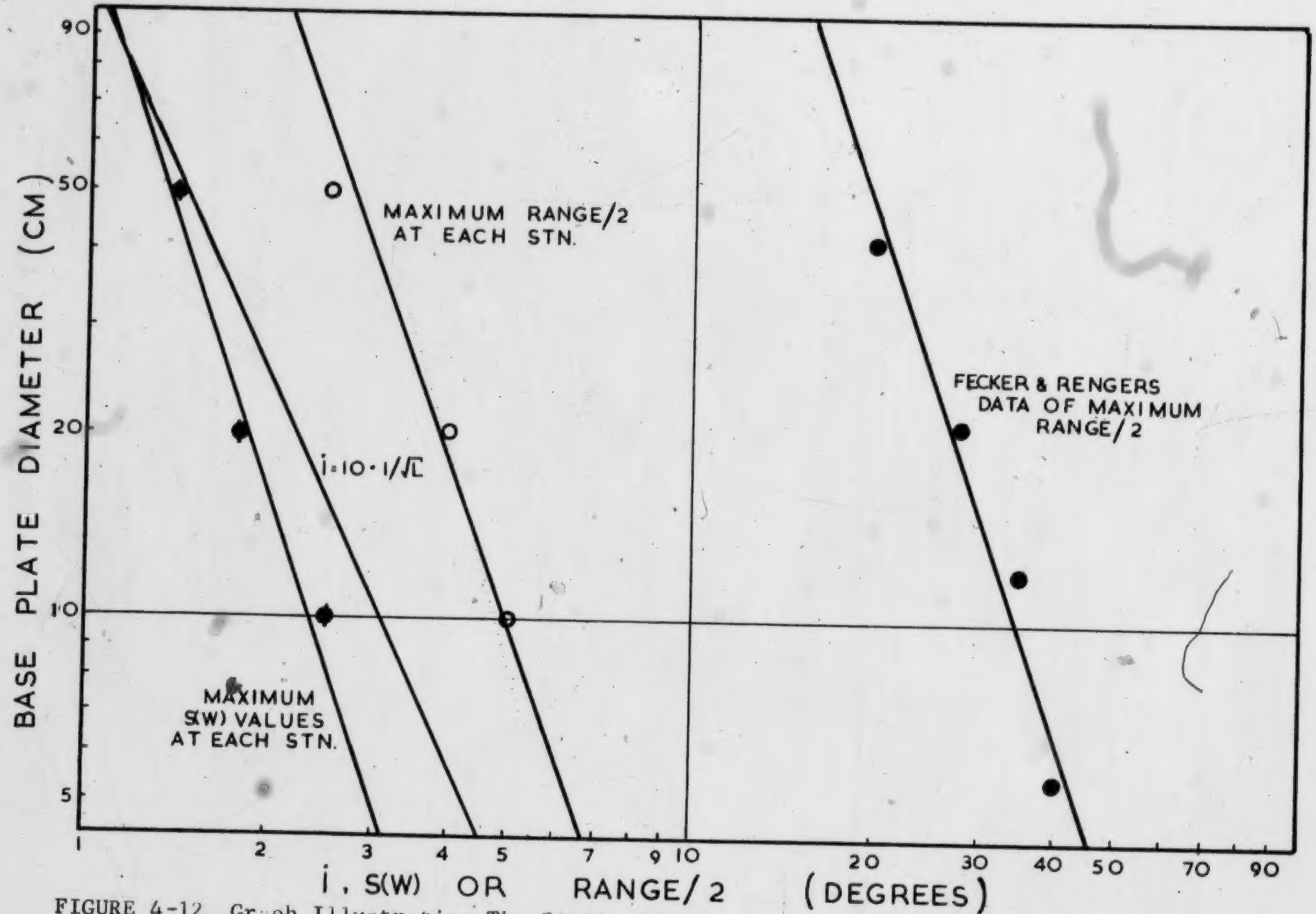

FIGURE 4-12 Graph Illustrating The Similarity In Trend Bet een Fecker and Renger's Original Data and Maximum Range/2 Values And S( ) Values.

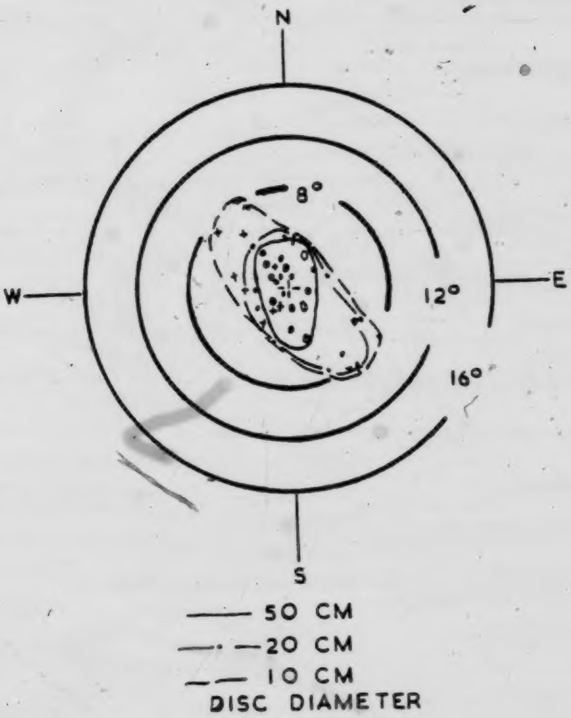

FIGURE 4-13 Results From Fecker And Rengers Approach At Stations 1 to 4 At Whitehorse Creek.

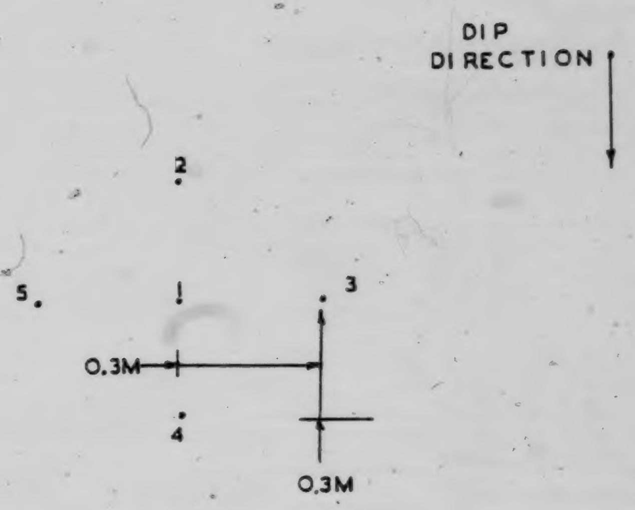

Station # 20				Yik	Yi	$\frac{(Yik-Yi)^2}{3}$
point	240/30	226/30	226/30	90	30	0.0
Xij	238/31	241/30	243/31	92	30.7	0.67
	218/34	218/34	218/35	103	34.3	0.67
	235/25	232/26	232/26	77	25.7	0.67
	198/30	198/31	207/27	88	29.3	8.67

Avg. $S^2\ (e) = 10.68/10 = 1.07$

FIGURE 4-14 Schematic Diagram Of A Station With A Worked Example Showing How To Find The Operator Error.

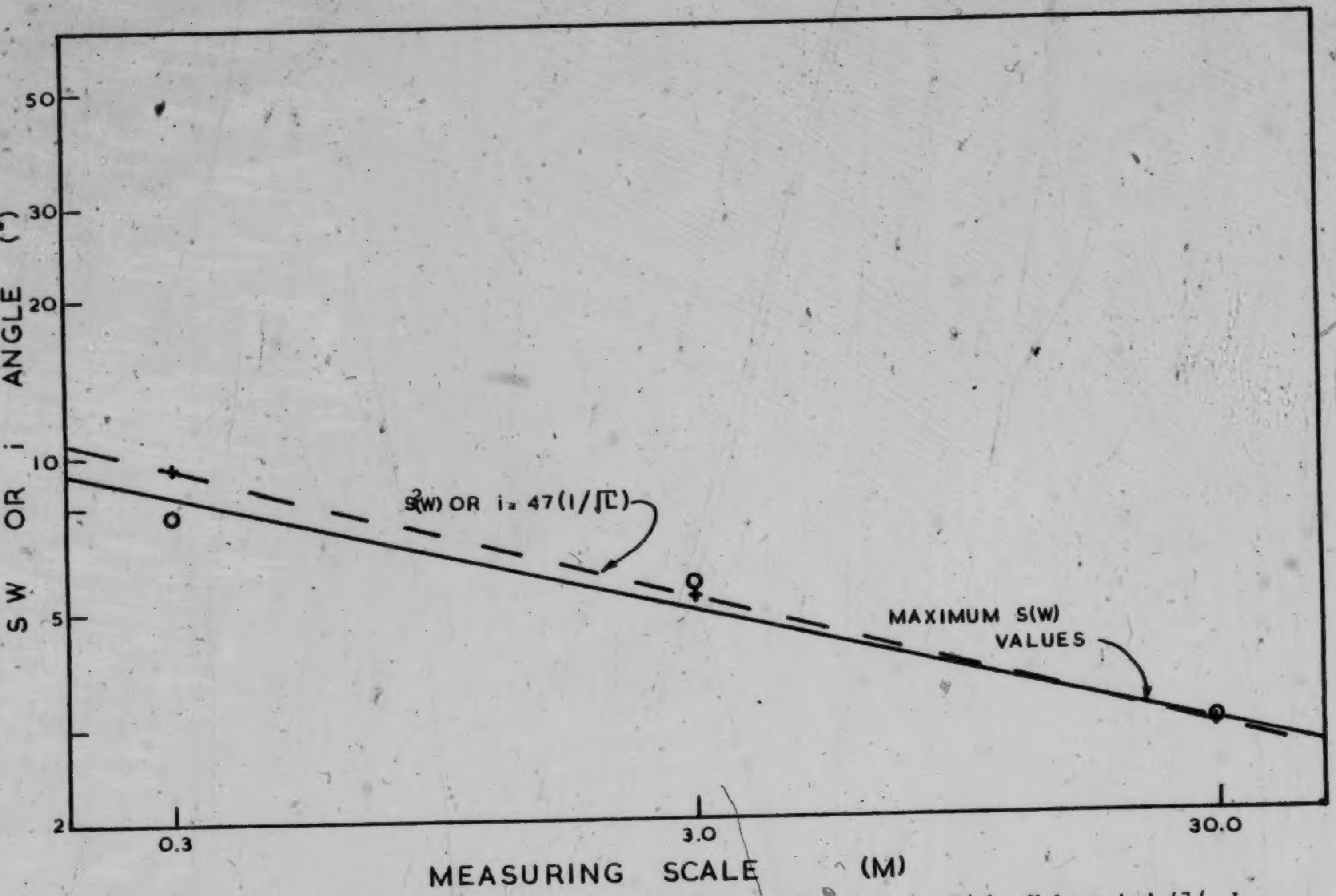

FIGURE 4-15 Graph Illustrating. The Similarity Between The Maximum S(w) Values And 47/ L.

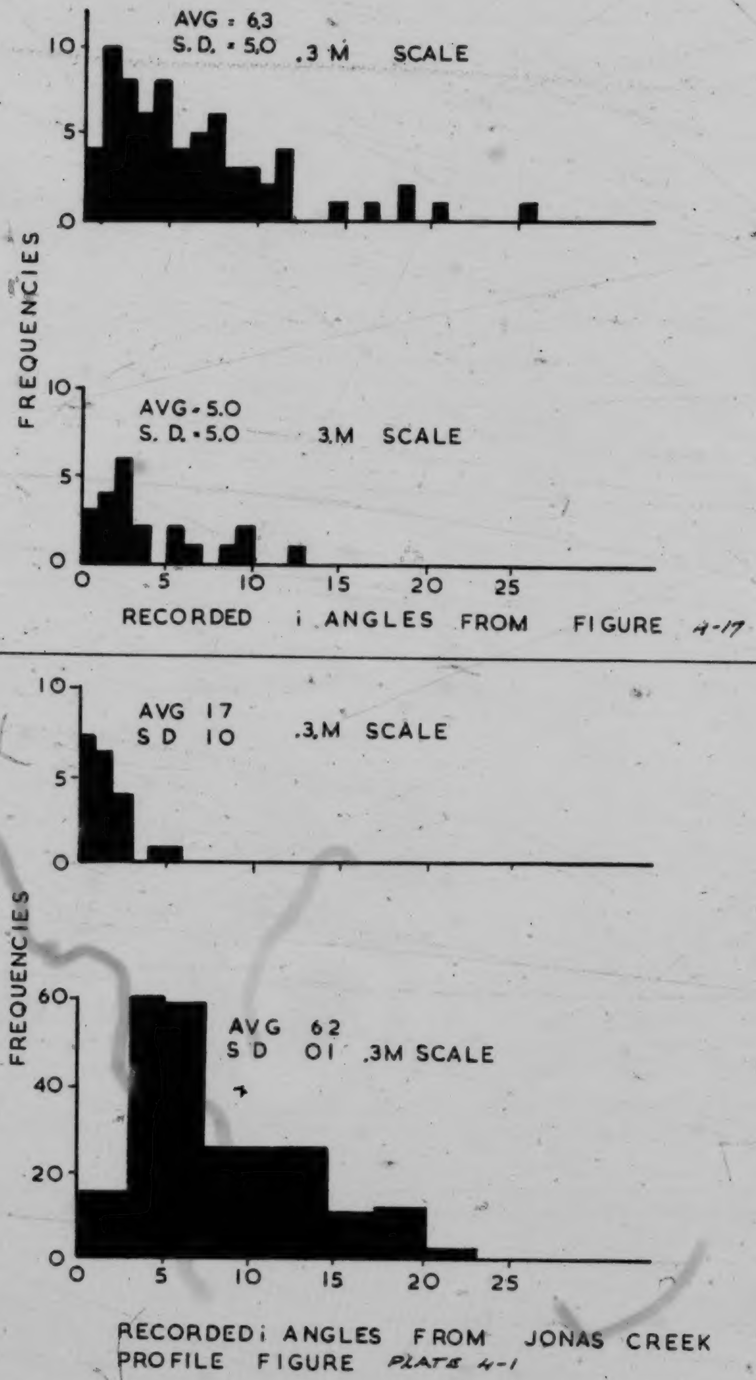

FIGURE 4-16 Histograms Of i Angles Recorded From Profiles.

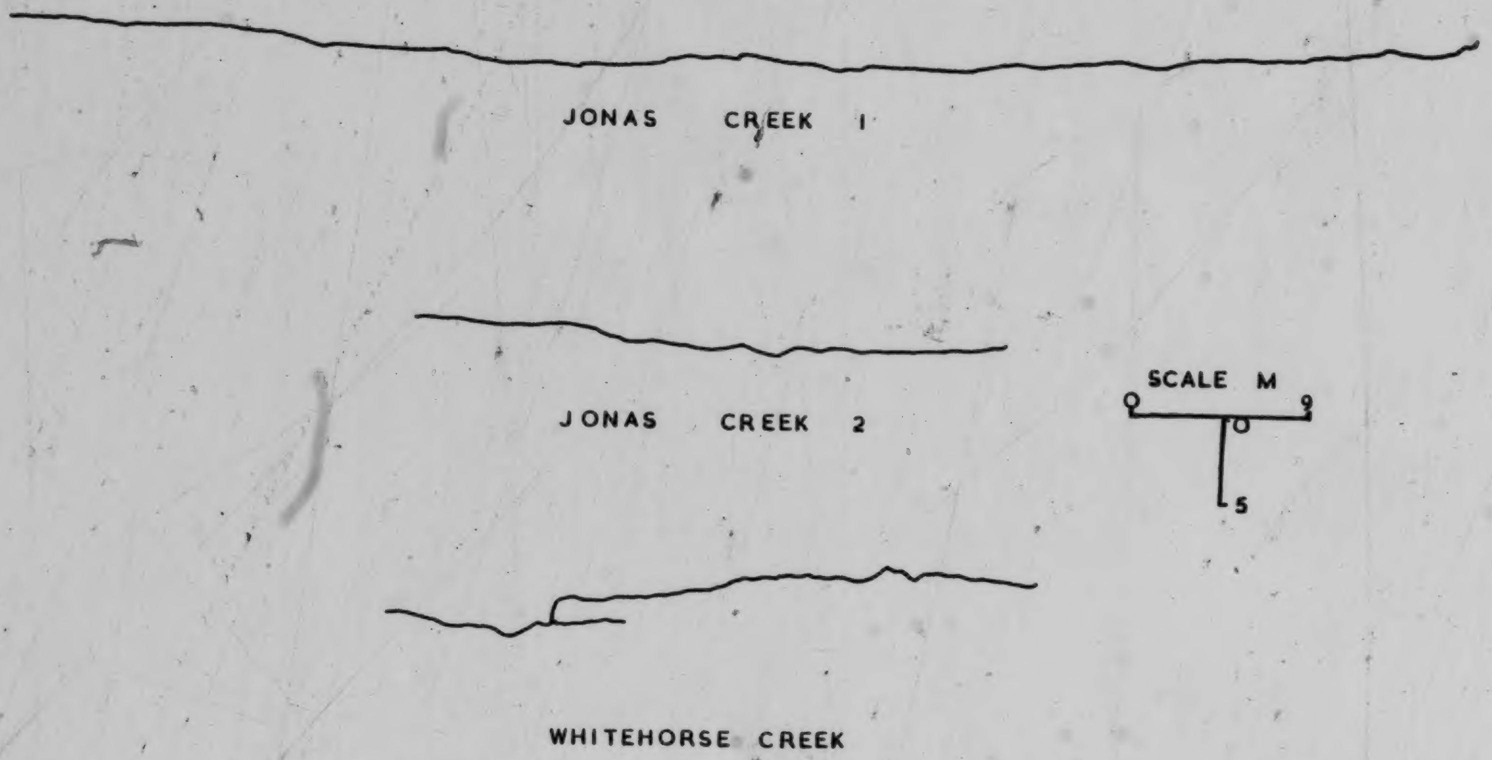
JONAS CREEK 1
JONAS CREEK 2
SCALE M
0
9
0
5
WHITEHORSE CREEK

FIGURE 4-17 Topographic Profiles Measured Using A Theodolite (To Determine i Angles).

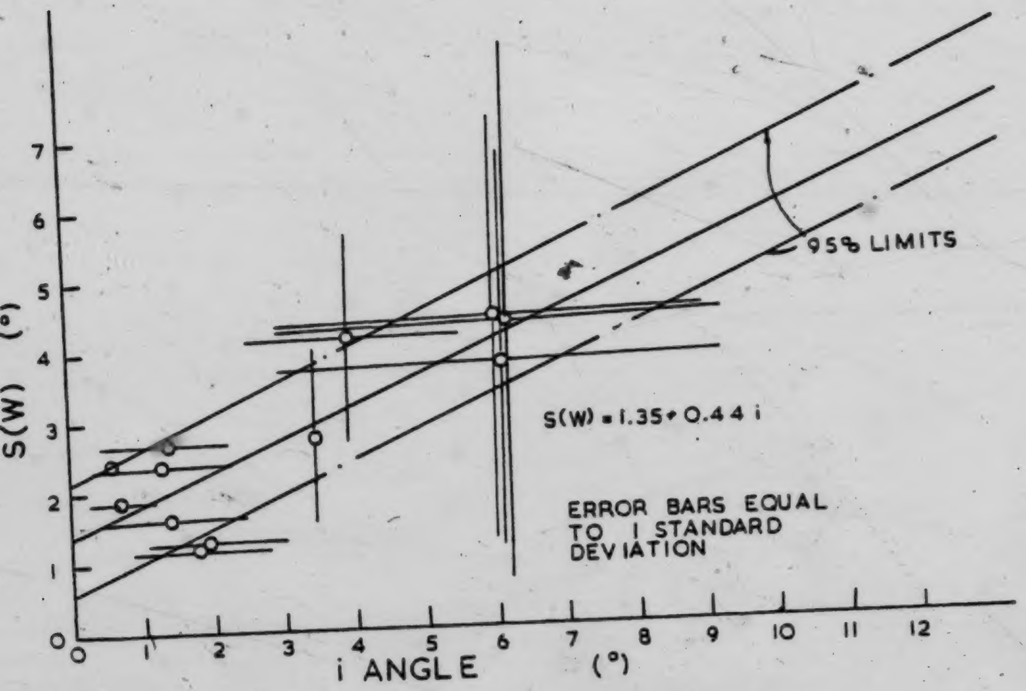

FIGURE 4-18 Experimentally Defined Relationship Linking S(w) With The Roughness Angle i.

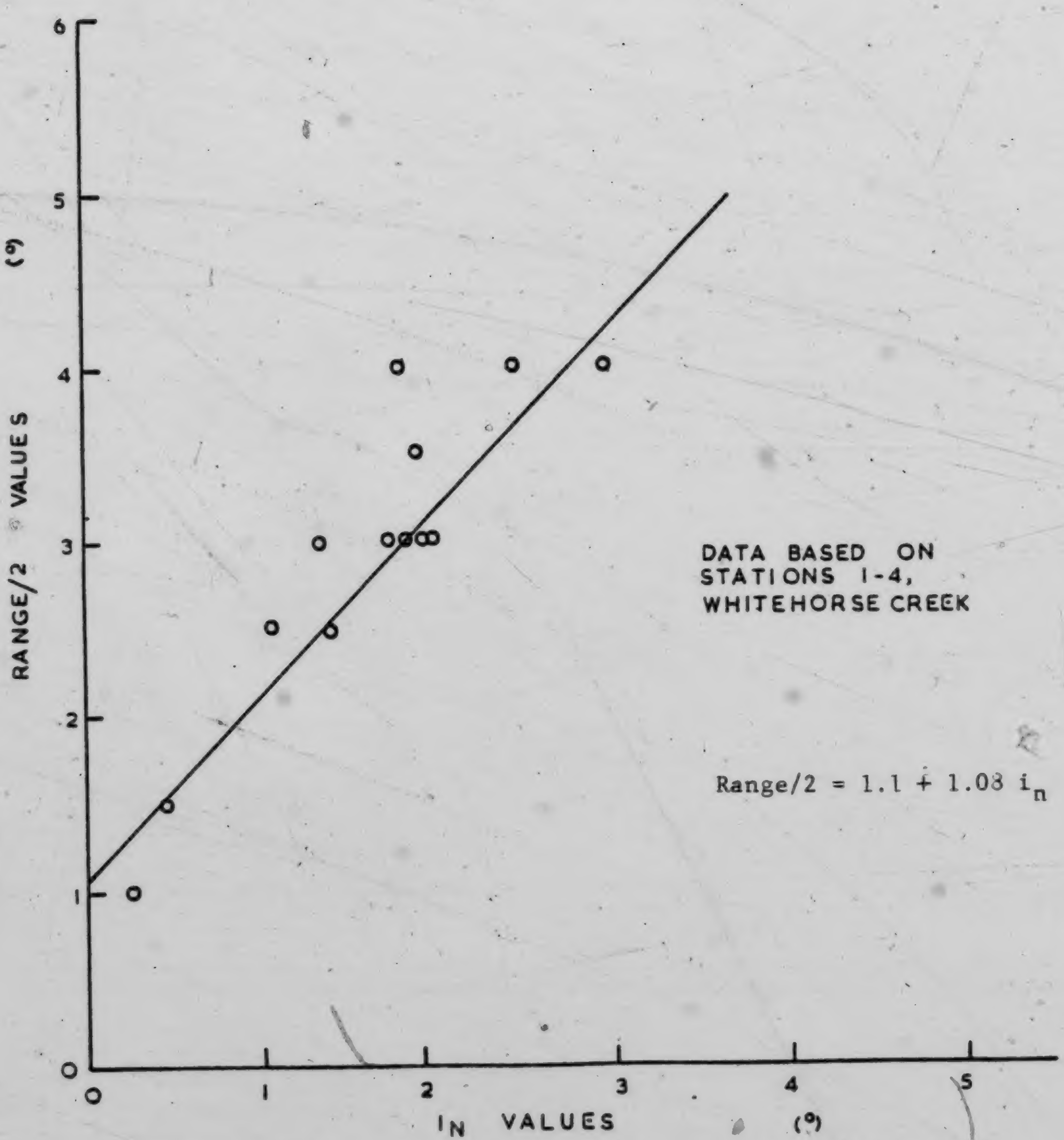

FIGURE 4-19 Comparison Between Roughness Values Evaluated By Fecker And Rengers Range/2 versus i_n Values.

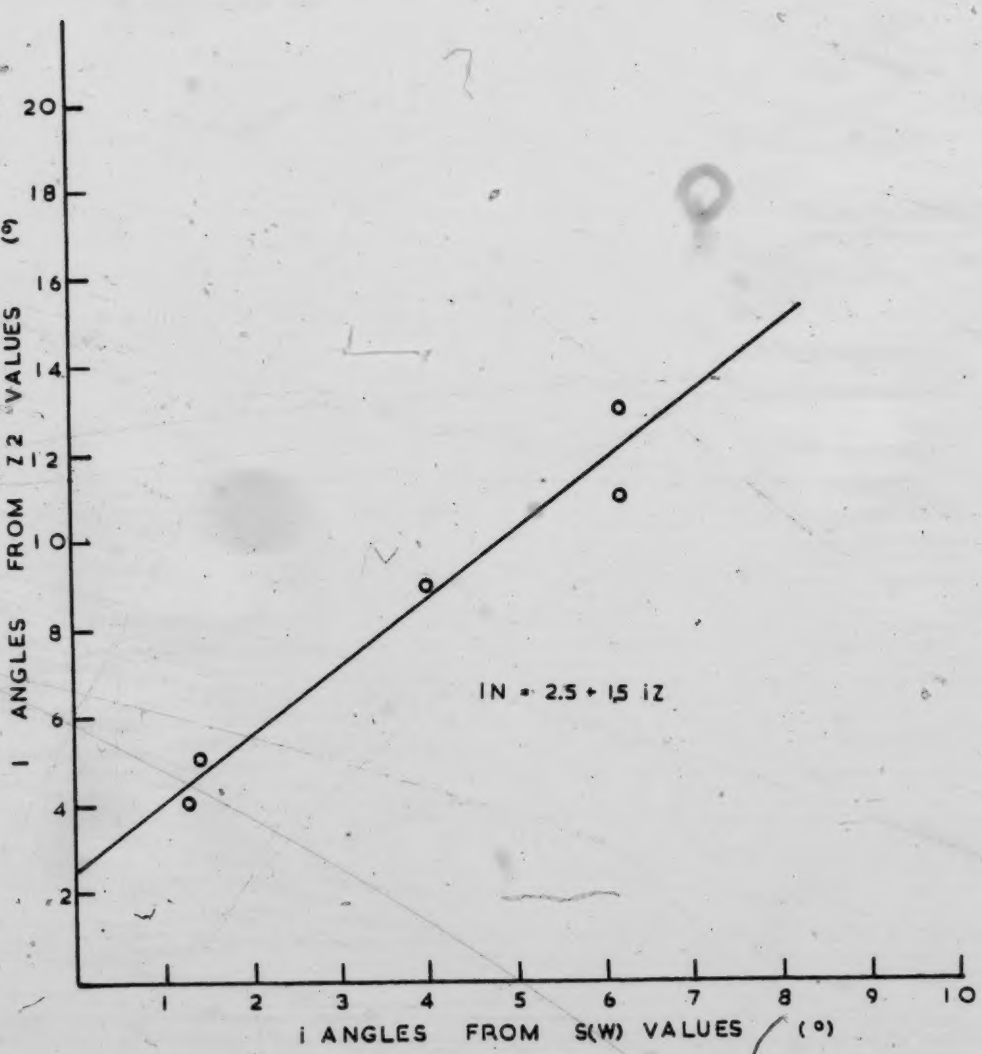

FIGURE 4-20 Relationship Between i_n Values And Z_2 Values For Large Scale Profiles Measured At Jonas Creek And Whitehorse Creek.

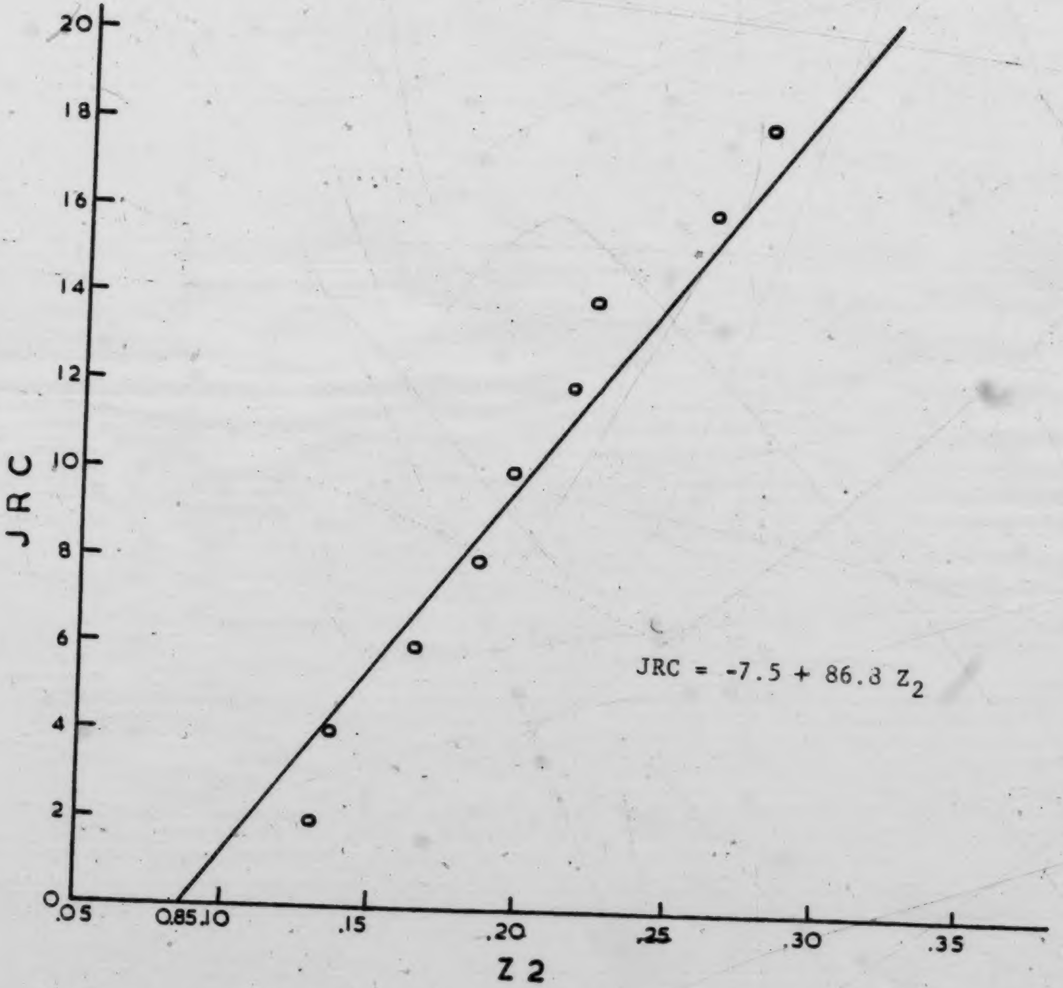

FIGURE 4-21 Relationship Between Z_2 Parameter And JRC Values. (After Tse, 1973).

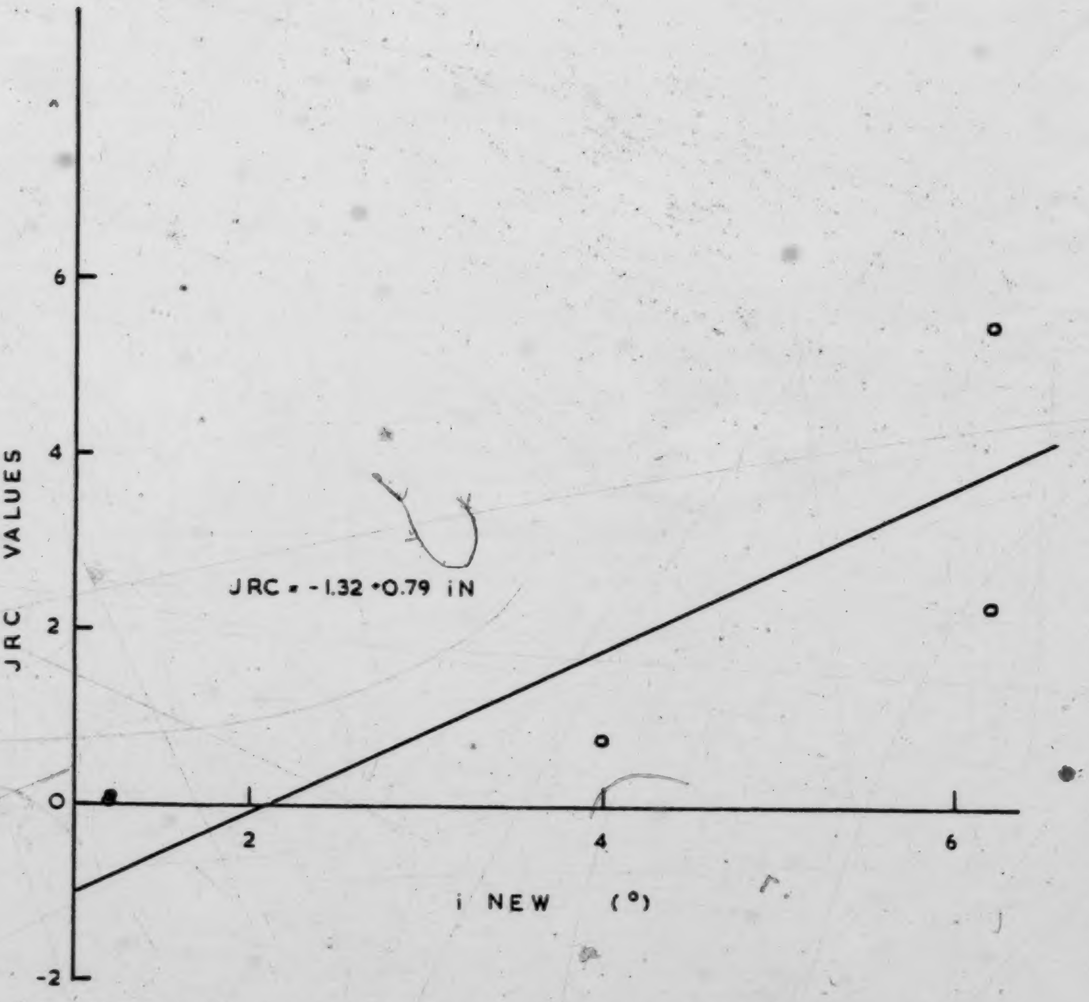

FIGURE 4-22 Graph Illustrating The Relationship Between in Values Ans JRC Values.

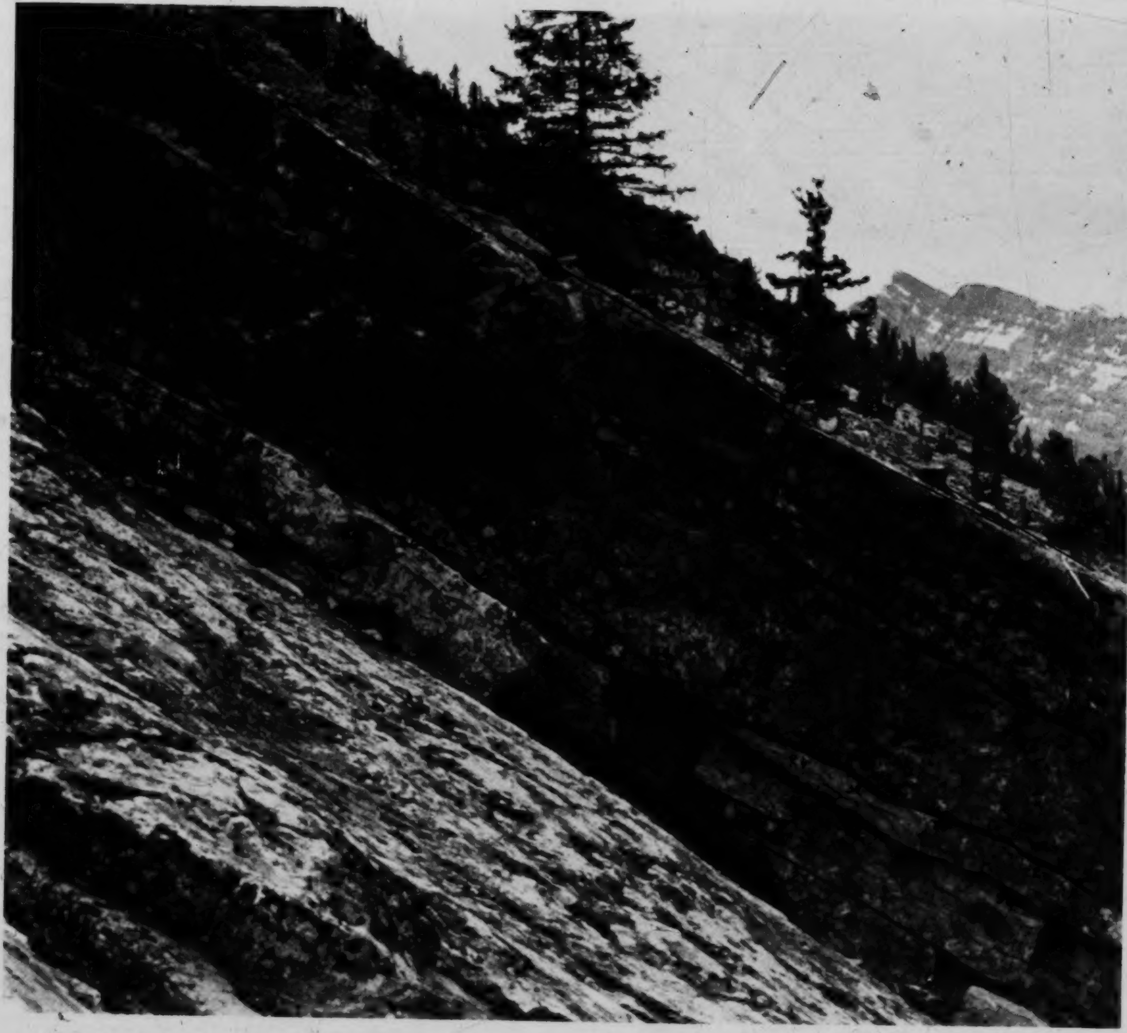

PLATE 4-1 A Profile Of A Bedding Plane At Jonas Creek Illustrating Various i Angles.

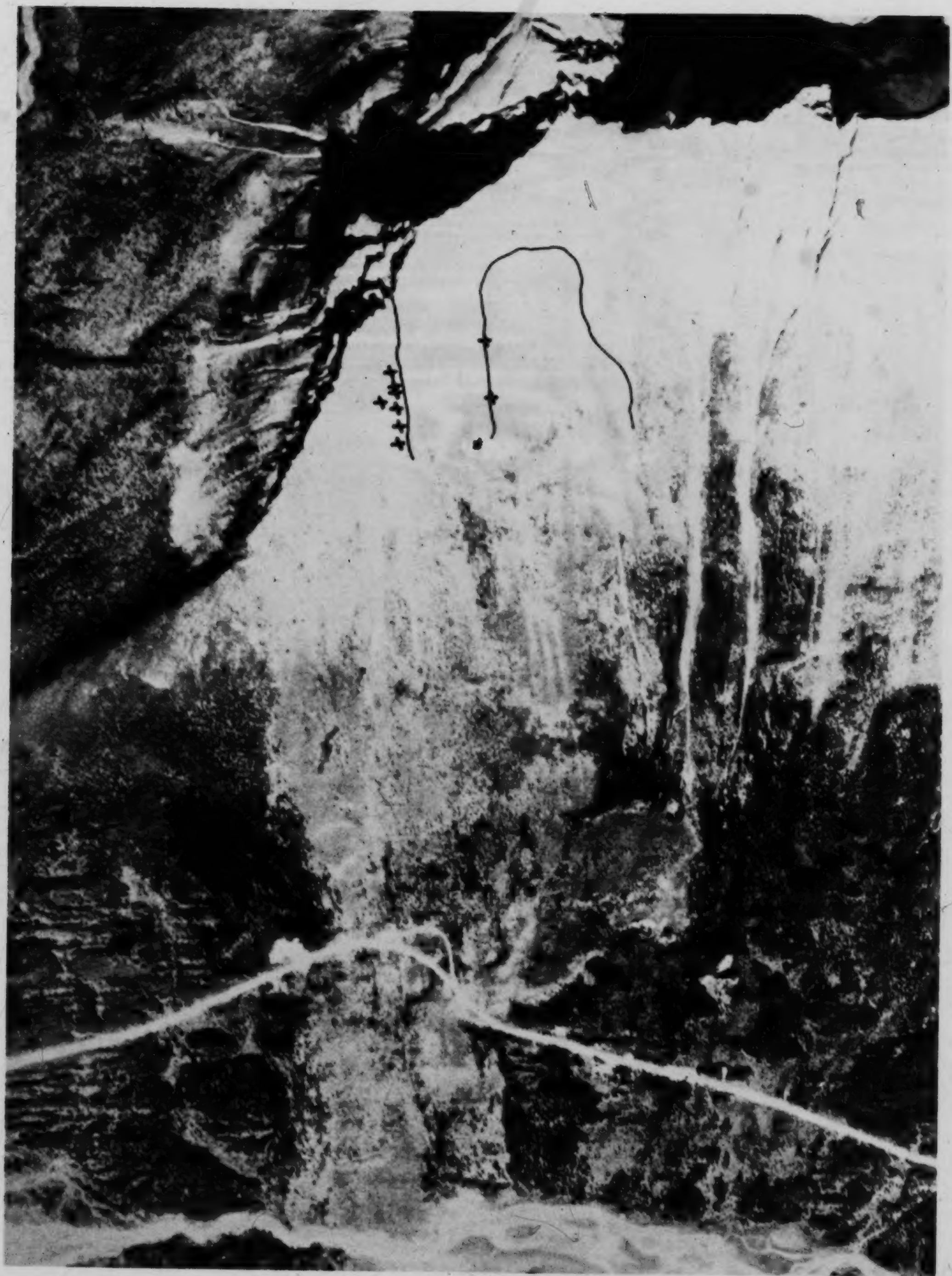

PLATE 4-2 Air Photo Illustrating The Rough Bedding Plane Locations At Jonas Creek.

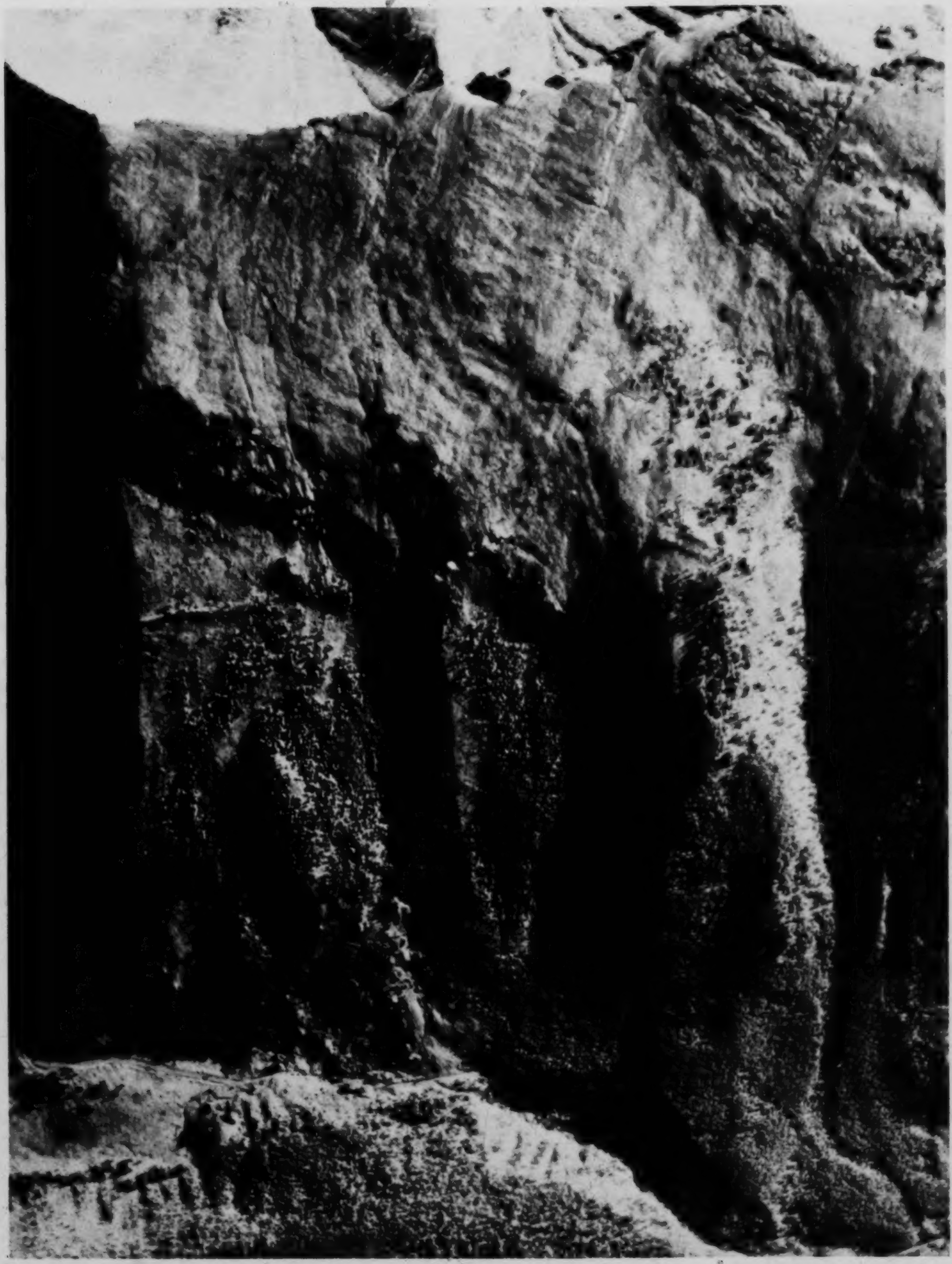

PLATE 4-3 Air Photo Illustrating The Rough Bedding Plane Locations At Whitehorse Creek.

Chapter V

Laboratory Determination Of Shear Strengths

5-1 INTRODUCTION

Detailed geologic investigations carried out in the initial stages of a slope stability investigation often reveal a series of possible failure modes governed by various sets of rock discontinuities. In order to evaluate which set or sets of discontinuities control failure, and in order to evaluate the slope stability in quantitative terms, the representative shear strengths acting along each discontinuity must be estimated. The shear strengths must be evaluated prior to the onset of slope design.

A laboratory shear testing programme was devised using conventional techniques to estimate values of peak and ultimate friction angles on clean, mating surfaces of quartzite and dolomite samples. The values of the Øp derived from direct shear test results were compared with peak friction angles evaluated using Barton's technique outlined in Chapter 4-2. The two values of Øp were then compared with back calculated values of friction thought to be acting at failure to find out how closely conventional shear tests on small samples predicted the in situ friction angles at the Jonas Creek and Whitehorse Creek rock slides.

In addition, an in situ shear test was performed on a large block of quartzite, 4 m long, 2.4 m wide, and 0.7 m thick, found on the slope beneath the north slide at Jonas Creek. This test was performed to evaluate the shear strength acting beneath the block and to evaluate how closely the field determination of ϕb + i matched the measured shear resistance. Only one test was performed. The results of the test were difficult to interpret, however, so the test procedure and results have been detailed in Appendix A-2.

Conventional shear tests were also used to evaluate basic friction values on several different surface preparations using a technique outlined by Coulson (1972). These values were compared with the ultimate friction angles determined by direct shear tests of naturally surfaced samples and with sliding friction angles evaluated using a new piece of apparatus, the tilting table. The sliding angles are thought to be representative of the basic friction angles.

This Chapter outlines the steps taken during each stage of the laboratory and field determination of shear strength and summarizes and compares the results from the various testing techniques.

5-2 PREVIOUS WORK IN SHEAR STRENGTH EVALUATION

The most common method used to evaluate the shear strength along discontinuities is the direct shear test. Hoek and Bray (1974) indicate that direct shear tests performed in the laboratory or in situ best simulate the loading and failure conditions which occur in the field and hence are the most appropriate of various testing techniques. Unfortunately, it has been amply demonstrated by back analysis (Krahn, 1974), and by direct shear tests on various sample sizes that peak shear strengths measured along discontinuities may be scale dependent (Deere et. al.,1967, Stagg,1968 and Hoek and Bray, 1977). Figure 5-1 illustrates the scale effect on peak friction angles evaluated by James (1970) and Pratt, Black and Brace (1974). The peak friction angles decrease by as much as 14° over a change in sample size from 80 cm^2 to 5000 cm^2 for clean jointed quartz diorite surfaces (Pratt,Black and Brace, 1974). James' tests (1970) were conducted on weathered mudstone, a much softer material. The peak friction angle did not vary as markedly with this material as with the quartz diorite.

Londe (1973a) indicated that scale dependency does not influence all test results. A joint in limestone infilled with soft clay showed virtually no scale dependence over a change in area from 1.25 m^2 to 4.4 m^2. Variations in friction angles caused by scale effects vary with the rock type and the nature of the geologic discontinuity. Very smooth tectonically disturbed surfaces such as slickensided bedding surfaces, may exhibit very little scale dependence. Clean rough undisturbed bedding surfaces or joints in relatively hard rock material may exhibit considerable scale dependence.

This problem of scale dependence is what gave such great impetus to defining the field values of i to fit into Patton's (1966) equation of

$$\phi p = \phi b + i \qquad 5.1$$

The basic friction angle, ϕb, can be evaluated in the laboratory in several ways. Patton (1966) advocated measuring ϕb by shearing rough sawn surfaces past each other. Coulson (1970) expanded on this method with an extensive investigation to further define the basic friction angle. Coulson recommended that ϕb be measured on surfaces rough sawn then lapped with #80 grit sandpaper. Barton (1971) recommended the use of sandblasted surfaces to determine ϕb.

Krahn (1974) noted that a review of case histories by Deere et. al., (1967) indicated that the ϕb determined on rough sawn surfaces was similar to the ϕ required by back analysis for a factor of safety of 1. This led Krahn to the belief that the best method of obtaining ϕb was either Patton's or Barton's technique.

Tests conducted during this thesis indicated that the sandblasted specimens gave similar results to those found on surfaces lapped with #80 grit paper (Section 5-5). This effectively tied all three methods of determinig Øb together and indicated that all gave similar results. This angle of Øb can then be applied in the field as Øb is independent of scale (Hoek and Bray, 1974, p.90). The angle i can then be evaluated in the field at the appropriate scale (Chapter 4) and added to Øb. In this manner a peak friction angle can be defined at an appropriate scale even though shear tests at that scale cannot be conducted. The appropriate scale has yet to be determined.

Hoek and Bray (1974, p. 149) suggested that the shear strength along discontinuities could be estimated using a simple tilting test. The slope angle of a discontinuity at which the upper half of a specimen slid from the top of the lower half of the specimen is recorded as the friction angle. This technique for evaluating friction is simple and fast. Test results reported by Coulson (1972) indicate that Øb is relatively constant over the normal loads found in many rock slope problems. For similar rock types (dolomites and sandstones), Øb values varied less than 3° on average over a normal stress range from 0.07 MPa to approximately 2.00 MPa. This indicates that Øb is not noticably stress dependent.

Following this, Cawsey and Farrar (1976) published a short discussion pertaining to the use of this apparatus. They attempted to measure the peak friction angles acting along naturally rough surfaces of soft Chalk samples. They suggested that this test simulated the in situ conditions of failure as closely as a conventional drained direct shear test. They concluded that the tilting table successfully measured the peak friction angle of the samples as the results were equivalent to those found by previous authors using conventional drained direct shear tests and triaxial tests. Hencher (1976), however, dismissed this comparison and stated that although the results were similar the mechanics of failure for the tilt test were not equivalent to the mechanics of the conventional tests noted above.

Hencher (1976) also investigated the use of the tilting table apparatus. His samples, however, unlike the soft Chalk samples, consisted of artificially prepared surfaces of hard rock, similar to those tested here. Hencher concluded on the basis of his tests that the tilt table is a useful research tool which yields results equivalent to those obtained using direct shear or triaxial tests on hard rock.

Barton and Choubey (1977) also used a tilt table to evaluate Øb on smooth unweathered rock surfaces. They suggested that for artificial surfaces this test yielded the mineralogic properties of the sample because for all practical purposes the surfaces were non dilatant. Barton and Choubey (1977) used flat sawn surfaces to determine Øb. The actual roughness of their test surfaces was never quantified. It would appear to be the equivalent of a sand blasted surface as the Øb values reported were approximately 30°, similar to the range of values of Øb reported by

Coulson for a sand blasted surface on various rock types.

Barton and Choubey (op. cit.), also performed tilting tests on naturally rough samples and found that the results were difficult to interpret. The maximum angle measurable was a function of the sample block configuration. With naturally rough surfaces the tilt table often was inclined to the point that the normal resultant fell outside the middle third of the base of the slider, the upper block was free to fail, and hence induced tension near the top of the block. This resulted in a toppling failure which could not be evaluated in terms of a sliding friction angle. As a result, Barton and Choubey recommended that the tilt table tests should not be attempted in the case of naturally rough joints. Similar results were found in this thesis investigation..

5-3 SAMPLING LOCATION

The geologic investigations undertaken at Jonas Creek and outlined in Chapter 2, indicated that the rock type involved in the failure did not vary noticeably in composition throughout the slid mass. In addition failure occurred on several bedding surfaces. No single unique bedding surface or other single geologic discontinuity, such as a shear zone or a fault was responsible for the failure. All of the bedding surfaces examined on the failed slope were indistinguishable with respect to mineralogy and roughness. It was thought, therefore, that any bedding surface would yield shear strength values representative of the shear strengths acting on the slope at the time of failure.

The rock slides at Jonas Creek are easily accessible as the Banff-Jasper Highway actually traverses the slide debris. Samples could not be obtained from the actual failure surface which is located 4 km northeast and 1 km vertically above the highway. The area between the failure plane and the road is covered with loose blocky debris which makes vehicle access impossible. This prevented the use of any mechanical drilling apparatus for sampling.

In addition the large size of the blocks of quartzite existing on the failure surface, coupled with the high degree of interlock between blocks made sampling and backpacking of the samples to the road impossible. The interlocking was caused by the surface roughness on the mating discontinuity halves. This held the rock together like a jigsaw puzzle. As a result, block samples approximately 50 cm square by 20 cm thick containing representative bedding discontinuities were retrieved from the debris directly below the centre of the north rock slide on the northeast side of the highway (Plate 2-2). The sample surfaces within these blocks all appeared to be similar in mineralogy and roughness to those surfaces exposed on the failure surface.

At Whitehorse Creek a quarry road allowed vehicle access to the rock slide debris. Once again however, it was impossible to gain vehicular access to the failure surface so samples could not be retrieved by drilling apparatus. In addition, blocks in excess of 1.0 m² near the failure surface prevented hand sampling and backpacking of the samples to the road. Block samples were therefore taken from the centre of the debris pile on the north side of the access road (Plate 3-2).

The failed material all belongs to the Turner Valley Formation. Examination of the stratigraphic column (Figure 3-4) indicates that several sub-units exist within the formation. The failure surface again consisted of several bedding planes and it was concluded that no single discontinuity was responsible for failure. The bedding surfaces along which failure occurred were similar in nature and appeared to be contained within one rock type of the Turner Valley Formation. Visual examination of the rock type around the failure surface was made before samples were collected. Samples were then located within the debris pile with bedding surfaces which resembled as closely as possible those surfaces found at the failure plane. The samples varied from 50 cm square to 75 cm square and were between 15 to 25 cm thick. Several bedding discontinuities were sampled.

5-4 SAMPLING PROCEDURE

The sample blocks were usually rhombohedral in outline due to near vertical orthogonal joint sets which pervade the rock mass. Samples chosen were split open along existing discontinuities in the field using a hammer and chisel. Samples which failed to break evenly, or which revealed beddding surfaces dissimilar to those found near the failure plane, were discarded. Both halves of the sample were then repositioned in their original configuration and bound tightly together with fibre reinforced tape so that no movement could take place along the failure surface prior to testing. The sample was then wrapped in 2.5 cm thick rubber foam and transported to the laboratory.

No joint surfaces were sampled as failure had taken place along bedding surfaces. The debris piles were searched thoroughly but no trace of discontinuities other than tension joints or bedding surfaces were found anywhere within the debris pile.

5-5 SAMPLE PREPARATION

The large block samples were kept wrapped in fibre reinforced tape to minimize movement during trimming on a water cooled diamond saw. The large field blocks were trimmed to form individual 5 cm x 5 cm x 7 cm high samples. The bedding surface discontinuities were located at approximately mid height of the sample. Sample shear directions were determined prior to trimming so that all samples from one block were sheared in the same direction.

The shear direction was inferred by the presence of micro joints, small steps varying in height from 1 to 5 mm, on the discontinuity surface. The micro joints were similar in orientation to other micro joints, and macro joints 1/2 to 1 m high, found on the actual failure surface (Plate 2-4). All the joints examined in the field stepped down through the stratigraphic column as elevation decreased and so failure always occurred by opening the vertical joints which were striking parallel to bedding. Using this criterion the shear direction in the lab was always defined as the direction of least resistance which opened the near vertical micro joints in the sample. This corresponded to the down dip direction of the bedding plane in the field.

It was impossible to cut the rock samples accurately enough to fit directly into the direct shear box frame and so the samples were deliberately cut undersize. The dimensions were slightly less than the nominal dimensions cited above. The trimmed samples were then cast in Randustrial Bolt Anchor Sulfaset in order to standardize the size and orientation of the small blocks. Figure 5-2 is a pictorial summary illustrating how the samples were cut and molded. This is reported in detail in Appendix A-3.

The bottom halves of the samples were lightly sanded by hand to ensure a proper snug fit in the bottom half of the shear box. The upper half of the samples were sanded undersize on a belt sander so that 1.6 mm thick Teflon strips could be inserted between the samples and the upper shear box frame. This insured that dilation of the upper sample half could occur without being hindered by the interaction of the steel box and the Sulfaset casting.

Samples with natural surfaces were used to evaluate peak friction angles on the small scale. During casting and sanding, these natural surfaces were protected from contamination by a layer of brown paper held in place by masking tape. This was finally cut away and the surfaces cleaned with compressed air blasts prior to testing.

Samples which were used to evaluate the basic friction angle were cast in a similar manner. The lower half of the discontinuity shear surface was either sand blasted or sanded with clean sandpaper on a belt sander as a final step. This insured a uniform surface with little or no roughness on the 3 to 6 cm scale. Compressed air was used to clean this surface prior to testing.

Upon completion of casting and sanding, the samples were attached to a stationary platform and a mechanical tracer was used to record three discontinuity profiles for each sample. The rock surface profiles were traced by a metal stylus which was pulled over the rock surface at a constant rate. The stylus was attached to a linearly variable displacement transducer (LVDT) and the vertical displacements of the stylus tip were continuously recorded. The resulting profiles were traced by an X-Y recorder. Some example traces are shown in Figure 5-3.

Krahn (1974) devised a method of evaluating the roughness of a rock surface by digitizing the roughness profiles and calculating various mathematical parameters such as CLA, RMS or Z2 and Z3, to represent roughness on a scale of 0.01 m to 1.0 m in order to define a correlation between peak friction angles and surface roughness. He concluded however that the time and equipment demands were too great to warrant further pursuit of this method. Direct shear test results from samples up to 0.3 m square, the practical limit for shear testing at the University of Alberta laboratory, were easier to obtain than trying to predict friction angles on the basis of surface roughnesses.

In order to estimate the surface roughness of the 5 cm x 5 cm square samples prior to testing a straight edge and a modified protractor were used in conjunction with the graphical output profiles to evaluate the average i angle in a manner similar to that used by Patton (1966) on his field profiles.

In order to evaluate the uniaxial compressive strength of the material, 2.5 cm diameter cores were drilled from intact samples of rock using a modified drill press. Cores were extracted both parallel and perpendicular to bedding surfaces. The cores were then trimmed to a standard length of 6 cm prior to testing in a point load tester.

Small plates of intact rock material approximately 15 cm long,10 cm wide and 2 cm thick were cut from block samples of both the quartzite and the dolomite. Various techniques such as sandblasting, sanding or polishing with different grit sizes were used to prepare the surface finish of these plates. The plates were then used as the stationary plates which were anchored to the tilting table to define sliding angles. The samples cast in Sulfaset to be used in direct shear tests were also used in the sliding tests as the mobile slider blocks.

5-6 TESTING APPARATUS AND PROCEDURE

The direct shear test apparatus used to test the 5 cm x 5 cm square samples was designed and built at the University of Alberta. Shear deformations were applied at a constant strain rate to the lower half of the shear box by a worm gear connected by a chain drive to an electric motor. Horizontal and vertical deformations were recorded using LVDTS. The normal load was applied by a dead weight lever arm system. Shear load and vertical displacements were simultaneously recorded versus horizontal displacements on a dual channel Hewlett Packard X-Y-Y' recorder.

The shear load was measured on the upper half of the shear box by a 8.2 KN capacity load cell manufactured by Transducer Inc. The upper half of the shear box was supported by extension arms with roller bearings attached to movable stainless steel shafts. This arrangement meant there was no contact between the upper and lower halves of the shear box and so all the shear resistance measured was generated along the discontinuity only. This arrangement also prevented rotation of the upper shear box, a phenomenon which plagued earlier versions of this apparatus. Goodman (1976) notes that the majority of direct shear machines prevent rotation of the sample.

This arrangement also has the potential of increasing the normal stress acting along the discontinuity. Although the upper shear box was prevented from rotating, the sample within the upper box was still trying to rotate. It was thought prior to the start of testing, that the upper sample could thus jam in the upper box. This would prevent dilation and increase the normal stress. Consequently, the upper sample was sanded undersize and 1.5 mm thick Teflon strips were inserted between the sample mold and the steel shear box.

Tests were conducted to discern how the shear strengths evaluated in the new non-rotating shear box differed from results in which rotation had been allowed. Eight samples from a suite of rocks taken from an open pit mine, tested in 1975 using the old configuration, were tested. The peak friction angles were identical to those measured previously. In addition the original samples were retested and the results indicated that the ultimate friction angles had not changed. During the testing the dilation of the samples was monitored using an LVDT. The results indicated that the dilation rate was continuous and smooth, therefore no jamming or dilation suppression was occurring. There was no evidence of jamming or surface damage either on the upper sample mold or on the Teflon strips. As a result, it was concluded that no increase in normal stress was occurring during testing and that the shear box gave representative shear strengths. Dilation values that were measured during shear, however, were thought to be more accurate than values obtained in the old box as no component of rotation about projecting asperities was allowed.

Samples were inserted into the lower half of the shear box in a mated position. The lower half of the sample was forced into the shear box frame to ensure a snug fit. Often the sample had to be forcibly removed after the test. The upper half of the shear box was carefully lowered over the upper half of the sample and secured by the removable steel rods. The vertical load was then applied to the sample via the hanger system. The vertical and horizontal LVDT's and the horizontal load cell were placed in position and secured such that all were set to record maximum deformations and loads. The X-Y-Y' recorder was started and the initial load cell and LVDT readings were recorded. Shearing was initiated and all loads and deformations were monitored. The samples were sheared approximately 0.7 cm in one direction before the horizontal deformation direction was reversed. The samples were then sheared 1.4 cm in the opposite sense before being sheared back to their original positions. The normal load was held constant throughout the test. Peak shear loads occurred after only 1 to 2 mm of shear. As a result normal stress changes were not great.

Testing of the rock cores to define the uniaxial compressive strengths was relatively easy. The 6 cm long rock cores were placed between the conical plattens of the point load tester such that the plattens were across the diameter of the core at the mid length point. A hydraulic ram system was used to apply a force between the plattens across the core diameters. The maximum force applied across the plattens, which caused failure of the rock, was measured on a hydraulic dial gauge. The force measured was then converted to the uniaxial compressive strength of the rock materials.

JRC values, which are also a necessary component needed to define Øp using Barton's method, were evaluated from the traces of profiles measured from the direct shear test specimens. The roughness traces were then compared with the standard traces developed by Barton (Figure 4-10) and a JRC value for each profile was estimated.

Sliding tests were conducted using a new tilting table apparatus which was built at the University of Alberta. The table was a very simple piece of equipment which consisted of a heavy steel box constructed of 1.25 cm thick steel plate within which there was a rotating plate hinged at one end. The opposite end of the plate was connected to a finely threaded rod by a universal joint so that by rotating the threaded rod the table could be tilted. The whole tilting table could be securely clamped to a lab bench to eliminate vibrations. A metal pointer attached to the rotating table measured the angular rotation on a fixed protractor.

Clamps were attached to the rotating table to securely hold specially prepared blocks of rock, referred to as plates, in a fixed position. A rock sample which had been cut and molded for direct shear was then placed on the horizontal plate. The samples, referred to as sliders, had either natural or sand blasted surfaces. The horizontal table was then rotated at a constant rate until the upper block or slider slid down the inclined plane.

The angle at which sliding occurred was used to represent the angle of friction between the moving slider and the fixed plate. Figure 5-4 illustrates the simple statics involved.

In the case of sliding tests on natural surfaces, the two mating halves of a direct shear test sample were placed on the tilting table in a mated position. The lower half of the sample was clamped to the table so that the average failure surface orientation was horizontal. The table was then raised until failure occurred.

5-7 TESTING PROGRAMME

Direct shear tests to evaluate the peak friction angles and ultimate friction angles were performed on 30 5 cm x 5 cm samples with natural surfaces taken from the debris piles. Normal loads were varied from 0.05 to 0.8 MPa. This corresponded roughly to a normal load range imposed by 0 to

34 m of rock. The maximum thickness of rock thought to have been overlying the failure surface was 30 m so the normal loads applied easily encompassed the range of normal loads acting in the field. All the natural discontinuity surfaces tested were bedding surfaces along which no discernable movement had taken place.

Fourteen direct shear tests were also run on a variety of artificial surfaces in order to define the basic friction angle. The normal loads used during this stage of testing also ranged from 0.05 to 0.8 MPa. The upper halves of the shear test specimens were always sand blasted surfaces whereas the lower halves of the specimens consisted of a variety of roughnesses. The sand blasted specimens were consistently used for the upper block to avoid the problems of stick slip associated with shear tests performed between two smooth surfaces (Bowden and Tabor, 1950).

In addition to the direct shear tests a series of tilting table tests were run on samples with artificially prepared surfaces. The objective of these tests was to investigate the possibility of evaluating ϕb in a simple fast manner. The ϕb values from the tilting table tests were compared with the ϕb values evaluated using the more conventional techniques. All the samples used in this part of the testing programme were taken from one block of dolomite or one block of quartzite in order to minimize mineralogical differences.

It was originally thought that due to the very low normal loads imposed on the tilting table tests even micro roughnesses would alter the angles of sliding and that in order to remove the topographic effect very smooth plates would be needed. Highly polished plates of dolomite and quartzite were prepared using a special polishing technique used in ore mineralogy. Samples were ground smooth using progressively finer grades of carborundum grit and finally polished using tin oxide on a vibrating table covered with felt cloth. Naturally rough or sand blasted samples were used as sliders on the very smooth polished plates in order to eliminate the effect of stick slip found between two smooth surfaces.

The initial angles recorded during these tests were much lower than expected. As a result other plates were prepared with artificial surfaces of various roughnesses. These plates were sanded with #80 grit sand paper, sand blasted or lapped with #200 grinding powder. The various values of sliding angles were then compared with the angles recorded in direct shear and by other authors (Patton, 1966 and Coulson, 1972 and Barton, 1971). Sliding tests were performed on the polished surfaces and some sand blasted surfaces in both a dry environment (RH = 10 %) and a wet environment (RH =100%) at 25°C to investigate the effect on tilting table results. The majority of the tests were run dry at 25°C.

Naturally rough samples were also tested on the tilting table. These samples were always naturally rough mating surfaces which were taken from the set of direct shear test specimens prior to shear testing.

The testing programme associated with the point load tests consisted of breaking seven 2.5 cm diameter cores of quartzite and five 2.5 cm diameter cores of dolomite. All cores tested were 6 cm long. The cores were allowed to air dry for 30 days after being extracted from the block sample by a water-cooled diamond drill. The cores were then tested in a relative humidity of 10% and a temperature of 25°C. Cores were extracted from the rock both parallel and perpendicular to bedding surfaces to investigate the range of strengths imposed by anisotropy.

5-8 DIRECT SHEAR TEST RESULTS

All of the direct shear test results were recorded directly onto the X-Y-Y' recorder and the peak shear load T p, the ultimate shear load, T ult, and the respective dilation angles i, were all measured directly from this graph.

The peak shear load, measured in the direction of least resistance, was taken as the maximum shear load which occurred during the first deformation cycle. The ultimate shear load was evaluated near the graph's origin where the dilation curve indicated that there was no influence in the i angle (dy/dx=0). The ultimate values were recorded for both directions of shearing and then averaged. This eliminated any variations in shear resistance caused by non horizontality of the discontinuity surface due to misalignment of the bedding surfaces in the mold. The ultimate shear strengths were recorded after approximately 2.4 cm and 4.8 cm of displacement. Figure 5-5 is a representative example of one of these graphs. All of the test results are included in Appendix A-3.

The shear loads measured from the graphs and the vertical loads applied for each test were divided by the original nominal surface area of each sample, measured prior to testing, to convert all loads to stresses. The resulting peak and ultimate stresses are summarized in Tables A 4-1 and A 4-2 in Appendix A-4.

A certain amount of slack in the deformation system was recorded on the X-Y-Y' graphs and is labelled in Figure 5-5. This slack was inherent in the system and was impossible to eliminate.

The resulting values of normal stress and shear stress were plotted on Mohr-Coulomb diagrams and shear strength envelopes were fitted to the data. A straight line envelope defined by T =a(0) +a(1)N, and a power law envelope defined by T =aN exp.b, were tested using simple regression analyses. The term exp. b means raised to the power b. In all cases the normal stresses, N, were assumed to be known accurately. Confidence limits were then defined for the best fit lines by assuming that all deviations from the best fit line were due to variations in shear strength values. The shear strength data are summarized in Figures 5-6 and 5-7.

In order to establish how closely the peak and ultimate data points were described by a straight line the power law curves were altered to the form of log T =log a +b log N. A linear regression analysis was performed on this data and the 95% confidence limits for b were established. The results indicate that for the Jonas Creek peak and ultimate values and for the Whitehorse Creek ultimate values, the exponent b could equal 1. The Whitehorse Creek peak values, however, ranged from 0.423 to 0.875 (Table 5-1). The best fit line had an exponent of 0.649. The best fit power law line is shown in Figure 5-7.

Both the power law envelope and the straight line envelope appear to fit the data equally well over the central part of the graph.

The straight line Mohr-Coulomb envelopes for the peak and ultimate data points for both the Jonas Creek and the Whitehorse Creek samples did not intersect the origin of the graphs and small values of cohesion were obtained. Since the sample halves had been separated prior to testing these values do not reflect a true cohesion mechanism. The 90% confidence limits for the cohesion intercepts were calculated and the result implied that for both peak and ultimate Jonas Creek values, and the ultimate Whitehorse Creek value, the value of c could be zero. The 95% confidence limits about the cohesion value for the peak Whitehorse Creek data, indicates that the value of cohesion could also be zero.

Table 5-2 summarizes the shear test results for natural and artificial surfaces and these results indicate that the peak and basic friction angles are well within the values recorded by previous authors who conducted small scale direct shear tests (Krahn, 1974 and Coulson, 1972). The peak values, however, were considerably higher than those predicted on the basis of back analyses of the rock slides (Chapter 6).

5-9 ROUGHNESS EVALUATION RESULTS

The small scale roughness of the profiles recorded were visualized as being caused by a series of small asperities each of which could be represented by an i angle. The average i angles for each profile were evaluated and compared with the other two profiles run on each sample. All were found to be of similar roughness. Krahn (p.54, 1974) found similar results and concluded that roughnesses taken anywhere on one sample would not be significantly different.

Krahn also found that there was a significant difference in surface profiles of a sample measured before and after shearing (Figure 5-8). Six samples from Jonas Creek, however, profiled before and after direct shear tests, showed no significant differences between the i angles recorded. Table 5-3 summarizes the i angles measured before and after shear. In the case of dolomite samples from

Whitehorse Creek surface damage during shear was considerably greater than that found in the Jonas Creek samples and in many cases this led to small pieces of loose rock being dislodged from the surface. When profiles were run on these surfaces the various sizes of crushed rock would loosen and interfere with the stylus of the roughness profiler and cause binding. This led to non-representative profiles. In some instances the steep shattered surfaces appeared rougher after shearing. After three abortive attempts to measure the post shear roughness on the dolomite samples this procedure was stopped.

The i angles evaluated prior to shear for each sample were averaged and tabulated in Table 5-4. The corresponding i angle for each sample measured by dilation during shear were also recorded. The samples from Jonas Creek exhibited a straight line relationship between the two methods of measuring i as shown in Figure 5-9. However, the amount of scatter surrounding the best fit straight line prevented the use of this method in a predictive capacity. The samples from Whitehorse Creek showed considerably more scatter than the Jonas Creek results. The i angles evaluated in profile were considerably larger than the i angles measured during shear. This poor correlation between the i angles was probably due to the crushing or shearing through of the small steep asperities. The very hard quartzite from Jonas Creek did not crush easily and areas of surface damage were small. These areas were approximately 1% of the area of the shear surface. The dolomite samples, however, exhibited a much larger area of surface damage. The area of surface damage was very hard to evaluate for the dolomite samples but appeared to vary from 10 to 20 % of the area.

Ladanyi and Archambeault (1970) proposed equation 4.4 {$(As = 1-(1-N/Nt)^{1.5})$} to predict areas of shearing through, (As). Assuming a transition pressure of 100 MPa and a maximum normal load of 1.5 MPa for the Jonas Creek quartzite, then the predicted maximum area of shear is approximately 2.2%.

Assuming that the transition pressures for dolomite and quartzite vary in the same ratio as the uniaxial strengths, then the N/Nt ratio for Whitehorse Creek is 1500/33,000 (Section 6-9). The calculated shear area is 6.7% or 3 times greater than that expected for Jonas Creek samples. (Tp/N) for each sample and the corresponding i value measured by dilation at peak shear load were recorded. The resulting relationships illustrated in Figure 5-10 indicate a similar trend to that defined by Barton (1974). Barton indicated that there was a relationship linking the Øpeak values measured during laboratory shear testing with the i values measured at the point of peak shear by dilation. Barton attempted to show that the relationship of Øp-Øb = 2i(dilation) represented the behaviour of artificial samples tested in the lab. This relationship also appeared to represent the results from Jonas Creek and Whitehorse Creek. The results of this comparison indicated that the approach used by Barton to predict the lab shear strengths on the basis of $\phi b + i$ accurately predicted the relationship between the i measured during shear and the i measured prior to shear.

5-10 RESULTS OF THE POINT LOAD TESTS

The maximum force F, applied across the conical plattens of the point load tester was recorded for each rock core tested. The force values were then divided by the square of the core diameter to convert the forces to stress units;

$$I = F/D^2 \qquad 5.2$$

The I value, in this case evaluated for a core diameter D of 25 mm, was then modified using a graph presented by Broch and Franklin (1972) to give an I value for a core diameter of 50 mm, the standard around which the test was calibrated by Broch and Franklin (1972). The uniaxial compressive strength of the rock material was then given by

$$C = 24 I \qquad 5.3$$

The uniaxial strengths of the cores were highly anisotropic and depended greatly upon whether the sample was split parallel or perpendicular to bedding. The values are summarized in Table 5-5. The values of the uniaxial strengths C, when used in Barton's general equation with various values of normal load, yield various values of i given by

$$i = JRC \log_{10}(C/N) \qquad 5.4$$

which often lead to a curved Mohr envelope. The value of i is modified by an empirical evaluation of roughness, the joint roughness coefficient (JRC). In cases where weathering has occurred the uniaxial compressive strength of the material is replaced by the joint compressive strength (JCS) of the rock (Barton and Choubey, 1977). The discontinuity surfaces at Jonas Creek and Whitehorse Creek were not noticeably weathered so the uniaxial compressive strength values were used.

One further modification must be made. When dealing with very low normal loads such that the ratio of (C/N) is greater than 100, where C is the uniaxial compressive strength of the material and N is the normal stress for which the shear strength is being evaluated, then Barton (1974) recommended using a straight line from the origin to the point defined by C/N =100 to define the Mohr-Coulomb envelope. All the results from Table 5-5 indicate that for the maximum normal loads used in the direct shear tests (0.8 MPa), the ratio of C/N should be replaced by 100 and a straight line envelope used.

Using the value of C/N=100 Barton's equation for i simplifies to

$$i = 2(JRC) \qquad 5.5$$

Barton (1974), originally evaluated the JRC of a rock sample by qualitatively comparing the trace of a discontinuity surface with three roughness profiles having known JRC values. Barton and Choubey (1977) later refined the JRC values and presented a set of ten curves with known JRC values (Figure 4-10). Using these curves in comparison with the profiles of the rock samples made earlier, estimates of JRC were made for Jonas Creek and Whitehorse Creek sample profiles. The mean and standard deviations of the JRC values for all the profiles grouped were 9.4°± 4.4° at Jonas Creek and 16.7°± 3.1° at Whitehorse Creek. These corresponded to i angles of 18.8°± 8.8° and 33.4°± 6.2° (Equation 5.5). Peak friction angles were therefore given by 48.8°± 8.8° and 58.4°± 6.2°, assuming Ø basic values of 30° and 35° respectively. The peak angles so defined were very close to the peak friction angles of 48.1°± 3.5° and 51.6°± 7.0° evaluated using the direct shear apparatus.

5-11 TILTING TABLE TEST RESULTS

The tilting table tests were originally intended to be used as a fast means of establishing Øb without using a direct shear box. This type of approach could perhaps be useful during preliminary investigations. Results can be obtained at low cost within 1 or 2 hours after sampling. Shear tests results often take 6 to 8 days to evaluate. The first set of tests were conducted using naturally surfaced block sliders resting on very smooth polished plates. The very smooth plates were used because it was thought that even small asperities on the plate would significantly change the angle at which sliding occurred due to the very low normal loads imposed on the sample. The naturally rough sliders were used to overcome the frictional phenomenon known as stick slip which occurs when two very smooth surfaces are sheared past each other. Stick slip occurs due to the presence of very thin layers of contaminant which form on the smooth surfaces. Rough surfaces tend to break up the layer of contaminants and hence are not as susceptible to stick slip. The naturally rough sliders used for these tests were the direct shear test samples used to measure Øp and Øult in Section 5-7. The tilt tests were performed prior to the direct shear testing. Tilt table results reported in this section were all obtained from tests performed in a room with a relative humidity of approximately 10% and a temperature of approximately 25° C.

Roughnesses on the polished plates were measured using a Talysurf roughness measuring device, as the larger profiler used to measure the roughness of natural samples was too coarse. The Talysurf yielded a single average value of roughness measured as a center line average value which gave a quantitative measure of plate roughnesses for comparison purposes.

The CLA values for the quartzite and dolomite polished plates were 0.75 micro-m. Table 5-7 summarizes the various CLA values measured for various surface preparations and indicates that the CLA values found on the smooth surfaces had by far the lowest values of roughness. Roughnesses on the polished surfaces were at least one order of magnitude smaller than sandblasted surfaces and several orders of magnitude smaller than roughnesses on 5 cm x 5 cm samples. This means that for all practical purposes the roughness on the polished plates was neglible. In addition, inspection of this surface profile under a microscope at 100x magnification indicated that no roughness was visible and so the resistance to sliding was the result of mineral to mineral contact. As a result future reference to the sliding angle defined using a polished plate will use the term mineralogic friction angle and will be represented by the symbol ϕm.

Initial sliding angles recorded for 9 quartzite sliders on the polished quartzite plate had a mean and standard deviation of 12.3°± 2.6°. The initial sliding angle for 10 dolomite sliders was 16.8°± 2.7°. The mean value of 12.3°± 2.6° recorded for the quartzite sample is similar to the value of 12.8°± 0.9° found by shearing a sand blasted surface over a polished surface in direct shear tests (Section 5-7).

Tilting table tests were also performed using sand blasted sliders on polished plates in order to compare the sliding angles using this surface combination with the results established using direct shear tests. The sliding angles were not significantly different from those established using naturally surfaced sliders on a polished surface. The means and standard deviations of three tests for each of the quartzite and dolomite samples respectively were 11.5°± 0.5° and 16.3°± 1.2°. The differences of between 4° and 5° in the mean values of sliding friction, Øm, between the quartzite and dolomite, were similar to the differences in Øb found by Coulson (1972) for similar rock types. Coulson sheared two sand blasted samples past each other and found a difference of 5° between the Øb values of quartz rich and carbonate rich rocks (Coulson, 1972, p.99).

The low angles of friction, Øm, recorded for the tilting tests agreed well with values of friction reported by Horne and Deere (1965) who sheared smooth buttons of rock with low surface contact areas (to avoid the problem of contaminants) over smoothly polished plates of rock.

A series of tests were performed using naturally surfaced sliders of quartzite on quartzite plates lapped with #200 grit abrasives. CLA measurements recorded on this sample indicated that the roughness was intermediate between the smooth polished plate and the rough sand blasted surfaces. The CLA value was 26 micro-m. The angle of sliding for nine tests had a mean and standard deviation of 22.2°± 1.6°.

Similar sliding tests were also conducted using plates of quartzite and dolomite artificially roughened by sand blasting or by lapping with #80 grit sandpaper. Roughnesses measured on the dolomite samples were 150 micro-m and on the quartzite samples were 200 micro-m. No significant differences were noted between the values established using sand blasted or sanded plates and sand blasted or sanded sliders. The sliding angles for the various combinations are summarized in Table 5-8. The mean sliding angles and their standard deviations however were 30.8°± 1.1° for the quartzite and 34.2°± 1.0° for the dolomites. These were similar to the basic friction angles of 32.0°± 4.4° and 35.8°± 3.1° measured on equally rough surfaces in the direct shear box. The normal loads applied during direct shear tests were significantly higher than those used in the tilting table tests. However, for purposes of evaluating Øb this is of little concern as Øb does not change significantly over the normal loads commonly investigated in surface workings (Coulson, 1972). Results of Øb shear tests conducted over the normal stress range expected at either Jonas or Whitehorse Creeks indicate that Øb is stress independent for this stress range.

Sliding tests performed on mating natural surfaces gave extremely variable results which appeared to be controlled only by surface roughnesses and not at all by mineralogy. The angles of sliding varied from 36° to 66° and averaged 45.2°. The rougher samples consistently gave the higher values of sliding friction. Due to the large scale of the asperities with respect to the total block size being tested, and due to the configuration of the sample blocks, interlocking between asperities occurred and a rotating toppling failure was seen to occur in all but the smoothest of samples.

The maximum allowable angle of rotation was dependent upon the block configuration of the sliders which was previously determined due to the size of direct shear specimens. The maximum angle which could be reached without inducing tension near the top of the failure plane was 35 to 40°. At this point the normal resultant of the upper slider fell outside the middle third of base of the slider. At 60-65° the resultant fell outside the base of the block and toppling occurred. The failure angle could no longer be regarded as a sliding friction angle.

In order to establish the relevance of the tilting table test for measuring Øb, a variety of rock types were tested using sliders and plates both of which had been lapped with #80 grit sandpaper. The tests were performed at a relative humidity of 10% and a room temperature of 25°C. Rock types tested included fine grained felsite, coarse grained granodiorite, and coarse and fine grained poorly cemented sandstones in addition to the quartzites and dolomites already tested. Five sliding tests were performed for each sample and the slider and plate were blown clear of debris using compressed air after each slide. These results were compared with Øb results recorded by Coulson (1972) using direct shear tests on sanded surfaces of limestone, coarse grained granite, fine grained granite and sandstones. Table 5-8 summarizes Coulson's results. A comparison of the tilting table results with those presented by Coulson (1972) indicates that the tilt table tests give reliable friction angles comparable with those found using conventional techniques.

5-12 TILTING TABLE TEST RESULTS : PART 2

Further tests were conducted on the polished surfaces of both quartzite and dolomite plates using naturally surfaced blocks of the same lithology as the plates for sliders. In the first instance, after each sliding failure, both the slider and the plate were blown clean with compressed air and the sliding angles did not increase noticeably after 9 slides (Section 6-8).

During these tests no surface damage occurred to either of the polished plates anchored by clamps to the tilting table. However, a very loose cohesionless powder of silt size particles was left on the polished dolomite surface after each slide. This powder was derived from the crushing of the fine asperities which formed the contact points between the polished plates and the natural surface of the slider. If the powdered debris was left to accumulate on the polished surface the angle at which sliding occurred increased from 16.8° ± 2.8° to 29.6° ± 3.6° over 6 or 7 continuous slides. The angle then remained constant during further sliding. If the powder debris was blown from the surfaces by compressed air the sliding angle immediately decreased to about 20°± 2° but never again did it regain the original low value of 16.8°± 2.8°.

The increase in the sliding angle, Øm, measured on the dolomite blocks was apparently due to the interaction between the sliding block and the loose very fine grained debris on the polished surface. This prompted a closer look at the sand blasted surfaces used to represent Øb which yielded sliding angles very similar to those recorded on polished plates after several slides without cleaning. The sand blasted surfaces had tiny asperities equal in size to the sand grains used to sand blast the rock. In the case of the quartzite these asperities were formed by individual sand grains protruding from the quartzite matrix. In the dolomite sample the soft fine grained dolomite was forced to assume a profile similar in form to the sand grains bombarding the surface. The asperities consisted of small pieces of dolomite surrounded by indentations left from the sand blasting process.

The orientations of the small scale asperities were examined under a microscope and the inclinations of the asperity faces were evaluated using a straight edge and a protractor. The average orientations established on the basis of over 50 random measurements had a mean and standard deviation of 18.7°±6.1°.

The sliding angles on the sand blasted surfaces for quartzite and dolomite had means of 30.8° and 34.2° respectively. The Øm values established by sliding tests had means of 11.5° and 16.3° for quartzite and dolomite respectively. The differences between the two were 19° and 17.9° respectively. It appears on the basis of these findings therefore that Øb is in reality a combination of Øm, the angle of friction determined on perfectly smooth surfaces, and an i angle, i microscopic, which forms as a result of sand blasting.

A series of sliding tests were also conducted in order to define how the sliding angles varied with moisture content. Tests were conducted in a humid environment with a relative humidity of 100% and a room temperature of 25°C. Sand blasted sliders were used in all cases and both polished and sand blasted plates were used. The smooth plates showed an increase in Øm of about 8° to 10° for both quartzite and dolomite samples. The sandblasted surfaces showed less than 2° increase in the mean sliding angle when sliding occurred on a wet surface as opposed to a dry surface..

Bromwell noted that the presence of surface water greatly affected the coefficients of friction of smooth surfaces (Lambe and Whitman,1969, p. 66). This effect diminished, however, as the surface roughness increased. This effect was indeed noted here as the increase in sliding angles from "wet" to"dry" conditions varied from 9° on average for smooth plates to 2° on average for sand blasted plates.

5-13 SUMMARY OF THE RESULTS

Peak friction angles recorded on natural discontinuities were much higher than those found by back analysis to be acting during failure. This result is thought to be a consequence of the scale effect of direct shear tests. The peak shear strengths defined by Barton's analysis using JRC values evaluated from the shear test sample profiles yielded peak friction angles very similar to those evaluated by direct shear.

The ultimate friction angles, the angles measured after a large degree of displacement, when very little topographic component was acting, were very similar to Øb in the case of Jonas Creek samples and friction angles about 5° higher than Øb for the Whitehorse Creek samples. The Whitehorse Creek samples had rougher discontinuity profiles prior to testing than the Jonas Creek samples and so it was thought that even after a large amount of displacement the friction angle was still being influenced by roughness. It would seem therefore that ultimate values of friction evaluated on very rough natural surfaces should not be used to estimate the basic friction angle, Øb.

The peak shear stresses plotted on a Mohr-Coulomb diagram over the normal stress range thought to be acting at the rock slide failure surfaces were represented very well by a straight line relationship, thereby reinforcing the Øb + i theory previously explained in Section 4-2. The i angles measured during dilation for the quartzite samples were equal to the i angles measured on the profiles prior to shearing and these i angles were equal to one half of the difference between Øp and Øb ; a relationship defined by Barton in 1971. The same relationship was not as clearly defined in the softer dolomite samples due to the shearing through of asperities rather than riding over. This also explains why the Mohr-Coulomb envelope for the dolomite samples had an effective cohesion intercept. The resulting Øp friction values, recorded on 5 cm x 5 cm square samples, however, grossly overestimated the shear strengths acting in the field.

Basic friction angles were also evaluated using conventional shear tests in a manner outlined by Patton (1966) and Coulson (1972). The Øb values defined for the quartzite and dolomite samples tested were very close to the values commonly assumed for Øb for the various rock types (30° for quartzite and sandstones and 35° for dolomites and limestones).

Tilting table tests using natural surfaces as sliders and sandblasted surfaces as plates yielded similar Øb values to those given by Coulson (1972). Use of the tilting table also illustrated very clearly how Øb is dependent on surface roughness. A very smooth surface in the field caused by geologic deformations may have a much lower basic friction angle than the commonly quoted 30° to 35°. Krahn (1974) reported peak and ultimate friction angles of 28° and 15.6°

respectively for limestone samples of bedding surface discontinuities which had undergone flexural slip. Bruce and Cruden (1977) reported peak and ultimate friction angles of 30° and 20° for discontinuities contained within felsite samples. The basic friction angle is in reality a combination of ϕm and i microscopic and varies directly as the i microscopic values vary. ϕ mineralogic is a function of mineral to mineral contact only.

5-14 RECOMMENDATIONS

The results for the tilting table tests indicate that a different procedure for evaluating discontinuity shear strengths may be used, especially for preliminary assessments. The tilt test can be applied to hard rock surfaces which do not have a pronounced topography. Weathered surfaces or clay covered surfaces cannot be tested in this manner due to a cohesive strength component. The tilt test is simple to perform and is much faster to perform than a direct shear test. The results, evaluated in detail for dolomite and quartzite samples and superficially for several other rock types, are similar in magnitude to direct shear test results for equivalent surface roughnesses.

The tilting table plate can easily be changed to simulate a variety of roughnesses. This becomes necessary when the discontinuity in the field is smoother than a sandblasted surface. This can occur in a fault zone or along beds deformed by flexural slip. The sliding angles recorded for the smooth surfaces vary depending on the relative humidity of the testing environment. Tests should be conducted at low relative humidities as this gives rise to the lowest possible angles and hence is a conservative estimate of the friction angle. In addition, at normal loads higher than can be obtained on the tilting table, the effect of the surface contaminants, which are responsible for altering the sliding angle, may be reduced.

Barton and Choubey (1977) have recommended the use of the tilting table tests to evaluate the basic friction angle. The surfaces recommended were flat saw cut surfaces similar to those recommended by Patton (1966).

The procedure being recommended here uses naturally rough slider blocks on plates of equivalent lithology finished to an appropriate degree of roughness. This allows tests to be performed on surfaces smoother than sawn surfaces. The use of a naturally rough slider also eliminates the effect of stick slip. This becomes necessary when the discontinuity in the field is smoother than a sandblasted surface.

TABLE 5-1

Summary of shear test results and their confidence limits

FORM	JONAS CREEK	WHITEHORSE CREEK
Power law	$T=0.975\ N^{0.913}$	$T=1.241\ N^{0.649}$
(peak)		
T = a N exp.b	95% conf. b ±0.20	95% conf. b ±0.226
(ultimate)	$T=0.575\ N^{1.190}$	$T=0.731\ N^{1.026}$
	95% conf. b ±0.16	95% conf. b ±0.55
Straight Line	T=-0.013 +1.115 N	T=0.166 + 1.262 N
(peak)		
	90% a = ± 0.068	95% a = ±0.190
	90% b = ± 0.135	90% b = ±0.330
(ultimate)	T=-0.035 +0.664 N	T=0.021 +0.862 N
	90% a =± 0.025	90% a = ±0.520
	90% b =± 0.069	90% a = ±0.120

TABLE 5-2

Summary of Direct Shear Test Results

Sample	Surface	Natural	Natural	Sandblasted	Polished
Quartzite	Angle=	Peak	Ultimate	Øb	Øm
	Ø value	48.1°	33.6°	32.0°	12.8°
assumed cohesion value was zero throughout					
Dolomite	Angle=	Peak	Ultimate	Øb	Øm
	Ø value	51.6°	40.7°	35.8°	------
	cohesion	0.16MPa	0.0	0.0	0.0

TABLE 5-3

Summary of i angles recorded before and after shear for 6 samples of quartzite.

BEFORE

sample	avg. i from profiles	standard deviation
JC-1	5.5	4.0
JC-2	6.0	4.1
JC-3	14.6	4.7
JC-5	7.0	2.5
JC-6	4.5	2.0
JC-7	4.7	2.1

AFTER

JC=1	5.3	3.2
JC-2	5.4	4.8
JC-3	14.7	5.7
JC-5	8.2	1.1
JC-6	5.0	1.8
JC-7	4.3	2.4

TABLE 5-4

A comparison of the i angles measured on the profiles with those measured by LVDT during shear.

Sample #	i from the profile	i from the LVDT
JONAS CREEK		
JC-1	5.5°	4.5°
JC-2	6.0°	9.6°
JC-3	14.6°	16.0°
JC-4	6.1°	5.8°
JC-5	7.0°	6.5°
JC-6	4.5°	5.5°
JC-7	4.7°	7.0°
JC-8	5.5°	3.5°
JC-9	11.4°	7.5°
JC-10	4.3°	4.5°
JC-11	5.0°	2.0°
JC-12	5.5°	1.0°
JC-13	5.3°	6.7°
JC-14	8.6°	10.0°
JC-15	11.9°	7.5°
JC-16	7.1°	4.5°
JC-17	10.5°	4.5°

TABLE 5-4 CONTINUED

WHITEHORSE CREEK

WC-1	4.5°	6.0°
WC-2	15.3°	14.5°
WC-3	10.4°	0.0°
WC-4	20.9°	3.0°
WC-5	11.5°	3.0°
WC-6	11.2°	4.0°
WC-7	8.3°	6.0°
WC-8	15.1°	8.0°
WC-9	14.1°	9.0°
WC-10	11.9°	16.0°
WC-11	11.2°	7.5°
WC-12	11.3°	8.0°

TABLE 5-5

A summary of uniaxial compressive strengths as obtained by the point load tester.

bedding orientation

JONAS CREEK	4 cores	3 cores
quartzite	mean C=539.3 MPa	233.2 MPa
	std.dev. =±98.55 MPa	±48.6 MPa
WHITEHORSE	2 cores	3 cores
CREEK	mean C=179.8 MPa	85.1 MPa
dolomite	std.dev. =±41.0	±33.3 MPa

TABLE 5-6

A summary of the CLA values encountered on the artificial surfaces.

rock	polished	#200 grit	sandblasted
quartzite	0.75 micro m	26.0 micro m	150.0 micro m
dolomite	0.75 micro m	------------	200.0 micro m

* Natural surfaces could not be evaluated using the Talysurf but an approximation, made from the profiles of the samples was approximately 4000 micro m.

TABLE 5-7

A summary of the sliding angles ϕ_s,measured by tilt table

QUARTZITE

Plates lapped with

	tin oxide	#200 grit	#80 grit	sandblas
natural sliders	12.3±2.6°	22.2±1.61°	31.3±1.5°	30.8±2.4°
sandblasted sliders	11.5±0.5°		31.0±2.2°	30.2±2.2°
DOLOMITE				
natural sliders	16.8±2.7°		34.3±1.2°	34.2±1.3°
sandblasted sliders	16.3±1.2°		34.1±0.3°	34.2±2.6°

TABLE 5-8

A comparison of the sliding friction angles from the tilt table with those defined by Coulson.(surfaces lapped with #80 grit

rock type	sliding angles	direct shear results
quartzite	30.8±1.1°	32.0±4.4°
felsite	32.0±1.0°	
granodiorite	32.0±0.3°	
dolomite	34.2±1.0°	36.0±3.1°
crse.sandstone	37.5±0.5°	
fine sandstone	35.7±0.3°	

Coulson's Results

limestone	34 to 40°
fine granite	34 to 36°
coarse granite	32 to 36°
sandstone	28 to 39°

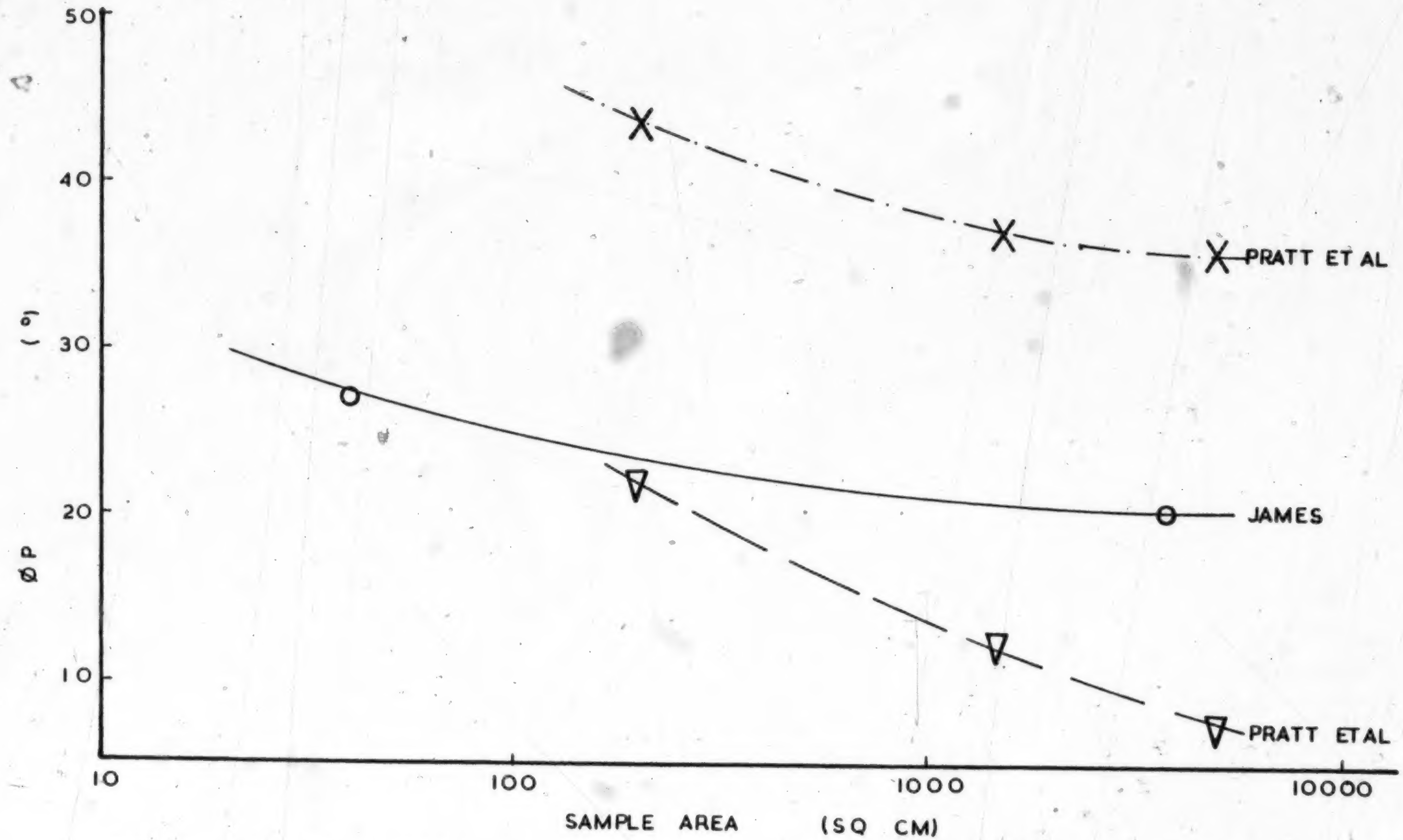

FIGURE 5-1 Scale Effects Of Sample Size On Peak Friction Angles (Modified After James, 1970, And Pratt Et.Al. , 1975).

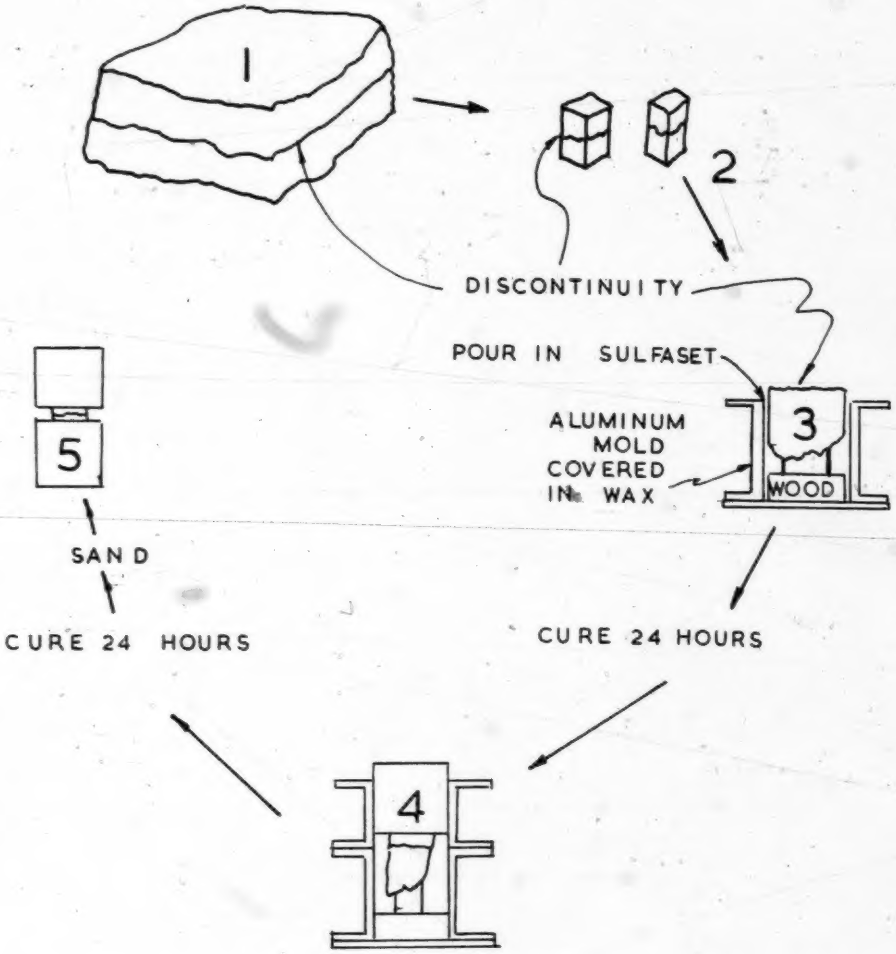
1
2
DISCONTINUITY
POUR IN SULFASET
3
ALUMINUM MOLD COVERED IN WAX
WOOD
CURE 24 HOURS
4
CURE 24 HOURS
SAND
5

FIGURE 5-2 Schematic Diagram Of Sample Preparation.

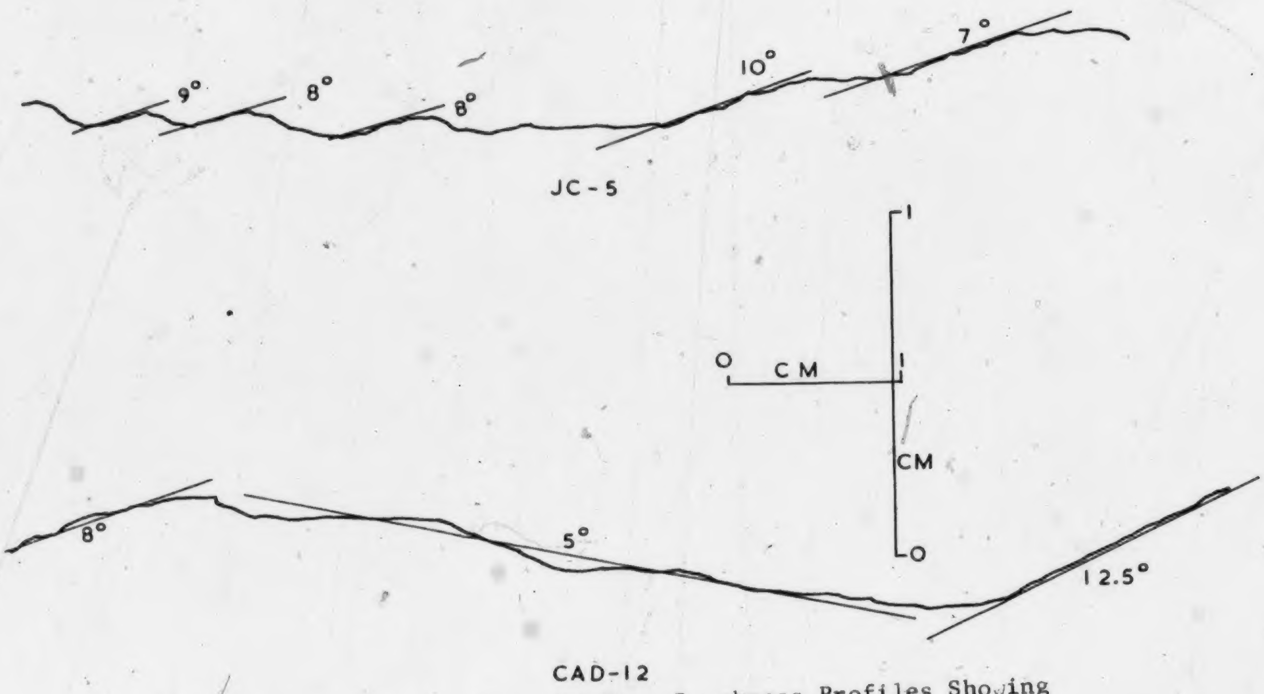

FIGURE 5-3 Example Traces Recorded From Roughness Profiles Showing Some Representative i Angles.

FOR LIMIT EQUILIBRIUM
THE DISTURBING FORCE
= THE RESISTING FORCE

$$W \sin\beta = W \cos\beta \tan\phi$$

$$\therefore \beta = \phi$$

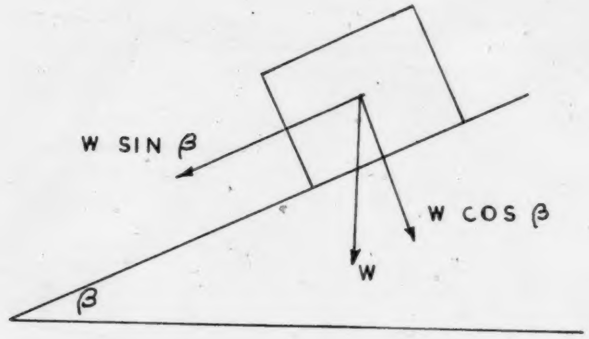

FIGURE. 5-4 Schematic Drawing Of Sliding Test Statics

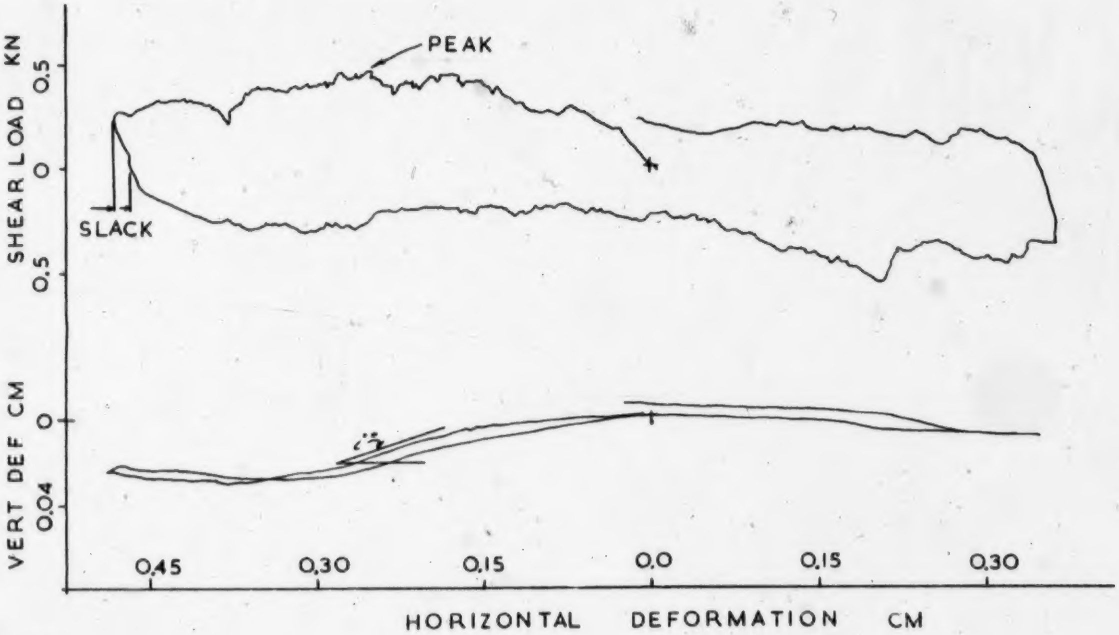

FIGURE 5-5 An Example Of A Direct Shear Test Graph Result.

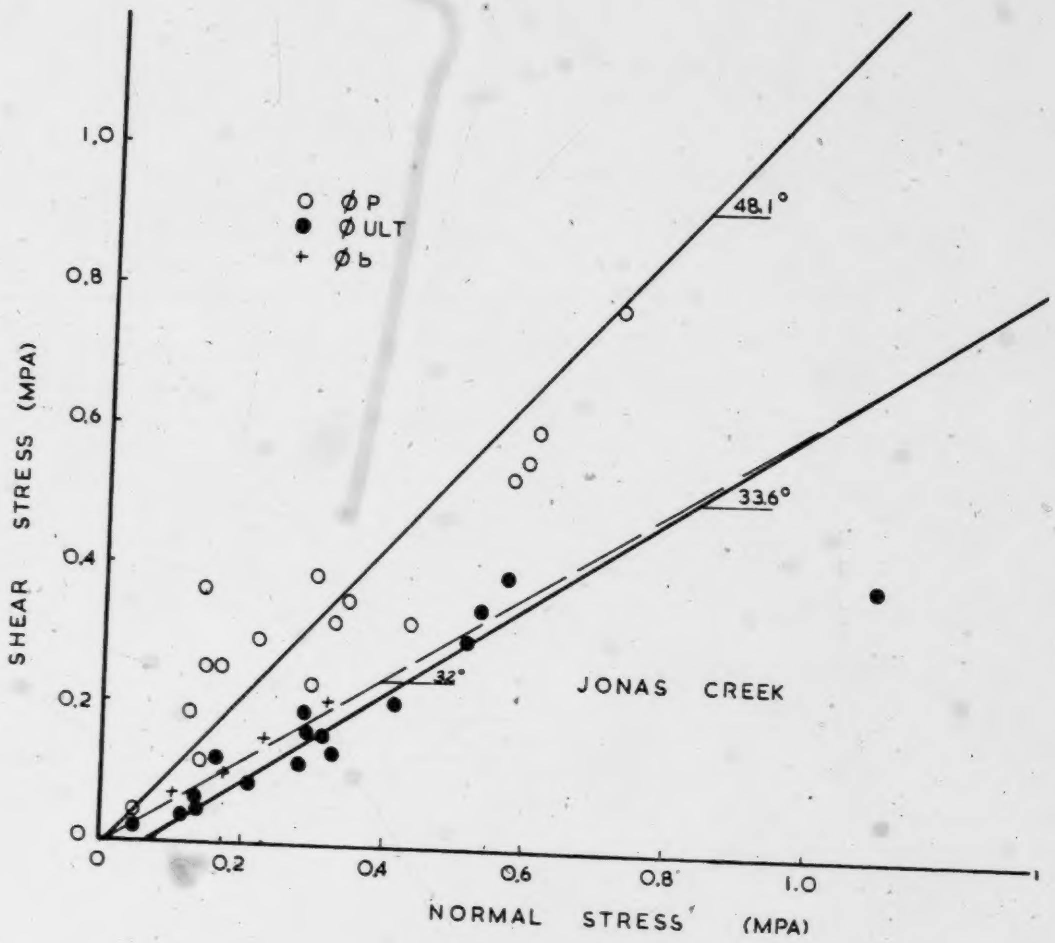

FIGURE 5-6 Mohr Coulomb Envelopes For The Results Of The 5 cm x 5 cm Direct Shear Tests At Jonas Creek.

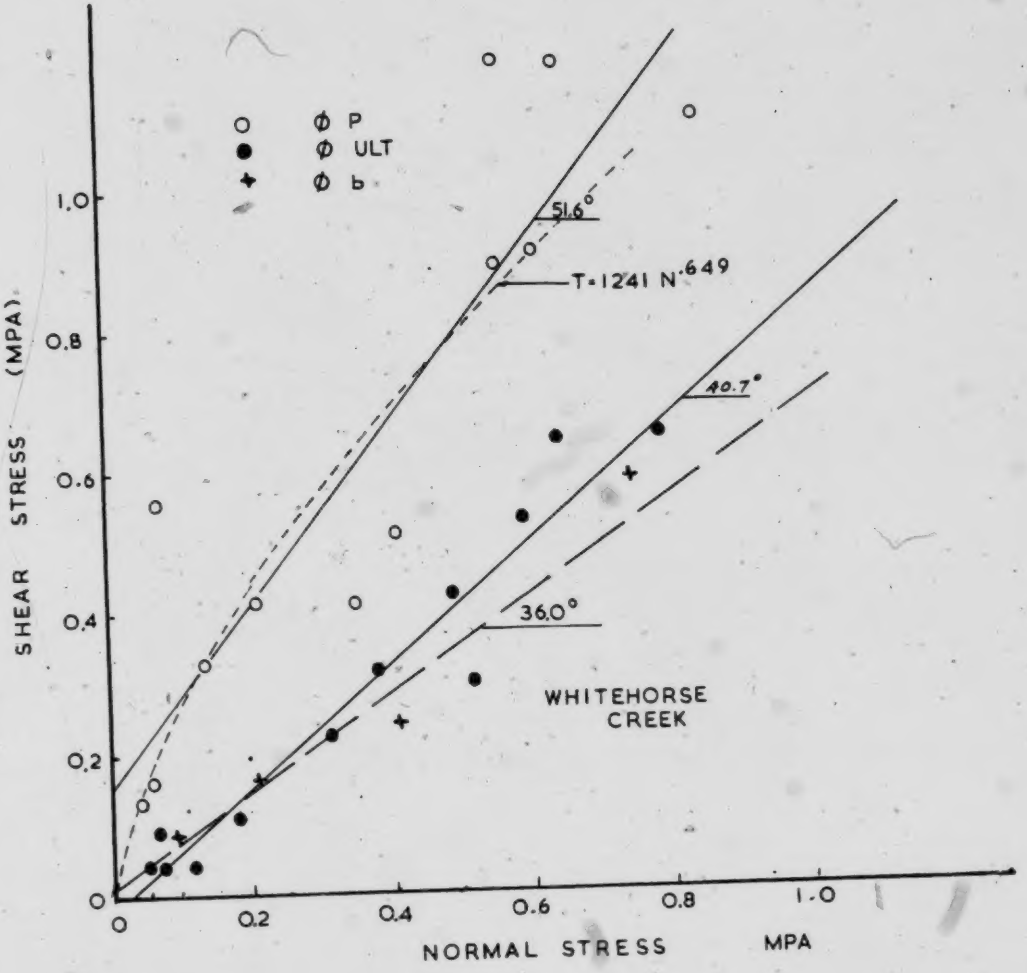

FIGURE 5-7 Mohr Coulomb Envelopes For The Results Of The 5 cm x 5 cm Direct Shear Tests At Whitehorse Creek.

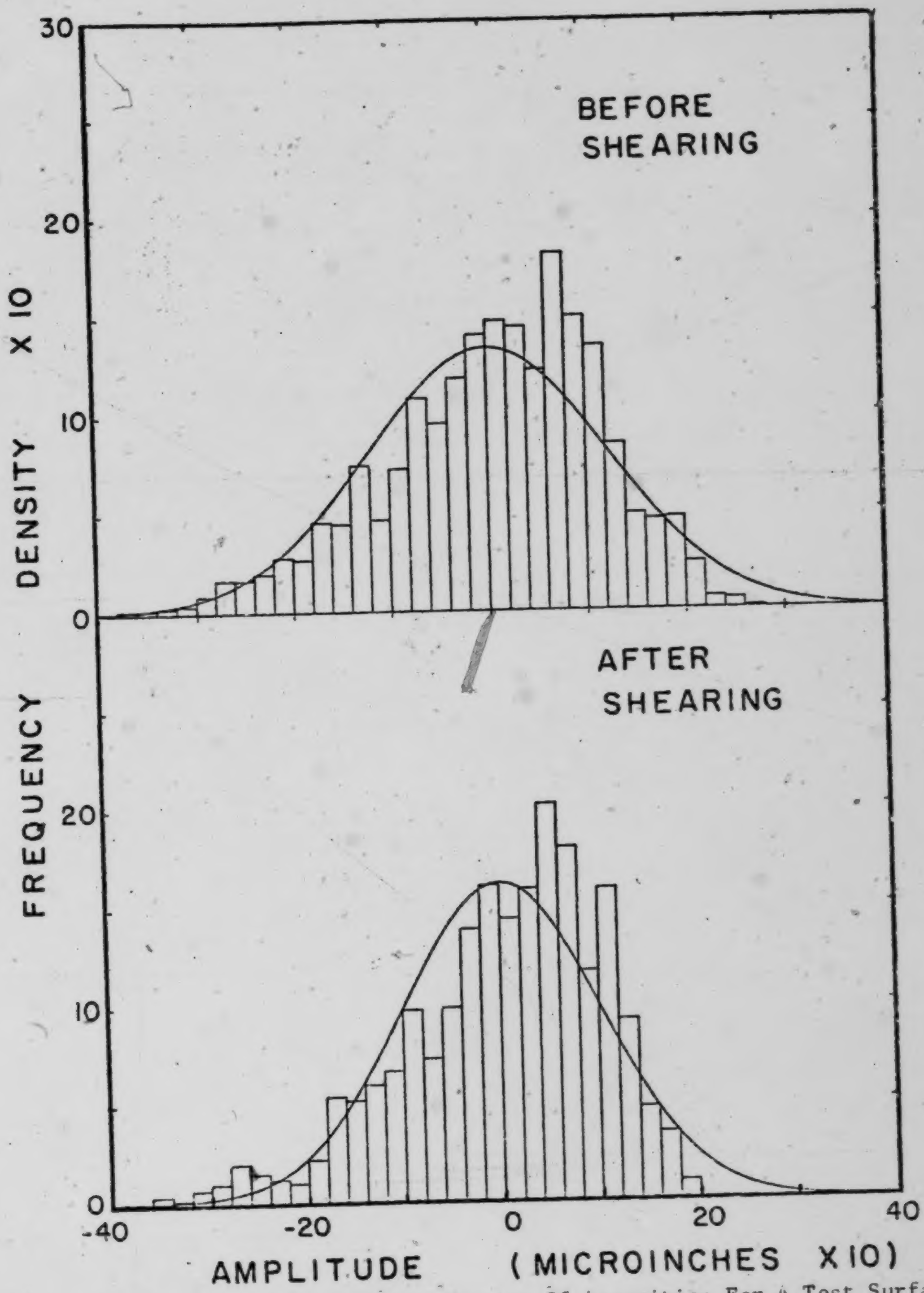

FIGURE 5-8 Amplitude Distribution Of Asperities For A Test Surface

(After Krahn, 1974)

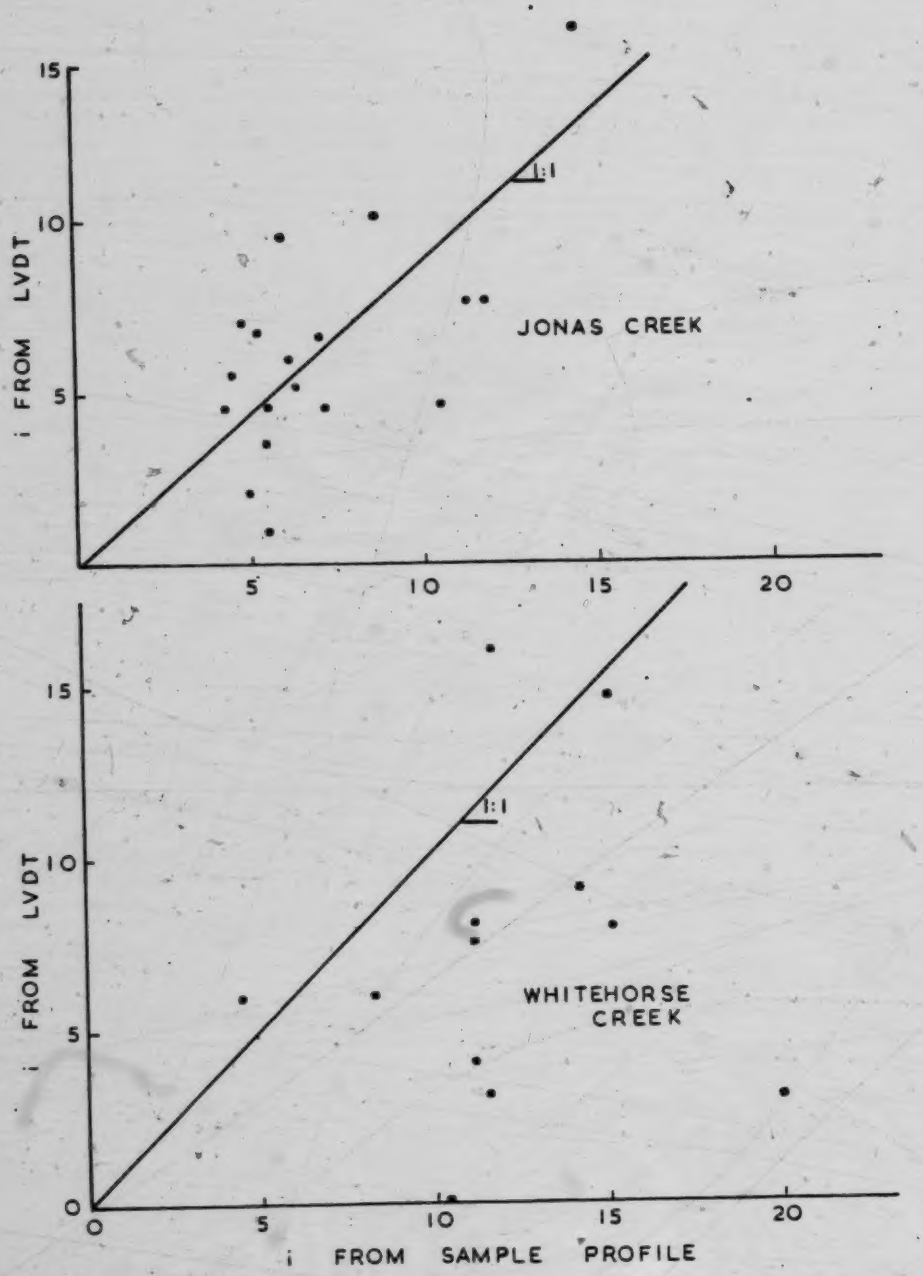

FIGURE 5-9 Graphical Presentation Of The Relationship Between The i Angle Measured By LVDT During Shear Versus The Average Profile i Angle.

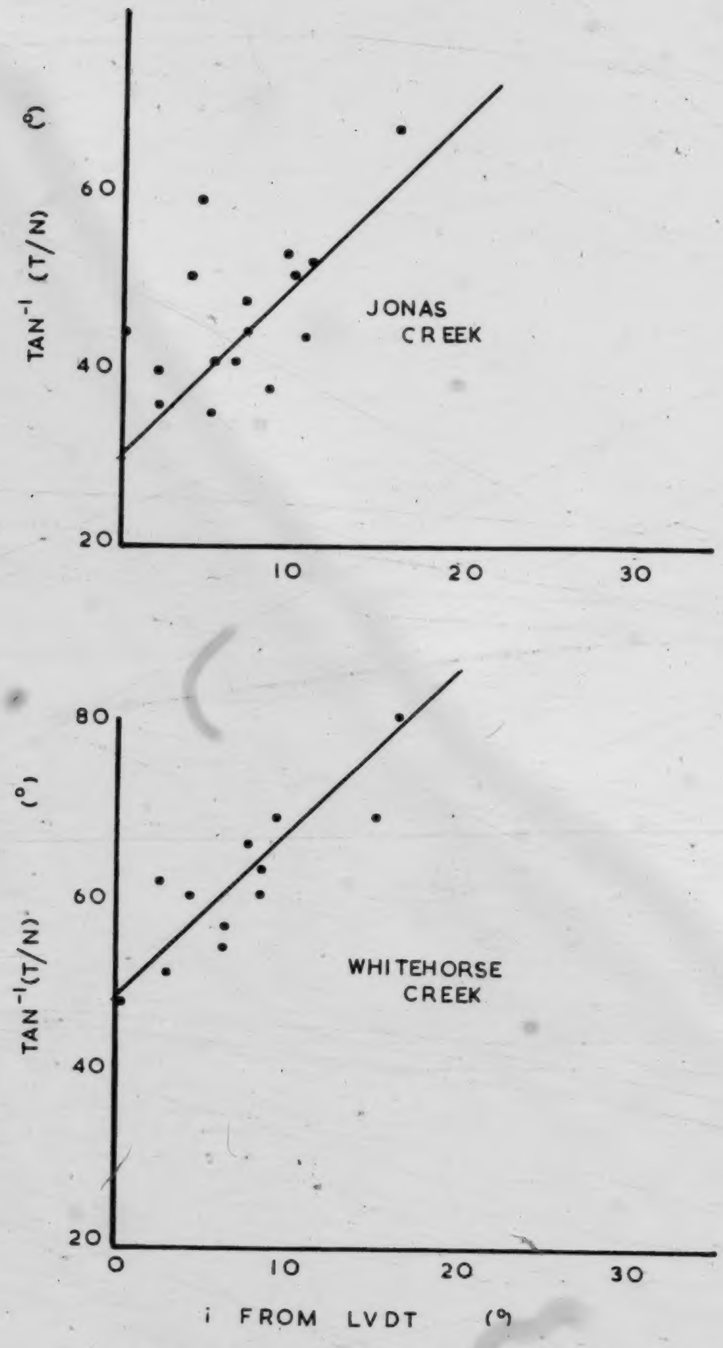

FIGURE 5-10 Graph Of Bartons' Relationship Of

$\emptyset_p = \emptyset_b + 2i_{LVDT}$

Found For The 5 cm x 5 cm Shear Samples.

CHAPTER VI

Rock Slide Back Analysis

6-1 INTRODUCTION

The final step in a slope investigation, prior to the choosing of a set of design or remedial parameters, involves a quantitative evaluation of slope stability. This step usually incorporates the results of field mapping and laboratory determination of shear strengths in a stability analysis which defines the factor of safety for various slope profiles and failure surfaces.

In the case of failed slopes it is possible to equate the factor of safety to unity. Then by evaluating the preslide topography and the failure surface or surfaces it is possible to calculate the average shearing resistance acting along a failure surface (Morgenstern and Sangrey, 1975). In this way a natural rock slide can be treated as a large scale in situ shear test and the back-calculated results can be compared with the experimentally derived shear strength parameters. This technique allows us to evaluate how closely our experimental methods predict the real shear strengths acting at failure.

Stewart (1974) indicated that for small slides an assumption of unity for the factor of safety could lead to unconservative results. This lack of agreement between back calculated parameters was thought to have been caused by the small size of the slides being investigated. The factors of safety of small slides are highly susceptible to small changes in cohesion values acting along the slide surface whereas larger slides can tolerate the small variations.

In the case of the Jonas Creek and Whitehorse Creek rock slides, back analyses were used to test the applicability of the field measurements of roughness. This chapter summarizes the results of these back analyses and discusses the various assumptions which had to be made in order to satisfy the needs of the stability methods.

6-2 SLOPE STABILITY METHODS

Current methods of evaluating slope stability fall into two broad categories; finite element or stress strain analysis, and limit equilibrium analysis.

Morgenstern (1968) has stated that the most rational approach to the design of rock masses would be based upon displacements, as the major aim of all design calculations is to limit rock mass displacements. A deformation analysis would predict the displacements of all the points composing a rock structure for the various load configurations. Such an analysis requires the equations of equilibrium for any element of the rock mass and the constitutive equations governing the rock material. Morgenstern stated that even if such relationships were known, computational difficulties would be enormous, as the relationship would probably be non-linear. Other complications such as variations in density, pore pressures, anisotropy and non homogeneity due to bedding and discontinuities in the rock mass makes this method impractical at present.

Goodman (1976) pointed out that many of the computational difficulties surrounding finite element programs have been overcome. The use of one dimensional joint elements has been used to model the discontinuities within a rock mass. However the use of this element requires a knowledge of shear strength along a discontinuity as well as the stiffnesses along and across the discontinuities. These last two values have not been satisfactorily measured to date.

Goodman (op.cit.) pointed out, however, that not all problems require a finite element solution. In situations where small displacements are of little importance, limit equilibrium methods of analysis are quite sufficient to analyse the problem. Furthermore, Morgenstern and Sangrey (1975) indicated that deformations are controlled semi-empirically by designing to an appropriate factor of safety using limit equilibrium analysis.

In a failed slope back analysis, where small deformations and stress changes are not known prior to failure, the finite element method is of little use. As a result, for this investigation, slope stability was assessed solely through the use of limit equilibrium methods.

Several computational methods exist for assessing the states of limiting equilibrium in a slope. The advantages and disadvantages of some of the more common methods have been discussed by Fredlund and Krahn (1975). The simplified Bishop circular arc method, and the Morgenstern-Price non circular arc method of limit equilibrium analyses were used to define the shear strength parameters associated with a factor of safety of unity (Bishop, 1954 and Morgenstern and Price, 1965).

The Bishop circular arc analysis is seldom used in rock slope investigations as most rock slope failures occur along planar discontinuities. The presence of the well defined folded failure surface on Jonas Ridge, however, gave an opportunity to apply this method to rock slopes. One of the advantages to this approach was that computer calculations could be checked easily for the north failure surface at Jonas Creek using hand calculations.

The non-circular arc analysis was performed on both failure surfaces at Jonas Creek, a potential failure surface in the unfailed portion of Jonas Creek, and on the failure surfaces of the two slides at Whitehorse Creek. A verification of the non-circular arc analysis computer results were made at Whitehorse Creek using a simple stereonet analysis (Hoek and Bray, 1974, Chapter 8).

A limit equilibrium method of analysis proposed by Barton (1972) was also investigated. This method assumes the existence of a planar failure surface on a slope with a steep face and a horizontal top broken up into sections by vertical joints striking parallel to the face of the slope (Figure 6-1). This analysis utilizes friction values and cohesion values and predicts the location of a vertical back scarp formed by blocks stabilized by cohesion (Barton, 1972). The location of a back scarp in a back analysis will therefore tend to confirm or contradict the choice of cohesion values used.

The limits set by Barton (1972) for this model were not strictly adhered to at Jonas Creek or Whitehorse Creek. The slope profiles did not have the required topographic profile shown in Figure 6-1. In addition the failure surface at Jonas Creek was curved whereas the model failure surface was planar. At Whitehorse Creek the location of the back scarp was apparently caused by a change in slope of the failure surface and was independent of cohesion values. As a result this method was found to be unsuitable for evaluating the shear strength parameters at either location.

Goodman and Bray (1976), and later Hoek and Bray (1977), presented a limit equilibrium technique for evaluating rock slope stability where the dominant failure mode was attributed to toppling failures. Goodman and Bray (1976), noted that this type of failure was common in steeply dipping slates, schists, thinly bedded sediments, columnar jointed volcanics and regularly jointed granitics. The rock types found at Jonas Creek and Whitehorse Creek do not fall into this category and hence would not appear to be susceptible to this type of failure.

Hoek and Bray (1974) presented a criteria for establishing whether or not toppling failures were likely to occur. This method indicated that, because of the geometry of the failing blocks and the slope angles involved at both study areas, failure could only occur by sliding. In addition, there was no evidence at either Jonas Creek or Whitehorse Creek to indicate that a toppling failure had occurred. As a result, no further investigations were carried out with respect to toppling failures.

In order to define the limiting equilibrium shear strength parameters thought to be acting during a sliding failure, the pore water pressures and sliding mechanisms must be specified (Morgenstern and Sangrey, 1975).

Patton and Hendron (1975) expand this further and list five parameters for a successful limit equilibrium analysis. These are:

1) Determination of the shape, orientation and location of the failure surface.
2) The prefailure topographic profile of the slide mass.
3) An estimation of pore pressures acting on the failure surface prior to failure.
4) Determination of the shear strength parameters acting along the failure surface and
5) Slope displacement measurements prior to failure.

In the case of back analyses conducted on pre-historic slides such as the Jonas Creek and Whitehorse Creek slides it is impossible to evaluate all of the above parameters with the same degree of accuracy. Slope displacements prior to failure, for example, cannot be ascertained to any degree. In other cases, pore pressure estimations for example, generalizations and assumptions have to be made and often a range of probable values have to be used in the final analyses. The following sections discuss the assumptions made with respect to the back analyses at Jonas Creek and Whitehorse Creek.

6-3 GEOMETRY OF THE FAILURE MASSES

The shapes, locations and orientations of the failure surfaces used in the limit equilibrium analyses were evaluated by field mapping as outlined in Chapters 2 and 3, in conjunction with detailed topographic maps of the slide area.

The exposed failure surface of the north slide at Jonas Creek was found to have a circular arc profile and did not have a back scarp. Bedding dips varied from 28° to 39° over the length of the failure surface. A circular arc was fitted to the geologic data and topographic profiles of the failure surface by trial and error in order to run the Bishop's circular arc method of analysis. The topographic profiles were drawn from a detailed topographic map of the slide area constructed on a scale of 1 cm = 48 m. The north slide was the only section amenable to circular arc analysis however, as the steep back scarp of the south slide altered the shape of the failure surface. The shape and attitudes of the south slide failure surface and back scarp of the unfailed central portion, were extrapolated from the profile of the north slide failure surface and the existing south slide scarp. The preslide topographic profile of the two failed sections at Jonas Creek were extrapolated horizontally from the profile of the unfailed central section. The slide masses outlined in the above fashion were fitted with small straight line segments and non circular arc analyses were performed on all three sections.

The field data recorded from Whitehorse Creek indicated that the failure surfaces of both slides were planar. The dip of the failure surfaces was 32°. The location of the failure surface and the location and orientation of the back scarps of the slides at Whitehorse Creek, were recorded from a topographic map constructed from air photos on a scale of 1 cm = 24 m. The preslide topography was extrapolated horizontally from the nearest unfailed portion of the ridge over to the middle of each slide. The final profiles used for the back analyses are illustrated in Figures 6-2 to 6-7.

6-4 PORE PRESSURE ASSUMPTIONS

Hoek and Bray (1974) have noted that the pressure of water can lead to a loss of slope stability through several mechanisms:

1) Water pressures which reduce the stability of slopes by reducing the effective normal stresses and increases the shear stresses tending to cause sliding.
2) Increased moisture content which increases the rock unit weight and accelerates weathering thus decreasing shear strength parameters.
3) Freezing of groundwater which gives rise to shear stresses due to wedging or more importantly the freezing of groundwater on an exposed face thus blocking drainage and increasing water pressures.
4) Erosion of the surface materials due to fast ground water flow which leads to instability and reduced effectiveness of drain.
5) Liquefaction which leads to instability. This is a special case of point number 1.

The most important of the above water effects is the reduction in stability resulting from increased water pressures within a rock mass (Hoek and Bray, 1974). As a result, if a reliable estimate of stability is to be obtained it is essential that water pressures within the slope being investigated are measured. In the case of a back analysis conducted on prehistoric slides, pore pressure measurements are not available and so reasonable estimates of water pressures must be made.

At the Jonas Creek slides, the areas of sliding lie very close to the crest of Jonas Ridge, a cuesta. This portion of the cuesta is unlikely to be in connection with the regional groundwater flow. It would seem reasonable therefore to suggest that pore pressure fluctuations would mainly be in response to local variations in recharge and discharge.

The possibility of high pore pressures developing behind a frozen face seems small at Jonas Creek. Freezing of the sheltered lower portions of the slope face causing a blockage in discharge is unlikely without the exposed upper boundary of Jonas Ridge freezing and thus causing cessation of the groundwater recharge cycle. As mentioned above, the slide areas on Jonas Ridge are unlikely to be affected by regional groundwater patterns and hence deep regional water probably could not percolate into the mass and build up behind a frozen face.

At Jonas Ridge, there is no area other than the dip slope face for snow or water to accumulate on and cause high water pressures. The ridge is quite unprotected from winds from the southwest and so snow accumulation would probably not be great. Avalanches down chutes visible on the air photos (Figure 2-5) would discharge some of the remaining snow. These avalanche chutes also provide channels for surface runoff and locally depress groundwater tables. A large avalanche chute exists near the south margin of the south slide.

Regardless of the amount of meltwater available as recharge it would seem unlikely that high pore pressures could have existed within the slide areas at Jonas Creek. In the case of the north slide the failed area extended to the skyline of the ridge and the very steep 55° slope below the upper failure surface at the crest indicated that very little recharge could enter the slope. No catchment area existed behind the slope.

The north lateral margin of the triangular slide was unobstructed and thus probably was free draining. The joints are not filled with gouge and hence allowed water to flow easily to the slide margins . This probably allowed a reduction of pore pressures. The assumed toe of the failure surface was approximately 600 m above the valley bottom, was apparently unobstructed, and did not appear to have been covered with low permeability material. The smallest grain size observed anywhere in the slide debris at Jonas Creek corresponded to fine-grained sand size. As a result, the lower margin of the north slide also appeared to be free draining. The south margin of the north slide butted against an unfailed portion of the ridge which was covered with loose frost shattered blocks which would not hinder drainage.

The south slide at Jonas Creek also occurred near the top of the ridge. A very small dip slope catchment area existed behind the vertical back scarp. The area of this catchment basin was less than one-third of the area of the slid mass so recharge from this area was probably negligible. Joints observed around the perimeter of the failed mass were again continuous and clean. The assumed toe location was also apparently unobstructed and was also approximately 600 m above the valley bottom. It would appear therefore, that this second slide was also well drained and hence pore pressures were probably negligible.

Conditions at Whitehorse Creek were somewhat similar. The failure occurred on a dip slope of part of a cuesta which was probably isolated from a regional groundwater pattern. The steep inslope of the cuesta dipped at 45° and provided little access for water. A small catchment area behind the scarp, flatter lying than the failed portion, (dip of 20 degrees), provided a small local recharge area approximately equivalent in size to the slide area. This was probably of little consequence.

Joints within the area examined were clean and widely spaced. They appeared to be continuous and thus probably provided free drainage. In addition the north west lateral margin of the slide was open and hence could easily discharge water thereby reducing excess pore pressures. The inferred toe of the failure was 100 m above the valley bottom and was again apparently unobstructed so drainage was probably not impeded.

It would appear from the above considerations that the values of pore water pressures, were probably not high. As a result, for back analysis purposes the initial value of pore water pressure was assumed to be zero.

The author is aware that back analyzed shear strength parameters are highly dependent upon assumed pore pressure values and that pore pressure values can be quite high even though only small quantities of water were present. As a result a variety of pore pressure values were used in the limit equilibrium analyses to define the sensitivity of the relationship between Ø and the porewater pressure parameter Ru.

6-5 SHEAR STRENGTH PARAMETERS

For purposes of the back analysis, the shear strength parameters were assumed to be constant over the failure surface. The rock density was assumed to be 2614 Kg/m^3 an average density for quartzite (Hoek and Bray, 1974), and the initial pore pressures were assumed to be zero.

The value of cohesion was assumed to be zero for the following reasons:

1) In Chapter 5 it was explained that the value of the shear strength was given by, $T=N \tan(Øb + i)$ for low normal loads. The value of cohesion was zero.
2) Hoek and Londe (1974) indicate that values of cohesion used in rock analyses are highly variable and cannot be relied upon.

It is not yet possible to evaluate the area of rock bridges acting within a slope and hence determine a reliable average cohesion value. Hoek and Londe therefore suggest that values of cohesion being used in rock slope design should equal zero. This approach is too conservative for consideration in most open pit mines where slopes are open for short periods and some failures can be tolerated. For slopes which must stand for long periods of time, where failures cannot be tolerated, such as in civil engineering projects, this approach errs on the safe side and is acceptable.

Limit equilibrium analyses were performed on three cross sections at Jonas Creek and two cross sections at Whitehorse Creek in order to define the Ø value which gave a factor of safety of one.

6-6 DISCUSSION

At Jonas Creek, the experimental Øp value, evaluated by adding together the Øb values evaluated from sandblasted surfaces on the tilt table and the average i angles from the 0.3 m scale in the failed areas was 34.6°. The Øb value evaluated by the direct shear box was slightly higher and the resulting Øp value was 35.8°. The back analyzed values of Øp for the two failed sections, calculated using assumed values of zero cohesion and zero pore pressure, was 34°. This was only 0.6° or 1.8° less than the experimentally derived values. This led to a calculated factor of safety of 1.02 or 1.07 depending on the choice of Øb.

Using the average roughness angle of 8.9°, measured on the perimeter of the unfailed section at Jonas Ridge, a Øp value of 39.7° or 40.9° was calculated. The back analyzed shear strength parameters needed for equilibrium in this unfailed section were also C=0 and Øp =34.0° . The factor of safety, defined as that factor necessary to reduce the strength parameters to those necessary for limiting equilibrium, varied from 1.2 to 1.3 depending on the choice of Øb. These factors of safety were calculated assuming zero cohesion and zero pore pressures.

The close correlation found between the back calculated and the predicted values of Øp for the failed portions at Jonas Creek indicate that the assumptions made with respect to water pressures, cohesion, i angles and Øb were consistent.

Mention was made in Chapter 5 of Øb values measured on a variety of polished surfaces. These were thought to correspond to Øb values found on flexural slip or fault surfaces. These lower values of Øb, observed on the polished surfaces are apparently too low to be consistent with previous assumptions and were probably inapplicable. This is consistent with the results of field mapping at Jonas Creek which revealed very few areas of flexural slip surfaces.

The back analyzed values calculated for the younger slide at Whitehorse Creek did not agree as well with the experimental values derived as did those at Jonas Creek. The Øb value obtained from the tilting table was 34.2° and Øb from the shear box was 35.8°. The average i angle on the 0.3 m scale was 3.5° . The resulting Øp values were 37.7° and

39.3°. The back calculated Øp value was 32°. This yielded a factor of safety of 1.2 and 1.3 respectively. The back calculated value of Øp was 2.2° to 3.8° lower than the values of Øb evaluated on sand blasted surfaces. This indicates that the assumptions made with respect to this back analysis may have been slightly in error.

Pore pressures may have been acting on the failure surface prior to failure even though the previous pore pressure analysis indicated that free drainage would probably occur. Because the toe of the slope was close to the valley bottom it may have been covered with a thin layer of impermeable till prior to failure. A deposit of till was found on the unfailed portion of the ridge beside the slide margins(Chapter 3). This may have decreased the drainage and thus caused an increase in the porewater pressure.

Various values of pore pressure were tried using the non circular arc analysis and an Ru value of 0.2 was found to be necessary to bring the slope to a state of limiting equilibrium. This corresponds to a height of water of approximately 15 m which is approximately one half the height of the failure scarp at the back. If the arguments made previously with respect to pore pressures being equal to zero are correct this would appear to be a little high.

A second possibility is that the choice of a sand blasted surface to evaluate Øb is not appropriate. There is no field evidence to support this, however, as no tectonically disturbed surfaces were found on the failure surface. However the soft and soluble nature of the rock and the age of the slide may have combined to erase the traces of such a surface, a remote but nevertheless conceivable possibility.

A final possibility which can not be ignored is the existence of an earthquake in the vicinity of the slide adding energy to the slope and causing failure. This last possibility is impossible to evaluate however due to the slide age.

The previous analysis made with respect to pore water pressures indicated that at Jonas Creek the assumption of zero pore water pressure was acceptable. At Whitehorse Creek an Ru value of 0.2 was needed to cause failure assuming that the friction angle acting was equal to Øb plus the average 0.3 m scale i angle measured in the field. However, the final friction angle found by back analysis is highly susceptible to the assumed Ru values. An Ru value of 0.5, the worst groundwater configuration possible, yielded back analyzed friction angles of 64° at Jonas Creek and 57° at Whitehorse Creek for a factor of safety of unity.

This is the upper bound. Back analyses using these high values of Ru would indicate that small scale laboratory specimen shear strength could be relied upon; an unlikely but nevertheless possible hypothesis which cannot be disproved at present.

6-7 POST FAILURE BEHAVIOUR

The problem of estimating how far a rock slide will travel after the factor of safety has dropped to one is of considerable importance. In open pit mines, where failures are a normal occurrence due to the low working factors of safety, the horizontal travel distance may control whether or not a failure can be tolerated. This type of analysis is also important for natural slope stability problems. How far back from a transportation corridor should slope stability be checked for example?

Eisbacher (1978) reported that rock slides in the MacKenzie Mountains, a future potential area for transport and utility corridors, travelled down tributary valleys for many kilometers before emptying into a main valley. Large horizontal distances have also been travelled by historic rock slides such as the Elm, Vaiont, Flims and Blackhawk slides (Scheidegger,1973). Attempts to predict the travel distances on the basis of dry sliding friction have met with little success and so non sliding failure models have been introduced (Shreve, 1968, and Hsu, 1975 and Habib, 1975).

There have been instances where the mass has not travelled excessively large distances but has moved a distance commensurate with distances predicted using the laws of friction. The Schachental, Airolo and Lecco slides all fit this category (Scheidegger,1973). An analysis performed on the Hope Slide indicated that the horizontal travel of this slide, similar to the three mentioned above, was governed by the basic friction angle of the debris

(Bruce and Cruden, 1977) .

The equations governing the post-failure behaviour of the mass are based on energy balance considerations. The kinetic energy of the slide is equal to the gravitational potential energy of the mass plus external energy introduced by earthquakes minus the energy consumed in overcoming frictional resistance. The energy gained by a slide from earthquakes is hard to evaluate. If this energy input was ignored the average distance travelled by the slide debris in a frictional sliding mode could be calculated.

Scheidegger (1973) presented the governing equation for post failure behaviour as;

$$1/2\ mv^2 = mgs \sin B - mgs \cos Bf \qquad 6.1$$

where m is the mass moving with velocity v a distance s down a slope of B degrees and g is the gravity constant. Figure 6-8 illustrates this principle.

The quantity f was designated the fahrboschung by Heim and corresponds to the coefficient of friction along the slide path (Hsu, 1975). Scheidegger (1973) illustrated f as the slope of a straight line joining the crown of the slide to the toe of the debris. Integration of the above governing equation from the crown to the toe of the slide yielded the simplification:

$$f=h/x \qquad 6.2$$

where;

h is the total vertical drop and x is the horizontal distance, measured from the crown to the toe (Figure 8-2).

Clearly this relationship for f depends on at least three assumptions:

1) Pore pressures during sliding are neglible, and
2) The particle mass of m slides from the crown to the toe of the slide.

These assumptions are somewhat restrictive. Results may easily be obtained for the motion of the centres of mass for the slide debris in the presence of a constant pore pressure, p. If a small portion of the slide mass Dm, initially at rest, moves through a distance of Ds, the resulting governing equation becomes:

$$1/2 \ Dm \ v^2 = Dmg \ Ds \sin \theta - Ds(Dmg \cos \theta - p) f \qquad 6.3$$

As $Ds \sin \theta = Dh$ and $Ds \cos \theta = Dx$, the above equation may be rewritten as

$$1/2 \ Dmv^2 = Dmg \ Dh - (DMg \ Dx - pDs) f \qquad 6.3a$$

This equation may be integrated twice. The first integration replaces the slide mass with an effective mass, M acting at the center of gravity of the slide mass. The second integration sums the displacements over the slide path. These quantities may be evaluated separately as the summations are independent. The limits of integration for the slide path now become the initial and final positions of the centre of gravity of the slide mass. The resulting equation becomes

$$1/2\ Mv^2 = Mgh' - (Mgx' - ps)f \qquad 6.4$$

where h' and x' are the vertical drop and the horizontal travel of the centre of gravity of the slide mass (Figure 6-8).

After sliding, the kinetic energy of the mass is zero. Thus

$$0 = Mgh' - (Mgx' - ps)f \qquad 6.5$$

and so

$$Mgh' / (Mgx' - ps) = f' \qquad 6.6$$

In areas where pore pressures are zero this reduces to

$$f' = h'/x' \qquad 6.7$$

In order to evaluate f' the positions of the centre of gravity of the slide mass both before and atfer movement are required.

This analysis was successfully performed for the Hope Slide where the pre slide and the post slide topography were well defined and the pre and post slide centres of gravity could be easily located. As a result of this success a similar analysis was conducted on the slides being studied at Jonas and Whitehorse Creeks to test the applicability of this method.

At Jonas Creek, limit equilibrium analyses implied that pore pressures and earthquake effects acting at failure were neglible so it seemed possible to apply the above simple technique. Although the limit equilibrium analysis at Whitehorse Creek implied that either pore pressures or external earthquake effects were present at failure this method was used to determine how closely the results agreed with known movements. This technique should give a minimum horizontal distance travelled.

In order to define the centres of gravity in the pre and post slide masses where pre slide topography was not available, certain approximations had to be made. A hypothetical topographic surface, probably more uniform than that which existed prior to failure, was extrapolated from the unfailed portions of the slides to give an indication of the preslide rock thickness. In the case of the failed mass two techniques were used to define the rock thicknesses.At Jonas Creek an attempt was made in the field to evaluate the geometry and thickness of the debris. Straight line traverses were run in a grid pattern over the debris and the debris thickness was estimated. These thicknesses were then transferred to a detailed topographic map.

At Whitehorse Creek, due to the greater thickness of debris, this technique was not practicable. However the very distinctive outline of the slide debris was obvious on a topographic map constructed on a scale of 1:4800. Original ground contours on the side of the debris could be extrapolated beneath the debris and so thicknesses could be estimated at various points on the map.

A square grid, consisting of squares 60 m x 60 m was overlain on the topographic maps of Jonas Creek and Whitehorse Creek. An arbitrary origin was established outside of the rock slide area. The distances from the origin of the grid to any specific point, measured parallel to the grid axes, were recorded as moment arms. The sum of the moments taken about the origin, divided by the the sum of the debris thicknesses marked on the map gave the resultant moment arms. The intersecton of all three moment arms established the centre of gravity of the failed mass. Plate 3-1 illustrates the use of this technique at Jonas Creek. The horizontal and vertical distances between the centres of gravity were then known and it was a simple matter to calculate the f values for each slide. The older slide at Whitehorse Creek could not be evaluated in this way due to the lack of debris.

The values of f were converted to equivalent angles of friction and were found to be 24° and 27° respectively for the north slide and the south slide of Jonas Creek. The average values of Øb as defined by the sliding friction tests was 30.8° ± 1.1° .The close agreement between the Øb value and the arctan f values for Jonas Creek once again implies that the assumptions made with respect to zero earthquake forces and pore pressures are reasonable. The difference between the equivalent angles of 24° and 27° for the two slides at Jonas is small considering the precision with which thicknesses were measured. The somewhat poorer agreement between the value of 27° and the Øb value of 34.2°±1.0° at Whitehorse Creek was not unexpected. The limit equilibrium analysis indicated that either pore pressures or earthquakes may have been acting at the time of failure.

6-8 CONCLUSIONS

The factors of safety evaluated by comparing the experimental values with the back analyzed values of shear strength lay within 2 to 7 % of the assumed value of unity at Jonas Creek thereby lending credibility to the methods of evaluating field values of shear strength. The factor of safety at Whitehorse Creek lay within 24 to 31 % of unity. Although this value does not agree as closely with unity as at Jonas Creek the results should also be compared with previous rock slope analyses where estimates have been out by as much as several hundred percent (Krahn, 1974) .

The distances travelled by the slides at both Jonas and Whitehorse Creeks indicated that the mode of failure following initiation of movement was dominantly that of sliding. At Whitehorse Creek, excess energy or pore pressures in the mass allowed the debris to travel a short distance farther than would be expected on the hypothesis of frictional sliding. The slide at Jonas Creek behaved almost as dry frictional sliding theory would predict.

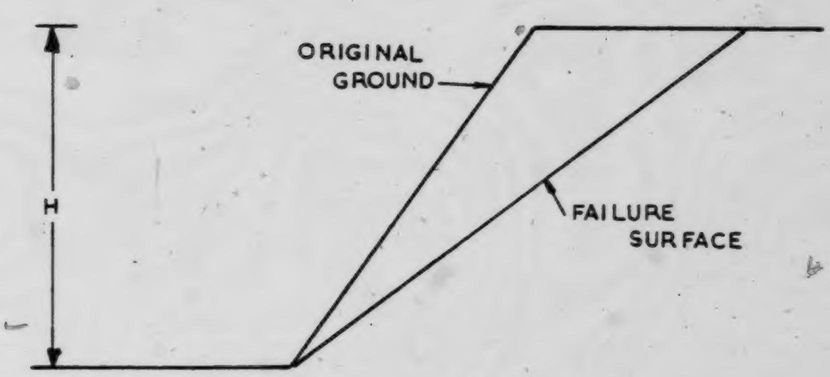
ORIGINAL GROUND
H
FAILURE SURFACE

FIGURE 6-1 Failure Geometry Proposed By Barton.
(After Barton, 1972).

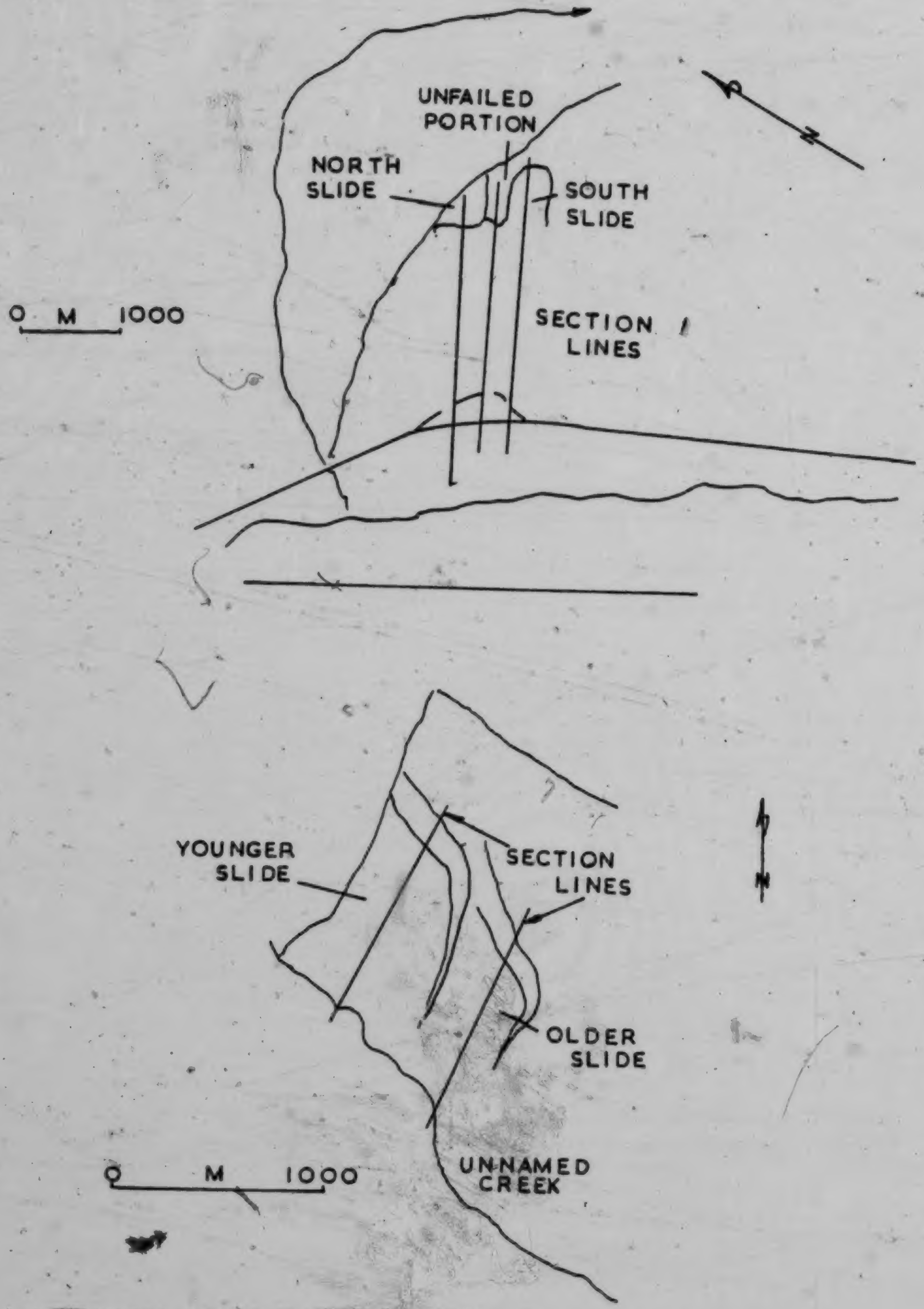
UNFAILED PORTION
NORTH SLIDE
SOUTH SLIDE
N
0 M 1000
SECTION LINES
YOUNGER SLIDE
SECTION LINES
N
OLDER SLIDE
0 M 1000
UNNAMED CREEK

FIGURE 6-2 Location Map Showing The Section Lines Illustrated In Figures 6-3 to 6-7.

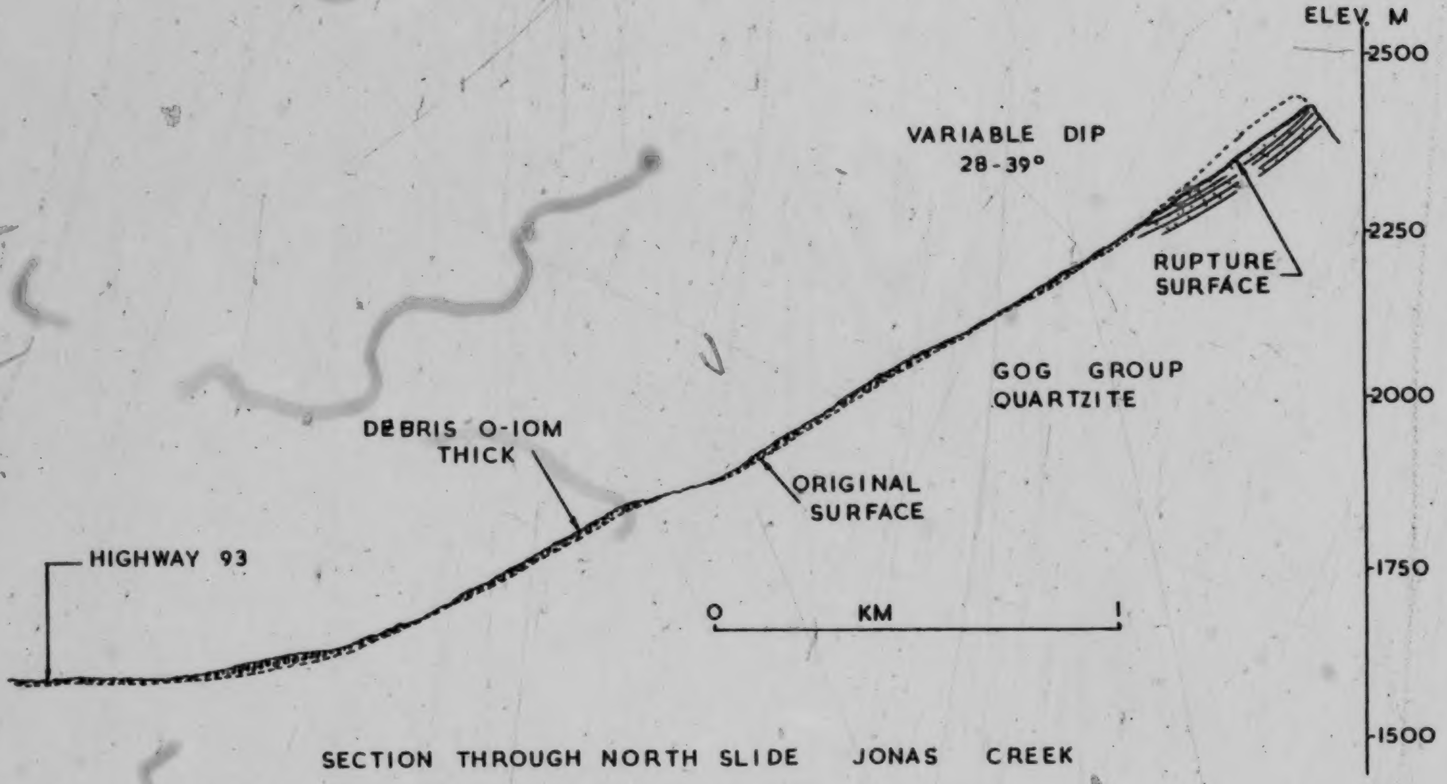
ELEV. M
2500
2250
2000
1750
1500
VARIABLE DIP
28-39°
RUPTURE
SURFACE
GOG GROUP
QUARTZITE
ORIGINAL
SURFACE
DEBRIS 0-10M
THICK
HIGHWAY 93
0
KM
1
SECTION THROUGH NORTH SLIDE JONAS CREEK

FIGURE 6-3 Cross Section Of The North Slide At Jonas Creek.

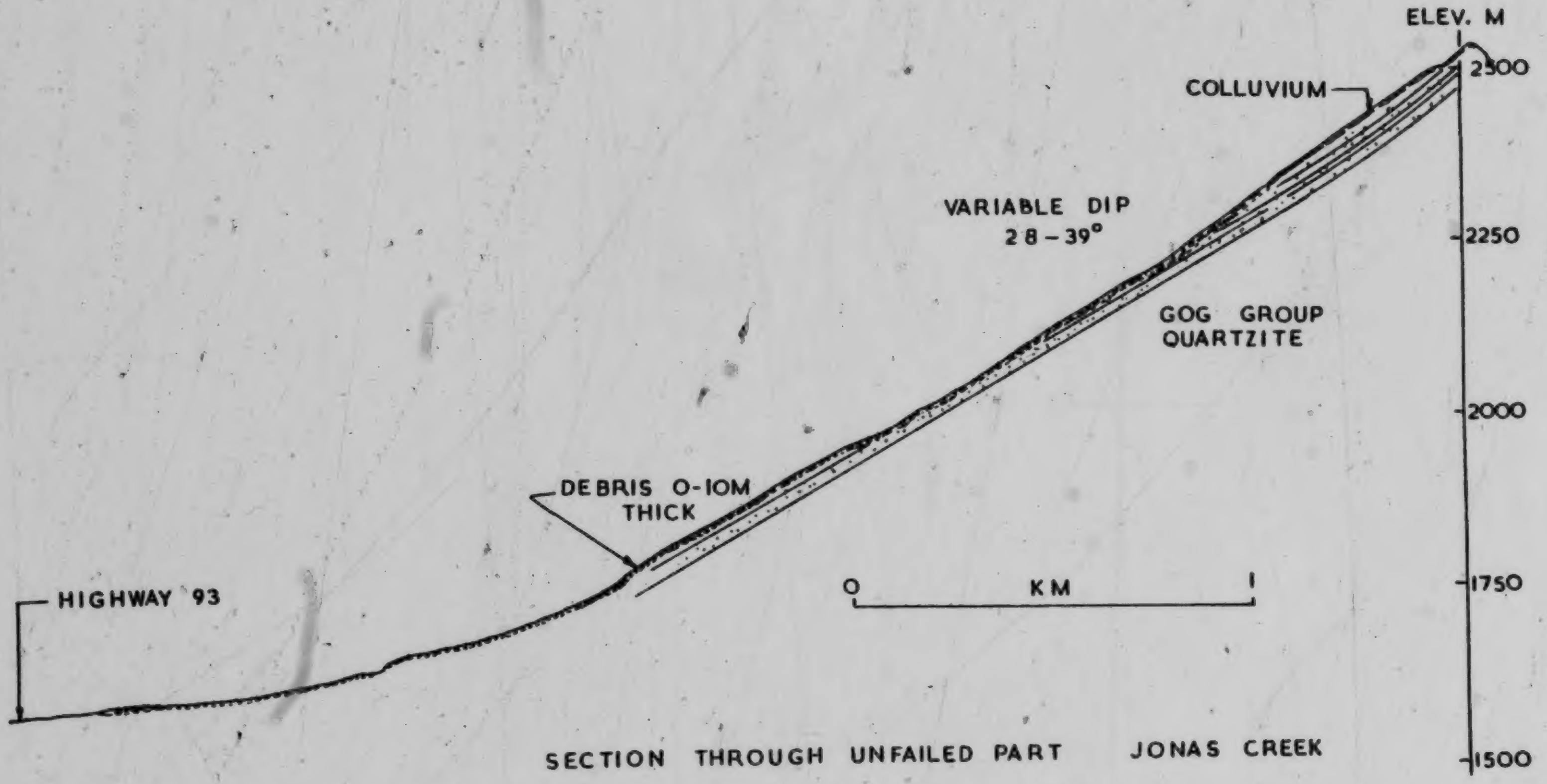
ELEV. M
2500
2250
2000
1750
1500
COLLUVIUM
VARIABLE DIP
28 - 39°
GOG GROUP
QUARTZITE
DEBRIS 0-10M
THICK
HIGHWAY 93
0
KM
1
SECTION THROUGH UNFAILED PART JONAS CREEK

FIGURE 6-4 Cross Section Of The Unfailed Section At Jonas Creek.

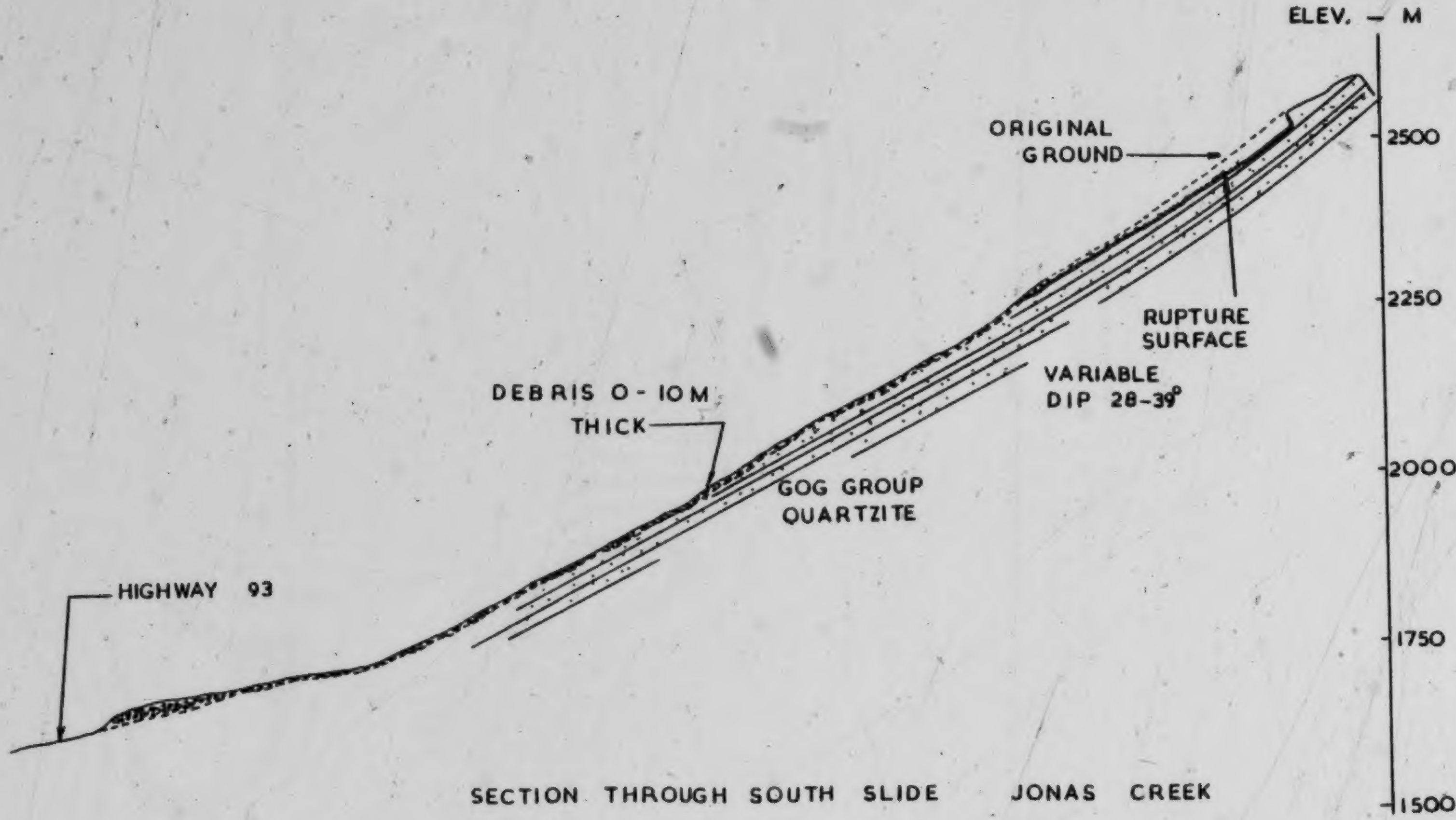
ELEV. — M
2500
2250
2000
1750
1500
ORIGINAL GROUND
RUPTURE SURFACE
VARIABLE DIP 28-39°
DEBRIS 0-10M THICK
GOG GROUP QUARTZITE
HIGHWAY 93
SECTION THROUGH SOUTH SLIDE JONAS CREEK

FIGURE 6-5 Cross Section Of The South Slide At Jonas Creek.

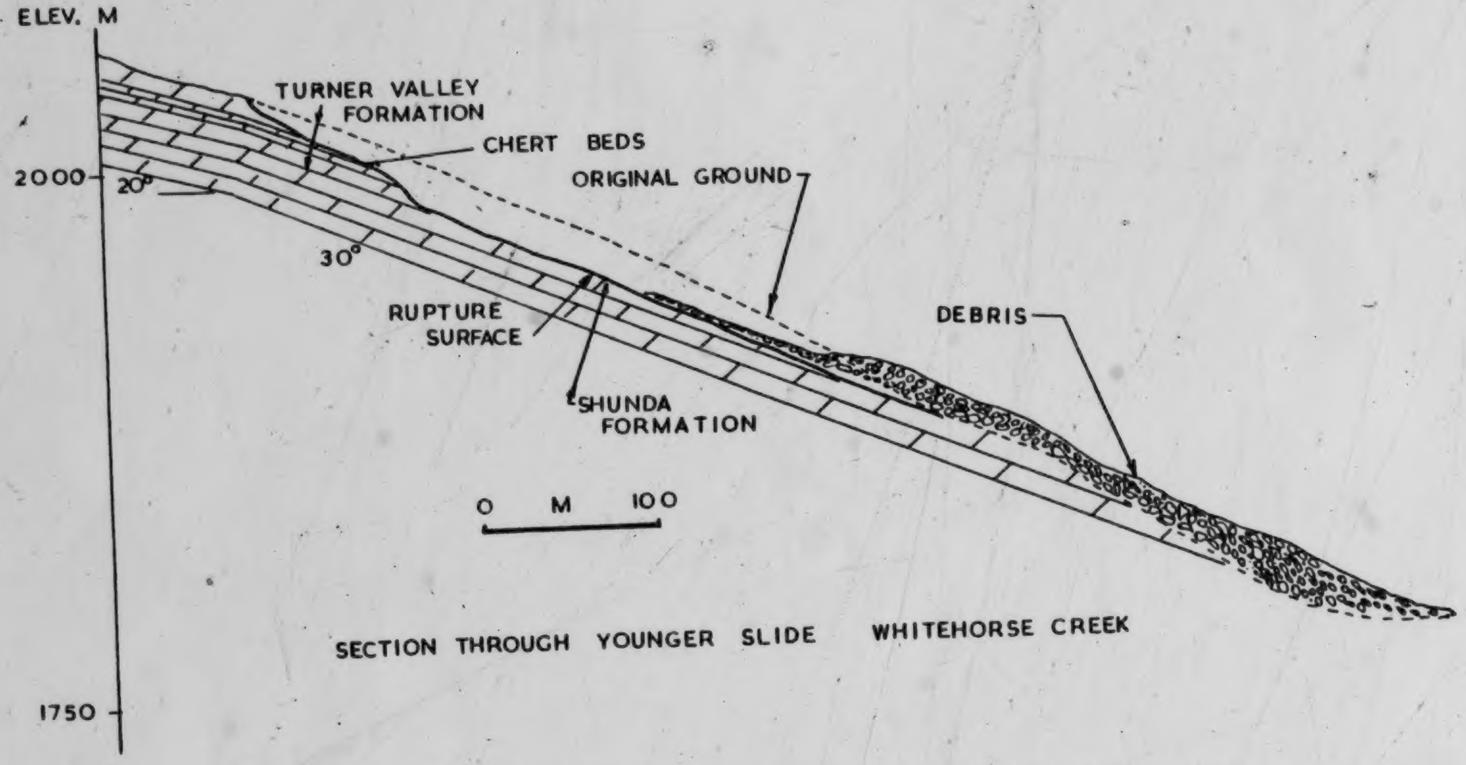
ELEV. M
2000
1750
20°
30°
TURNER VALLEY FORMATION
CHERT BEDS
ORIGINAL GROUND
RUPTURE SURFACE
SHUNDA FORMATION
DEBRIS
0 M 100
SECTION THROUGH YOUNGER SLIDE WHITEHORSE CREEK

FIGURE 6-6 Cross Section Through The Younger Slide At Whitehorse Creek.

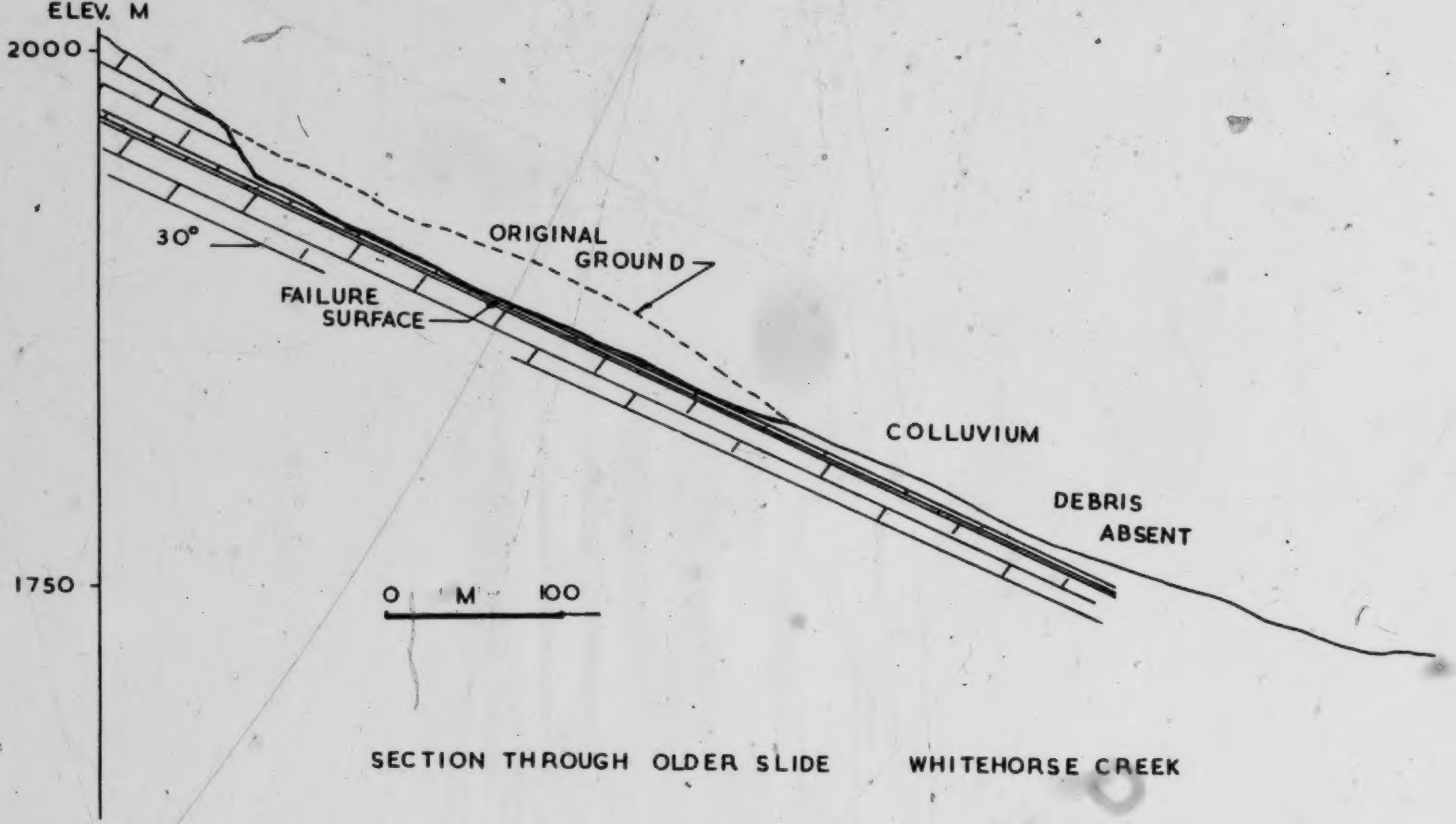
ELEV. M
2000
1750
ORIGINAL GROUND
30°
FAILURE SURFACE
COLLUVIUM
DEBRIS ABSENT
0 M 100
SECTION THROUGH OLDER SLIDE WHITEHORSE CREEK

FIGURE 6-7 Cross Section Through The Older Slide At Whitehorse Creek.

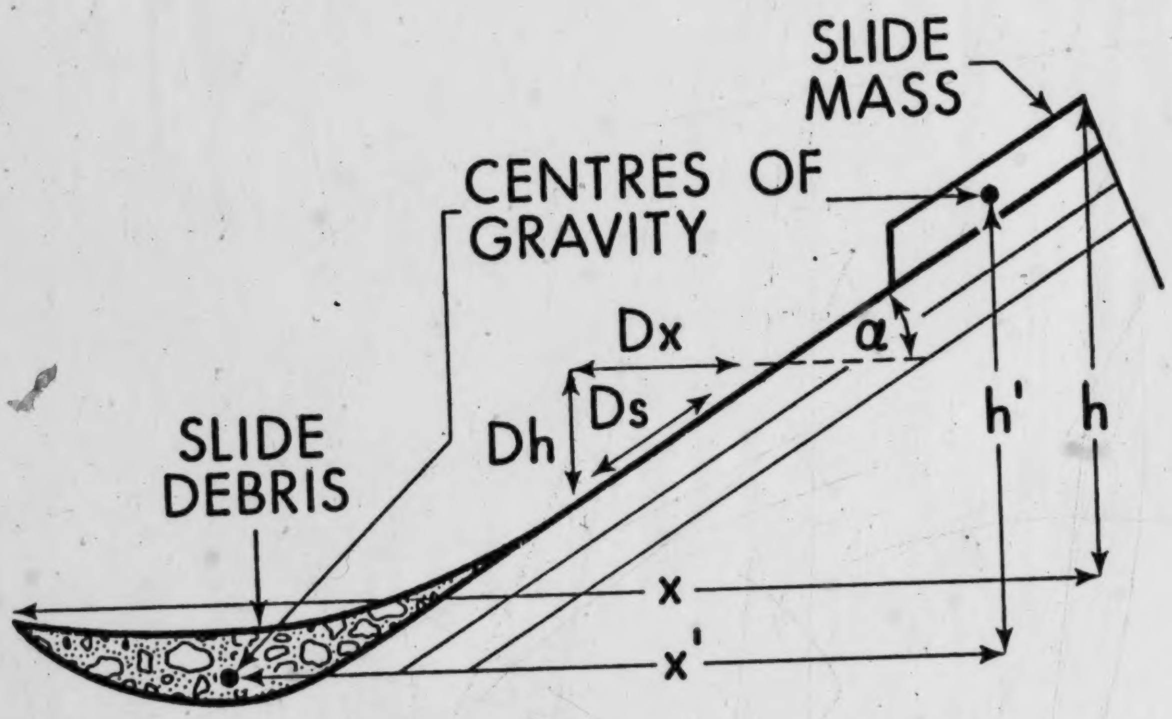
SLIDE MASS
CENTRES OF GRAVITY
Dx
α
Ds
Dh
SLIDE DEBRIS
h'
h
x
x'

FIGURE 6-3 A Figure Illustrating The Horizontal And Vertical Distances Travelled By The Centres Of Gravity Of The Failed Mass.

CHAPTER VII

Conclusions

In 1966 Patton introduced a simple bilinear failure theory to explain the behaviour of rough unweathered discontinuity surfaces in direct shear. Ladanyi and Archambeault (1970), Barton (1971), and Hoek and Bray (1974) indicated that this relationship was too simple to be used over large ranges in normal stress. In the case of slope stability problems the range of normal stresses encountered is very often small and the normal stresses are low. Hoek and Londe (1974) indicate that under these conditions the shear strength envelopes can be represented by $\phi b + i$.

The shear strength which can be mobilized along various discontinuities depends upon several variables. These are, the nature of the discontinuity, the presence or absence of soil infilling, the degree of interlock between discontinuity surfaces and the geologic tectonic history. Discontinuities which have undergone tectonic deformations and which as a result may be almost planar, non-interlocking, or filled with gouge-like material are the most dangerous with respect to stability. As a result these have recieved the most attention in recent years. Many comparisons were made using this type of discontinuity between large scale in situ tests and small scale laboratory tests. The results have indicated a very low degree of scale dependence. In many instances the stress strain behaviour of the discontinuity has closely resembled that of a soil. This may be characterized by a gentle rise to a peak shear strength with a small post peak drop in shear resistance. This type of discontinuity has been successfully tested in the laboratory and the results can be treated with a high degree of confidence. In addition, in situ tests, although expensive, can also be performed easily and accurate strengths obtained.

Patton (1966), Hoek and Londe (1974) and Goodman (1976) indicate that the stress-strain behaviour during direct shear of rough clean discontinuities is characterized by a rapid rise in shear stress to a peak followed by a marked drop in post-peak shear strength or highly irregular behaviour. Hoek and Londe (1974) indicate that for this type of surface the peak shear strength behaviour is scale dependent both with respect to cohesion and roughness. The variability of the roughness means a variability exists in the peak friction angle as defined by any of Patton's (1966), Ladanyi and Archambeault (1970), or Barton's (1971) criteria. All of these depend to some degree on roughness angles i.

Recent work by Pratt, Black and Brace (1974), on clean unweathered interlocking surfaces of quartz diorite have shown a high degree of scale dependence. This scale dependence has until now been partially responsible for the low accuracy with which the factor of safety has been evaluated for this type of discontinuity. A drop of 14° in peak friction angle occurs over a change in surface area from 60 to 5,000 cm^2.

Hoek and Londe (1974) indicated that the ϕb values are independent of scale over the range of normal loads associated with slope problems. This implies that all scale dependence of friction angles is due to roughness. ϕb values can be ascertained very accurately by several methods. This implies that all inaccuracy in the peak friction angles $(\phi b + i)$ has been associated with the evaluation of roughness.

Part of this problem has been a lack of technical knowledge with which roughness angles can be evaluated. The purpose of this thesis was first and foremost to design and test a method of evaluating field roughness. The results were then tested for accuracy using detailed back analyses of two rock slides in the Canadian Rocky Mountains.

The initial steps of the investigation involved an examination of the geology of the site in order to define the failure surfaces and the pertinent geologic factors which had influenced slope stability. The failures at Jonas Creek were originally classified as planar slides following the nomenclature of Hoek and Bray (1974). However, the slides had actually failed along several folded bedding surfaces. The presence of a large fold was defined using a dip isogon map. A number of small amplitude fold axes running parallel to the bedding dip direction were defined using a stereonet analysis. The failure surface was contained entirely within the Lower Cambrian Gog Group quartzite.

The slides at Whitehorse Creek occurred along several planar bedding surfaces within the Turner Valley Formation. The slides at both locations occurred on dip slopes of sedimentary strata dipping into the valley at 30 to 40°.

During the field investigations a new method of evaluating field scale roughness was designed and implemented. A series of compass readings were taken over the failure surfaces. A mean and standard deviation of the readings were taken at various scales and the roughness was calibrated with the standard deviations. The roughnesses for various scales were calculated and a pattern of roughness established. At the slides studied, the first order roughness, the 0.3 to 3.0 m scale, appeared to control failure. The average i angles for all scales up to the 30 to 300m scale were also evaluated. The i angles for the larger roughness scales were all smaller than those recorded for the first order scale. As a result, when the first order roughness was overcome failure could not be averted.

The new method of analysis has several advantages over previous methods of roughness evaluation.

1) Outcrop exposure does not have to be continuous in order to evaluate i using the new method.

2) Roughness can be evaluated on scales varying by as much as three orders of magnitude.

3) No special equipment is necessary to conduct a survey.

4) The i angle values on a specific discontinuity can be expressed statistically as a mean and standard deviation. This lends itself well to a probabilistic approach of rock slope stability (McMahon,1975, Jennings,1970). In addition, the measurements needed to establish the i angles are similar to those needed to establish the mean orientation of the failure surfaces another parameter needed for probabilistic design.

Shear strengths were evaluated using direct shear tests conducted on 5 cm x 5 cm samples of various roughnesses. Results indicated that the peak friction angles could be represented by a straight line over the range in normal loads tested and that the simple model of $\phi p = \phi b + i$ was adequate. The shear strengths of the small laboratory samples overestimated the ϕp values found in the field.

A back analysis, based on the assumption that the most likely water pressures acting in the slope were low, indicated that the laboratory samples overestimated the shear strengths believed to be acting in the field. Nevertheless, if the worst possible ground water configuration is assumed to have been present, it is possible to accomodate the peak friction angles measured in the laboratory. Although this possibility does exist, the author feels that it is not a realistic appraisal of the porewater pressures which were most likely acting on the sliding surface at failure.

Basic friction angles evaluated on sandblasted surfaces also yielded straight line envelopes over the range in normal loads tested. The friction angles for the sandblasted surfaces fell within the normally quoted 30 to 35° range for certain rock types. No attempts were made to evaluate these values statistically. Only mean values were used.

Highly polished smooth samples were also tested in direct shear and friction angles as low as 12° were obtained for the quartzite and 15° for the dolomite samples. The angle varied with the surface preparations. The range of normal loads did not cause any surface damage to these samples.

Tilting table tests were conducted using 5 cm x 5 cm sliders on plates of quartzite and dolomite. The values measured on the tilting table were equivalent to the values measured in direct shear using similar surfaces. This indicated that the tilting table apparatus may be used to define ϕb values. The advantage of this technique over the direct shear box is the ease and inexpensiveness with which friction values may be defined. This type of apparatus may be useful in the early stages of an investigation for perhaps a feasibility study where many different rock types have to be quickly evaluated. This type of test will also yield a large number of test results quickly and easily, a result which could be beneficial to a probabilistic approach for defining ϕb. This test is of course only of use for hard rock surfaces.

Analysis of failed slopes based on the laboratory determination of shear strength in conjunction with field values of i yielded a factor of safety of 1.02 to 1.07 at Jonas Creek and a factor of safety of 1.2 to 1.3 at Whitehorse Creek. The value of cohesion used in both cases was zero. The close agreement of the factors of safety with unity at Jonas Creek indicated that the i angles measured in conjunction with the friction angles adequately reflected the shear strengths being mobilized at failure and indicated that the factor of safety of a rock slope may be identified accurately given that a) the proper failure surface and failure mode can be identified in the field and b) that the slide is of sufficient size to overcome the sensitivity of the factor of safety to the value of cohesion. Stewart (1974) indicated that the value of cohesion chosen for small slides controlled the factor of safety to a high degree. Any inaccuracies in the cohesion then led to inaccuracies in the factor of safety. Krahn (1974) meanwhile indicated that for the large Frank slide, the factor of safety was insensitive to the chosen cohesion value.

At this time no satisfactory method of evaluating cohesion for conventional approaches or probabilistic approaches has been derived. McMahon (1975) has proposed a method for determining the probable extent of rock bridges given a number of measurements of discontinuity extent. The strengths to be assigned to the rock bridges are themselves time dependent and not completely understood.

It would appear then, that in a rock mass with clean open discontinuities with no rock bridges, the possibility of evaluating the shear strength is good. The potential for evaluating the factor of safety of a slope in which cohesion is playing a major role is at this time not as satisfactory.

The calculated factors of safety for the Jonas Creek slide indicate that in all probability the assumptions made with respect to pore water pressure values were correct. However, at Whitehorse Creek this was not the case. The factors of safety calculated were 20 to 30% higher than unity. The most likely cause of this inconsistency rests in the assumptions made with respect to water pressures. Very little water is needed to cause high pressures in areas where joints may be tightly closed. It would appear, however, on the basis of section 6-6 that perhaps a number of factors could all have combined to give the higher factor of safety. These are pore pressures, ϕ_b values and the possible presence of an earthquake.

The two slide areas studied here appeared to be controlled in their pcst failure movements by dry sliding friction. The friction angles defined by using the tan f values (section 6-7) were slightly lower than the tan ∅b values previously estimated, however, a lower friction angle would be expected due to the decrease in ∅ caused by the differences between static and dynamic coefficients of friction. Given this argument it would appear that for some slides at least, it is possible to predict how far debris will travel.

REFERENCES

Babcock, E.A.,1974. "Jointing In Central Alberta." Canadian Journal of Earth Sciences, Vol. 11, pp. 1181-1186.

Baird, D.M., 1963. "Jasper National Park, Behind The Mountains and Glaciers." Geol. Surv. Can., Misc. Rept. #6, Queen's Printers,pp. 92-93.

Banks, D.C. and Strohm, W.E.,1974. "Calculations of Rock Slide Velocities." 3rd ISRM Congress, Vol.2b, Denver, pp. 839-847.

Barton, N., 1974. "Rock Slope Performance As Revealed By A physical Joint Model." 3rd ISRM Congress, Vol. 2b, Denver, pp. 765-779.

Barton,N.,1974b. "Estimating The Shear Strength Of Rock Joints." 3rd ISRM Congress , Vol.2a, Denver, pp.219-220.

Barton, N., 1973a. "Review Of A New Shear Strength Criterion For Rock Joints." Eng. Geol. Vol. 7, pp. 287-332

Barton, N.,1972. "Progressive Failure Of Excavated Rock Slopes." 13th Symp. On Rock Mechanics, ASCE, New York, p. 139.

Barton,N., 1971. "A Relationship Between Joint Roughness And Joint Strength." Proc. Of The Symp. On Rock Fracture, Nancy, Paper 1-8.

Barton, N. and Choubey, V.,1977. "The Shear Strength Of Rock Joints In Theory And Practice." Rock Mechanics, Vol. 10, pp.1-54.

Bayrock, L.A. and Reimchen, T.H.F., 1976. "Terrain Analysis Of Jasper National Park." Consultants Report For Parks Canada, Bayrock and Reimchen Surficial Geology Ltd., 23p.

Bayrock, L.A.and Reimchen, T.H.F.,1975. "Surficial Geology And Erosion Potential -Foothills Of Alberta Noth Of 52• Latitude ." Consultants Report For Alberta Environment, Bayrock And Reimchen Surficial Geology Ltd. 58p.

Benjamin,J. and Cornell,A., 1970. "Probability Statistics And Decisions For Civil Engineers." McGraw-Hill, 345p.

Bernaix, J., 1969. "New Laboratory Methods Of Studying The Mechanical Properties Of Rocks. Internat. J. of Rock Mech. And Min. Sci. , Vol. 6, pp. 43-90.

Bieniawski, Z.T.,1970. "Insitu Large Scale Testing Of Coal." in: Insitu Investigations In Soils And Rocks, The British Geotech. Soc., Dawes and Sons Ltd, London, pp. 67-74.

Bieniawski, Z.T., 1968. " Propogation Of Brittle Fractures In Rock " Proc.Of The 10th Symp. on Rock Mechanics, AIME, pp. 409-427.

Bishop, A.W.,1954. "The Use Of The Slip Circle In The Stability Analysis Of Slopes." Geotechnique, Vol. 4, p.7.

Bowden,F.P.and Tabor, D.,1950. "The Friction And Lubrication Of Solids." Clarendon Press, Oxford.

Brace,W.F. et.al.,1966. "Dilatency In The Fracture Of Crystalline Rocks." J. of Geophys. Research, Vol. 71, pp. 3939-3953.

Brawner,C.O.,1971. Introduction To Stability In Open Pit Mines. Proc. Of The 1st Int. Conf. On Open Pit Mines. ed: Brawner, C.O. and Milligan, V.,p.1.

Broch, E., 1974. "The Influence Of Water On Some Rock Properties." 3rd ISRM Congress. Vol 2a, p.33.

Broch, E.and Franklin, J.A., 1972. "Point Load Strength Test." Int. J. Rock Mech. Min. Sci. Vol. 9, pp. 669-697.

Browning, J.M., 1973. "Catastrophic Rock Slides, Mount Huascaran, North Central Peru." Am. Ass. Petrol. Geol. Bull. Vol. 57, pp.1335-1341.

Bruce, I. and Cruden, D.M., 1977. "The Dynamics Of The Hope Slide." Bull. Of IAEG. No. 16 P. 94.

Byerlee, J.D., 1967. "Frictional Characteristics Of Granite Under High Confining Pressures." J. Of Geophys. Res. Vol.72, pp.36-39.

Cawsey, D.C. and Farrar, N.S., 1976. " Simple Apparatus For Finding Rock Joint Friction." Geotechnique, Vol.26, pp.382-386.

Charlesworth, H.A.K., et.al. 1967. " Precambrian Geology Of The Jasper Region, Alberta." Research Council Of Alberta, Bull. 23, 74p.

Christensen, R.J., Swanson, S.R. and Brown, W.S., 1974. "Torsional Shear Measurements Of The Frictional Properties Of Westerly Granite." 3rd ISRM Congress, Vol. 2a p.221-224 .

Colbach, P.B. and Wiid, B.L., 1965. "Influence Of Moisture Content On The Compressive Strength Of Rocks." 3rd Canadian Rock Mech. Symp. pp.65-71.

Coleman, A.P., 1911. "The Canadian Rockies." Frode Publishing, Toronto, 123p.

Cook, D.G., 1975. Structural Style Influenced By Lithofacies, Rocky Mountain Main Ranges." Geol. Surv. Canada, Bull. 233, 73 p.

Coulson, J.H., 1972. "Shear Strength Of Flat Surfaces In Rock." 13th Symposium On Rock Mechanics, p.77-105.

Coulson, J.H., 1970. "The Effects Of Surface Roughness On The Shear Strengths Of Joints." Ph.D. Thesis, University Of Illinois.

Cruden, D.M.,1974. " Major Rock Slides In The Rockies." 29th Canadian Geotechnical Conf. Edmonton. p.59-71.

Cruden, D.M. and Charlesworth, H.A.K.,1976. "Errors In Strike And Dip Measurements." Bull. Of G.S.A. Vol. 87, pp.977-980.

Currie, J.B. and Reik,G.A., 1977. "A method Of Distinguishing Regional Directions Of Jointing And Of Identifying Joint Sets Associated With Individual Geologic Structures." Can. J. Earth Sci. Vol. 14 p. 1211.

Deere, D.U., Hendron, A.J., Patton, F.D. and Cording, E.J., 1967."Design Of Surface And Near Surface Construction In Rock." Eighth Symp. On Rock Mech. Failure And Breakage Of Rock, pp. 272-302.

Dietrich, K.,1972. "Time Dependent Friction In Rocks." Jour. Geophys. Res. Vol. 77 p.20.

Drozd, K.,1967. "Variations In The Shear Strength Of A Rock Mass Depending On The Displacement Of Test Blocks." Proc. Oslo Geotech. Conf. Vol. 1 p. 265.

Eigenbrod, K.D. and Morgenstern, N.R.,1972. "A Slide In Cretaceous Bedrock At Devon, Alberta." in: Geotech. Practice For Stability In Open Pit Planning, Ed: Brawner, C. and Milligan, V., pp. 223-238.

Eisbacher, G., 1978. " Lecture Presentation To The Edmonton Geological and Geotechnical Society. Edmonton, 1978.

Everall, M.D. et. al. 1974. "Mechanical Properties Of Rocks And Rock Masses." 3rd ISRM Congress , Vol. 2a , p. 101.

Fecker,E. and Rengers,N.,1971. "Measurement Of Large Scale Roughness Of Rock Planes By Profilograph And Geological Compass. Proc. Of Symp. On Rock Fracture, p. 1-18.

Flanagan,R., 1978. Letter to D.M. Cruden, Jan.11, From R. Flanagan, Superintendent of Jasper National Park, Alberta.

Franklin, J.A. and Chandra, R., 1972. " Slake Durability Test." Int. J. Of Roch Mech. Min. Sci. Vol. 9 pp. 325-341.

Fredlund, D.G. and Krahn, J., 1976. "Comparison Of Slope Stability Methods Of Analysis." 29th Canadian Geotech, Conf., Vancouver, p. VII-56.

Friedman, M. and Stearns, D.W.,1971. "Relationship Between Stresses Inferred From Calcite Twin Lamellae And Macrofractures,Teton Anticline , Montana. G.S.A. Bull.82, pp.3151-3162.

Giuseppe, B., 1970. "The Shear Strength Of Some Rocks By Laboratory Tests." 2nd ISRM Congress, Vol. 2. p. 165.

Goldstein, M., Goosev, B., Pyrogovsky, N., Tulinov, R. and Turovskaya, A.,,1966. "Investigation Of The Mechanical Properties Of Cracked Rock." 1st ISRM Congress, Vol. 2.p. 521.

Goodman,R.E., 1976. "Methods Of Geological Engineering." West Publishing, 472 pp..

Goodman, R.E., 1974. "The Mechanical Properties Of Joints." 3rd ISRM Congress, Vol. 1a pp. 127-140.

Goodman,R.E. and Bray,J.,1976. "Toppling Failure", ASCE Specialty Conf. Boulder, Vol.2, p.201.

Goodman, R.E.and Ohnishi, Y. 1973. "Undrained Shear Tests On Jointed Rock." Rock Mechanics, Vol. 3, pp.129-149.

Goodman,R.E., Taylor, R.L. and Brekke, T.L.,1968. " A Model For The Mechanics Of Jointed Rock." ASCE Journal SM #6 Vol. 94, p.637.

Habetha, E. 1976. "Large Scale Shear Tests For The Waldeck II Pump Fed Storage Station." Proc. 2nd Int. Congress of The IAEG. Sao Paulo, Vol. 2, p. IV-35.

Habib, P. 1975. "Production Of Gaseous Pore Pressures During Rock Slides." Rock Mechanics, Vol. 7, p.193.

Hald,A.,1952. "Statistical Theory." Wiley and Sons , pp. 847 pp..

Hamel, J.V., 1976. "Libby Dam Left Abutment Rock Wedge Stability." ASCE Specialty Conf. Rock Engineering For Foundations And Slopes. Boulder p.361.

Hencher, S.R., 1976. Discussion Of Cawsey And Farrar's Simple Method Of Evaluating Joint Shear Strength, Geotechnique, Vol.26 p.382-387.

Heuze, F.E. 1974. "Analysis Of Geological Data For The Design Of Rock Cuts." 3rd ISRM Congress , Vol. 2a pp. 798-802.

Hoek,E., 1971. "The Influence Of Structures Upon The Stability Of Rock Slopes." in: The Proc. 1st Symp. on Stability of Open Pit Mining. Vancouver, P. 49.

Hoek, E. and Bray, J. 1977. "Rock Slope Engineering, 2nd ed. " Inst. of Mining and Mett. , London, 309pp.

Hoek, E.and Bray, J. 1974, "Rock Slope Engineering." Inst. of Mining And Mett. , London, 402 pp.

Hoek, E. and Londe, P. 1974. " Surface Workings In Rock." 3rd ISRM Congress Vol. 2, p. 613.

Horne, H.M. and Deere, D.U., 1962. " Frictional Characteristics Of Minerals." Geotechnique, Vol. 22, p.319.

Hsu, K.J., 1975. "Catastrophic Debris Streams Generated By Rock Falls." Bull. Of G.S.A. Vol. 86, pp. 129-140.

Hoskins, E.R. and Jaeger, J.C. and Rosengren, K. S., 1968. " A Medium Scale Direct Friction Experiment." Int. J. Rock Mech. Min. Sci. Vol.5 pp.143-154.

Hughes,R.D., 1955. "Geology Of Portions Of Sunwapta And Southesk Map Areas, Jasper National Park, Alberta." in: Fifth Annual Field Conf. Guidebook. Alta. Soc. Pet. Geol. pp. 69-116.

Jaeger, J.C., 1971. "Friction Of Rocks And The Stability Of Rock Slopes." Geotechnique, Vol. 21, pp. 97-134.

Jaeger, J.C., 1959. "The Frictional Properties Of Joints In Rock." Geofisica Pura Applicata, Vol. 43., pp. 148-158.

James, P.M., 1970. "Insitu Shear Tests At Muda Dam." in: Insitu Investigations In Soils And Rocks. The British Geotech. Soc. London, p. 75.

Janke,N.C.,1972. "Field Measurements With Common Equipment." Photogrammetric Engineering, Vol. 38, p. 7.

Jennings, J.E.,1970. " A Mathematical Theory For The Calculation Of The Stability Of Slopes In Open Pit Mines." Symp. Of Planning Open Pit Mines, Johannesburg, pp. 33-53.

Kerrich, J.E., 1974. "Notes On The Orientation Of Sets Of Joints." Internal Report At The University Of Witwatersrand, 45 pp.

Krahn, J.,1974. " Rock Slope Stability With Emphasis On The Frank Slide." Ph.D. Thesis, University Of Alberta, 244 pp.

Krsmanovic,D., 1967. "Initial And Residual Shear Strengths Of Hard Rocks." Geotechnique V.17 pp. 145-160.

Kutter, H.K., 1974. " Rotary Shear Testing Of Rock Joints." 3rd ISRM Congress V2a, Denver, p. 254-257.

Ladanyi, B. and Archambeault, G,. 1970. Simulation Of Shear Behaviour Of Jointed Rock Mass." Proc. 11th Symp. on Rock Mech. AIME pp. 83-104.

Lajtai, E.Z., 1975. "Failure Along Planes Of Weakness." Can. Geotech. J., Vol. 12, pp. 118-125.

Lambe, T.W.and Whitman, R.V., 1969. "Soil Mechanics." Wiley And Sons Inc. pp. 61-69.

Londe, P. 1973a. "The Role Of Rock Mechanics In The Reconnaisance Of Rock Foundations." Quart. Jour. Of Eng. Geol. Vol. 6 ,p. 57-74.

Londe, p., 1973b, "Water Seepage In Rock Slopes." Quart. J. Of Eng. Geol. Vol. 6, pp. 75-92.

Locker, H.G., 1968. "Some Results Of Direct Shear Tests On Rock Discontinuities." 2nd ISRM Congress, Vol.1 pp. 171-173.

Lyell, K.A., 1970. "The Interpretation Of Water Pressure Factors For Use In Slope Theory." Symp. Of Planning Open Pit Mines, Johannesburg, p. 73.

Macauley, G., Penner, D.G., Proctor,R.M., and Tisdall,W.H., 1966. "Chapter 7 Carboniferous." in: The Geol. History Of Western Canada. ed: McCrossan,R.P. and Glaister,R.P., pp. 89-101.

MacKay, B.R., 1929. "Geologic Maps Of Map Sheets NTS #83C/14 and 83F/3." No Report.

MacQueen, R.W.,1966. "Mississippian Stratigraphy And Sedimentology At Cadomin Alberta." in: Field Guide Of The Edmonton Geol. Soc. p.39.

Martin,G.R. and Millar, P.J., 11974. "Joint Strength Characteristics Of Weathered Rock." Proc. Of The 3rd ISRM Congress, V 2a.

Maslov,N.N., and Pavlishev, T.V., 1974. "Creep and Pseudocreep Of Rocks And Their Effect When Estimating The Stability of Jointed Rock Mass." 3rd ISRM Congress.

McMahon, B.K., 1975. "Probability Of Failure And Expected Volume Of Failure In High Rock Slopes." 2nd Australian -New Zealand Geomechanics Conf. pp. 308.

McMahon, B.K., 1974. "Design Of Rock Slopes Against Sliding On Preexisting Fractures." 3rd ISRM Congress, Vol. . pp.803-808.

McMahon, B.K., 1971. "A Statistical Method For The Design Of Rock Slopes." Proc. Of The 2nd Australian-New Zealand Conference On Geomechanics. p. 314- 321.

Millar, P.J.and Martin, G.R., 1975. "A Note On The Shear Strength Of Rock Joints In Direct Shear." 2nd Australian -New Zealnd Geomechanics Conf., pp. 248-252.

Mogilevskeya, S.E., 1974. "Effect Of Geological Factors On The Shearing Resistance Along Joints In Rock." 3rd ISRM Congress, Vol. 2a p. 276.

Moore, P., 1958. "Late Paleozoic Stratigraphy In The Rocky Mountains And Foothills Of Alberta. in: A Critical Historical Review In The Jurassic and Carboniferous Of Western Canada. ed: Goodman, A.J. Am. Ass. Of Pet. Geol. pp. 145-189.

Morgenstern, N.R. and Sangrey, D., 1975. "Chapter 7, Stability Analysis." in: HRB. Special Report.

Morgenstern, N.R., 1972. " The Influence Of Groundwater On Stability."in: Stability In Open Pit Mining. ed: Milligan, V.and Brawner, C. ,p. 65.

Morgenstern, N.R., 1968. "Ultimate Behaviour Of Rock Structures." in: Rock Mechanics In Engineering Practice, ed: Stagg, K.G. and Zienkiewicz, O.C., pp.321-351.

Morgenstern, N.R. and Noonan, D., 1974. "Fractured Coal Subjected To Direct Shear." 3rd ISRM Congress, Vol. . p.282.

Morgenstern, N.R. and Price, V.E., 1965. "The Analysis Of The Stability Of General Slip Surfaces." Geotechnique Vol. 15, pp.79-93.

Mountjoy, E.W. and Aitken, J.D., 1963. "Early Cambrian And Late PreCambrian Paleocurrents, Banff and Jasper National Parks." Bull. Can. Pet. Geol. Vol. 7, pp. 161-168.

Newland, P.L.and Allely, B.H., 1957. "Volume Changes In Drained Triaxial Tests On Granular Materials." Geotechnique, Vol. 7, p. 17-34.

Nieble, C. et.al. 1974. "Shear Strength Of Typical Features Of Basaltic Rock Masses." 3rd ISRM Congress, Vol. 2a p. 294.

North, F.K.,1966. "Chapter 3 Cambrian." in: The Geological History Of Western Canada ed: McCrossan, R.G.,and Glaister, R.P. p. 28.

Onodera,T.F., Yoshinaka,R. and Oda,M.,1974. " Weathering And Its Relation To Mechanical Properties of Granite." 3rd ISRM Congress,Vol. 2a P. 71.

Patton,F.D., 1966. "Multiple Modes Of Shear Failure In Rock And Related Materials." Ph.D. Thesis, University Of Illinois, Urbana.

Patton,F.D.and Deere, D.U., 1971. "Geologic Factors Controlling Stability In Open Pit Mines." in: Stability In Open Pit Mines.ed: Brawner,C.and Milligan, V., AIME, Vancouver p.23.

Patton, F.D. and Hendron,A.J., 1975. "General Report On Mass Movements." Proc. Of The 2nd Int. Congress of The IAEG. Sao Paulo,Vol. 2, p.1.

Piteau, D.R., 1970. "Geologic Factors Significant To The Stability Of Slopes Cut In Rock." Symp. of Planning Open Pit Mines, Johannesburg, pp.33-53.

Piteau, D.R., 1971. "The Question Of Characterizing And Extrapolating Joint Properties In Engineering Practice." 20th Colloquium On Geomechanics, Salzburg.

Pratt,R.,Black,A.,Brown,W. and Brace,W.,1974. " A New Technique For Determining The Deformation And Friction Characteristics Of Insitu Rock." ASTM STP 554 Field Testing And Instrumentation Of Rock, p. 3-10.

Pratt,R.,Black,A., Brown,W. and Brace, W., 1972. "The Effect Of Specimen Size On The Mechanical Properties Of Unjointed Diorite."Int. J. Of Rock Mech. Min.Sci. Vol. 9 pp.513-529.

Pratt,R.,Black,A.and Brace,W.,1974. "Friction And Deformation Of Jointed Quartz Diorite." 3rd ISRM Congress, Vol 2a p.306-311.

Price,R.A. and Mountjoy,E.W., 1970. "Geologic Structure Of The Canadian Rocky Mountains Between Bow And Athabasca Rivers, A progress Report." G.A.C. Sp. Report #6 p.7.

Ramsden,J.,1977. "Numerical Methods In Fabric Analysis." Ph.D. Thesis University Of Alberta, p.89.

Ramsay, J.G., 1967. "Folding And Fracturing Of Rock." McGraw Hill Book Co. 568 pp.

Rengers,N., 1970. "Influence Of Surface Roughness On The Friction Properties Of Rock Planes." 2nd ISRM Congress, Vol. 1. p. 229.

Ripley,C.F.and Lee,K.I., 1961. "Sliding Friction Tests On Sedimentary Rock Specimens." 7th Int. Cong. Of Large Dams. p.42.

Ritchie, A.M., 1958. "Recognition And Identification Of Landslides." in: Landslides And Engineering Practice, Hwy. Res. Board Sp.Report 29. ed: Eckel,E.B., NAS-NRC Publication 544, p. 48.

Robertson, A.MacG., 1971. "The Interpretation Of Geological Factors For Use In Slope Theory." Symp. Of Planning Open Pit Mines, Johannesburg,pp. 55-71.

Rocha, M., 1971. "Some Problems On Failure Of Rock Masses." Rock Mech. And Engineering Geology, Supplementum I.

Rodrigues, F.P. 1968. "Determination Of Shear Throughout The Rock And Sliding On Joints." 2nd ISRM Congress, p.175.

Romero,S.and Molina, R.,1974. "Kinamatic Aspects Of The Vaiont Slide." 3rd ISRM Congress, Vol. 2b p. 865.

Rosengren, K.J. and Jaeger, J.C.. 1968. "The Mechanical Properties Of An Interlocking Low Porosity Aggregate." Geotecnique, Vol. 18, p.317-335.

Rowe, P.W.,1962. "The Stress Dilatency Relationship For Static Equilibrium Of An Assembly Of Particles in contact." Geotechnique Vol.12 p.500.

Ruiz, M.D., 1975. "Rock Slope Stability Analysis Discontinuities Shear Strength Parameters And Prestressing Costs." 2nd Int. Congress of The IAEG., Sao Paulo,Vol.2 p. V-PC-1.

Ruiz, M.D., Camargo,F., Midea,N.F. and Nieble, C.M.,1968. "Some Considerations Regarding The Shear Strengths Of Rock Masses. " 2nd ISRM Congress , Vol. 2,p. 159.

Scheidegger, A.E., 1973. "On The Prediction Of The Reach And Velocity Of Catastrophic Landslides." Rock Mechanics, Vol.5, pp. 231-236.

Schneider, H.J., 1976. "The Shear Strength And Deformability Of Rock Joints." Rock Mechanics, Vol.8, pp.169-184.

Schneider, H.J., 1975. "Investigations Into The Question Of the Residual Friction On Rock Joints." 2nd Int. Congress Of The IAEG, Sao Paulo, Vol.1, p. IV-11.

Schneider, H.J., 1974. "Rock Friction-A Laboratory Investigation." 3rd ISRM Congress, Vol. 2a p. 311.

Shreve,R.,. 1968. "Leakage And Fluidization In Air Layer Lubricated Avalanches." Bull. Of G.S.A. Vol. 79, pp. 653-658.

Singh, D.P. and Bamford,W.E., 1971. "The Prediction And Measurement Of The Long Term Strength Of Rock." Proc. Of The First Australian- New Zealand Conference On Geomechanics. Vol. 1 p. 37.

Sowers,G.,1976. "Dewatering Rock For Construction." ASCE Specialty Conference, Rock Engineering For Foundations And Slopes. Vol. 1 pp. 200-215.

Stagg, K.G., 1968. "In Situ Tests In Rock Masses." in: Rock Mechanics In Engineering Practice, ed: Stagg,K.G. and Zienkiewicz. O.C., p.125.

Stearns, D.W.,1967. "Certain Aspects Of Fractures In Naturally Deformed Rocks." Nat.Sc. Fdn. Advanced Seminar In Rock Mechanics. ed: Riecker, R.F., Air Force Cambridge Research Laboratory. Special Report 1, pp. 97-116.

Steffen, O.K.H. and Jennings, J.E., 1974. "Definition Of Design Joints For 2-Dimensional Rock Slope Analysis." 3rd ISRM Congress, Vol. 2b p. 827.

Stewart, W.P., 1974. "Stability Of Three Rock Slopes." M.Sc. Thesis, University Of Alberta, 155 pp.

Stott,D.F. and Taylor, G.C.,1972. "Stratigraphy And Structure Of The Rocky Mountains Of West Central Alberta And Northeastern B.C." Int. Geol.Congress, Guidebook For Excursion A10. 71pp.

Terzaghi, K., 1962. "Stability Of Steep Slopes On Hard Unweathered Rock." Geotechnique, Vol. 12, pp. 251-270.

Till, R., 1974. "Statistical Methods For The Earth Scientist." Macmillan Publishing, 152 pp.

Tse, R., 1978."In Preparation." M.Sc. Thesis,University Of Alberta, In Preparation.

Walpole,R.E., 1968. "Introduction To Statistics." Macmillan Co. New York, 365 pp.

Washburn,R.E.,1973. "Periglacial Processes And Environments." Arnold, 320 p.

Wheeler, J.O., Campbell, R.B., Reesor,J.E., and Mountjoy, E.W., 1972 "Structural Style Of The Southern Canadian Cordillera." Int. Geol. Congress, Guidebook For Excursion A01-X01, 118pp.

Witherspoon,P.A. and Gale,J.E., 1975. "Mechanical And Hydraulic Properties Of Rocks Related To Induced Seismicity." First Int Symp. On Induced Seismicity, Banff.

Woodcock,N.H., 1976. "The Accuracy Of Structural Field Measurements." Journal Of Geology, Vol. 4, p.350.

APPENDIX

APPENDIX A-1

The method used to detect the presence of the small folds on the north failure surface at Jonas Creek was first proposed by Ramsden(1977). The technique was devised in order to detect small differences in orientation of geologic structures which were similar in orientation.

In the graphical modification of the method proposed here, the average orientation of a group of poles to the discontinuities was found by plotting the data on an equal area net and contouring the data points. The average pole was then rotated to the centre of the stereonet about an axis parallel to the average strike of the discontinuities and the individual points were rotated an equal amount. Straight lines joining the centre of the stereonet to each of the individual points were then constructed. The direction of each line then indicated the direction of the departure of the individual point from the mean orientation of the surfaces and the length of the line the size of the departure. If such lines are plotted on a map (Figure A-1-1), very small systematic differences in orientation can be detected and various structural features could be more easily recognized.

FIGURE A-1-1 SKETCH MAP ILLUSTRATING RAMSDENS GRAPHICAL MODEL

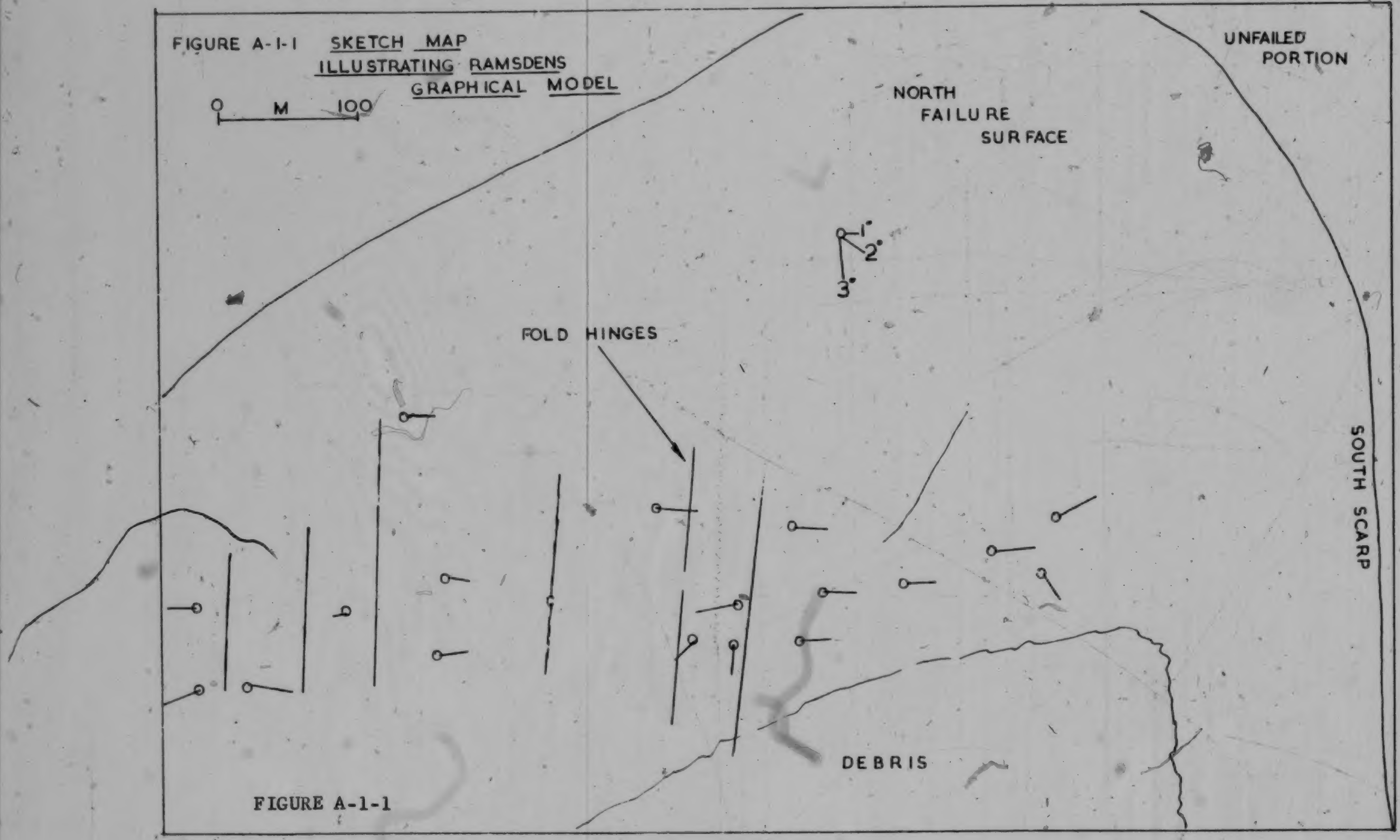
0 M 100
UNFAILED PORTION
NORTH FAILURE SURFACE
1°
2°
3°
FOLD HINGES
SOUTH SCARP
DEBRIS

FIGURE A-1-1

APPENDIX A-2 In Situ Shear Test

INTRODUCTION

One of the problems found in correlating the field measurements of roughness with the peak shear strengths found in the field during failure, is the lack of shear strength data performed on a large scale (Krahn, 1974). In situ large scale shear tests are often extremely expensive to obtain and hence are limited to very large projects.

In the case of natural slopes, very large scale shear tests can be evaluated using back analysis of failed areas. Small scale shear tests on 5cm x 5cm samples are inexpensive to perform and are common but they are of somewhat limited value.

During field mapping at Jonas Creek, a large block of quartzite over 4.0 m long was found separated from the main mass of a bedding surface. The rock had slid along a bedding plane for a distance of 0.6 m before coming to rest. The back and lateral margins of the block were defined by near vertical joints. The lateral margins were open and were apparently not restricting movement. It was thought prior to testing that the block had moved down the slope along a bedding plane surface until it had encountered an asperity upon which it had become stabilized. It was thought that a direct shear test performed on this block to yeild a peak friction angle of Øb + i, could be used to verify the field measurement of roughness evaluated prior to the test.

The block was located on the north west margin of the north slide at Jonas Creek. It was bounded on the back side and both lateral margins by vertical joints which were open and continuous. There did not appear to be any joint contact between the side of the sample and surrounding bedding surfaces from which the sample block had moved. The toe of the block was unobstructed.

The block measured 4.0 m long, 2.4 m wide and 0.7 m thick. The weight of the block was 144 kN. The block was resting on a slope with an average dip of 30°.

ROUGHNESS EVALUATION

The roughness was evaluated using a variety of techniques on the upper surface of the unsheared block prior to failure and the failure plane after the test left the failure plane exposed. The roughness on the upper surface of the block , evaluated using the new variance technique, was based on 75 measurements located at 5 stations on the surface. The roughness evaluated in this manner had an average i angle of 3.7°.

Following the test, the roughness was evaluated on the exposed surface using only 2 stations and the average i angle was 3.2°. This agreed well with the average i angle recorded from a profile of the bedding surface found below the test block. This average i angle was 2.6°.

PREPARATION

Prior to testing small loose rocks and soil debris were removed from the back and lateral margins of the block. During this operation tree roots were exposed at the back margin of the test block and these were thought to be responsible for initiating the original movement of the sample block.

Black painted aluminum strips, 2.5 cm wide and 1 m long were anchored by adhesive to the sliding block. Similar strips were erected on the stable portion of the slope approximately 1 to 2 m away from the lateral margin of the test block. Survey ribbon was used to tie the strips together and to identify each strip. The rods were all positioned vertically on the rock and the horizontal distances between the rods was recorded. A 35 mm camera was positioned 18.2 m away from the centre of the test block along the strike of the beds. Photographs were then taken of the test set up every 10 seconds during the test and displacements of the block were recorded by measuring the relative displacements between the stationary and moving aluminum strips.

In addition a steel tape was epoxied to the moving sample block. The tape was stretched from the sample block to a cut cross on the stable bedding plane behind. As the block was moved forward during the test displacements were measured with respect to time.

The shear load was applied by a pair of hydraulic rams placed in the already open joint at the back of the sample block. The rams were individually controlled by a gate valve so that one ram could be shut off if the block strted to turn in its track. Aluminum plates were placed between the rams and the rock surfaces to accomodate the roughness of the joint walls.

The shear load developed during the test was measured on two hydraulic gauges which had a working range of 60 to 5000 psi. Quick-connect hoses were used on all connections. Aluminum pipe spacers of various lengths were used as spacers between the jacks and the stationary bedding surface behind. This bedding surface extended for well over 30 m back upslope and hence served as a reaction block. All readings of load and displacement and all photographs were taken every 10 seconds. The load time and deformation time curves were then used to construct the load deformation graph.

POST SLIDE OBSERVATIONS

During the test, a very loud groaning sound was heard followed by a sudden crack and a sudden acceleration of the block. The block only moved 1.1 m , however, as the lateral margins wedged and caused a sudden stop.

Following the test the exposed failure surface was examined for surface damage. One small scratch less than 5 cm long was found. Large areas of sheared rock were found an the edges of the block where crushing of asperities had occurred. Unfortunately, this component of the total measured shear resistance, was unknown.

The failed block was found to be raised up off the failure surface at the end of the test. The block was firmly wedged between the unfailed portions of the bedding planes on the lateral margins of the test block. Several small spherical pieces of rock approximately 7 - 10 cm in diameter, were trapped beneath the sample block and were apparently supporting its weight. This, in conjunction with the very little surface damage which occurred on the basal surface, indicated that perhaps the block had moved on very small contact areas.

RESULTS

The resulting load time and deformation time graphs are highly irregular (Figure A-2-1). However, it would appear from the displacement-time curve that a constant displacement per unit time occurred midway through the test. Using the average load developed during this period a peak angle of 36° to 37° was calculated. This implies that the i angle was 6° to 7°, almost twice the angle measured before and after shearing. The excess strength derived from the crushing of the sides was unknown.

DISCUSSION

Due to the loss of frictional contact along the base of the sample, and due to the interference of the side effects, it is not possible to isolate the component of shear resistance provided by the bedding surface roughness. The roughness of the vertical joints was unknown but because of the high degree of local crushing which occurred in places, it is doubtful that a value of i would have been of any significance. The value of 36-37° for a peak shear strength of the block is considerably below peak strengths measured in the laboratory tests.

The results of the in situ test are inconclusive. A continuous recording of the load versus displacement is necessary during these tests and should be incorporated into any future tests of this nature.

A movie of the failure was taken on 8mm film. The results of this were unfortunately of little significance due partially to the angle of shooting and also due to the small film size. Future tests should look into the possibility of getting above the plane of sliding of the block to record the failure on film.

This method is definately a viable testing method but more expense in both time and money should be done for future tests of this nature.

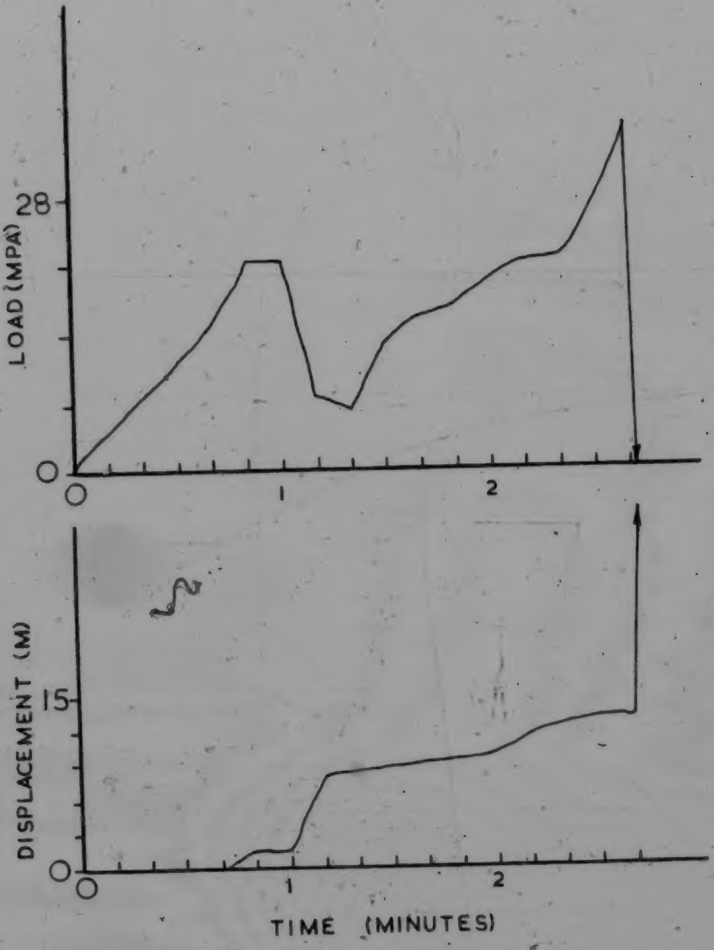

FIGURE A-2-1 Results Of The Insitu Shear Test At Jonas Creek.

APPENDIX A-3 SAMPLE PREPARATION

Section 6-3 outlines the procedure for obtaining large block samples in the field. The blocks are separated in the field to insure that the discontinuity being sampled represents the desired surface. The sample is then wrapped to avoid movement and transported to the lab.

The samples were kept wrapped in fibreglass reinforced tape after transport. The direction of shear was established in the lab on the basis of the orientation of micro joints (section 6-4). Ideally the direction of shear should be marked on the sample as it is removed from the site near the failure plane. The in situ dip and dip direction of the sample should be marked on the rock in order to orient the sample with respect to the failure surface in the lab. This procedure was not performed at the areas studied as the material was recovered from the slide debris and the original dip and dip direction could only be inferred.

Following the evaluation of sample shear direction, the upper surface of the sample was divided into squares using a felt pen marker and steel scale. The directions of shear were then marked on each sample. The large block sample was then placed in a water cooled diamond saw and the samples were sliced to their 4.5 cm x 4.5 cm dimensions. In most cases the samples were too high to be used directly so the ends were trimmed off. This left a sample of 4.5 cm x 4.5 cm and approximately 7 cm high. The discontinuity was approximately at the mid height of the sample. Masking tape was wrapped around the sample at the mid point to avoid the seepage of molding material into the discontinuity.

The casting of the sample to insure a snug fit in the direct shear box was a simple procedure. Aluminum molds with interior dimensions of 5 cm x 5 cm were used. The molds were capable of being dismantled for easy removal of the cast specimens.

A block of plywood 4.95 cm square and 1.87 cm thick was then used as a base. Four 2.5 cm long finishing nails were hammered into the wood then withdrawn several times until they could move easily into and out of the wood. The block with the wood was then placed in the mold. The bottom half of the sample block was then placed on top of the nails and pushed by hand until the discontinuity surface was level with the top of the mold. The rock sample was then removed from the mold.

The molds were placed in hot wax and allowed to heat for approximately 1 minute. Upon removal the wax flowed out of the mold leaving a very thin skin of wax which hardened in about 5 minutes. When the wax had hardened the rock sample was replaced in the mold in the original position. A mixture of Randustrial bolt anchor sulfaset and water was then made. The mix had enough water to give it the consistency of white glue. The mixture was then poured into the mold around the edges of the sample. The mold was filled to within 2 or 3 mm of the discontinuity line. The sample was then allowed to cure for 24 hours before being removed from the mold. The markings on the rock sample were then transferred to the outside of the sulfaset.

The second half of the sample was prepared in a similar manner. An extension of the mold ensured that the second half of the sample being molded lined up with the previously molded sample. The sulfaset was then added to the mold and left for 24 hours.

The sample was removed from the mold and the plywood blocks and the protruding finishing nails were removed by a small trimming saw. The samples were then stored in the lab prior to sanding and testing. Prior to testing the bottom half of samples were sanded on a flat surface to ensure a snug fit in the shear box. The upper halves were sanded undersize on a sanding belt with a sanding jig clamped in place. This ensured flat sides and true corners. The masking tape was then removed from around the discontinuity surface.

The samples were then stored in the testing room at approximately 25° C and a relative humidity of 10% . The samples were air blown clean immediately prior to testing.

APPENDIX A-4 SHEAR TEST RESULTS

This appendix presents the results of the direct shear tests and the tilting table tests performed on the bedding surface discontinuities retrieved from Jonas Creek and Whitehorse Creek.

TABLE A-4-1

Shear Strength Data for Jonas Creek

sample	area (cm^2)	N (mPa)	Tp (mPa)	Tult (mPa)	i dilation degrees
1	18.9	0.130	0.181	0.038	4.5
2	19.1	0.220	0.289	0.073	9.5
3	16.8	0.140	0.361	0.047	16.0
4	19.0	0.333	0.313	0.133	5.8
5	18.3	1.222	1.551		12.0
6	21.0	0.595	0.554	0.341	5.5
7	20.6	1.060	1.162		7.0
8	20.8	0.052	0.043	0.020	3.3
9	20.8	0.144	0.251	0.064	4.5
10	16.6	0.144	0.114	0.050	8.5
11	20.6	0.302	0.218	0.134	2.0
12	21.0	0.434	0.321	0.206	1.0
13	19.7	0.577	0.526	0.291	6.7
14	23.1	0.296	0.227	0.112	
15	21.1	0.170	0.251	0.120	10.0
16	14.6	0.343	0.344	0.156	7.5
17	21.4	0.604	0.597	0.389	0.0
18	21.3	0.308	0.386	0.158	4.5

TABLE A-4-2

Shear Test Data Whitehorse Creek

sample	area	N	Tp	Tult	i dilation
	(cm^2)	(mPa)	(mPa)	(mPa)	degrees
1	14.0	0.622	0.906	0.519	6.0
2	17.6	0.127	0.334	0.039	14.5
3	16.8	0.356	0.404	0.227	0.0
4	16.4	0.210	0.413	0.109	2.5
5	17.2	0.849	1.092	0.653	3.0
6	14.1	0.414	0.512	0.306	4.0
7	13.4	0.569	0.894	0.411	6.0
8	17.0	0.578	1.185	2.970	8.0
9	17.9	0.062	0.165	0.091	9.0
10	15.6	0.077	0.561	0.046	16.0
11	14.1	0.052	0.126	0.038	7.5
12	18.1	0.659	1.179	0.620	8.0

TABLE A-4-3

Summary of the Artificial Surface Shear Test Results

sample	area (cm²)	N (mPa)	Tp (mPa)
POLISHED QUARTZITE			
1	16.6	0.053	0.020
2	17.1	0.141	0.029
3	17.3	0.139	0.031
4	19.1	0.255	0.062
5	19.4	0.343	0.087
6	16.0	0.766	0.176
SANDBLASTED QUARTZITE			
1	20.1	0.114	0.075
2	18.4	0.174	0.104
3	17.9	0.234	0.159
4	18.1	0.324	0.208
SANDBLASTED DOLOMITE			
1	15.2	0.110	0.082
2	15.0	0.224	0.163
3	15.3	0.422	0.245
4	15.5	0.759	0.581

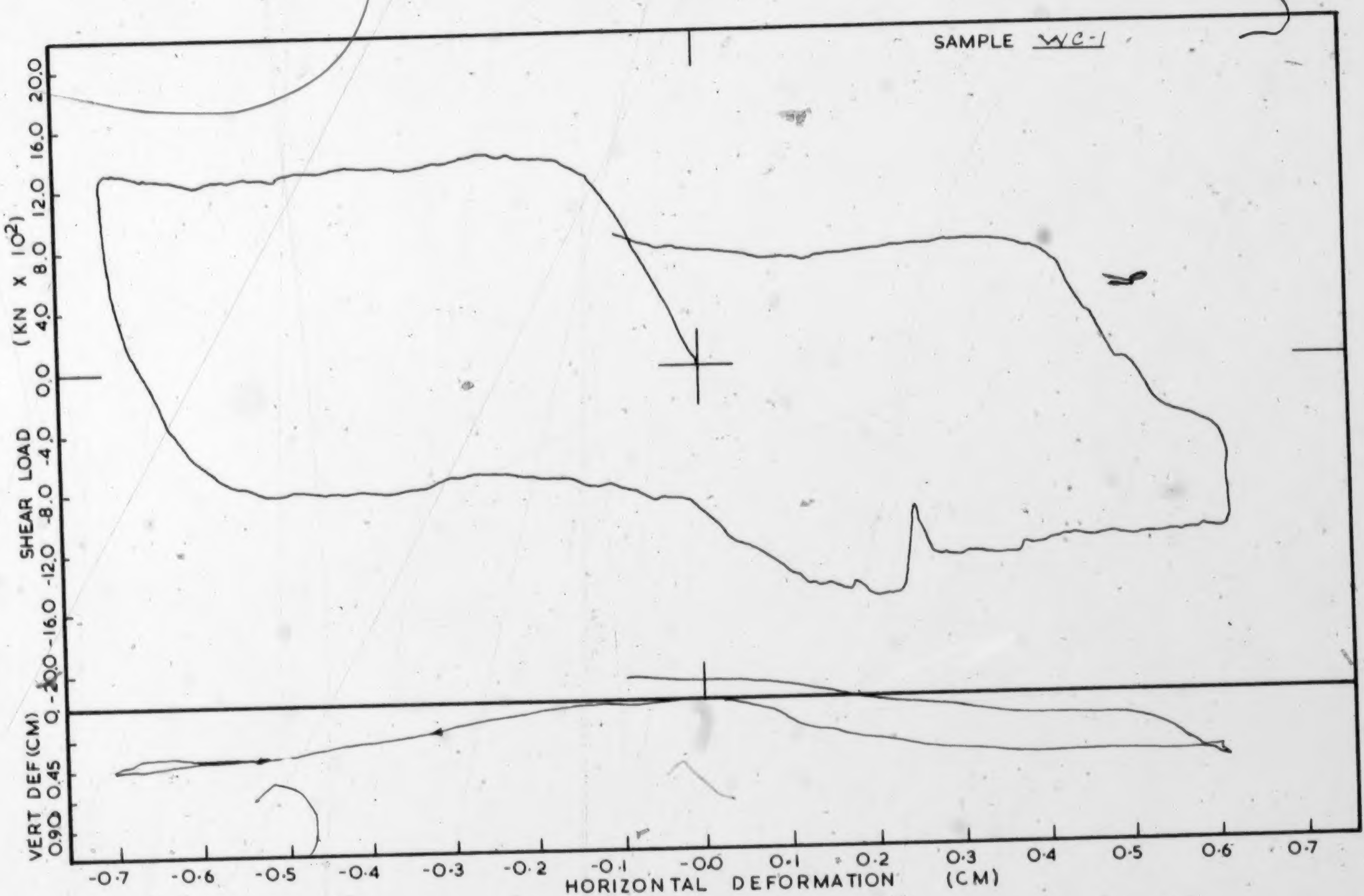
SAMPLE WC-1
SHEAR LOAD (KN X 10²)
20.0
16.0
12.0
8.0
4.0
0.0
-4.0
-8.0
-12.0
-16.0
-20.0
VERT DEF (CM)
0
0.45
0.90
-0.7
-0.6
-0.5
-0.4
-0.3
-0.2
-0.1
-0.0
0.1
0.2
0.3
0.4
0.5
0.6
0.7
HORIZONTAL DEFORMATION (CM)

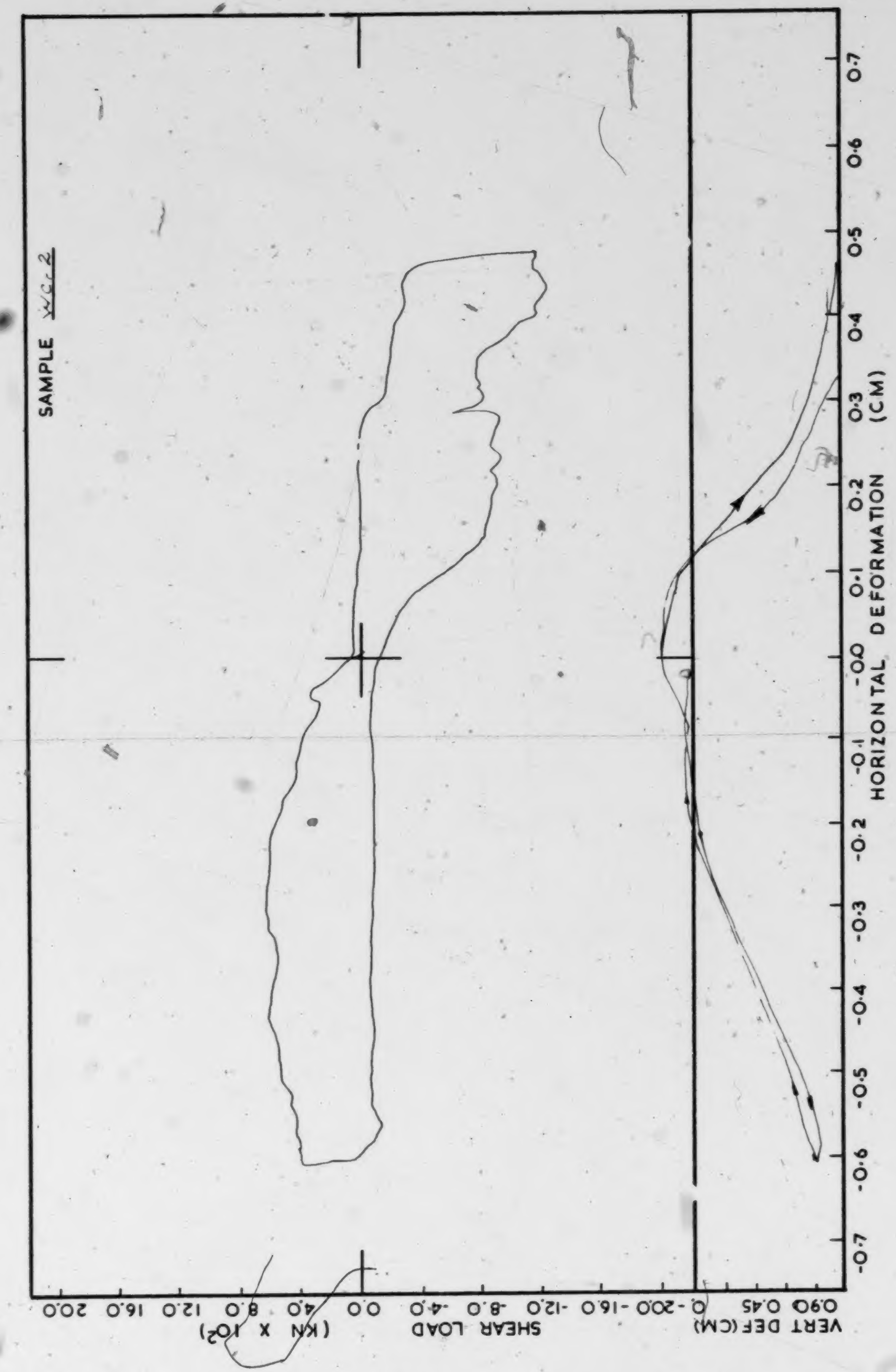
SAMPLE ycc 2
SHEAR LOAD (KN X 10²)
20.0
16.0
12.0
8.0
4.0
0.0
-4.0
-8.0
-12.0
-16.0
-20.0
VERT DEF (CM)
0.
0.45
0.90
-0.7
-0.6
-0.5
-0.4
-0.3
-0.2
-0.1
-0.0
0.1
0.2
0.3
0.4
0.5
0.6
0.7
HORIZONTAL DEFORMATION (CM)

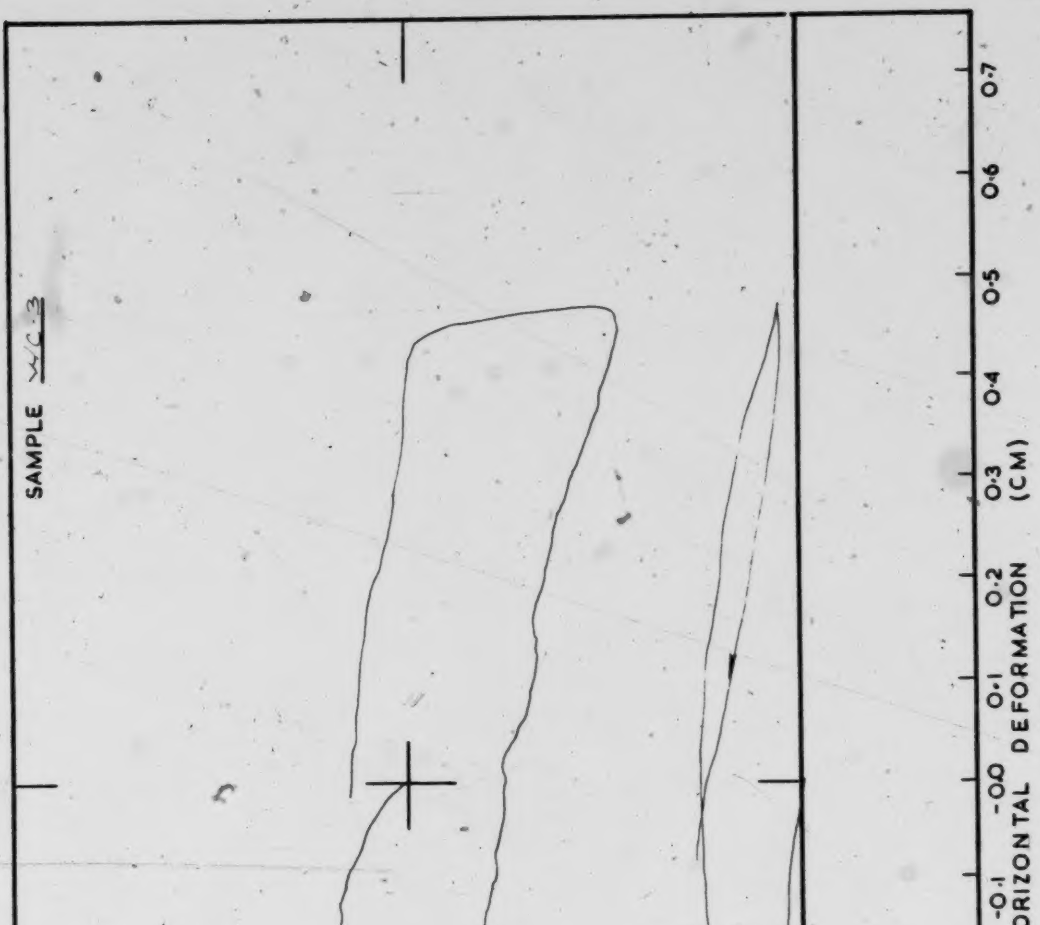
SAMPLE W/C 3
HORIZONTAL DEFORMATION (CM)
-0.7
-0.6
-0.5
-0.4
-0.3
-0.2
-0.1
0.0
0.1
0.2
0.3
0.4
0.5
0.6
0.7
SHEAR LOAD (KN X 10²)
20.0
16.0
12.0
8.0
4.0
0.0
-4.0
-8.0
-12.0
-16.0
-20.0
VERT DEF (CM)
0.
0.45
0.90

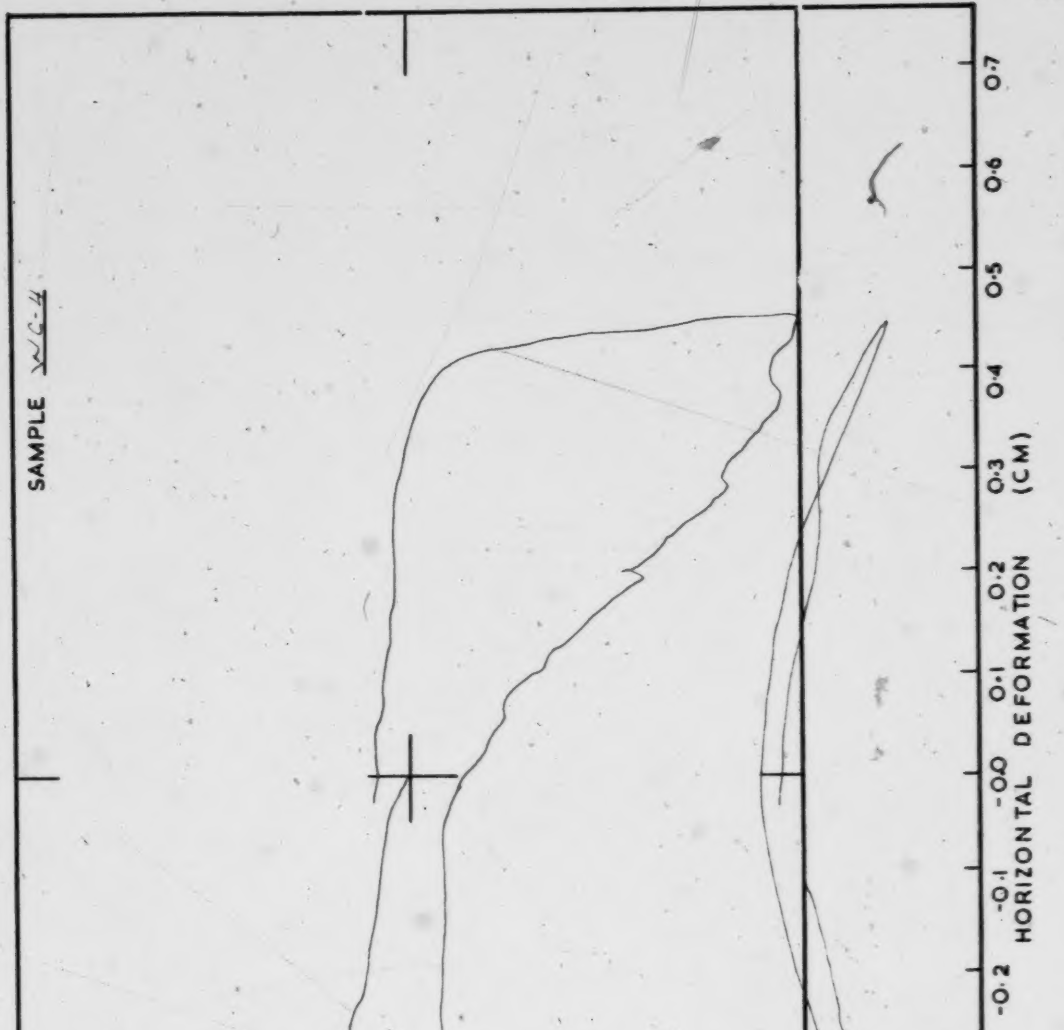
SAMPLE WC-4
SHEAR LOAD (KN X 10²)
20.0
16.0
12.0
8.0
4.0
0.0
-4.0
-8.0
-12.0
-16.0
-20.0
VERT DEF (CM)
0.
0.45
0.90
HORIZONTAL DEFORMATION (CM)
-0.7
-0.6
-0.5
-0.4
-0.3
-0.2
-0.1
-0.0
0.1
0.2
0.3
0.4
0.5
0.6
0.7

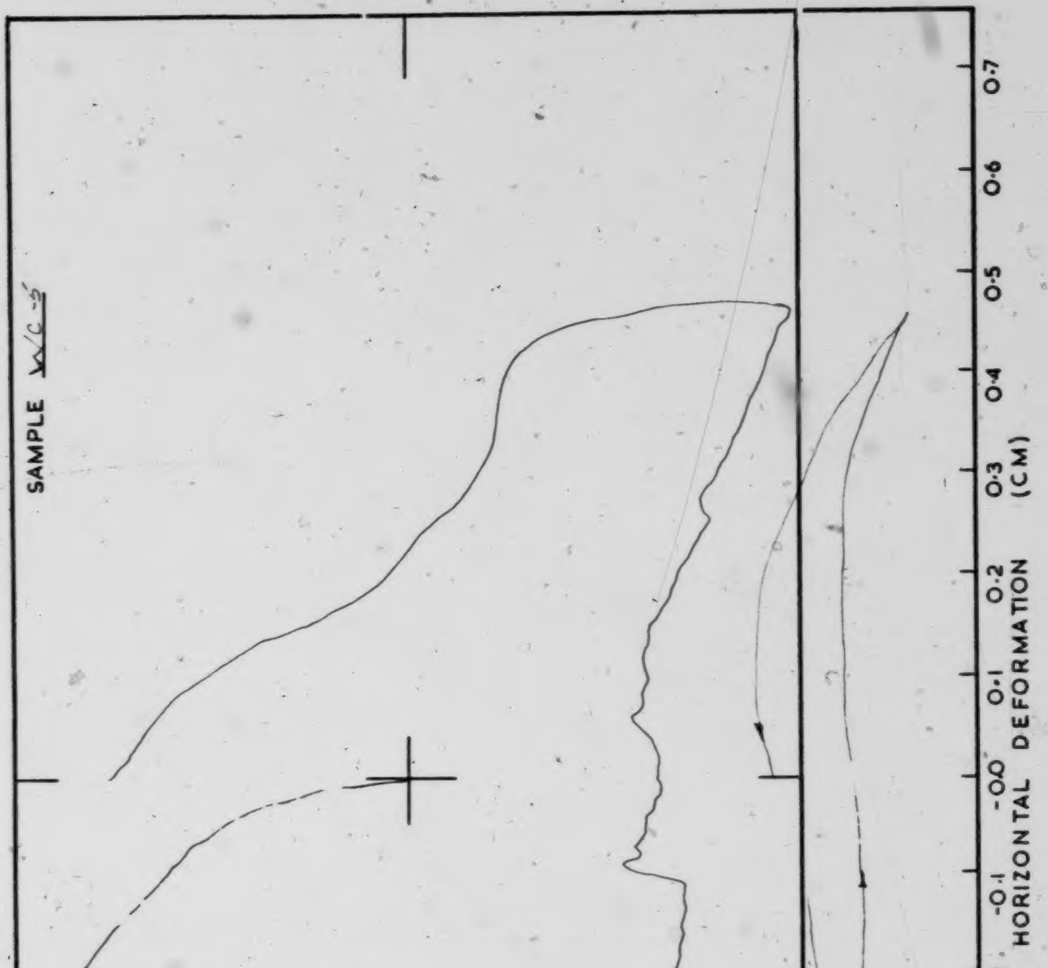
SAMPLE W/C-5
SHEAR LOAD (KN X 10^2)
20.0
16.0
12.0
8.0
4.0
0.0
-4.0
-8.0
-12.0
-16.0
-20.0
VERT DEF (CM)
0.90
0.45
0
HORIZONTAL DEFORMATION (CM)
-0.7
-0.6
-0.5
-0.4
-0.3
-0.2
-0.1
-0.0
0.1
0.2
0.3
0.4
0.5
0.6
0.7

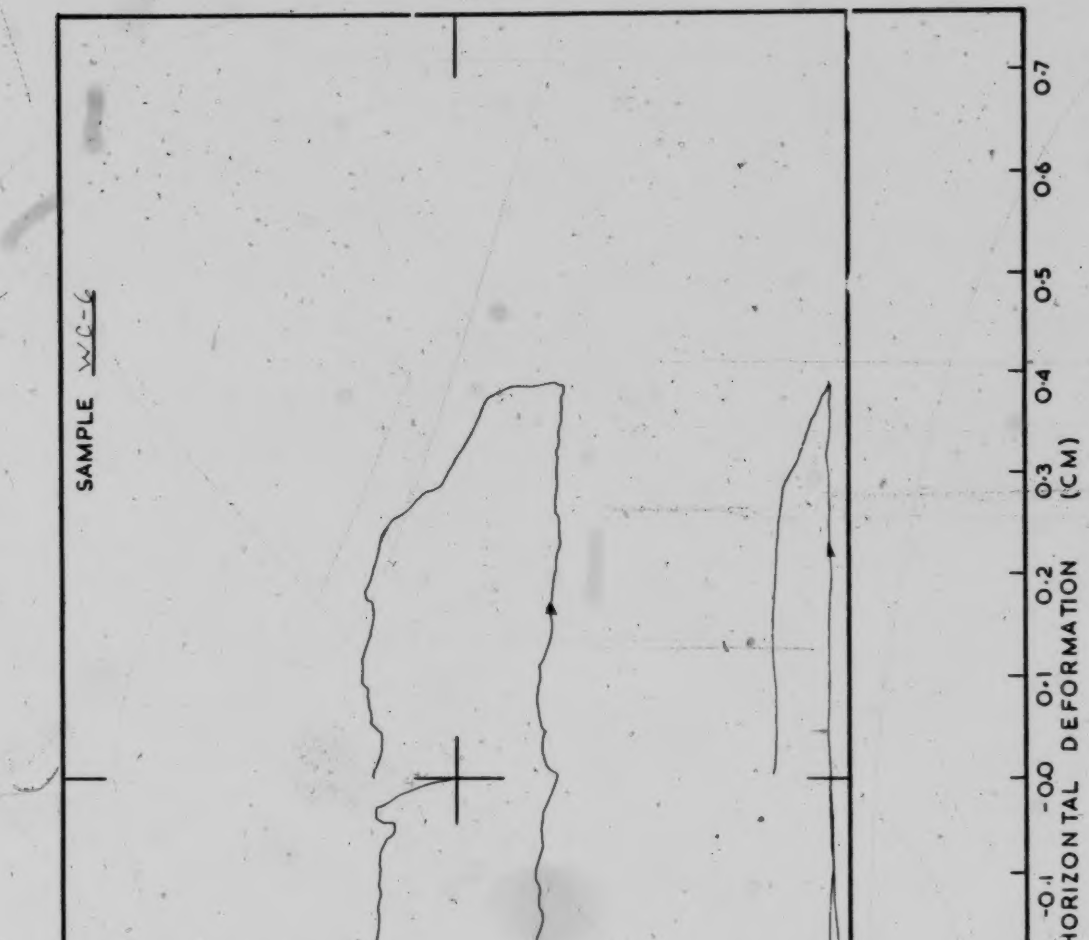
SAMPLE WC-6
SHEAR LOAD
(KN X 10²)
20.0
16.0
12.0
8.0
4.0
0.0
-4.0
-8.0
-12.0
-16.0
-20.0
VERT DEF (CM)
0.
0.45
0.90
-0.7
-0.6
-0.5
-0.4
-0.3
-0.2
-0.1
-0.0
0.1
0.2
0.3
0.4
0.5
0.6
0.7
HORIZONTAL DEFORMATION (CM)

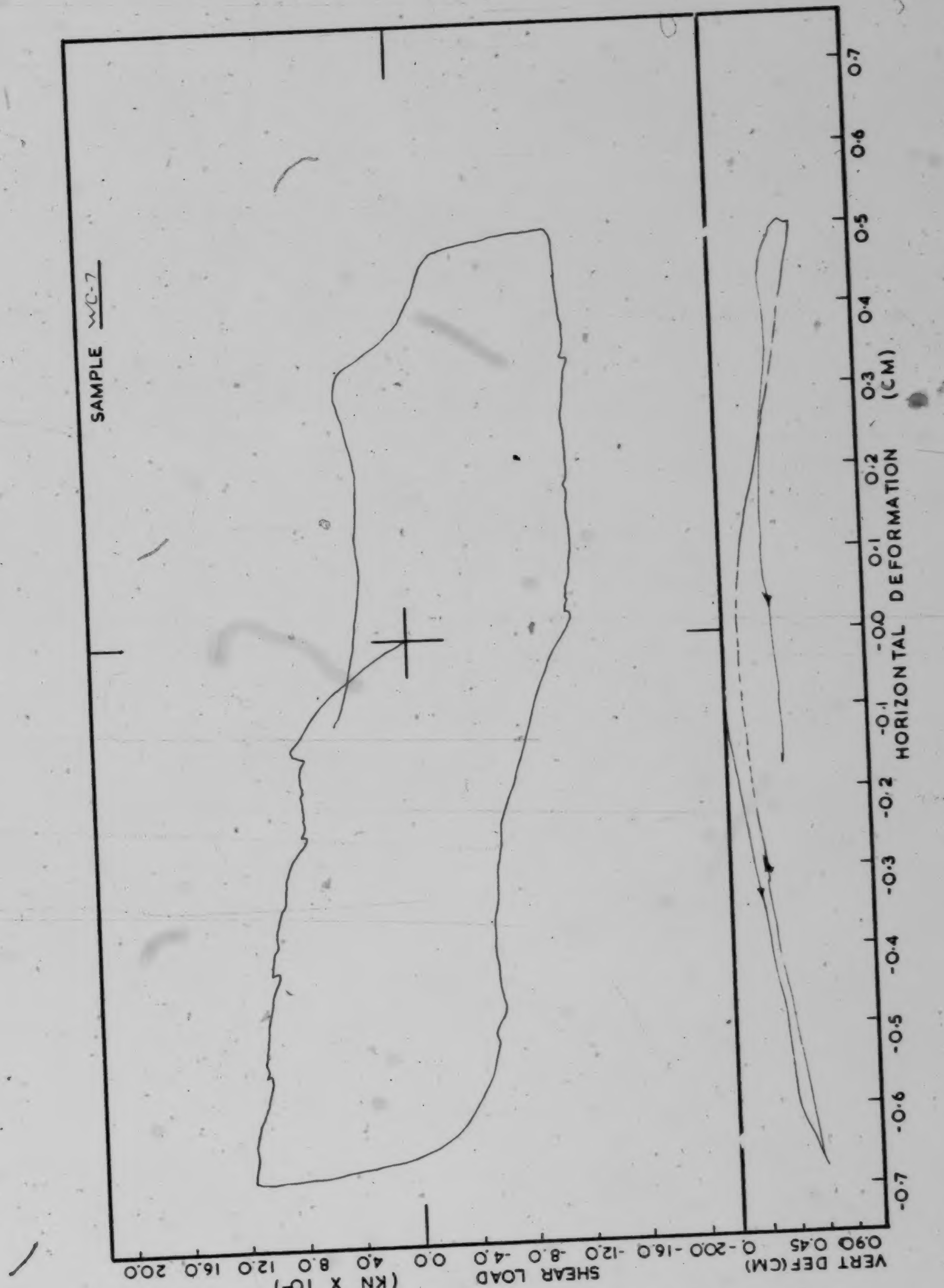
SAMPLE WC-7
SHEAR LOAD
(KN X 10^2)
20.0
16.0
12.0
8.0
4.0
0.0
-4.0
-8.0
-12.0
-16.0
-20.0
VERT DEF (CM)
0.90
0.45
0.
HORIZONTAL DEFORMATION (CM)
-0.7
-0.6
-0.5
-0.4
-0.3
-0.2
-0.1
-0.0
0.1
0.2
0.3
0.4
0.5
0.6
0.7

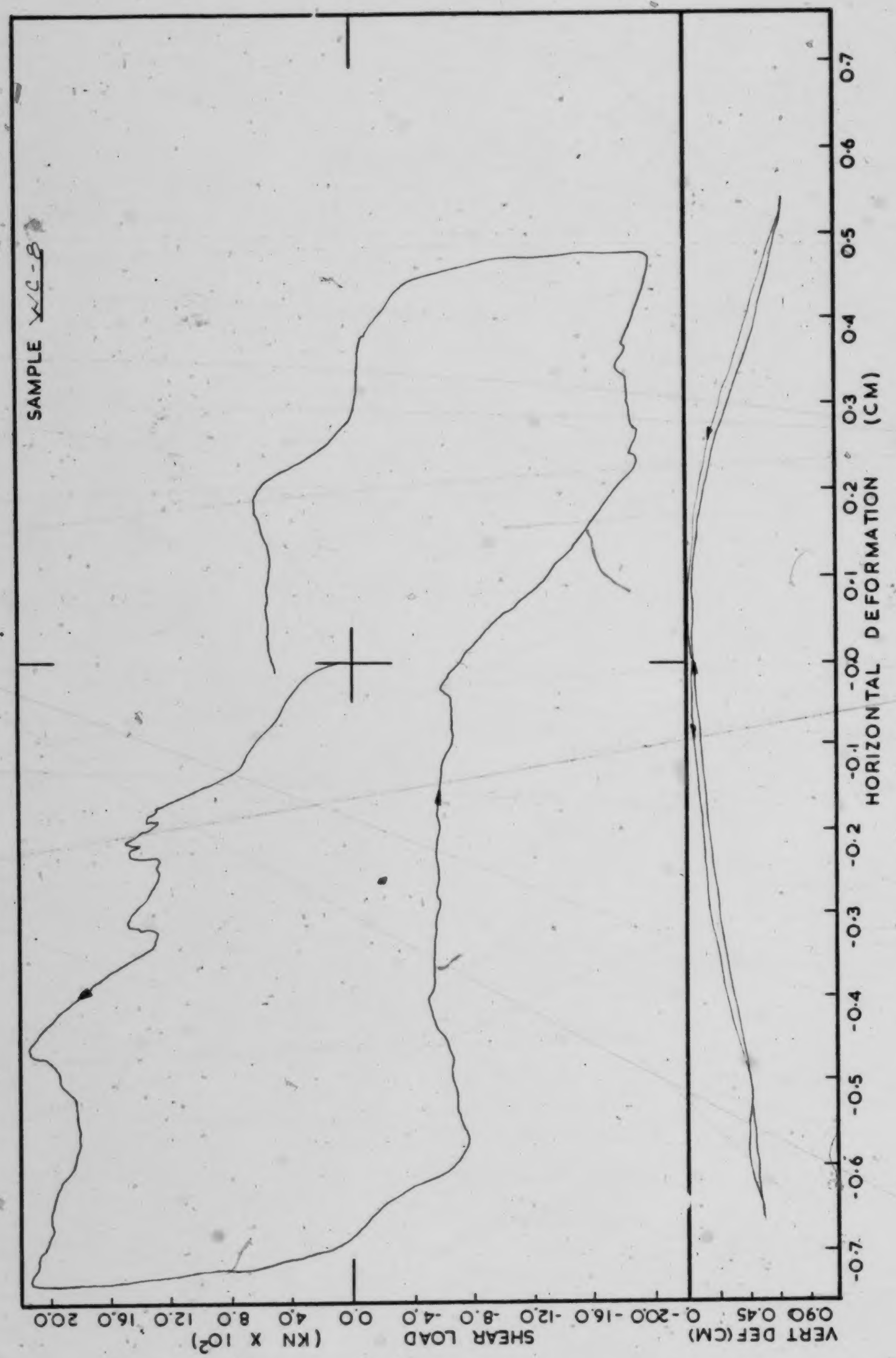
SAMPLE YC-8
SHEAR LOAD
(KN X 10^2)
20.0
16.0
12.0
8.0
4.0
0.0
-4.0
-8.0
-12.0
-16.0
-20.0
VERT DEF(CM)
0.
0.45
0.90
-0.7
-0.6
-0.5
-0.4
-0.3
-0.2
-0.1
-0.0
0.1
0.2
0.3
0.4
0.5
0.6
0.7
HORIZONTAL DEFORMATION (CM)

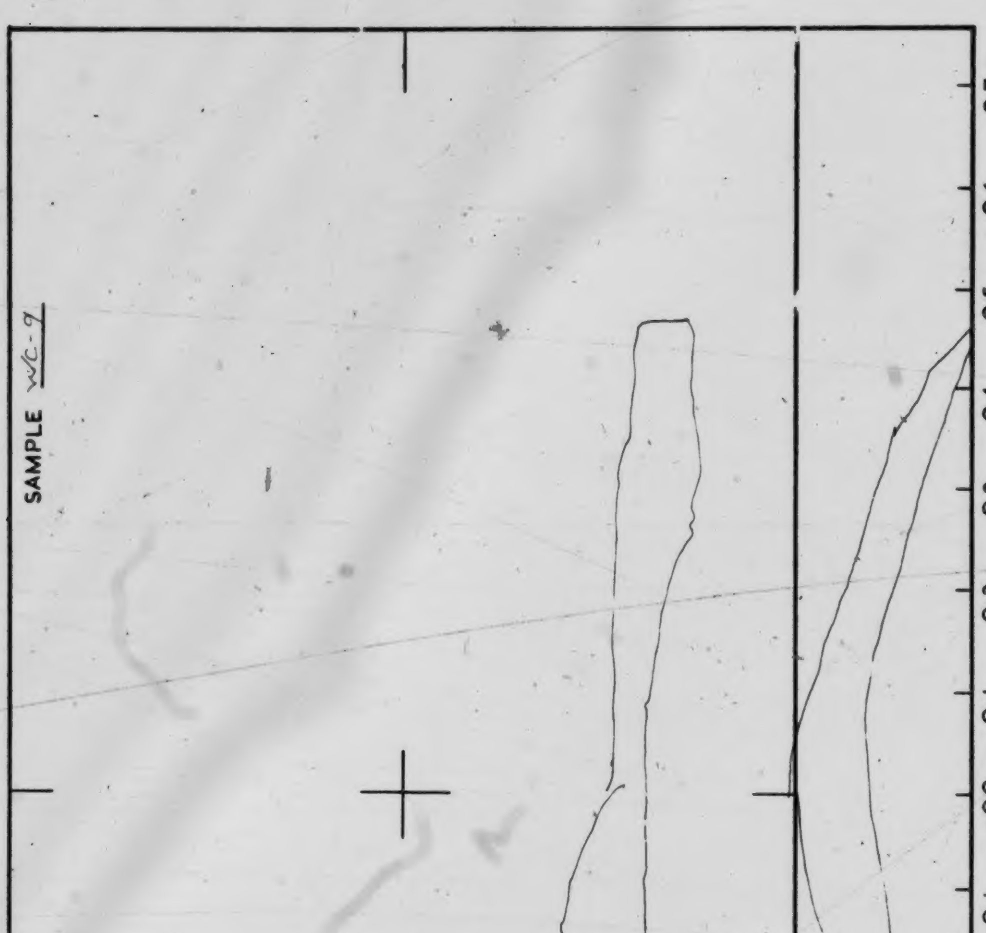
SAMPLE wc-9
HORIZONTAL DEFORMATION (CM)
-0.7
-0.6
-0.5
-0.4
-0.3
-0.2
-0.1
-0.0
0.1
0.2
0.3
0.4
0.5
0.6
0.7
SHEAR LOAD (KN X 10^2)
20.0
16.0
12.0
8.0
4.0
0.0
-4.0
-8.0
-12.0
-16.0
-20.0
VERT DEF (CM)
0.
0.45
0.90

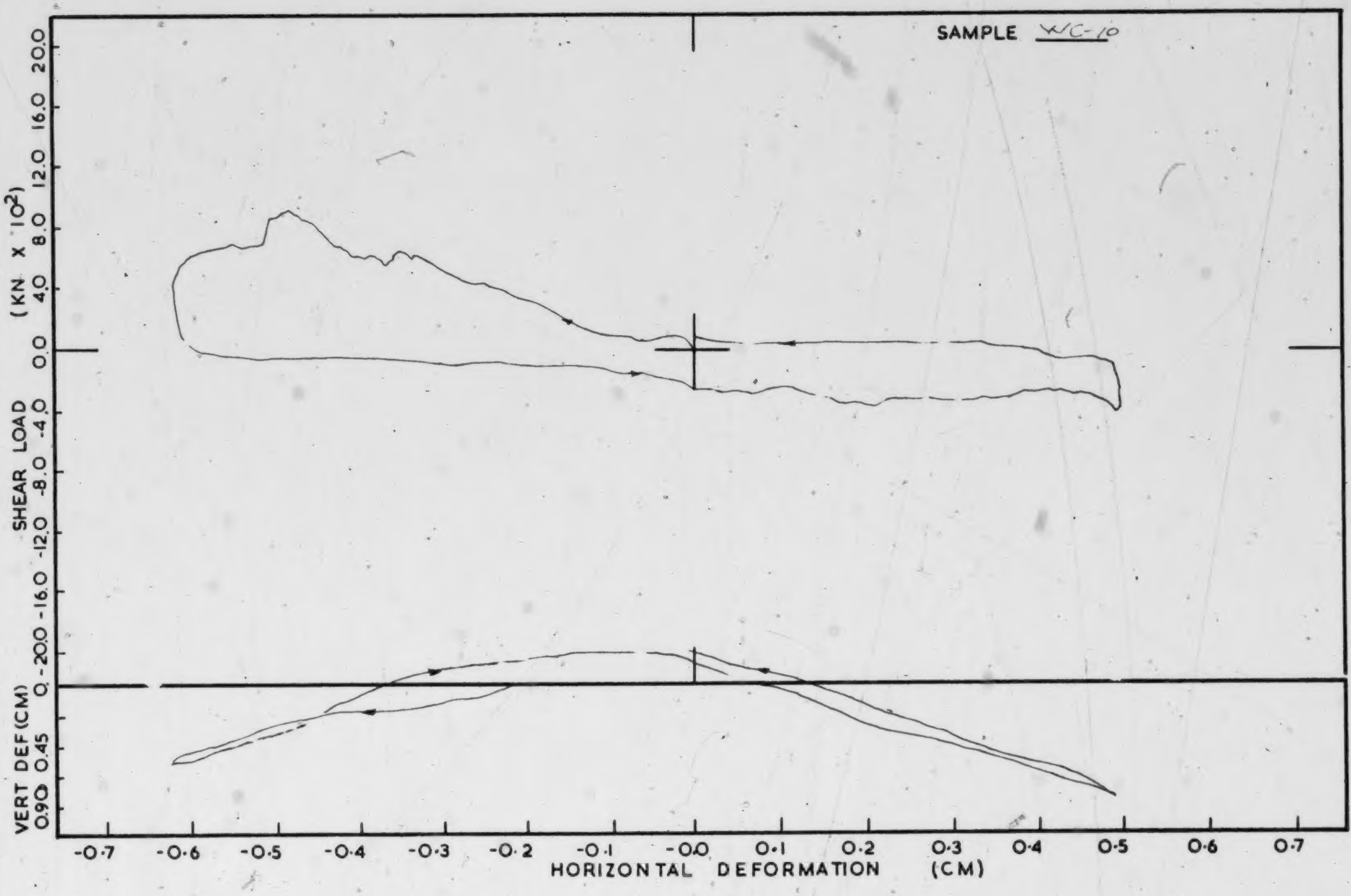
SAMPLE WC-10
SHEAR LOAD (KN X 10^2)
20.0
16.0
12.0
8.0
4.0
0.0
-4.0
-8.0
-12.0
-16.0
-20.0
VERT DEF (CM)
0.
0.45
0.90
-0.7
-0.6
-0.5
-0.4
-0.3
-0.2
-0.1
-0.0
0.1
0.2
0.3
0.4
0.5
0.6
0.7
HORIZONTAL DEFORMATION (CM)

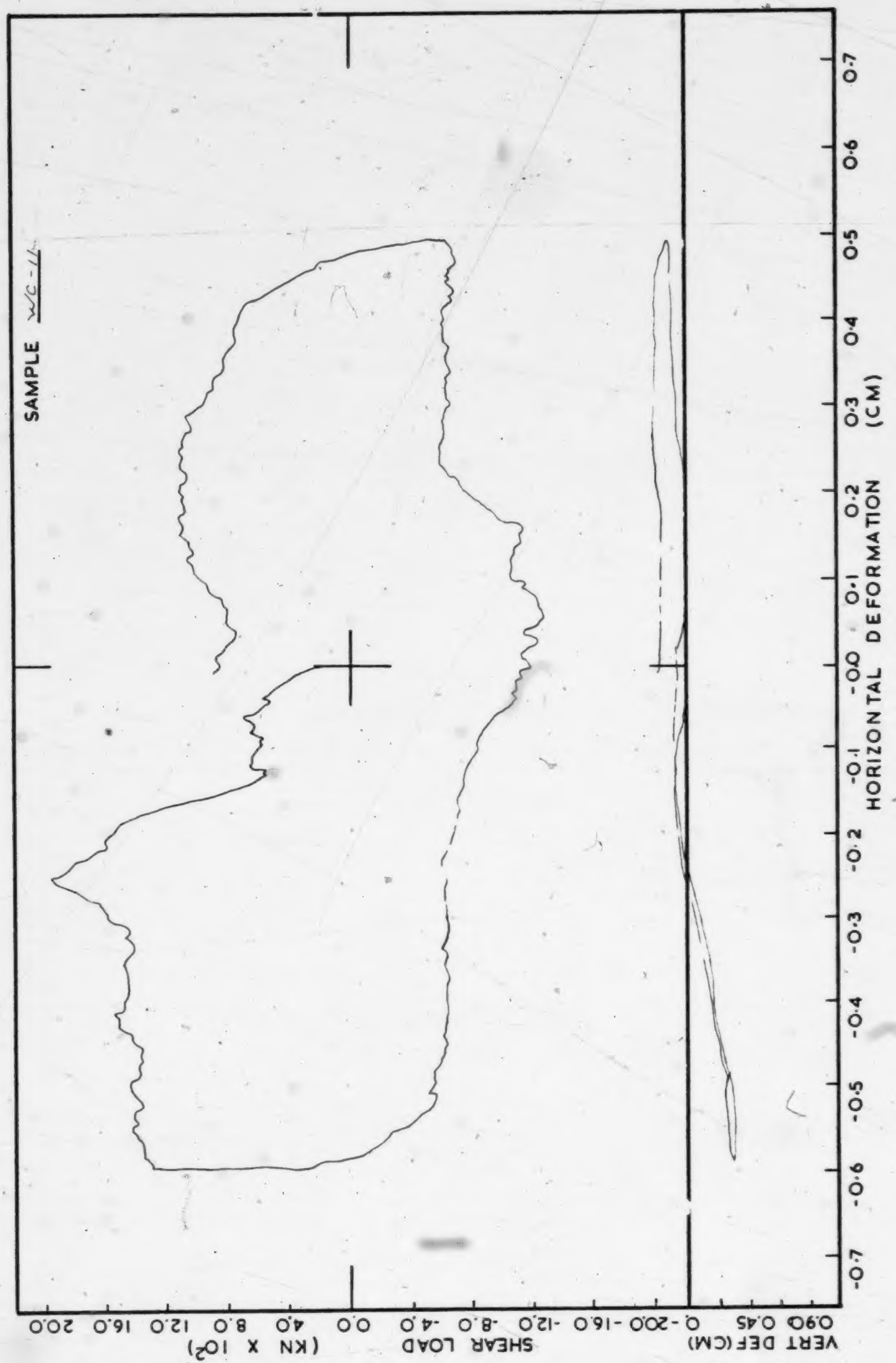
SAMPLE WC-11
SHEAR LOAD (KN X 10²)
20.0
16.0
12.0
8.0
4.0
0.0
-4.0
-8.0
-12.0
-16.0
-20.0
VERT DEF (CM)
0.
0.45
0.90
-0.7
-0.6
-0.5
-0.4
-0.3
-0.2
-0.1
-0.0
0.1
0.2
0.3
0.4
0.5
0.6
0.7
HORIZONTAL DEFORMATION (CM)

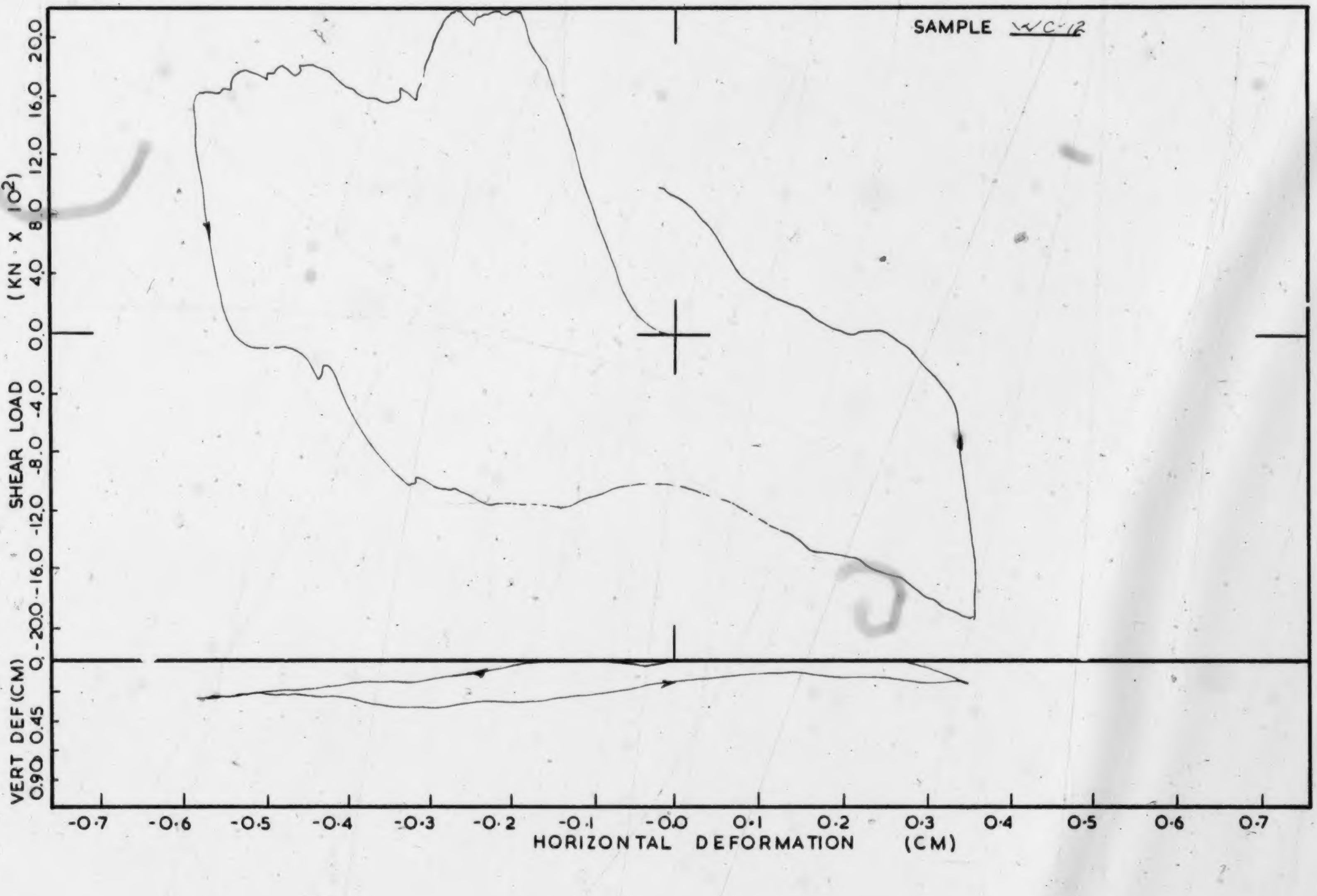
SAMPLE WC-12
SHEAR LOAD (KN · X 10^2)
20.0
16.0
12.0
8.0
4.0
0.0
-4.0
-8.0
-12.0
-16.0
-20.0
VERT DEF (CM)
0
0.45
0.90
-0·7
-0·6
-0·5
-0·4
-0·3
-0·2
-0·1
-0.0
0·1
0·2
0·3
0·4
0·5
0·6
0·7
HORIZONTAL DEFORMATION (CM)

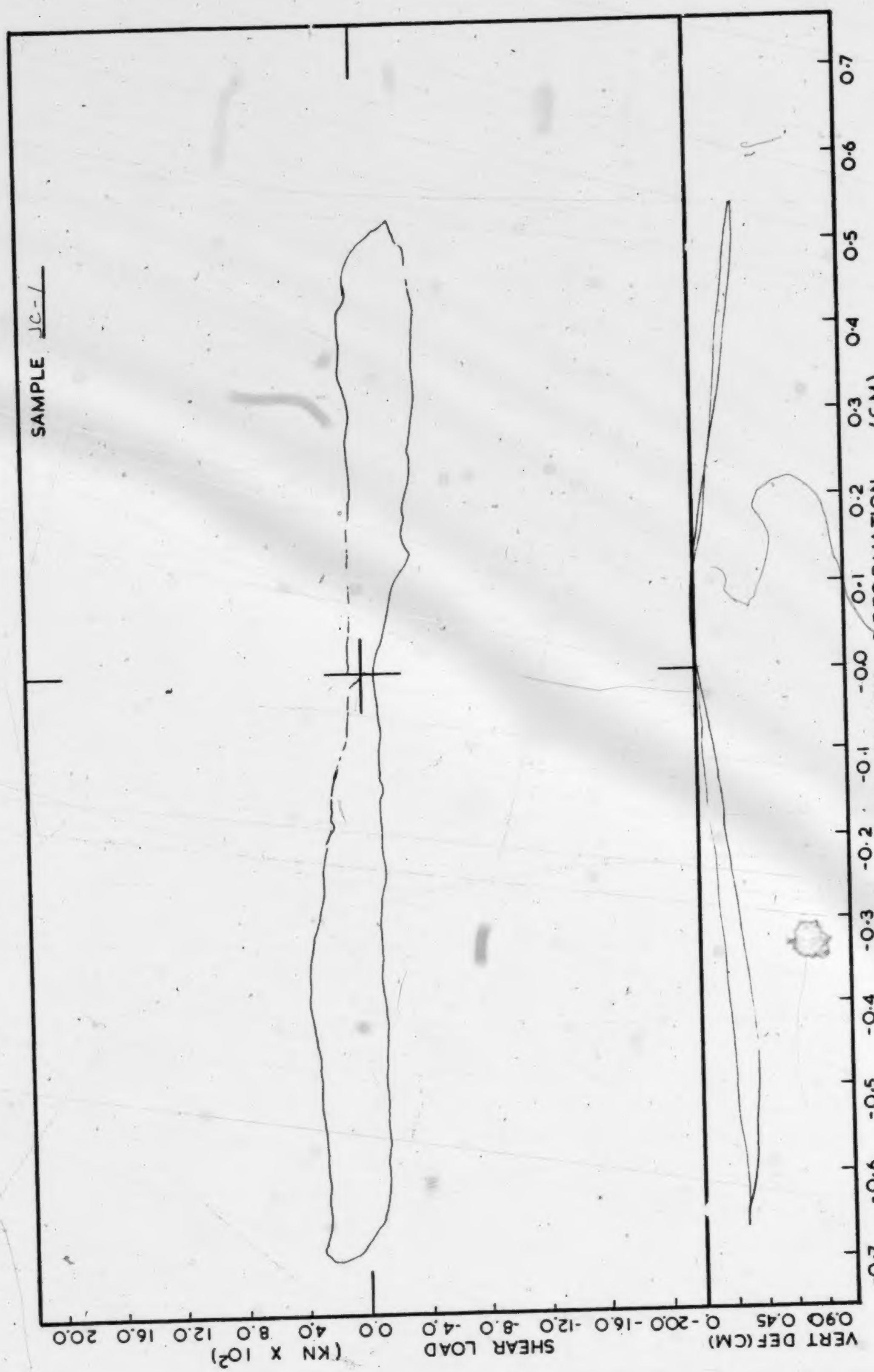
SAMPLE JC-1
SHEAR LOAD
(KN X 10^2)
20.0
16.0
12.0
8.0
4.0
0.0
-4.0
-8.0
-12.0
-16.0
-20.0
VERT DEF(CM)
0.
0.45
0.90
HORIZONTAL DEFORMATION (CM)
-0.7
-0.6
-0.5
-0.4
-0.3
-0.2
-0.1
-0.0
0.1
0.2
0.3
0.4
0.5
0.6
0.7

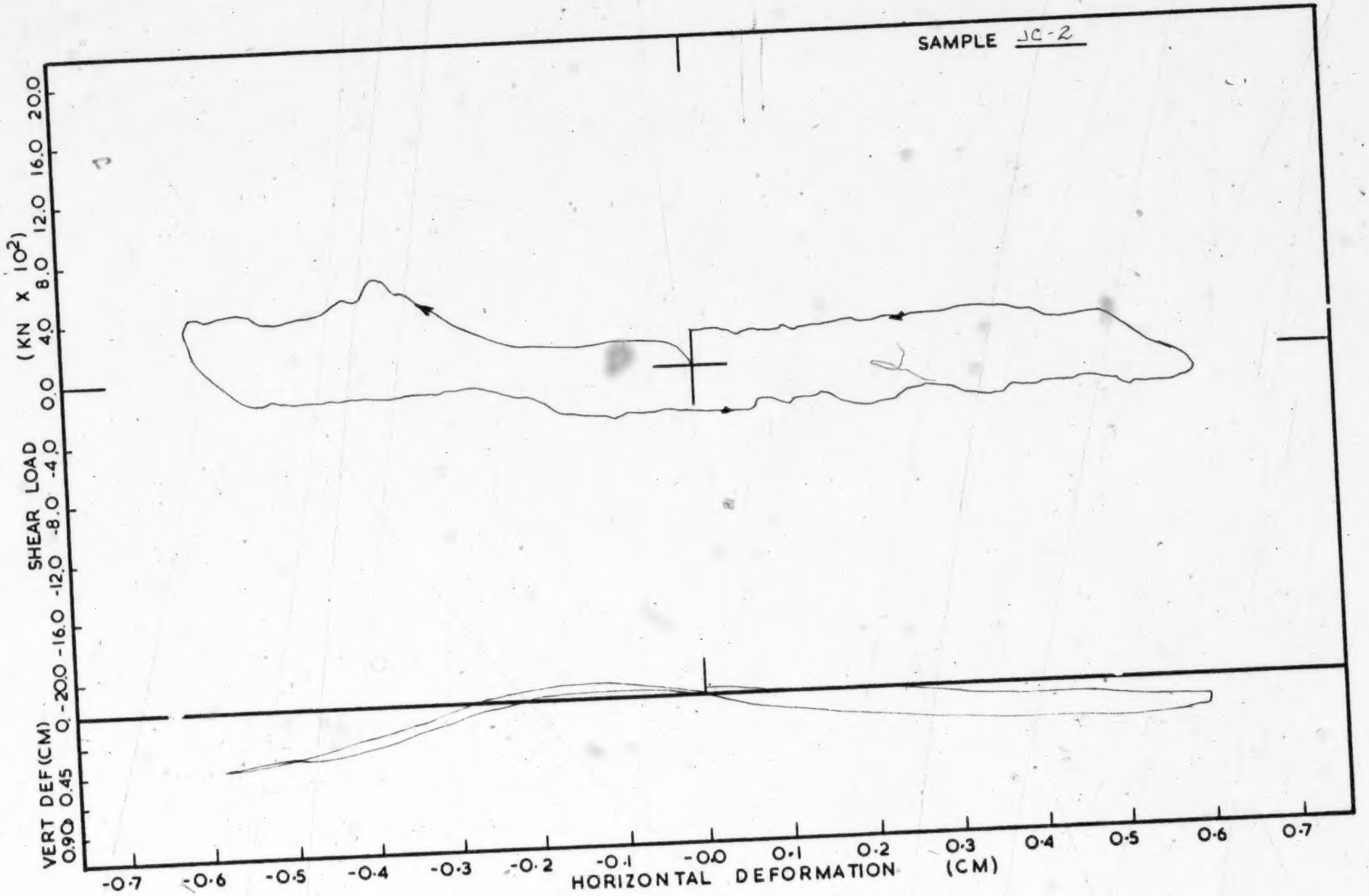
SAMPLE JC-2
SHEAR LOAD (KN X 10²)
20.0
16.0
12.0
8.0
4.0
0.0
-4.0
-8.0
-12.0
-16.0
-20.0
VERT DEF (CM)
0.
0.45
0.90
-0.7
-0.6
-0.5
-0.4
-0.3
-0.2
-0.1
-0.0
0.1
0.2
0.3
0.4
0.5
0.6
0.7
HORIZONTAL DEFORMATION (CM)

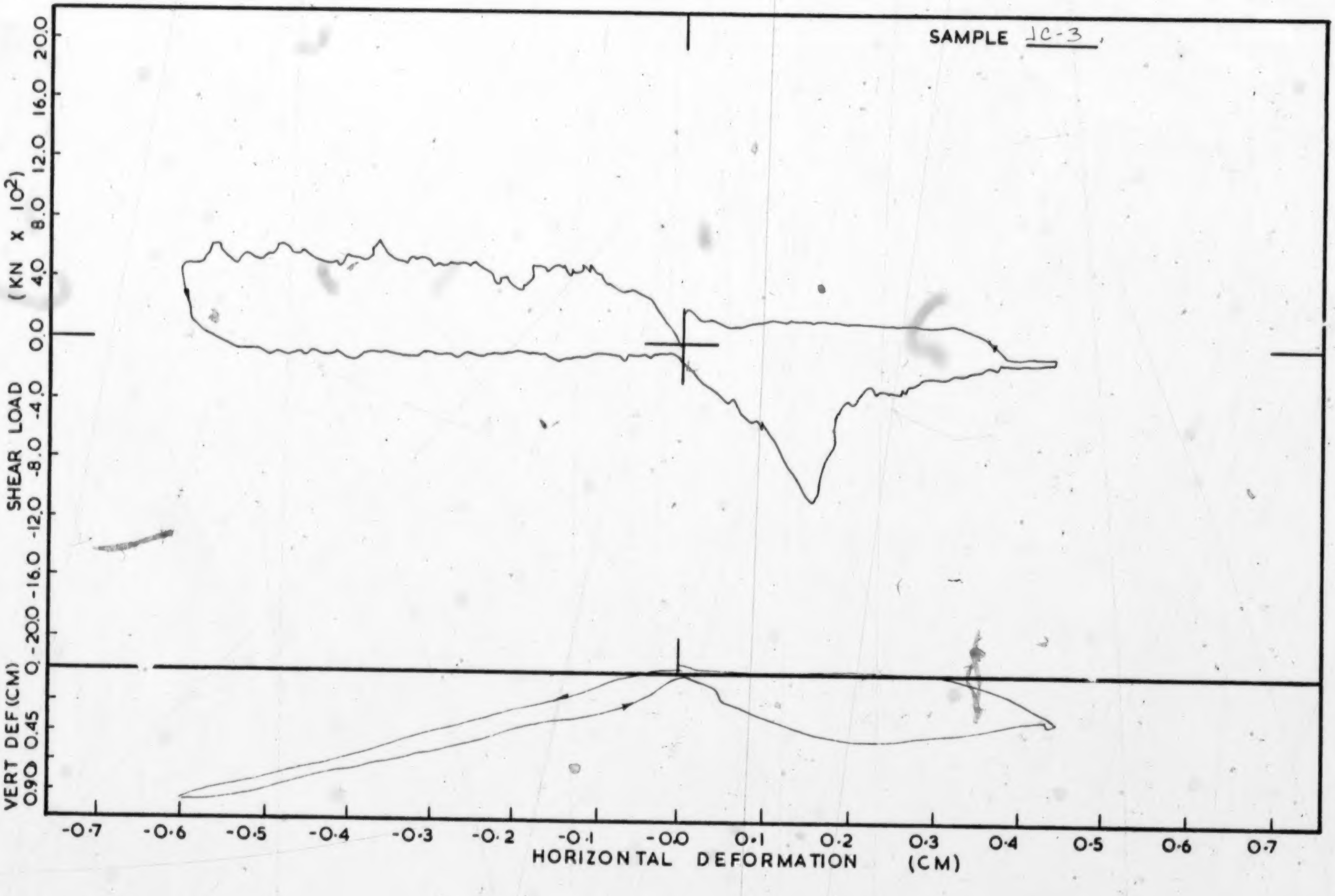
SAMPLE 1C-3
SHEAR LOAD (KN X 10^2)
20.0
16.0
12.0
8.0
4.0
0.0
-4.0
-8.0
-12.0
-16.0
-20.0
VERT DEF (CM)
0.
0.45
0.90
-0.7
-0.6
-0.5
-0.4
-0.3
-0.2
-0.1
-0.0
0.1
0.2
0.3
0.4
0.5
0.6
0.7
HORIZONTAL DEFORMATION (CM)

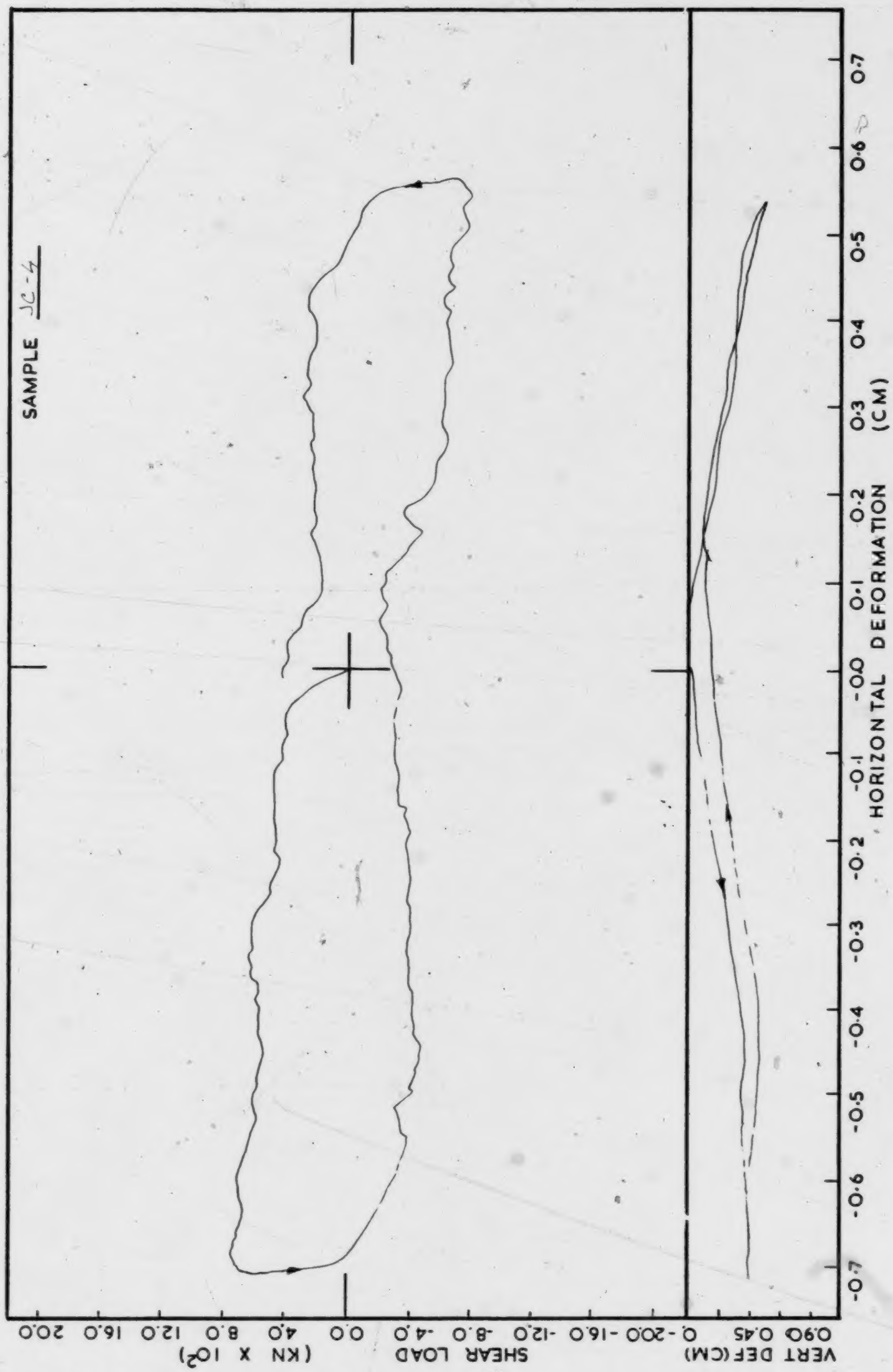
SAMPLE 3C-4
SHEAR LOAD
(KN X 10^2)
20.0
16.0
12.0
8.0
4.0
0.0
-4.0
-8.0
-12.0
-16.0
-20.0
VERT DEF (CM)
0.
0.45
0.90
HORIZONTAL DEFORMATION (CM)
-0.7
-0.6
-0.5
-0.4
-0.3
-0.2
-0.1
-0.0
0.1
0.2
0.3
0.4
0.5
0.6
0.7

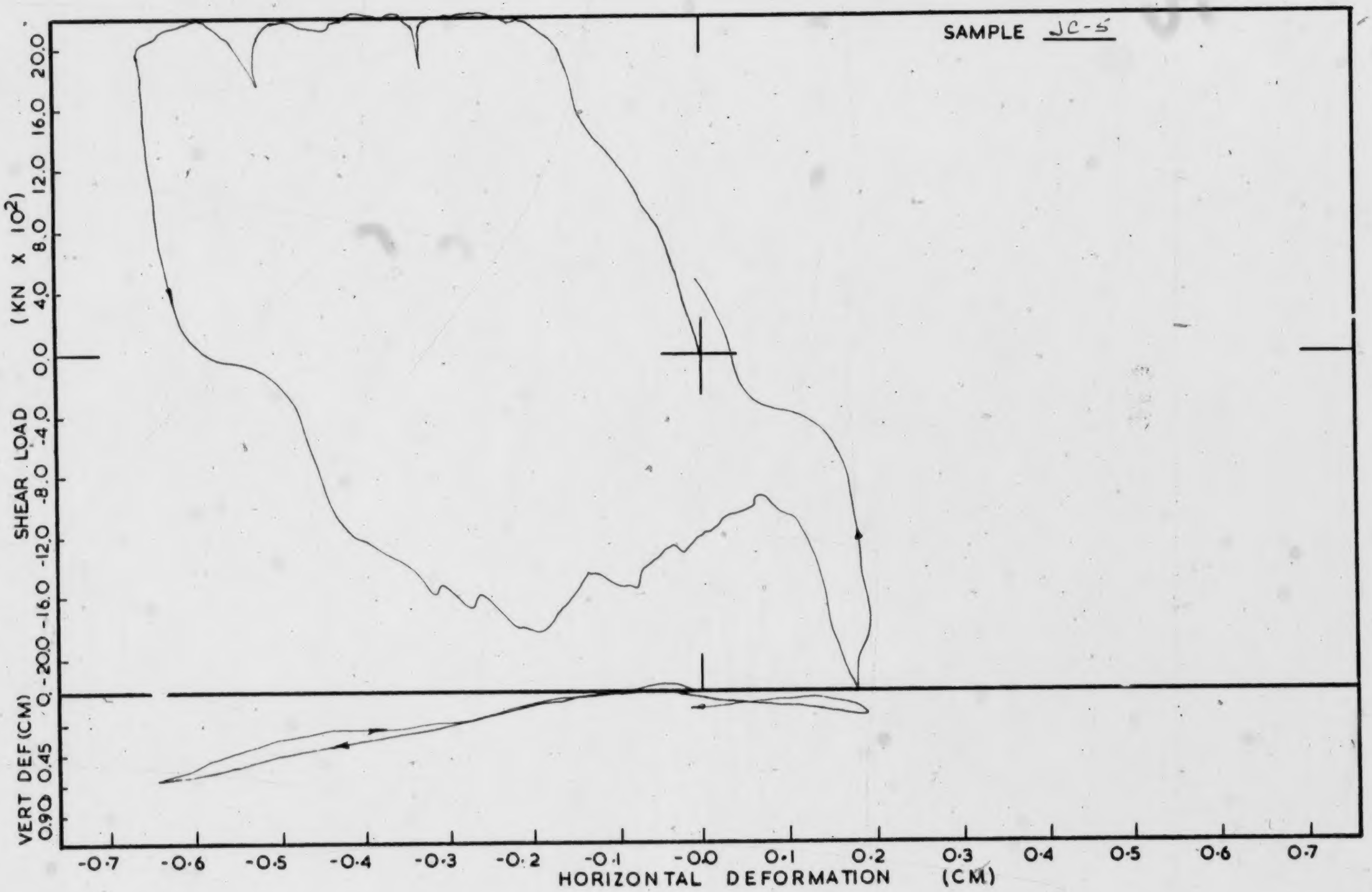
SAMPLE JC-5
SHEAR LOAD (KN X 10^2)
20.0
16.0
12.0
8.0
4.0
0.0
-4.0
-8.0
-12.0
-16.0
-20.0
VERT DEF (CM)
0.
0.45
0.90
-0.7
-0.6
-0.5
-0.4
-0.3
-0.2
-0.1
-0.0
0.1
0.2
0.3
0.4
0.5
0.6
0.7
HORIZONTAL DEFORMATION (CM)

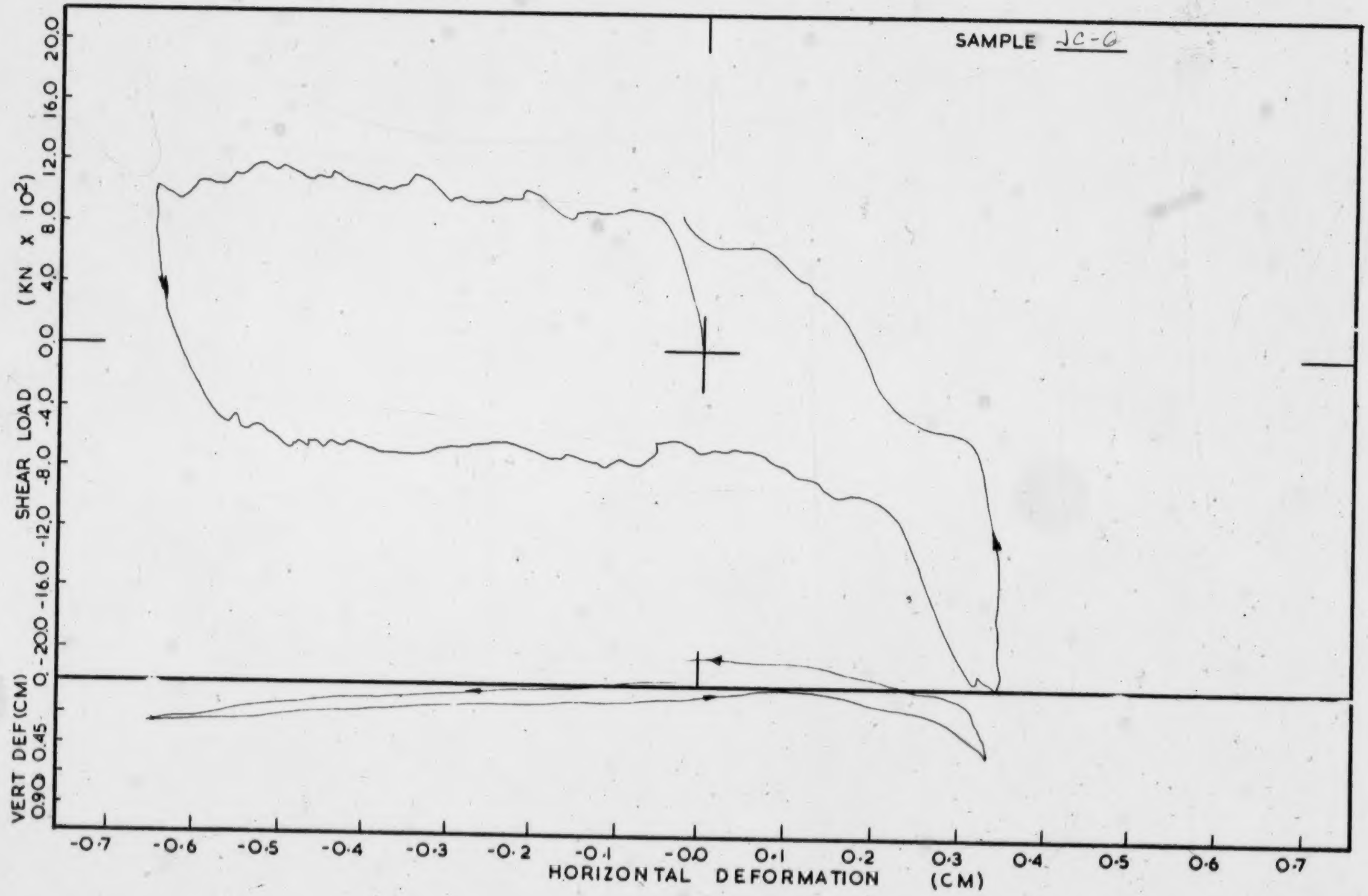
SAMPLE JC-6
SHEAR LOAD (KN x 10^2)
20.0
16.0
12.0
8.0
4.0
0.0
-4.0
-8.0
-12.0
-16.0
-20.0
0.
VERT DEF (CM)
0.45
0.90
-0.7
-0.6
-0.5
-0.4
-0.3
-0.2
-0.1
-0.0
0.1
0.2
0.3
0.4
0.5
0.6
0.7
HORIZONTAL DEFORMATION (CM)

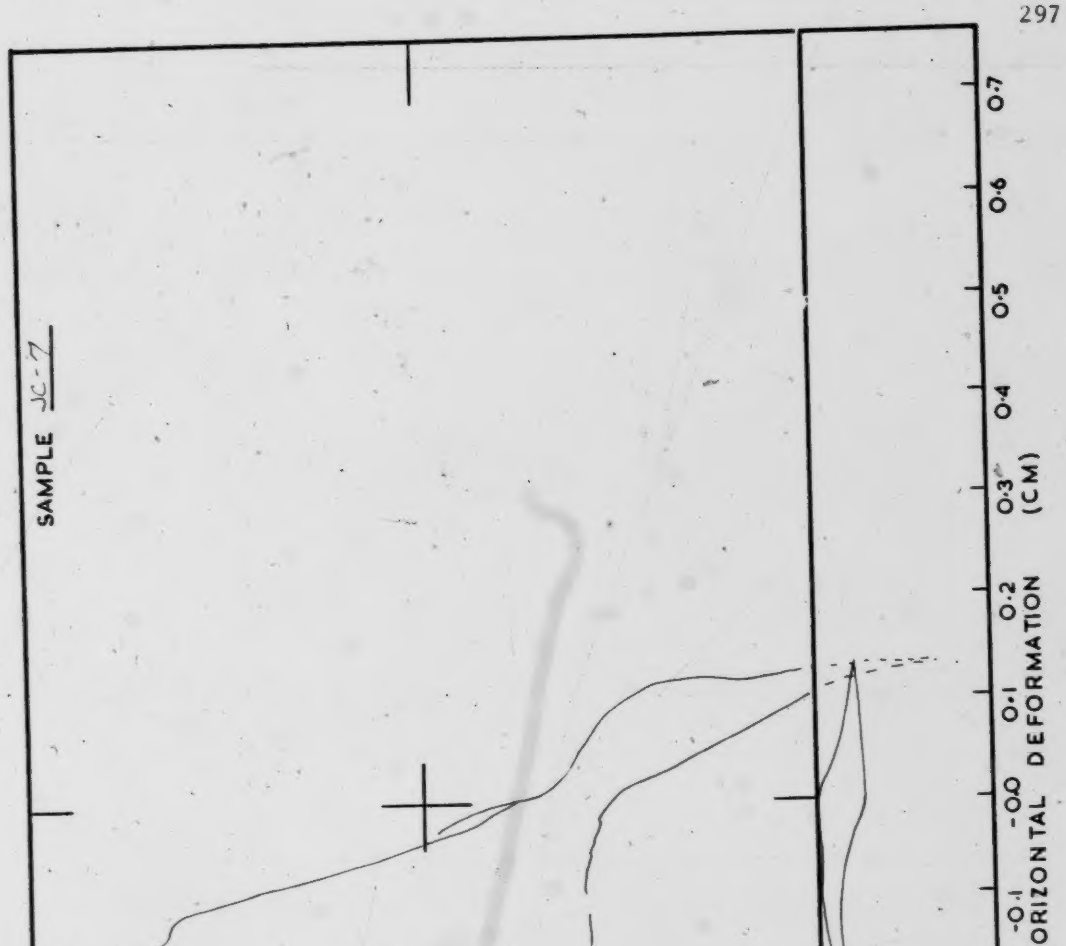
SAMPLE JC-7
SHEAR LOAD (KN X 10²)
20.0
16.0
12.0
8.0
4.0
0.0
-4.0
-8.0
-12.0
-16.0
-20.0
VERT DEF(CM)
0.90
0.45
0.
-0.7
-0.6
-0.5
-0.4
-0.3
-0.2
-0.1
0.0
0.1
0.2
0.3
0.4
0.5
0.6
0.7
HORIZONTAL DEFORMATION (CM)

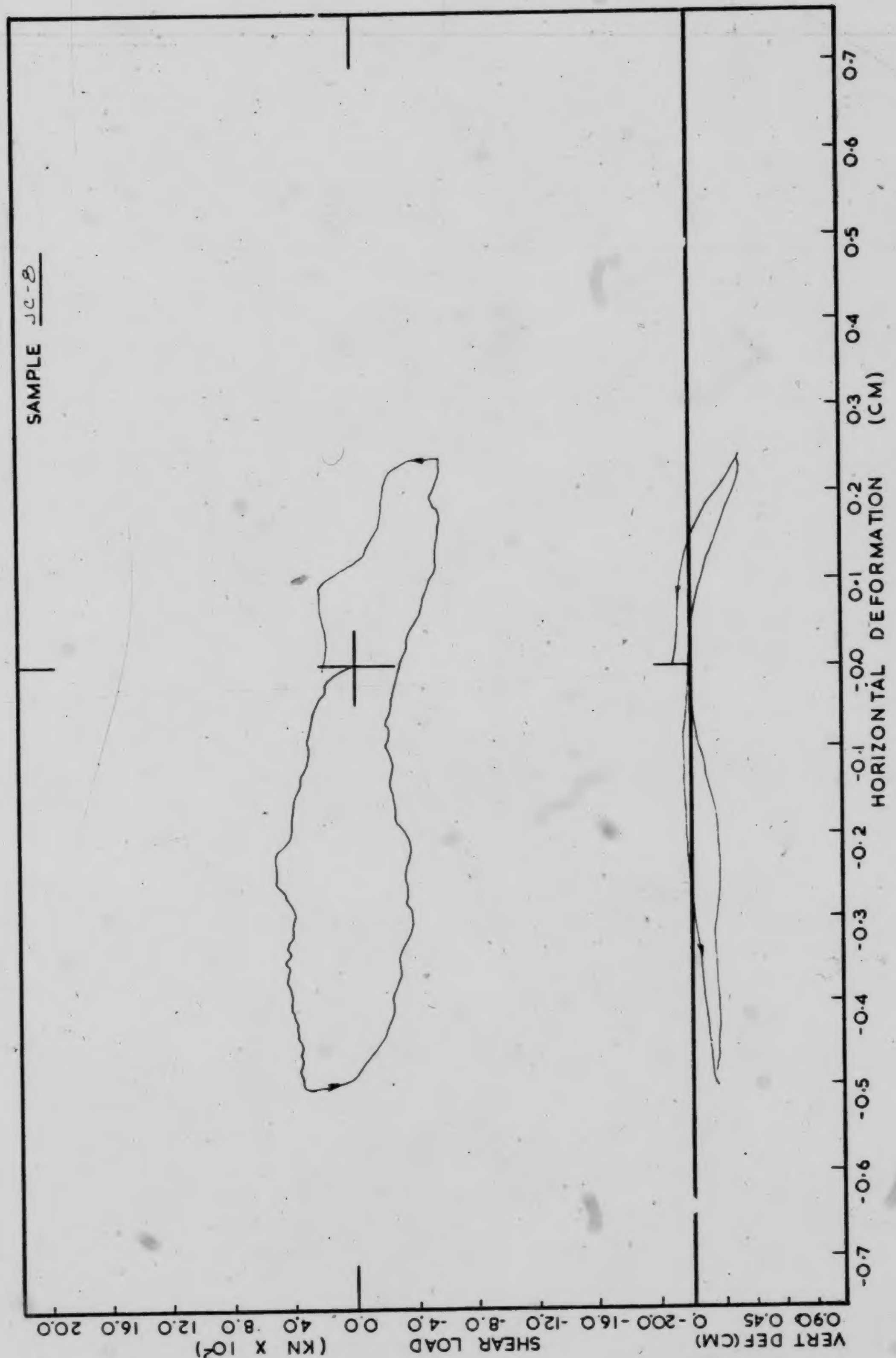
SAMPLE JC-8
-0.7
-0.6
-0.5
-0.4
-0.3
-0.2
-0.1
-0.0
0.1
0.2
0.3
0.4
0.5
0.6
0.7
HORIZONTAL DEFORMATION (CM)
20.0
16.0
12.0
8.0
4.0
0.0
-4.0
-8.0
-12.0
-16.0
-20.0
SHEAR LOAD (KN X 10^2)
0.
0.45
0.90
VERT DEF (CM)

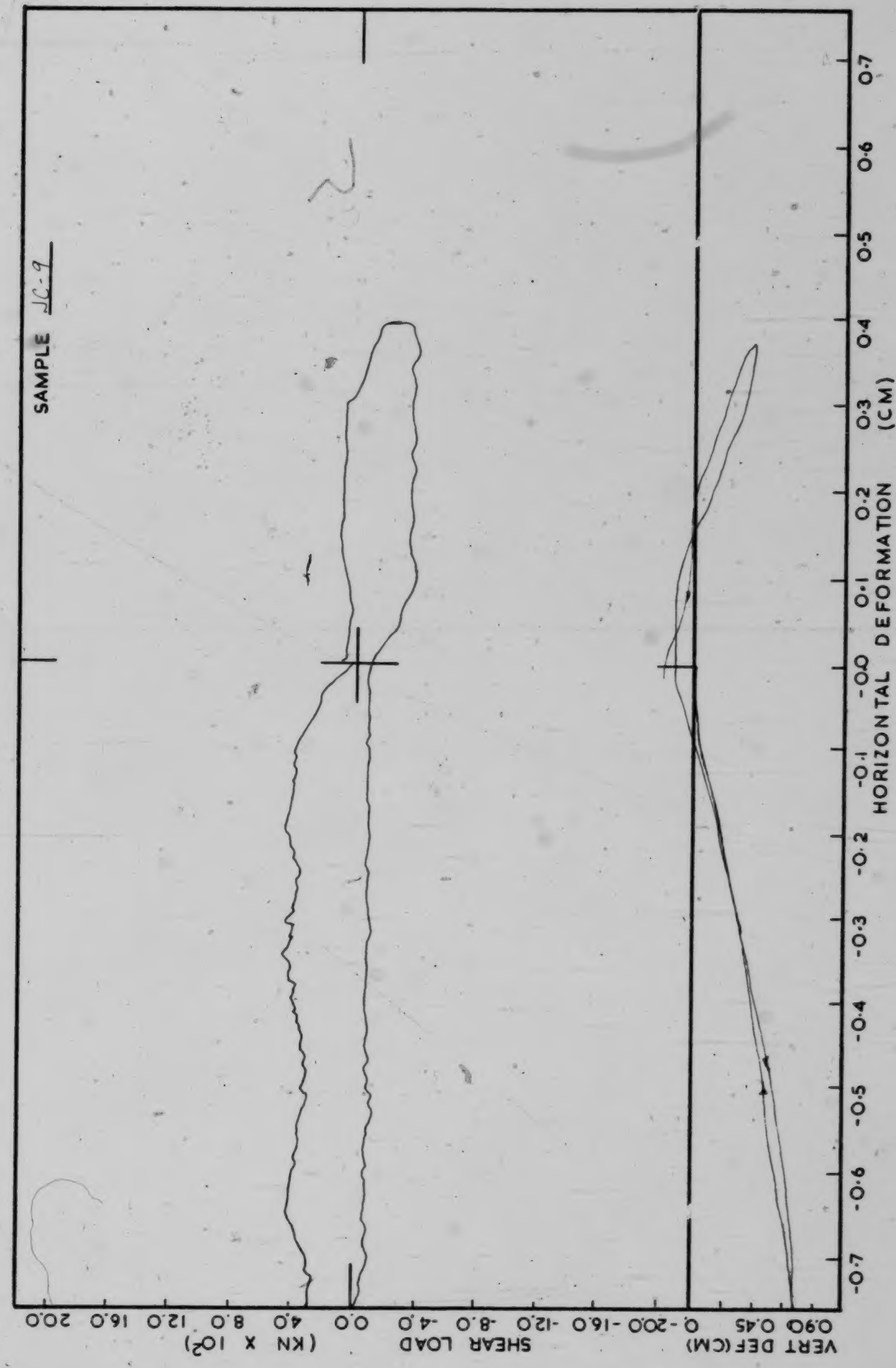
SAMPLE JC-9
SHEAR LOAD (KN X 10²)
20.0
16.0
12.0
8.0
4.0
0.0
-4.0
-8.0
-12.0
-16.0
-20.0
VERT DEF (CM)
0.
0.45
0.90
-0.7
-0.6
-0.5
-0.4
-0.3
-0.2
-0.1
-0.0
0.1
0.2
0.3
0.4
0.5
0.6
0.7
HORIZONTAL DEFORMATION (CM)

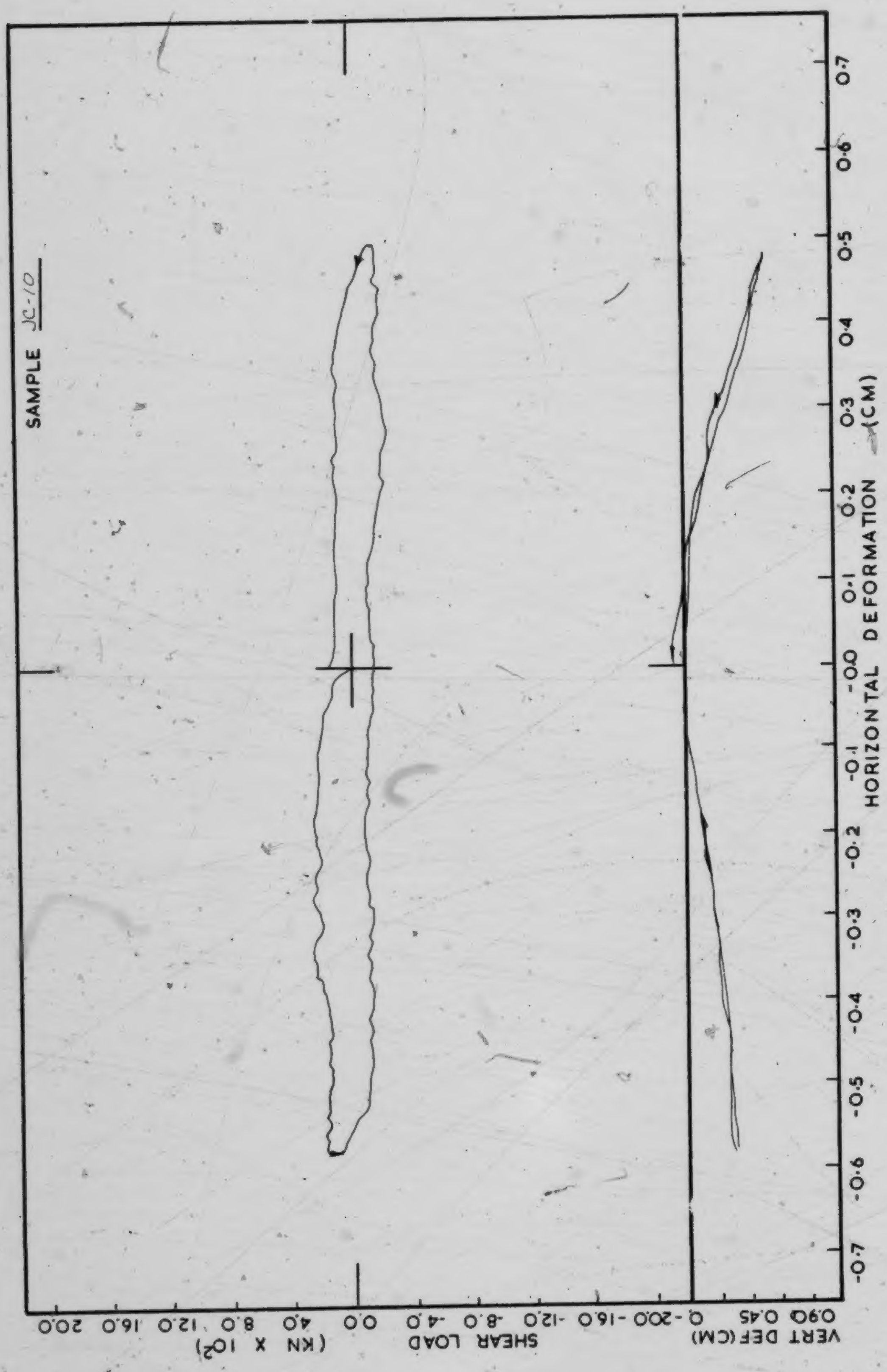
SAMPLE JC-10
SHEAR LOAD (KN X 10²)
20.0
16.0
12.0
8.0
4.0
0.0
-4.0
-8.0
-12.0
-16.0
-20.0
VERT DEF (CM)
0.90
0.45
0.
-0.7
-0.6
-0.5
-0.4
-0.3
-0.2
-0.1
-0.0
0.1
0.2
0.3
0.4
0.5
0.6
0.7
HORIZONTAL DEFORMATION (CM)

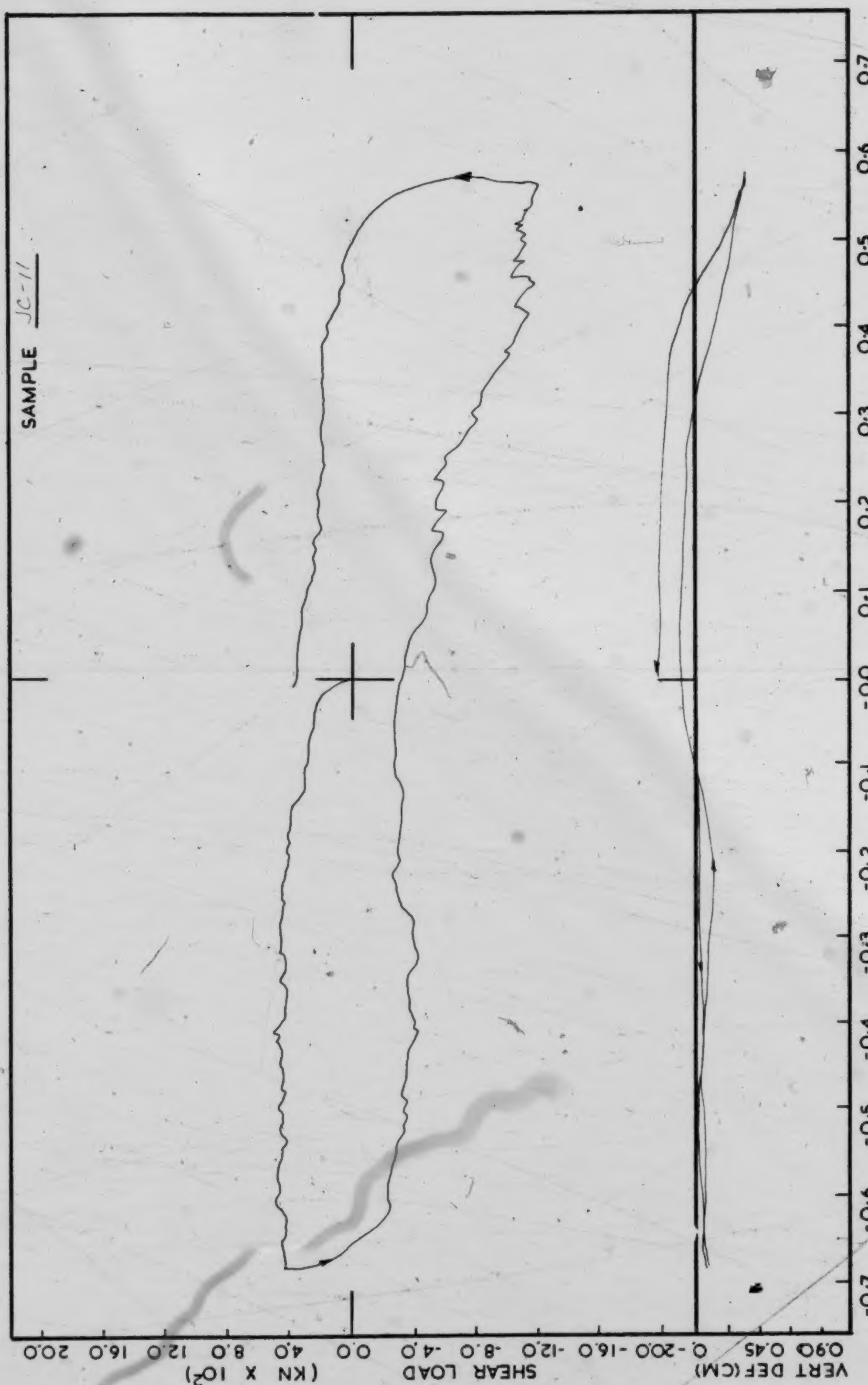
SAMPLE JC-11
SHEAR LOAD
(KN X 10²)
VERT DEF (CM)
0.90
0.45
0.
-20.0
-16.0
-12.0
-8.0
-4.0
0.0
4.0
8.0
12.0
16.0
20.0
-0.7
-0.6
-0.5
-0.4
-0.3
-0.2
-0.1
-0.0
0.1
0.2
0.3
0.4
0.5
0.6
0.7
HORIZONTAL DEFORMATION (CM)

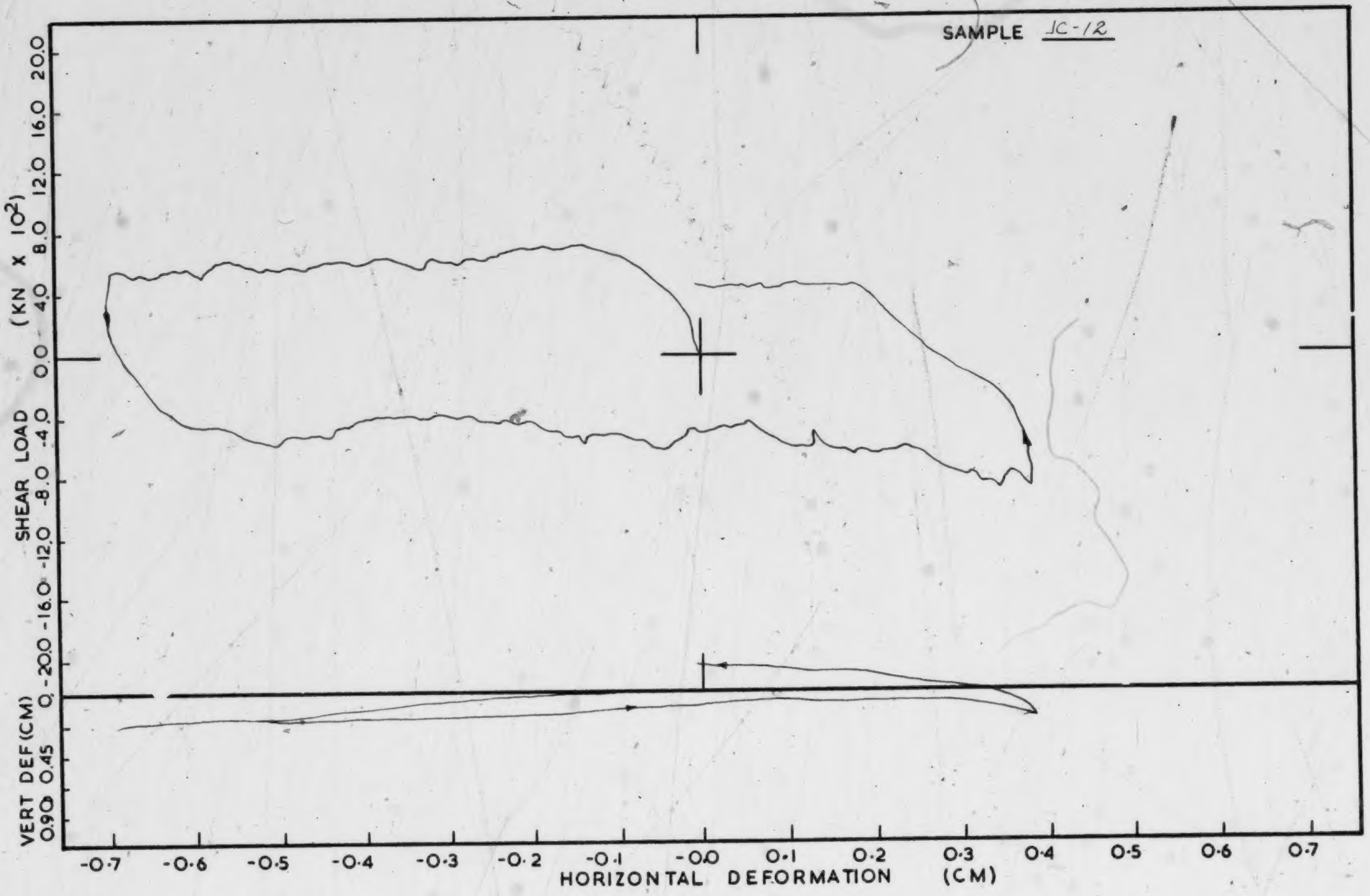
SAMPLE JC-12
SHEAR LOAD (KN X 10^2)
20.0
16.0
12.0
8.0
4.0
0.0
-4.0
-8.0
-12.0
-16.0
-20.0
VERT DEF (CM)
0.
0.45
0.90
-0.7
-0.6
-0.5
-0.4
-0.3
-0.2
-0.1
-0.0
0.1
0.2
0.3
0.4
0.5
0.6
0.7
HORIZONTAL DEFORMATION (CM)

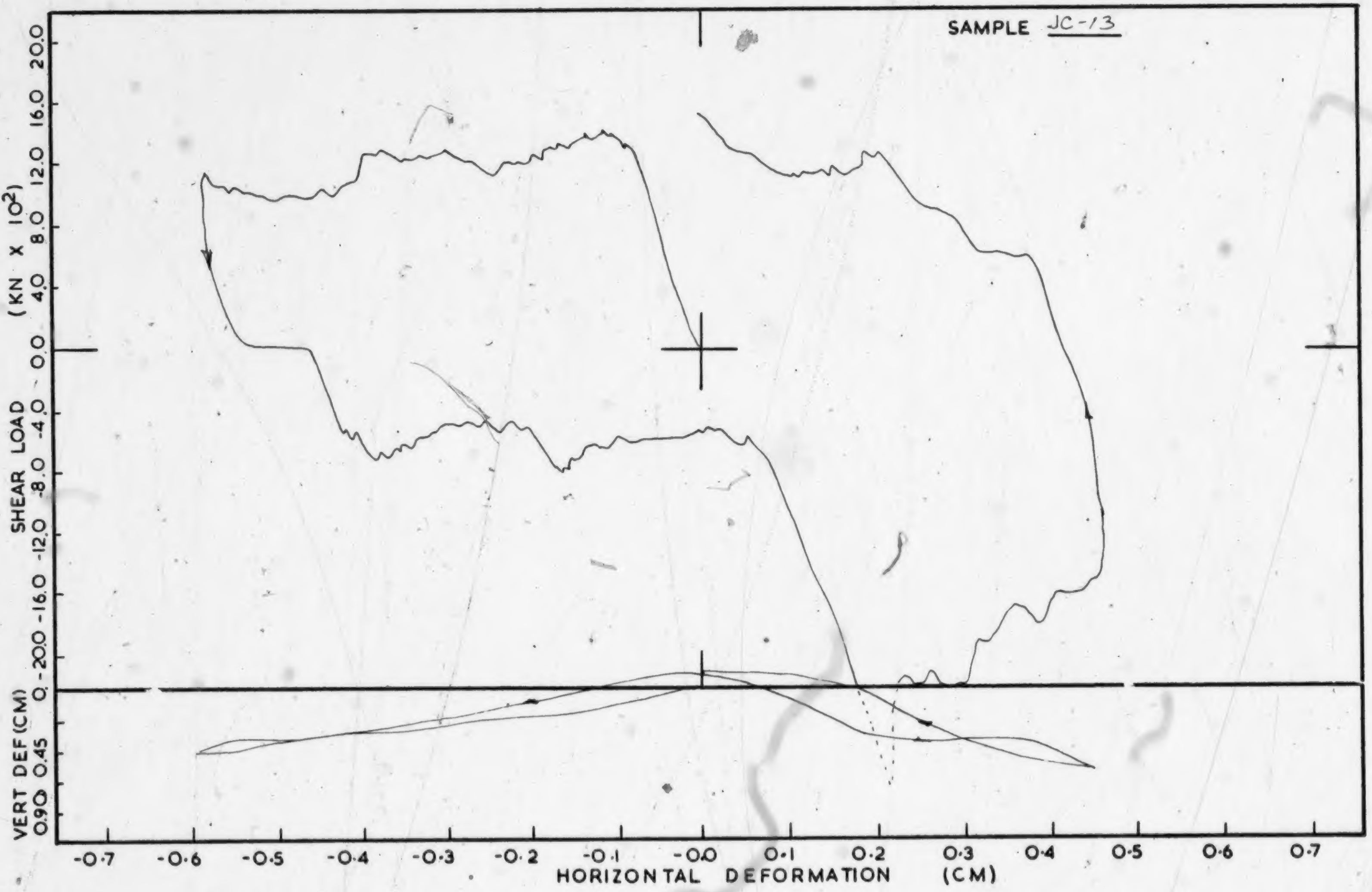
SAMPLE JC-13
SHEAR LOAD (KN X 10^2)
20.0
16.0
12.0
8.0
4.0
0.0
-4.0
-8.0
-12.0
-16.0
-20.0
VERT DEF (CM)
0
0.45
0.90
-0·7
-0·6
-0·5
-0·4
-0·3
-0·2
-0·1
-0.0
0·1
0·2
0·3
0·4
0·5
0·6
0·7
HORIZONTAL DEFORMATION (CM)

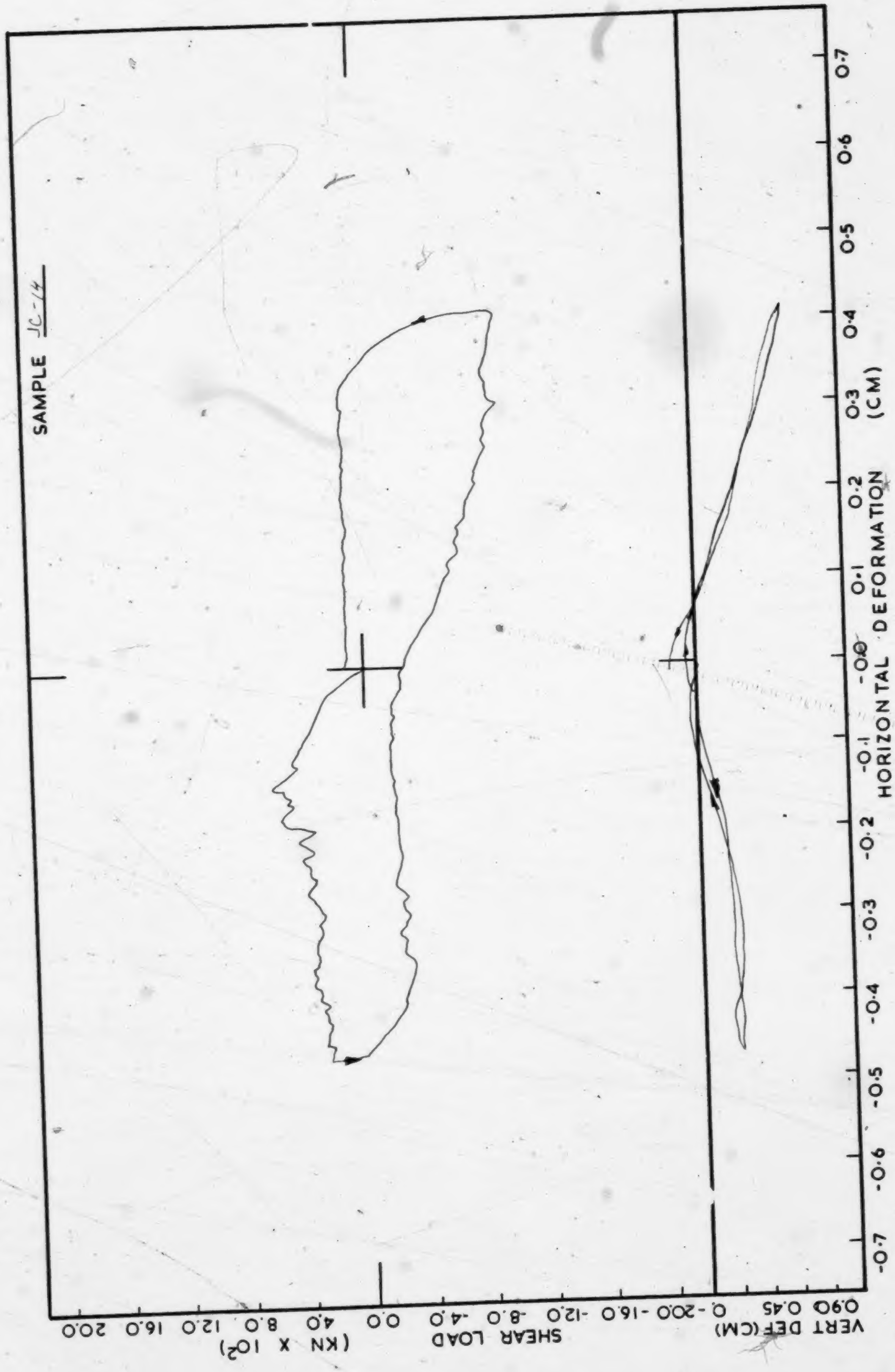
SAMPLE JC-14
SHEAR LOAD
(KN X 10²)
20.0
16.0
12.0
8.0
4.0
0.0
-4.0
-8.0
-12.0
-16.0
-20.0
VERT DEF(CM)
0.90
0.45
0.
HORIZONTAL DEFORMATION
(CM)
-0.7
-0.6
-0.5
-0.4
-0.3
-0.2
-0.1
-0.0
0.1
0.2
0.3
0.4
0.5
0.6
0.7

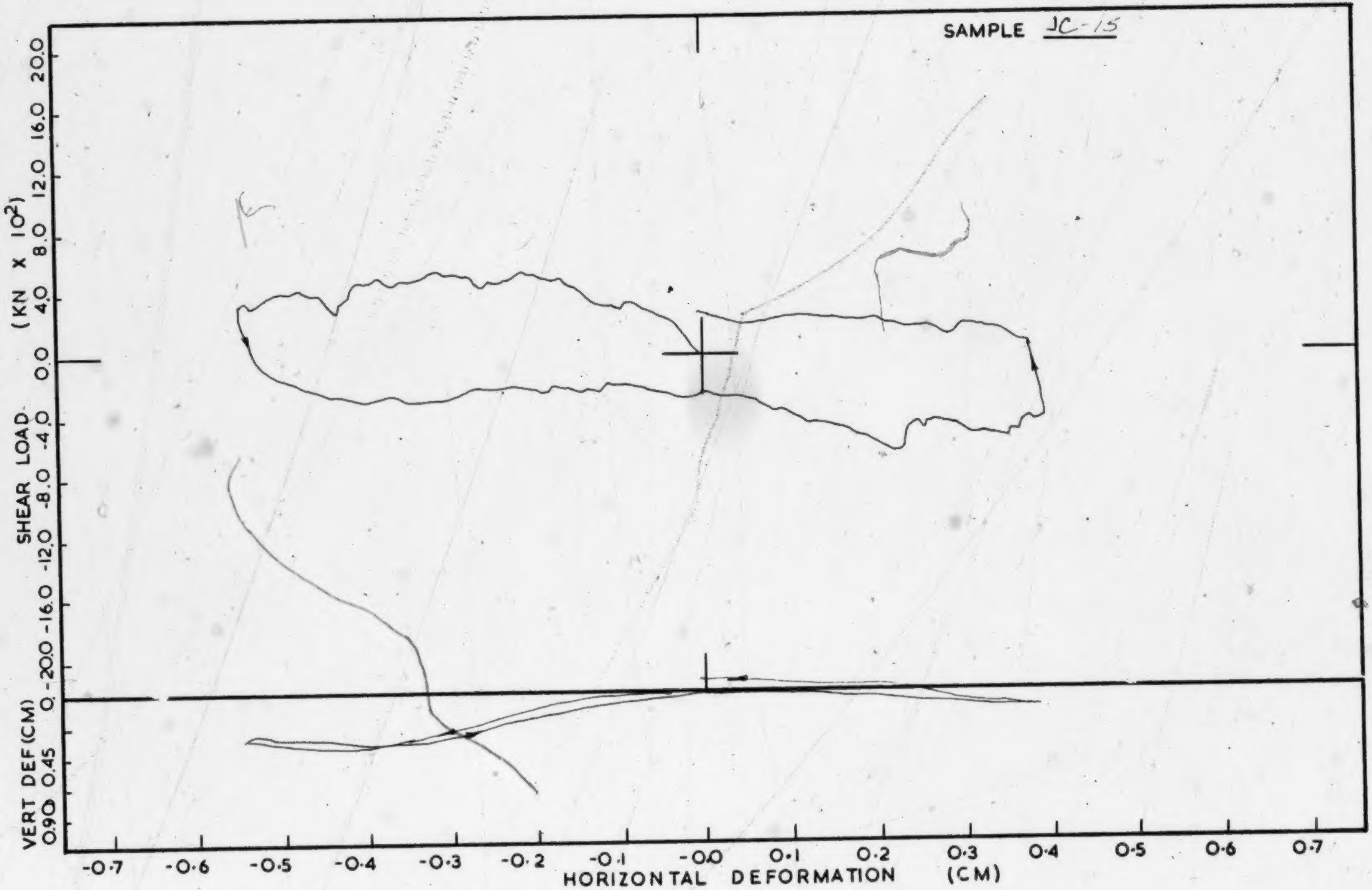
SAMPLE JC-15
SHEAR LOAD (KN X 10^2)
20.0
16.0
12.0
8.0
4.0
0.0
-4.0
-8.0
-12.0
-16.0
-20.0
VERT DEF (CM)
0
0.45
0.90
-0.7
-0.6
-0.5
-0.4
-0.3
-0.2
-0.1
-0.0
0.1
0.2
0.3
0.4
0.5
0.6
0.7
HORIZONTAL DEFORMATION (CM)

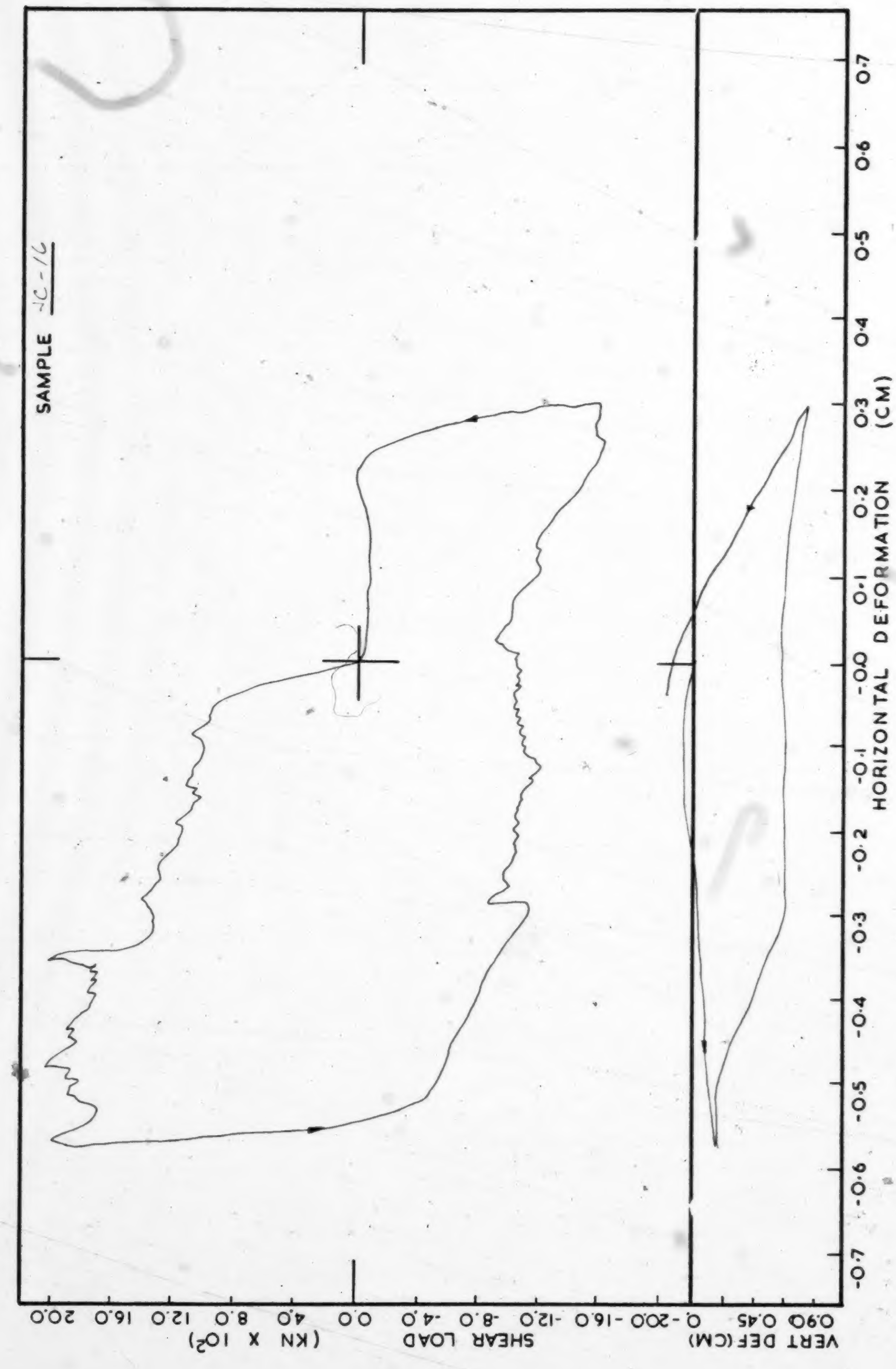
SAMPLE 4C-1C
SHEAR LOAD (KN X 10^2)
20.0
16.0
12.0
8.0
4.0
0.0
-4.0
-8.0
-12.0
-16.0
-20.0
VERT DEF (CM)
0.90
0.45
0.
-0.7
-0.6
-0.5
-0.4
-0.3
-0.2
-0.1
-0.0
0.1
0.2
0.3
0.4
0.5
0.6
0.7
HORIZONTAL DEFORMATION (CM)

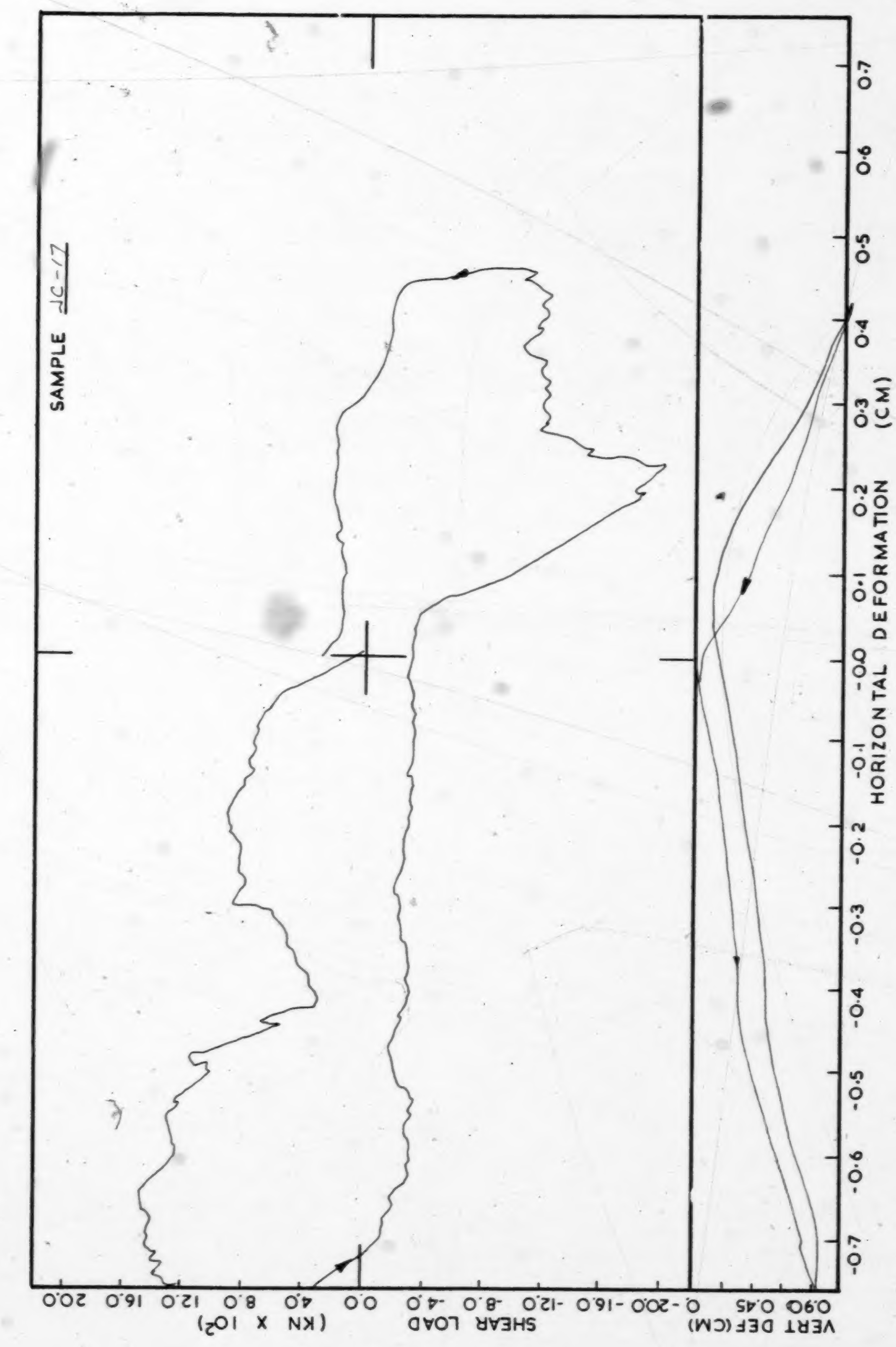
SAMPLE JC-17
SHEAR LOAD (KN X 10^2)
20.0
16.0
12.0
8.0
4.0
0.0
-4.0
-8.0
-12.0
-16.0
-20.0
VERT DEF (CM)
0.90
0.45
0
-0.7
-0.6
-0.5
-0.4
-0.3
-0.2
-0.1
0.0
0.1
0.2
0.3
0.4
0.5
0.6
0.7
HORIZONTAL DEFORMATION (CM)

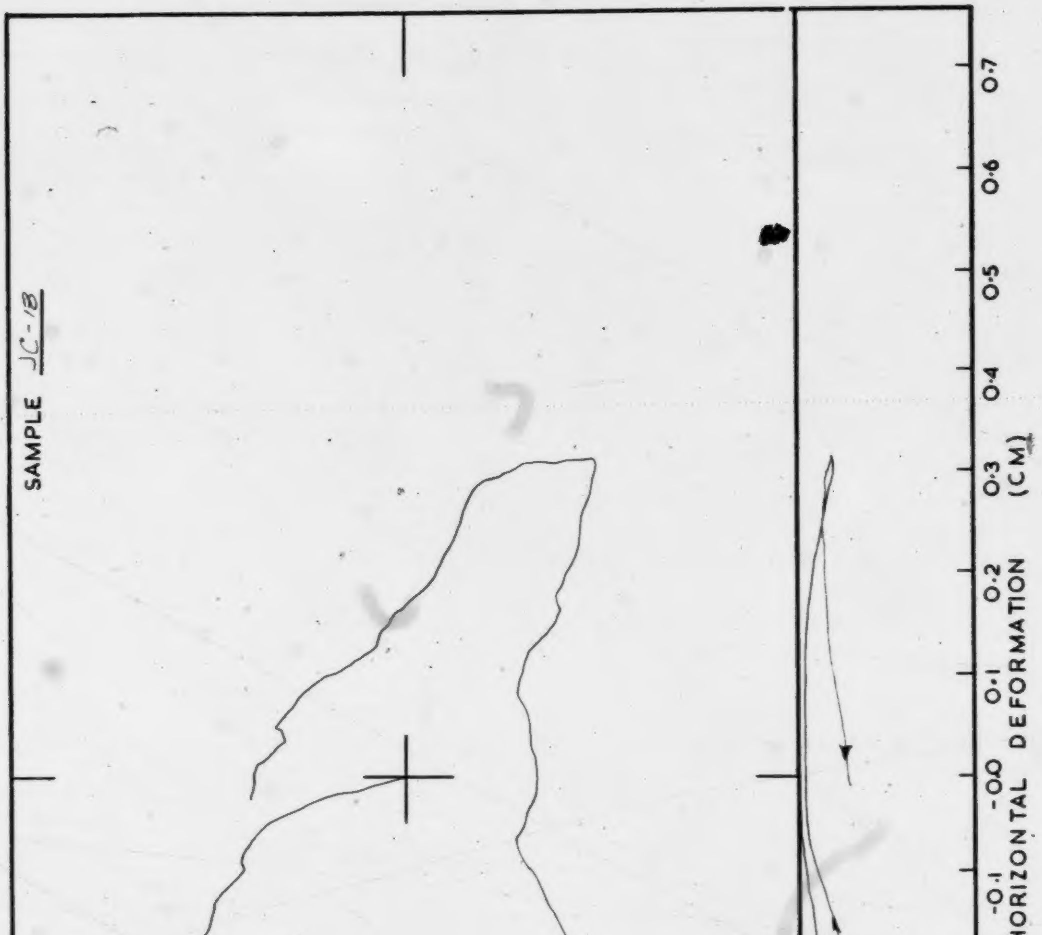
SAMPLE JC-1B
HORIZONTAL DEFORMATION (CM)
-0.7
-0.6
-0.5
-0.4
-0.3
-0.2
-0.1
-0.0
0.1
0.2
0.3
0.4
0.5
0.6
0.7
SHEAR LOAD (KN X 10^2)
20.0
16.0
12.0
8.0
4.0
0.0
-4.0
-8.0
-12.0
-16.0
-20.0
VERT DEF (CM)
0.
0.45
0.90